AN ABSTRACT OF THE DISSERTATION OF

Lijoy K. Mathew for the degree of Doctor of Philosophy in Toxicology presented on October 29, 2007.
Title: Unraveling Tissue Regeneration Using Chemical Genetics.

Abstract approved: _____

Robert L. Tanguay

The emerging field of regenerative medicine is mainly approached by two different aspects. First is the use of stem cell based models to generate a suite of differentiated cells for therapeutic applications and the alternative approach is to utilize the non-mammalian models that have the inherent capacity to regenerate their body parts. Zebrafish caudal fin regeneration is a well established research system to understand the basic principles of tissue regeneration. We combined a toxicological, a chemical genetic and a candidate gene approach to define the molecular signaling pathways important for regeneration. TCDD, an aryl hydrocarbon receptor (AHR) ligand was used as a chemical probe to impair regeneration and we identified that AHR2 and ARNT1 are the *in vivo* molecular partners for TCDD-mediated inhibition of regeneration. We further performed a global genomic analysis in the regenerating fin tissue after TCDD exposure to identify the downstream target genes modulated by AHR activation. Functional grouping of the differentially expressed genes by TCDD revealed misexpression of Wnt signaling genes as well as Wnt target genes, suggestive of a cross talk between AHR and Wnt signaling pathways. We hypothesized that, mis-expression of R-Spondin1, a TCDD-induced gene as well as a novel ligand for Wnt co-receptor LRP6 was responsible for the differential expression of the Wnt target genes. Partial antisense repression of R-Spondin1 or LRP6 prevented the inhibition of regeneration by TCDD, indicating that mis-induction of R-Spondin1 which mediates through LRP6 is absolutely required for TCDD-mediated inhibitory effect on fin regeneration.

Understanding the advantages of chemicals to probe tissue regeneration, we developed a rapid throughput regeneration assay to identify additional small molecules that modulated regeneration. Glucocorticoids were identified as inhibitors of regeneration and we demonstrated that glucocorticoid receptor activation is absolutely required for mediating the inhibition of regeneration. We further illustrated that, signaling from exogenous glucocorticoids impairs blastema formation and limits regenerative capability in vertebrates through an acute inflammation-independent mechanism and also report that, neutrophils and macrophages are not required for fin regeneration. Finally, we performed a comparative global genomic analysis between different zebrafish regeneration models and identified *raldh2*, a rate limiting enzyme for retinoic acid (RA) synthesis as a candidate gene across the distinct regeneration models. We demonstrated that, in addition to the well established role of RA signaling during the later phase of regenerative outgrowth, this signaling pathway is also critical for the initiation of regeneration, suggesting a dual phase of RA signaling during fin regeneration. Collectively, our results obtained through different experimental approaches suggest that, epimorphic regeneration is completed by a well orchestrated process of multiple molecular signaling events.

Unraveling Tissue Regeneration Using Chemical Genetics

by

Lijoy K. Mathew

A DISSERTATION

submitted to

Oregon State University

in partial fulfillment of
the requirement for the
degree of

Doctor of Philosophy

Presented October 29, 2007
Commencement June 2008

Doctor of Philosophy dissertation of Lijoy K. Mathew presented on October 29, 2007

APPROVED

Major Professor, representing Toxicology

Head of the Department of Environmental and Molecular Toxicology

---

Dean of the Graduate School

I understand that my dissertation will become part of the permanent collection of Oregon State University libraries. My signature below authorizes release of my dissertation to any reader upon request.

Lijoy K. Mathew, Author

ACKNOWLEDGEMENTS

I would like to thank a lot of people who helped me and guided me through the different phases of my graduate studies. Firstly, I have to express my deepest gratitude to my major advisor, Dr. Robert Tanguay who gave me an opportunity to join his lab in a very special situation. I had a great experience working with him and I have to thank him for providing the best guidance and support that helped in both academic as well as my personal development. I also wanted to thank Dr. Eric Andreasen, who supported me during the initial phase of my graduate studies and who also had the patience for teaching me various laboratory techniques. Jane LaDu has to be thanked her for all the help she provided at all technical as well as the non-technical levels. Sumitra Sengupta helped me with a lot of experiments and I would like to thank her for all her support. I wanted to thank all my committee members, namely, Dr. David Williams, Dr. Nancy Kerkvliet, Dr. Mark Leid and Dr. Jerry Heidel for serving in my graduate committee, helping me with the fellowship grants and guiding me throughout my graduate studies. I also wanted to thank Laura Young and Jessica Perry for helping with various experiments. My sincere thanks to everybody in the Department of Environmental and Molecular Toxicology for all the support. American Heart Association (AHA) provided pre-doctoral fellowship during my final year of graduate school and I have to thank AHA for the support. Most importantly, I wanted to thank my parents, my brother, my other family members and friends and very specially, my wife Usha who has been a great support for me all through my studies and my son Jacob. Finally, I wanted to dedicate my thesis to my parents, who spend their life teaching us and encouraging us to lead a good life by all means.

CONTRIBUTION OF AUTHORS

This dissertation is a collective effort of many collaborators from different universities and fellow members in Tanguay laboratory. In Chapter 1, Dr. Eric Andreasen provided intellectual contribution as well as helped with the preparation of the manuscript. In Chapter 2, Sumitra Sengupta performed certain exposure studies as well as in situ hybridization experiments. Dr. Eric Andreasen assisted me with the microarray analysis and quantitative-PCR experiments. Jane LaDu provided technical support for this project including assistance with morpholinos microinjections and animal care. In Chapter 3, Sumitra Sengupta worked with the screening of small molecule library and in situ hybridization experiments. Dr. Randall Peterson provided us the 2000-member small molecule library for rapid throughput regeneration assay. Dr. Eric Andreasen contributed intellectually and Dr. Atsushi Kawakami provided us with the reagents required for in situ hybridization experiments. Dr. Christiane V. Löhr conducted the histo-pathological analysis. Catherine A. Loynes and Dr. Stephen A. Renshaw provided the transgenic fish line (Tg(BACmpo:gfp)^{i114}) and helped with the neutrophil and macrophage migration assays. In Chapter 4, Sumitra Sengupta and Jessica Perry assisted with in situ hybridization experiments. Jane LaDu contributed technically regarding various microinjections and also supported with the fish care. Dr. Eric Andreasen assisted with the microarray analysis and also helped with the preparation of the manuscript. Most importantly, the work for this dissertation is the result of a group effort from all the past and present members of Tanguay laboratory who provided direct and indirect contributions.

TABLE OF CONTENTS

TABLE OF CONTENTS (Continued)

Page

LIST OF FIGURES

LIST OF FIGURES (Continued)

LIST OF FIGURES (Continued)

Figure Page

LIST OF TABLES

Unraveling Tissue Regeneration Using Chemical Genetics

Chapter 1. Introduction

The systematic functioning of all the organ systems in a human body is important as an injury or disease to a tissue/organ could lead to reduced quality of life or even fatality. Numerous disease conditions could be significantly improved if therapies that encourage tissue regeneration were available. The field of regenerative medicine is aimed at developing strategies to restore individual cell types, complex tissues, or structures that are lost or damaged. Most adult tissues and organs, especially in mammals, have lost their potential for further growth and differentiation. As a result, injury to a tissue or organ usually results in permanent damage (from scarring to disability). However, some non mammalian vertebrate animal models including salamanders, newts and zebrafish have retained the ability to regenerate their tissues, organs and appendages (Akimenko et al., 2003; Brockes et al., 2001; Poss et al., 2003). Since comparative genomics indicate significant genetic conservation between mammals and lower vertebrates, what are the molecular differences that permit tissue regeneration in the non mammalian models, and conversely make mammalian tissues recalcitrant to regeneration? By understanding the molecular and genetic pathways that coordinately function to accomplish regeneration in these "lower" animals, we will be in a stronger position to begin to understand why mammals fail to respond to tissue injury with a regenerative mechanism.

Zebrafish Regeneration

Zebrafish have the remarkable capability to regenerate their body parts including fins, optic nerve, scales, heart and spinal cord (Poss et al., 2003). Adult caudal fin regeneration is the most well-studied model for dissecting the molecular signaling that controls regenerative growth and angiogenesis (Bayliss et al., 2006; Poss et al., 2003).

This process is referred to as epimorphic regeneration. Epimorphic regeneration involves the reprogramming and migration of cells that differentiate and restore a tissue to its original form (reviewed in (Brockes and Kumar, 2005). Adult fin regeneration has been studied in a number of teleost fishes, including goldfish (Morgan, 1902; Santamaria et al., 1992; Santamaria et al., 1996), trout (Alonso et al., 2000), tilapia (Kemp and Park, 1970; Santamaria et al., 1992) and minnows (Geraudie and Singer, 1977; Morgan, 1900), indicating that regenerative growth is functionally similar in various fish species. In recent years, the emergence of the zebrafish model has reinvigorated the field of adult fin regeneration (Akimenko et al., 2003; Geraudie et al., 1995; Katogi et al., 2004; Lee et al., 2005; Mari-Beffa et al., 1996; Nechiporuk and Keating, 2002; Santamaria et al., 1996; Stoick-Cooper et al., 2007; Whitehead et al., 2005).

In zebrafish, the adult caudal fin consists of 18 bony rays attached to the skeleton by ligaments. Each ray, referred to as a lepidotrichia is comprised of two hemirays. The hemirays consist of repeating segments joined by ligaments. The area between the hemirays of a lepidotrichia contains blood vessels, nerves and mesenchymal cells. The fin grows by successive addition of hemiray segments to the most distal segment. After partial amputation of the caudal fin, an apical epithelial wound cap (AEC) forms over the clot at the amputation site within 12 hours post amputation (hpa). The AEC cells are derived from non-proliferating local epithelial cells that migrate laterally over the wound. Once the epithelial cap is formed, mesenchymal cells proliferate and migrate from sites beneath the wound plane and accumulate under the epithelial cap forming a structure called the blastema within 48 hpa. The precise origin of blastemal cells is currently unknown, but the body of evidence supports the conclusion that blastemal cells are derived by a process of de-differentiation from adult mesenchymal cells at the plane of amputation. The possibility remains that blastema cells could arise from a population of quiescent stem cells, which can rapidly proliferate following amputation (reviewed in (Akimenko et al., 2003). There is little experimental data in adult zebrafish for the presence of such stem cells, however it has been demonstrated that melanocytes originate from a population of stem cells which differentiate and migrate to the regenerating fin tissue (Rawls and Johnson, 2001). Although interesting, it is unlikely that these migrating melanocytes give rise to the other cell types required for regeneration as cellular

proliferation data is more consistent with the hypothesis that blastemal cells originate from the connective tissue between the hemirays which heavily incorporates BrdU as early 24 hpa (Poleo et al., 2001). The blastemal cells proliferate and re-differentiate, replacing the amputated tissues which are infused with nerves and blood vessels in a process called regenerative outgrowth. Regenerative outgrowth begins at 2 days post amputation (dpa) until the regenerative event is complete at about 14 dpa.

There is also growing evidence in zebrafish to suggest that heart regeneration has a high degree of commonality with fin regeneration with respect to the order of events which occur after a surgical wound. Both tissues regenerate through the blastema formation followed by proliferation of cells to complete outgrowth (Lepilina et al., 2006; Poss et al., 2003; Poss et al., 2002b; Raya et al., 2004; Raya et al., 2003). Gene expression of *msxB* and *msxC* encoding homeo-domain containing transcription factors were upregulated in regenerating zebrafish hearts as early as 3 dpa (Raya et al., 2003) and in regenerating fin blastema at 1dpa (Akimenko et al., 1995). Additionally, the expression pattern of *notch1b* and *deltaC*, members of the Notch signaling pathway, are induced very early after heart amputation as well as in the regenerating fin blastema (Raya et al., 2003). None of the four genes described above were detected in the non-amputated fin or heart tissue, indicating that the re-induction of these genes was specific to the regenerating tissue. Additionally, the *nightcap* zebrafish mutant harboring a temperature sensitive mutation in the *Mps1* gene, a kinase required for the mitotic checkpoint, failed to regenerate both heart and fin tissue (Poss et al., 2003; Poss et al., 2002a). The *nbl* zebrafish mutant having a missense mutation in *hsp60* failed to regenerate the fin as well as the heart. These studies underscores the mechanistic similarities between the two regeneration models (Makino et al., 2005).

Molecular Signaling During Zebrafish Caudal Fin Regeneration

The caudal fin regeneration is a well orchestrated process and is tightly controlled by multiple molecular signaling pathways in a spatio-temporal manner. Some of the earliest work in zebrafish has demonstrated an essential role of retinoic acid (RA) signaling in regeneration (Ferretti and Geraudie, 1995). Exposure to RA itself affects

regeneration by impacting the size of the wound epidermis thereby impinging on re-patterning within the blastema (Ferretti and Geraudie, 1995) in addition to inducing apoptosis in the AEC (Geraudie and Ferretti, 1997). One of the most well studied signaling pathways during zebrafish regeneration is Fibroblast growth factor (Fgf) signaling. This signaling pathway is absolutely critical for adult zebrafish fin and heart regeneration and this has been demonstrated using Fgfr 1 inhibitor (SU5402) as well as the transgenic line (*hsp70:dn-fgfr1*) that expresses the dominant negative Fgfr1 protein upon heat shock (Lee et al., 2005; Lepilina et al., 2006; Poss et al., 2000b). A genetic zebrafish mutant study revealed that *fgf20a* is absolutely required for the initiation and formation of blastema (Whitehead et al., 2005) and referred *fgf20a* as an initiator of regeneration. Recent studies illustrate that a proper balance of Wnt/β-catenin signaling is to be critical for the formation and proliferation of blastema cells that is required for complete regeneration (Kawakami et al., 2006; Stoick-Cooper et al., 2007). Moreover, it has also been established that *fgf20a* expression is controlled by Wnt/β-catenin signaling, suggesting that Wnt/β-catenin signaling acts upstream of Fgf signaling (Stoick-Cooper et al., 2007; Whitehead et al., 2005). Activin-βA(actβA) signaling is also reported to have functional role during regeneration and is important for the cell migration during wound healing and blastemal proliferation (Jazwinska et al., 2007). Even though major progress has been made in the identification of some of the essential molecular pathways for regeneration such as RA, Fgf, Wnt and actβA signaling, most would agree that we are still at the early stages of pathway discovery (Jazwinska et al., 2007; Kawakami et al., 2006; Poss et al., 2003; Poss et al., 2000a; Poss et al., 2000b; Stoick-Cooper et al., 2007; Whitehead et al., 2005).

Early Life Stage Fin Regeneration Model

Although adult zebrafish regeneration models have proven useful, many of the molecular and genetic tools that are useful for embryonic and larval studies are not easily applied to adult stage animals (Poss et al., 2003). Recent results indicate that these technical barriers may be overcome by using an early life stage regeneration model. Specifically, two-day-old zebrafish larvae completely regenerate their fin primordia

within three days following amputation (Kawakami et al., 2004; Mathew et al., 2006; Nakatani et al., 2007). The possibility of evaluating fin regeneration during this experimentally tractable life stage is enticing. It is recognized that the structure of the adult and larval fins are significantly different, however there is increasing evidence that there are remarkable similarities at the cellular and molecular level between adult and larval regeneration(Kawakami et al., 2004; Nakatani et al., 2007). Morphologically, the larval fin regenerates by a process that resembles that of the adult. A wound epithelium covers a pool of highly proliferating blastema-like cells as in adult regeneration (Kawakami et al., 2004). Also not surprisingly, similar to the adults, chemical inhibition of FGFR1 abrogates fin regeneration (Kawakami et al., 2004; Mathew et al., 2006). Since this life stage is inherently amenable to molecular and genetic manipulations such as transient and stable transgenics, genetic mutant screens and chemical genetics, this model offers a powerful new way to identify novel regulators of tissue regeneration.

Chemical Genetics and Regeneration

The use of small chemicals is an enormously powerful tool to help discover unknown players in biological processes. For instance, chemicals that inhibit protein function are useful for the identification of the key molecular target. To identify the principal molecular signaling pathways that control regeneration, chemical probes could be used to modulate regeneration. The underlying premise is that if a chemical inhibits or modulates an essential molecular target, then regeneration will be impacted and the identification of the target will help to unravel regenerative mechanisms. Previously it has been demonstrated that aryl hydrocarbon receptor (AHR) activation by TCDD impairs caudal fin regeneration in zebrafish (Andreasen et al., 2007; Andreasen et al., 2006; Zodrow and Tanguay, 2003). The AHR is a ligand activated, basic helix-loop-helix transcription factor and is a member of the PAS domain family of genes [reviewed in (Gu et al., 2000)]. The AHR signal transduction pathway in fish is similar to that in mammals, with the exception that fish have two or more AHR genes while mammals have only one [reviewed in (Hahn et al., 1997; Tanguay et al., 2003)]. Zebrafish and mammals also have two dimerization partners for AHR, AHR nuclear translocator proteins 1 and 2 (ARNT1, ARNT2), both of which can support AHR signaling (Prasch et al., 2004; Prasch

et al., 2006; Tanguay et al., 2000). Studying the inhibition of fin regeneration phenomenon by TCDD will provide more insight into the molecular mechanisms of AHR biology as well as greater understanding about tissue regeneration. We anticipated that, if one chemical could be used to identify important molecular signaling pathways required for regeneration, an unbiased chemical genetic approach will also lead to the identification of novel regenerative pathways.

Currently there are numerous gaps in our understanding of the complex regenerative pathways and interactions that mediate the different stages of regeneration. By thoroughly taking advantage of the early life stage zebrafish model, we will begin to dissect signaling events by mainly three approaches:

1. A toxicological approach to interfere a normal regeneration process and then to identify the molecular pathways affected by the AHR ligand, TCDD (Chapter 2 &3).
2. An unbiased chemical genetic approach to unravel novel regenerative pathways (Chapter 4).
3. A candidate gene approach with the utility of global genomic analysis to identify common molecular signaling between different regeneration platforms (Chapter 5).

References

Akimenko MA, Johnson SL, Westerfield M and Ekker M (1995) Differential induction of four msx homeobox genes during fin development and regeneration in zebrafish. *Development* **121**:347-57.

Akimenko MA, Mari-Beffa M, Becerra J and Geraudie J (2003) Old questions, new tools, and some answers to the mystery of fin regeneration. *Dev Dyn* **226**:190-201.

Alonso M, Tabata YA, Rigolino MG and Tsukamoto RY (2000) Effect of induced triploidy on fin regeneration of juvenile rainbow trout, Oncorhynchus mykiss. *J Exp Zool* **287**:493-502.

Andreasen EA, Mathew LK, Lohr CV, Hasson R and Tanguay RL (2007) Aryl hydrocarbon receptor activation impairs extracellular matrix remodeling during zebra fish fin regeneration. *Toxicol Sci* **95**:215-26.

Andreasen EA, Mathew LK and Tanguay RL (2006) Regenerative Growth is Impacted by TCDD: Gene Expression Analysis Reveals Extracellular Matrix Modulation. *Toxicol Sci* **92**:254-269.

Bayliss PE, Bellavance KL, Whitehead GG, Abrams JM, Aegerter S, Robbins HS, Cowan DB, Keating MT, O'Reilly T, Wood JM, Roberts TM and Chan J (2006) Chemical modulation of receptor signaling inhibits regenerative angiogenesis in adult zebrafish. *Nat Chem Biol* **2**:265-73.

Brockes JP and Kumar A (2005) Appendage regeneration in adult vertebrates and implications for regenerative medicine. *Science* **310**:1919-23.

Brockes JP, Kumar A and Velloso CP (2001) Regeneration as an evolutionary variable. *J Anat* **199**:3-11.

Ferretti P and Geraudie J (1995) Retinoic acid-induced cell death in the wound epidermis of regenerating zebrafish fins. *Dev Dyn* **202**:271-83.

Geraudie J and Ferretti P (1997) Correlation between RA-induced apoptosis and patterning defects in regenerating fins and limbs. *Int J Dev Biol* **41**:529-32.

Geraudie J, Monnot MJ, Brulfert A and Ferretti P (1995) Caudal fin regeneration in wild type and long-fin mutant zebrafish is affected by retinoic acid. *Int J Dev Biol* **39**:373-81.

Geraudie J and Singer M (1977) Relation between nerve fiber number and pectoral fin regeneration in the teleost. *J Exp Zool* **199**:1-8.

Gu YZ, Hogenesch JB and Bradfield CA (2000) The PAS superfamily: sensors of environmental and developmental signals. *Annu Rev Pharmacol Toxicol* **40**:519-61.

Hahn ME, Karchner SI, Shapiro MA and Perera SA (1997) Molecular evolution of two vertebrate aryl hydrocarbon (dioxin) receptors (AHR1 and AHR2) and the PAS family. *Proc Natl Acad Sci U S A* **94**:13743-8.

Jazwinska A, Badakov R and Keating MT (2007) Activin-betaA Signaling Is Required for Zebrafish Fin Regeneration. *Curr Biol*.

Katogi R, Nakatani Y, Shin-i T, Kohara Y, Inohaya K and Kudo A (2004) Large-scale analysis of the genes involved in fin regeneration and blastema formation in the medaka, Oryzias latipes. *Mech Dev* **121**:861-72.

Kawakami A, Fukazawa T and Takeda H (2004) Early fin primordia of zebrafish larvae regenerate by a similar growth control mechanism with adult regeneration. *Dev Dyn* **231**:693-9.

Kawakami Y, Rodriguez Esteban C, Raya M, Kawakami H, Martí M, Dubova I and Izpisua Belmonte JC (2006) Wnt/-catenin signaling regulates vertebrate limb regeneration. *Genes and Dev* **Dec 2006; 20: 3232 - 3237 ; doi:10.1101/gad.1475106**.

Kemp NE and Park JH (1970) Regeneration of lepidotrichia and actinotrichia in the tailfin of the teleost Tilapia mossambica. *Dev Biol* **22**:321-42.

Lee Y, Grill S, Sanchez A, Murphy-Ryan M and Poss KD (2005) Fgf signaling instructs position-dependent growth rate during zebrafish fin regeneration. *Development*.

Lepilina A, Coon AN, Kikuchi K, Holdway JE, Roberts RW, Burns CG and Poss KD (2006) A dynamic epicardial injury response supports progenitor cell activity during zebrafish heart regeneration. *Cell* **127**:607-19.

Makino S, Whitehead GG, Lien CL, Kim S, Jhawar P, Kono A, Kawata Y and Keating MT (2005) Heat-shock protein 60 is required for blastema formation and maintenance during regeneration. *Proc Natl Acad Sci U S A*.

Mari-Beffa M, Santanaria JA, Fernandez-Llebrez P and Becerra J (1996) Histochemically defined cell states during tail fin regeneration in telost fishes. *Differentiation* **60**:139-149.

Mathew LK, Andreasen EA and Tanguay RL (2006) Aryl hydrocarbon receptor activation inhibits regenerative growth. *Mol Pharmacol* **69**:257-65.

Morgan TH (1900) Regeneration in teleosts. *Arch Entw Org* **10**:120-131.

Morgan TH (1902) Further experiments on the regeneration of the tail fins of fishes. *Arch Entw MEch* **14**:539-561.

Nakatani Y, Kawakami A and Kudo A (2007) Cellular and molecular processes of regeneration, with special emphasis on fish fins. *Dev Growth Differ* **49**:145-54.

Nechiporuk A and Keating MT (2002) A proliferation gradient between proximal and msxb-expressing distal blastema directs zebrafish fin regeneration. *Development* **129**:2607-17.

Poleo G, Brown CW, Laforest L and Akimenko MA (2001) Cell proliferation and movement during early fin regeneration in zebrafish. *Dev Dyn* **221**:380-90.

Poss KD, Keating MT and Nechiporuk A (2003) Tales of regeneration in zebrafish. *Dev Dyn* **226**:202-210.

Poss KD, Nechiporuk A, Hillam AM, Johnson SL and Keating MT (2002a) Mps1 defines a proximal blastemal proliferative compartment essential for zebrafish fin regeneration. *Development* **129**:5141-9.

Poss KD, Shen J and Keating MT (2000a) Induction of lef1 during zebrafish fin regeneration. *Dev Dyn* **219**:282-6.

Poss KD, Shen J, Nechiporuk A, McMahon G, Thisse B, Thisse C and Keating MT (2000b) Roles for Fgf signaling during zebrafish fin regeneration. *Dev Biol* **222**:347-58.

Poss KD, Wilson LG and Keating MT (2002b) Heart regeneration in zebrafish. *Science* **298**:2188-90.

Prasch AL, Heideman W and Peterson RE (2004) ARNT2 is not required for TCDD developmental toxicity in zebrafish. *Toxicol Sci* **82**:250-8.

Prasch AL, Tanguay RL, Mehta V, Heideman W and Peterson RE (2006) Identification of zebrafish ARNT1 homologs: 2,3,7,8-tetrachlorodibenzo-p-dioxin toxicity in the developing zebrafish requires ARNT1. *Mol Pharmacol* **69**:776-87.

Rawls JF and Johnson SL (2001) Requirements for the kit receptor tyrosine kinase during regeneration of zebrafish fin melanocytes. *Development* **128**:1943-9.

Raya A, Consiglio A, Kawakami Y, Rodriguez-Esteban C and Izpisua-Belmonte JC (2004) The zebrafish as a model of heart regeneration. *Cloning Stem Cells* **6**:345-51.

Raya A, Koth CM, Buscher D, Kawakami Y, Itoh T, Raya RM, Sternik G, Tsai HJ, Rodriguez-Esteban C and Izpisua-Belmonte JC (2003) Activation of Notch signaling pathway precedes heart regeneration in zebrafish. *Proc Natl Acad Sci U S A* **100 Suppl 1**:11889-95.

Santamaria JA, Mari-Beffa M and Becerra J (1992) Interactions of the lepidotrichial matrix components during tail fin regeneration in teleosts. *Differentiation* **49**:143-50.

Santamaria JA, Mari-Beffa M, Santos-Ruiz L and Becerra J (1996) Incorporation of bromodeoxyuridine in regenerating fin tissue of the goldfish Carassius auratus. *J Exp Zool* **275**:300-7.

Stoick-Cooper CL, Weidinger G, Riehle KJ, Hubbert C, Major MB, Fausto N and Moon RT (2007) Distinct Wnt signaling pathways have opposing roles in appendage regeneration. *Development* **134**:479-89.

Tanguay RL, Andreasen E, Heideman W and Peterson RE (2000) Identification and expression of alternatively spliced aryl hydrocarbon nuclear translocator 2 (ARNT2) cDNAs from zebrafish with distinct functions. *Biochim Biophys Acta* **1494**:117-28.

Tanguay RL, Andreasen EA, Walker MK and Peterson RE (2003) Dioxin toxicity and aryl hydrocarbon receptor signaling in fish, in *Dioxins and Health* (Schecter A ed) pp 603-628, Plenum Press, New York.

Whitehead GG, Makino S, Lien CL and Keating MT (2005) fgf20 is essential for initiating zebrafish fin regeneration. *Science* **310**:1957-60.

Zodrow JM and Tanguay RL (2003) 2,3,7,8-tetrachlorodibenzo-p-dioxin inhibits zebrafish caudal fin regeneration. *Toxicol Sci* **76**:151-161.

Chapter 2. AHR Activation Inhibits Regenerative Growth

Lijoy K, Mathew, Eric A, Andreasen, and Robert L. Tanguay

Department of Environmental and Molecular Toxicology, Marine and Freshwater Biomedical Sciences Center, Environmental Health Sciences Center, Oregon State University, Corvallis, OR, 97331

Abstract

There is considerable literature supporting the conclusion that inappropriate activation of the aryl hydrocarbon receptor (AHR) alters cellular signaling. We have previously established that fin regeneration is specifically inhibited by TCDD in adult zebrafish and have used this *in vivo* end point to evaluate interactions between AHR and growth controlling pathways. Because there are experimental limitations in studying regeneration in adult animals, we have developed a larval model to evaluate the effect of AHR activation on tissue regeneration. Two day old zebrafish regenerate their amputated caudal fins within 3 days. Here we demonstrate that TCDD specifically blocks regenerative growth in larvae. The AHR pathway in zebrafish is considerably more complex than in mammals, with at least three zebrafish AHR genes (zfAHR1a, zfAHR1b and zfAHR2), and two ARNT genes (zfARNT1 and zfARNT2). Although it was presumed that the block in regeneration was mediated by AHR activation, it had not been experimentally demonstrated. Using antisense morpholinos and mutant fish lines, we report that zfAHR2 and zfARNT1 are the *in vivo* dimerization partners that are required for inhibition of regeneration by TCDD. Several pathways including FGF signaling are essential for fin regeneration. Even though impaired FGF signaling and TCDD exposure both inhibit fin regeneration, their morphometric response are distinct suggesting that the mechanisms of impairment are different. With the plethora of molecular and genetic techniques that can be applied to larval stage embryos, this *in vivo* regeneration system can be further exploited to understand cross talk between AHR and other signaling pathways.

Introduction

2,3,7,8-Tetrachlorodibenzo-*p*-dioxin (TCDD), an ubiquitous environmental contaminant causes a wide variety of toxicities including reproductive and developmental toxicity, immunotoxicity, cardiotoxicity, teratogenicity and neurotoxicity at low exposure levels. TCDD elicits toxicity by acting as a ligand for the aryl hydrocarbon receptor (AHR), [reviewed in (Schmidt and Bradfield, 1996)]. The AHR pathway has been studied in various disparate vertebrates including several species of fish. The AHR signal transduction pathway in fish species is akin to that of mammals except fish possess at least two AHR genes while the mammals have only one. AHR isoforms are designated as AHR1, and AHR2 (Hahn et al., 1997). zfAHR1a, zfAHR1b and zfAHR2 have been identified in zebrafish (Andreasen et al., 2002a; Karchner et al., 2005; Tanguay et al., 1999). *In vivo* antisense knockdown studies in zebrafish embryos have established that zfAHR2, and not zfAHR1, mediates the multiple end points of TCDD developmental toxicity in zebrafish (Prasch et al., 2003). Four splice variants of zfARNT2 denoted as zfARNT2a, b, c, x have been cloned and characterized (Tanguay et al., 2000; Wang, 2000). *In vitro* molecular and biochemical studies suggest that zfARNT2b functionally heterodimerizes with zfAHR2 to enhance the dioxin response element (DRE) driven transcription in the presence of TCDD (Tanguay et al., 1999; Tanguay et al., 2000). However, neither morpholino knockdown of zfARNT2 in zebrafish embryo, nor zebrafish ARNT2 mutants (*zfarnt2*$^{-/-}$) prevented TCDD mediated developmental toxicity (Prasch et al., 2004). This contradiction led to further investigation and identification of zebrafish ARNT1. Functional characterization by morpholino approach delineated that zfARNT1 is the functional heterodimer of zfAHR2 in zebrafish (Prasch et al., In Press).

Although AHR-driven transcriptional regulation has been extensively studied, the mechanism by which TCDD causes toxicity is not fully understood. The development of *in vivo* models to explore the complexity of AHR signal transduction is essential. Adult zebrafish have the remarkable capacity to regenerate their caudal fins completely within fourteen days after amputation (Geraudie et al., 1995) and it was previously demonstrated that TCDD inhibits this complex process (Zodrow and Tanguay, 2003). Recently it was

reported that the caudal fin primordia of zebrafish larvae are also capable of tissue regeneration in a process remarkably similar to that observed in adults (Kawakami et al., 2004). In the larval fin, within 10 min of amputation, epithelial cells surrounding the amputation plane begin migrate over the wound site. These epithelial cells accumulate to form a compact wound epithelium by 24 hours post amputation (hpa). Actively proliferating mesenchymal cells denoted as blastema cells are evident in the area adjacent to the amputation plane by 24-48 hpa. After blastema formation, both the adult and larval regenerating fins exhibit a common cell proliferation profile with the proliferation starting at the distal area (posterior to the amputation plane). The distal-most cells do not proliferate during the late phase of repair; instead, drastic cell proliferation occurs in the proximal (anterior to the amputation plane) region. In addition to the similar regenerative events between adults and larvae, fibroblast growth factor (FGF) signaling is necessary during fin regeneration suggesting a common regenerative molecular mechanism (Kawakami et al., 2004; Poss et al., 2000b).

Studies in adult fin regeneration were limited by barriers in molecular and genetic techniques which motivated us to develop a larval model to evaluate the consequence of AHR activation on early life stage regeneration. The objectives of this study were to first determine whether TCDD impairs larval fin regeneration, and then to determine which AHR pathway members mediate the response. Our observations demonstrate that TCDD specifically impedes larval fin regeneration. Activation of the AHR pathway was confirmed by immunohistochemical localization of induced cytochrome P4501A (zfCYP1A), a well studied AHR responsive gene. Antisense knockdown and mutant zebrafish lines demonstrate that zfAHR2 and zARNT1 are both required for the TCDD dependent block in regenerative growth. We also demonstrate that the inhibitory effects of TCDD exposure and FGF receptor antagonism on regeneration are distinct**.** In addition to the inherent advantages of zebrafish (i.e. rapid development and fecundity) the larval zebrafish model allows the use of many additional molecular and genetic techniques, such as transient and stable transgenics, mutant screens and antisense gene repression. Thus the larval zebrafish is an outstanding model to unravel tissue regeneration mechanisms.

Materials and Methods

Zebrafish lines and embryos

Fertilized AB strain embryos (University of Oregon, Eugene, OR) were used for all the experiments. *zfarnt2*$^{-/-}$ mutants (ARNT2 ^{hi1715}) in the TAB-14 background (Tubingen/AB cross no.14) was a gift of Nancy Hopkins (Center for Cancer Research and Department of Biology, Massachusetts Institute of Technology, Cambridge, MA). All embryos were raised in our laboratory according to standard procedures. Each experimental group consisted of 12 larvae.

Amputation of zebrafish larval fin primordia and chemical exposure

Embryos were dechorionated and anesthetized with 0.008% 3-amino benzoic acid ethylester (tricaine) in fish water. At 48 hours post fertilization (hpf), larvae were placed on an agar plate and the caudal fin primordia was amputated with a surgical razor blade just posterior to the notochord and transferred to a 24 well plate containing chemical free fish water. 2,3,7,8-Tetrachlorodibenzo-*p*-dioxin (TCDD)(>99% pure) was purchased from Chemsyn (Lenexa, KS); β-naphthoflavone (BNF, >99% pure) was obtained from Acros Organics (Morris Plains, NJ) and α-naphthoflavone (ANF) from Sigma, (St.Louis, MO). The amputated larvae (48 hpf) were exposed to vehicle (0.3% DMSO) or TCDD in vehicle (0.5 ng/mL of fish water) in a 24 well plate for 1 hr. After incubation, the embryos were rinsed multiple times and allowed to develop for 3 days in vehicle/TCDD-free water at 27^0C. Since BNF and ANF (both 0.3 μg/mL) were not soluble in DMSO, these ligands were dissolved in dimethyl formamide (DMF). ANF and BNF exposures were conducted in 24 well plates for 24 hours, followed by multiple rinses in water. After exposure to ANF and BNF, the larvae were reared for 3 days at 27^0C in ANF and BNF free water. The FGFR1 inhibitor (SU5402) was purchased from Calbiohem (SanDiego, CA). The amputated larvae were exposed to SU5402 at a final concentration of 5μM for 1 day, followed by multiple rinses with fish water.

Reverse Transcription Polymerase Chain Reaction (RT-PCR)

The caudal fin primordia of 48 hpf larvae were amputated and the animals were exposed to vehicle or TCDD in vehicle (0.5 ng/mL of fish water) for 1 h. After multiple rinses in TCDD free water, the embryos were reared at 27^0C. Regenerating fins were surgically amputated again at 3 dpa just posterior to the notochord. The amputated regenerating fins were directly immersed into TRI reagent (Molecular Research Laboratories, Cincinnati, OH) and RNA was isolated as previously described (Tanguay et al., 1999). Reverse transcription (RT) reactions were carried out using 100 ng of total RNA, 500 ng Oligo dT_{12-18} primer, 1mM dNTPs. The mixture was heated up to 65°C for 5 min and quick chilled on ice. The 20 µl reaction contained 1X First Strand Buffer (50 mM Tris-HCl (pH 8.3), 75 mM KCl, 3 mM $MgCl_2$), 0.01 M DTT, 40 units of RNaseOUT, and 200 units of SuperScript™ II Reverse Transcriptase (Invitrogen, Carlsbad, California). This reaction was incubated at 42°C for 50 min, followed by inactivation at 70°C for 15 min. Each 50 µl PCR reaction contained a 2 µl aliquot of cDNA as the template, 0.2 mM each dNTPs, 10X PCR Buffer, 1 mM $MgSO_4$, 0.2 µM forward and reverse primers for either AHR1, AHR2, ARNT1, ARNT2b/c, CYP1A, or β-actin (Table 1) and 1.0 unit of KOD Hot Start DNA polymerase (Novagen, San Diego, CA). The reactions were run in a PTC-100 Peltier thermal cycler (MJ Research, South San Francisco, CA) at the following conditions: 94°C for 20 s; 58°C for 30 s, 72°C for 80 s, for a total of 35 cycles. The PCR products were resolved by electrophoresis through a 2% agarose gel and visualized by ethidium bromide staining.

Morpholinos

Zebrafish aryl hydrocarbon receptor 2 morpholino (*zfahr*2-MO) (Gene Tools, Corvallis, OR) targeted the translation start site beginning 4 bp upstream of the AUG codon to 18 bp downstream of the sequence. The sequence of the *zfahr2*-MO was 5'TGTACCGATACCCGCCGACATGGTT3' and the 3' end was fluorescein tagged to assess microinjection success. Morpholinos were diluted to 2.8 mM in 1X Danieau's solution (58 mM NaCl, 0.7 mM KCl, 0.4 mM $MgSO_4$, 0.6 mM $Ca(NO_3)_2$, 5 mM HEPES, pH 7.6) as described (Nasevicius and Ekker, 2000). Zebrafish aryl hydrocarbon receptor nuclear translocator 1 morpholino (*zfarnt1*-MO)

(5'CTCTTACCTCAGTTACAATTTATA3') overlapped the translation start site of zfARNT1 mRNA, starting 4 bp upstream of the AUG start codon to 17 bp downstream of the sequence. The morpholinos were diluted to 1.5 mM in 1x Danieau's solution prior to microinjection. A standard control morpholino (Gene Tools, Corvallis, OR) (5'CTCTTACCTCAGTTACAATTTATA 3') was used as a control morpholino (Control-MO). The embryos were injected at the 1–2 cell stage with approximately 1-3 nl of the appropriate morpholino solution. Embryos were screened for fluorescence at 24 hpf to reveal successful injection. The caudal fin of selected embryos were amputated and exposed to TCDD or vehicle for 1 hour at 48 hpf. The morpholino injected embryos (morphants) were raised for 3 days following amputation and the regeneration of fin tissue was observed.

Genotyping of *zfarnt2* mutants

Embryonic DNA was extracted from individual embryos in extraction buffer (0.01 M Tris, 2 mM EDTA, 0.2% Triton-X, 0.2 mg/ml Proteinase-K) incubated at 55°C for 2.5 h. The extract was heated at 100°C for 10 min before centrifugation and the supernatant was used as the DNA template for PCR. The primers used were zfARNT2F1, zfARNT2R1 and TranspoR. zfARNT2F1 and zfARNT2R1 flank the knockout viral insertion and TranspoR lies within the transposon insert. zfARNT2F1and zfARNT2R1 were designed to distinguish *zfarnt2*$^{-/-}$ mutants from wild type (WT) and from heterozygous (HET) larvae, while zfARNT2F1 and TranspoR were used to distinguish WT from HET larvae. PCR was performed to amplify the appropriate sequence using KOD Hot Start DNA polymerase and the PCR products were examined by gel electrophoresis and ethidium bromide staining.

Whole mount immunolocalization of zfCYP1A and α-acetylated tubulin

The distribution of zfCYP1A protein in zebrafish larval fin tissue was assessed using the monoclonal antibody, C107 (mouse anti-CYP1A, 1:500; Biosense Laboratories, Bergen, Norway). Monoclonal antibodies generated against acetylated tubulin (mouse anti-AT, 1:1000; Sigma, St. Louis) label most axons and major peripheral processes in the developing embryo. On 3 dpa, TCDD exposed and control larvae were fixed

overnight in 4% paraformaldehyde in phosphate-buffered saline (PBS) and washed in PBS + 0.1% Tween-20 (PBST). The larvae were permeablized with 0.005% trypsin (4°C) in PBS on ice for 5 minutes, rinsed in PBST and postfixed in 4% paraformaldehyde. Permeablized larvae were blocked in 10% normal goat serum (NGS) in PBS + 0.5% Triton X-100 (PBSTx) for an hour at 22°C and incubated with the primary antibody overnight at 4°C in 1% NGS- PBSTx. Following 4x 30 min washes in PBST, the larvae were incubated with a secondary antibody (1:1000)(Alexa-546 conjugated goat anti mouse; Molecular Probes, Eugene, OR) for 5 h at 22°C. The larvae were then washed 4x for 30 min in PBST and visualized by epifluorescence microscopy.

Statistical Analysis

Each experiment comprised of 12 larvae per group. The larvae were exposed to vehicle or chemical with 2 larvae in each well. Significant difference in the area and length between the control and TCDD exposed animals was assessed by Students t-test ($p<0.05$) using SigmaStat 2.03 software.

Results

TCDD Inhibits Larval Zebrafish Caudal Fin Regeneration

Larval zebrafish caudal fin primordia have the remarkable ability to regenerate by a mechanism similar to that observed in adult fin regeneration (Kawakami et al., 2004). These studies were designed to determine if AHR activation would impact larval fin regeneration similar to adult zebrafish (Zodrow and Tanguay, 2003). The caudal fin primordia of the 48 hpf larvae were partially amputated just posterior to the notochord (Fig. 1). A range of TCDD concentrations was used (0.01 ng to 1 ng/mL) to determine the sublethal concentration that inhibits fin regeneration (data not shown). From these initial dose response studies, 0.5 ng/mL of TCDD was determined as the most effective concentration that impairs fin regeneration without causing mortality prior to 120 hpf, and was used for all of the described studies. The amputated larvae were exposed to

DMSO or TCDD and allowed to develop for 3 days. Zebrafish exposed to vehicle, regenerated their fin tissue in 3 days, while the process of regeneration was impaired in animals exposed to TCDD (Fig. 1). Although not the focus of these studies, exposed larvae also developed the typical TCDD toxicological signs including pericardial edema, yolk sac edema, reduced blood flow, impairment of the swim bladder (Henry et al., 1997; Prasch et al., 2004) at 3 dpa. This study suggests that larval and adult fin regeneration may be impaired by TCDD potentially through a common molecular mechanism. Importantly, these results allow full exploitation of the larval zebrafish model to elucidate the role of AHR activation and tissue regeneration.

Inhibition of Fin Growth by TCDD is Specific to the Regenerated Tissue

To determine if the effects of TCDD are specific to the regenerating fin, we performed partial fin amputations. The ventral halves of the caudal fins were amputated leaving the dorsal half of the developing fin intact to serve as a control and the larvae were exposed to vehicle or TCDD (Fig. 2). Images were taken immediately after partial amputation (0 dpa) and three days later (3 dpa). In the presence of vehicle, embryos completely regenerate their fins in 3 days. However, fin regeneration was significantly inhibited by TCDD (Fig. 2). Even though TCDD exposed larvae displayed classic signs of toxicity and regeneration of the ventral portion of the fin was inhibited, growth of the non-amputated dorsal half of fin was not affected (Fig.2). This suggests that AHR activation specifically interferes with the regenerative process and not just growth.

In order to quantify the growth response, the length of maximum outgrowth, the area of regenerated fin tissue (%) and the area of non-amputated fin tissue (%) were measured as depicted in the schematic diagram (Fig. 3A). The length of maximum outgrowth is defined as the distance from the plane of amputation to the tip of the regenerating fin. The area of regenerated fin tissue represents the newly grown ventral fin tissue after partial amputation. The area of the intact dorsal half of the fin was used to determine whether TCDD impacts non-regenerative fin development. The length of maximum outgrowth and the area of regenerated fin tissue (%) in TCDD exposed larvae were significantly lower when compared to the control larvae (Fig. 3B, C). Surprisingly, the increase in the area of non-amputated fin tissue (%) from 0-3 dpa in TCDD exposed

larvae was significantly greater than the control larvae (Fig. 3D). Together, these results establish that TCDD specifically inhibits the growth of the regenerating tissue. It is also important to emphasize that normal fin development and growth are not impeded by TCDD unless the fin is amputated.

Detection of AHR Pathway Members in the Regenerating Fin Tissue

To determine the expression profile of AHR members and regulated genes in the larval regenerating fin tissue, RNA was isolated from the regenerating fin tissue of DMSO or TCDD exposed larvae at 3 dpa. RT-PCR was performed using gene-specific primers for zfAHR1, zfAHR2, zfARNT1, zfARNT2b/c, zfCYP1A and β-actin as a control. The transcripts of *zfahr1, zfahr2, zfarnt1 and zfcyp1a* were expressed in both DMSO and TCDD exposed larval regenerating fin tissue, but the expression of *zfarnt2b/c* was faint (Fig. 4). Even though this method is non quantitative, *zfcyp1a* transcript level observed in the TCDD exposed fin tissue was apparently increased over DMSO levels suggesting that AHR pathway is active in regenerating fin tissue.

Whole Mount Immunolocalization of zfCYP1A

A common biomarker to evaluate the activation of AHR pathway by TCDD is to observe CYP1A expression. The temporal and spatial pattern is often associated with the toxicity (Andreasen et al., 2002b; Henry et al., 1997; Tanguay et al., 1999). Immunohistochemical staining of zfCYP1A protein was conducted with larvae exposed to vehicle or TCDD at 48 hpf. Specific immunolocalization of zfCYP1A was detected in the fin tissue of the TCDD exposed larvae, but was not observed in the control larvae (Fig. 5). zfCYP1A was consistently abundant at the distal tip of the caudal fin. TCDD induced expression of CYP1A in the intersegmental vessels (SE) was used to ensure the positive detection of zfCYP1A between the TCDD and vehicle exposed larvae (Fig.5). Elevated expression of zfCYP1A protein in the fin tissue of TCDD exposed larvae confirms that AHR pathway is activated

BNF, another AHR2 Ligand Inhibits Regeneration

To further test the hypothesis that TCDD blocks regeneration by inappropriately activating the AHR pathway, BNF was used as an alternative AHR ligand. BNF has been shown to bind and activate the zebrafish AHR2 (Wentworth et al., 2004). When amputated larvae were exposed to BNF (0.3μg/mL), regeneration was completely blocked as we observed in larvae exposed to TCDD. However, when zebrafish were exposed to the AHR2 antagonist, ANF (0.3 μg/mL) or vehicle, regeneration progressed and was completed in three days (Fig. 6). These results strongly suggest that ligand activation of AHR2 is necessary to block the regenerative process.

AHR2 is Necessary for TCDD to Impede Fin Regeneration

With the availability of the nearly complete zebrafish genomic sequence and the ability to use antisense modified oligonucleotides (morpholinos), the role of any protein in a biological process can be rapidly evaluated *in vivo* using zebrafish embryos or larvae (Nasevicius and Ekker, 2000). Morpholinos have been shown to be most effective between 0 and 96 hpf. Higher concentrations of morpholino (2.8 mM) can be used to prolong the repression of target genes up to 120 hpf (data not shown). The zfAHR2 and control morphants were amputated and exposed to vehicle or TCDD at 48 hpf and raised for 3 days. The control and zfAHR2 morphants exposed to vehicle regenerated completely indicating that the endogenous functions of zfAHR2 are not required for regeneration. As expected, the control morphants exposed to TCDD failed to regenerate (Fig. 7A). The caudal fins in zfAHR2 morphant animals exposed to TCDD were capable of complete regeneration indicating that inhibition of fin regeneration by TCDD is mediated through zfAHR2 (Fig. 7A). In other words, in the absence of zfAHR2, TCDD has no effect on tissue regeneration. Importantly, the zfAHR2 morphants also failed to develop other signs of TCDD toxicity including pericardia edema, yolk sac edema, reduced blood flow as previously detailed (Prasch et al., 2003). Immunohistochemical analysis was performed on the control and zfAHR2 morphants exposed to vehicle and TCDD to monitor *in situ* zfCYP1A protein expression. zfCYP1A was not detected in either control or zfAHR2 morphants exposed to vehicle (data not shown). Control morphants had significant vascular and extravascular zfCYP1A expression, and in

zfAHR2 morphants, zfCYP1A protein was not detected indicating complete and persistent knockdown of AHR2 (Fig. 7B). These results confirm that AHR pathway cannot be activated by TCDD in the absence of AHR2.

ARNT1, Not ARNT2 is Required for Inhibition of Fin Regeneration by TCDD

Since there are at least two ARNT genes expressed in the early embryo, zfARNT1 and zfARNT2, it was important to determine which ARNT is the *in vivo* partner for zfAHR2 that is necessary to block tissue regeneration. A genetic approach was used to specifically evaluate the role of zfARNT2. Insertional mutagenesis screens had previously identified zebrafish mutants that lacked ARNT2 expression (Amsterdam et al., 1999). These mutants were generously provided by Dr. Nancy Hopkins (Massachusetts Institute of Technology, Cambridge, MA). Embryos collected from *zfarnt2*$^{+/-}$ (HET) parents were raised to 48 hpf and 40 larvae were amputated and exposed to TCDD**.** In this pool of larvae, 25% should be *zfarnt2*$^{+/+}$ (WT), 50% should be *zfarnt2*$^{+/-}$ (HET) and 25% should be *zfarnt2*$^{-/-}$ mutants. TCDD completely inhibited the fin regeneration in all the larvae, irrespective of the ARNT2 genetic status (Fig. 8A). Genotyping of individual larvae were conducted with PCR to determine the larval genetic makeup (Fig. 8A).

To determine the role of zfARNT1 in fin regeneration, morpholinos were used to knockdown early life stage zfARNT1 protein expression. Control and zfARNT1 morphants were amputated at 48 hpf, followed by a waterborne exposure to vehicle or TCDD. The amputated larvae were allowed to regenerate their fins for 3 days. The control morphants exposed to TCDD displayed impaired fin regeneration, while the zfARNT1 morphants were able to completely regenerate their fins in the presence of TCDD (Fig. 8C). *In situ* immunolocalization of zfCYP1A protein confirms that zfCYP1A is highly induced in control morphants exposed to TCDD, while the zfARNT1 morphants had a significant decrease in the CYP1A expression (Fig. 8D). Together these results indicate that ARNT1 is a necessary *in vivo* dimerization partner for AHR2, which together, initiate a process that inhibits tissue regeneration.

Morphometrically, TCDD and FGFR1-mediated inhibition of fin regeneration are different

It is clear that AHR activation impairs or interferes with signaling pathways required for tissue regeneration, but these downstream targets remain unknown. To begin to understand the underlying cellular responses, the effects of TCDD were compared to the effects of another chemical known to impact regeneration. Inhibition of fibroblast growth factor receptor 1 (FGFR1) by a lipophilic drug (SU5402) has been shown to inhibit both adult and larval fin regeneration (Kawakami et al., 2004; Poss et al., 2000b). At the gross level, SU5402 inhibited fin regeneration, but to a lesser extent than TCDD (Fig. 9A, B). Importantly, over the course of the regeneration period (3 days), SU5402 had a significant reduction in the overall embryonic and larval growth, whereas TCDD had no measurable effect on overall growth during this developmental window (data not shown). During regeneration, neuronal axons and their peripheral processes grow and extend into the newly formed tissue (Tanguay, unpublished observation). The growth and pathfinding of these structures can be used to assess tissue reorganization. *In situ* immunolocalization using an α-acetylated tubulin antibody is a convenient way to label the axons and their peripheral processes. In the control larvae, the peripheral processes branch off the axonal trunks and fan out into the regenerate. After 3 days, a complex, but ordered network of branches is formed in the new tissue (Fig. 9C). In the TCDD exposed animals, the peripheral processes consistently extended toward the amputation plane, and then made lateral turns, nearly perpendicular to the plane of amputation. Importantly, the branches continued to extend in the presence of TCDD, but the pathfinding is altered. These observations are consistent with the concept that that TCDD impairs the ability of the neuronal processes to migrate directly into the tissue (Fig. 9C, D). Further illustration of this point is revealed when only the ventral half of the fin is amputated (Fig. 9E). TCDD consistently lead to an altered neuronal growth pattern where the new processes in the partially amputated fin continued to grow, but made lateral turns in the absence of sufficient new tissue to accommodate their length. These results suggest that, in TCDD exposed larvae, the peripheral processes in the regenerating fin maybe incapable of growing straight due to a physical barrier or improper growth factor signaling. The neuronal response in SU5402 exposed larvae was noticeably different. The pathfinding of the neuronal branches was not affected. The processes reached the end of the new tissue

and had a branching pattern indistinguishable from that in control animals (Fig.9E). Taken together, these results suggest that the inhibition of regeneration mediated by TCDD and FGFR1 inhibitor is different.

Discussion

Regeneration of tissue is a well orchestrated process where the injured or lost structure is completely replaced. In both adult and larval zebrafish, an epithelial wound covering is formed within 12hpa and this response does not involve cell proliferation (Nechiporuk and Keating, 2002; Santamaria et al., 1996). Wound closure is followed by the development of blastema and the wound epidermis is hypothesized to be a source of growth factors that stimulate and regulate the formation of the blastema. In adult zebrafish, fibroblast growth factors (FGFs) present in the wound epidermis interacts with the mesenchymal FGFR1. FFGR1 inhibitor studies suggest that active FGF signaling is required for the formation of blastema and regenerative outgrowth (Poss et al., 2000b). The differential expression of *mps1, shh, lef1, wnt3a, wnt5, RAR-γ* and *msx* homeobox genes illustrates the complexity of signaling pathways during the regeneration process (Akimenko et al., 1995; Poss et al., 2000a; Poss et al., 2000b; White et al., 1994). During regenerative outgrowth, cell proliferation propagates from distal zone to the proximal zone of fin primordia with intense proliferation occurring in the proximal region during the late phase of repair (Kawakami et al., 2004; Nechiporuk and Keating, 2002). In larvae, fin regeneration is completed in 3-5 days by controlled cellular proliferation and migration. It has been established that TCDD impairs the outgrowth phase of regeneration (Zodrow and Tanguay, 2003). Although it had been presumed that the block in regeneration is mediated by TCDD binding and activation of AHR signaling pathway, it had not been experimentally demonstrated.

In mammals, studies have demonstrated that *Ahr* null mice develop hepatic defects and have reduced liver size implicating a role of AHR in normal liver growth and development (Lahvis et al., 2000 ; Schmidt and Bradfield, 1996). The underlying deficit

appears to be a congenital vascular defect, failure of ductus venosus closure (Walisser et al., 2004). In addition to this endogenous developmental role, functional AHR is required to mediate TCDD toxicity (Gonzalez and Fernandez-Salguero, 1998; Mimura et al., 1999). Both zfAHR1 and zfAHR2 were present in the regenerating fin of vehicle and TCDD exposed larvae (Fig. 4). Previous studies have reported that zfAHR1 does not mediate TCDD toxicity as it does not bind to AHR ligands and has a very limited tissue distribution (Andreasen et al., 2002a). Knockdown of zfAHR2 by antisense morpholinos revealed that zfAHR2 mediates the endpoints of TCDD dependent developmental toxicity (Prasch et al., 2003). zfAHR2 morphants regenerated the fin tissue completely in the presence of TCDD confirming that AHR2 is necessary for TCDD to block fin regeneration. Recently, a third AHR gene was identified in zebrafish which is located adjacent to the AHR2 gene in the zebrafish genome. This duplicated gene was designated as AHR1b. *In vitro* studies indicate that AHR1b has AHR-like properties (Karchner et al., 2005). The AHR2 morpholino studies demonstrate that AHR1b cannot play a role in mediating the well-studied *in vivo* responses to TCDD. The endogenous role for AHR1b remains to be identified.

In mammals, ARNT1 is the functional dimerization partner for AHR mediating many endpoints of TCDD toxicity (Schmidt and Bradfield, 1996). *arnt2* knockout mice die within 24h of birth and have impaired hypothalamic development, confirming its function during normal development (Hosoya et al., 2001). In zebrafish, four splice variants of zfARNT2 have been characterized and zfARNT2b has been demonstrated to be transcriptionally active with zfAHR2 *in vitro* (Tanguay et al., 2000). Unexpectedly, antisense repression of ARNT2 did not impact embryonic responses to TCDD. Similar results were obtained in zebrafish *arnt2* mutants. Collectively, these results confirm that zfARNT2 is not the *in vivo* partner of zfAHR2 mediating the developmental toxicity by TCDD (Prasch et al., 2004). zfARNT1 was recently characterized in zebrafish (Prasch et al., In Press). In regenerating larval fin, zfARNT1 was highly abundant in both vehicle and TCDD exposed larvae, while the expression of zfARNT2 was low. Fin regeneration in ARNT2$^{-/-}$ was impaired when exposed to TCDD, while the zfARNT1 morphants completely regenerated, confirming that zfANRT1 is the heterodimer of zfAHR2.

Since TCDD inhibits adult zebrafish fin regeneration when dosed on either 0, 1, 2,

3, or 4 dpa, this suggests that TCDD interferes with multiple stages of regeneration (Zodrow and Tanguay, 2003). Similar results were found in larvae. When larvae were exposed to TCDD at 1 dpa, fin regeneration was also impaired (data not shown). Importantly, since wound healing and blastema formation occur in the first day, regenerative outgrowth may be the TCDD target.

Pharmacologic inhibition of FGFR1 inhibits blastema formation as well as outgrowth indicating that FGF signaling is required during fin regeneration (Kawakami et al., 2004; Poss et al., 2000b). Although FGFR1 inhibitor effectively reduced regenerative outgrowth, overall embryonic growth was also affected. Both FGFR1 inhibitor and TCDD impaired fin regeneration, but the tissue response to these chemicals was different. Using neuronal outgrowth as a marker, TCDD led to a significant disorganization of peripheral processes. Since matrix degradation and turnover are important in wound healing, tissue remodeling, tissue repair and inflammation, one possibility is that the extracellular matrix (ECM) metabolism is affected by TCDD. Matrix metalloproteinases (MMPs) are considered to be primarily responsible for the turnover of ECM. These proteolytic enzymes play a major role during development and morphogenesis. Improper regulation of these proteinases may result in pathologies such as arthritis, cancer, atherosclerosis, aneurysms, tissue ulcers and fibrosis (Visse and Nagase, 2003). It has also been reported that, after CNS injury, the optic nerve astrocytes are stimulated by regenerating axons by secreting active MMP and down regulating tissue inhibitors of metalloproteinases (TIMPs), resulting in the degradation of scar tissue creating a permissive growth environment (Ahmed et al., 2005). Tenascin-R, a glycoprotein deposited into the ECM acts as a repellant guidance molecule in boundaries during normal growth and regeneration of optical axons (Becker et al., 2004), clearly demonstrating that ECM components play critical roles in axonal guidance. We therefore propose that if matrix remodeling is impaired by TCDD, the neuronal growth cone may be unable to traverse through the matrix, resulting in abnormal pathfinding.

ECM is a dynamic environment that plays a crucial role in regulating cellular functions during normal and pathological remodeling processes such as embryonic development, tissue repair, inflammation, tumor invasion, and metastasis. ECM macromolecules are critical for creating a conducive cellular milieu for proper

proliferation and migration of different cell types. The MMPs are specifically controlled at the transcriptional level, activation of precursor zymogens, cell-ECM interactions and inhibition by endogenous TIMPs (Nagase and Woessner, 1999). The expression and functional role of MMPs has been studied in adult zebrafish regenerating fin, and have demonstrated that *membrane type mmp, mmp-2* and *timp-2* mRNA transcripts were expressed in the regenerating fin tissue. Fin outgrowth was significantly reduced by GM6001, a MMP inhibitor, emphasizing the magnitude of these proteinases during fin regeneration (Bai et al., 2005). Similarly, MMP inhibitor studies demonstrate that these enzymes are required for normal newt limb regeneration and *mmp3/10a, mmp3/10b* and *mmp-9* are upregulated within hours of limb amputation. The temporal expression of MMPs in the regenerating newt limb suggests that these enzymes are involved in blastema formation, maintenance and growth (Vinarsky et al., 2005). Interestingly, aryl hydrocarbons such as TCDD and Benzo (a) pyrene induced the expression of MMP-9 in PC-3 and DU145 human prostrate cancer cells (Haque et al., 2005). TCDD increased the expression and activity of MMP-1, MMP-2 and MMP-9 in transformed melanoma cell (A2058), as well as increased invasion (Villano et al., 2005). Gene expression in the fetal murine heart after TCDD exposure *in utero* suggest possible alterations in cell cycle control and ECM production and remodeling (Thackaberry et al., 2005). Furthermore, TCCD enhanced expression of MMP-1, 9 and TIMP-3 in lung airway epithelial cells by microarray analysis, implying that MMP expression maybe a common endpoint for AHR pathway activation (Martinez et al., 2002). In normal human keratinocytes, TCDD induces MMP-1 expression and co-treatment with all trans retinoic acid enhanced the MMP-1 expression additively (Murphy et al., 2004), suggesting the cross talk of AHR pathway with other signaling pathways. These studies correlate with the finding that ECM remodeling is impaired in the regenerating fins of TCDD exposed adult zebrafish (E. Andreasen, personal communication).

In summary, our data provide evidence that activation of AHR pathway inhibits larval zebrafish fin regeneration. The inhibition of fin regeneration is mediated by TCDD activation of zfAHR2 and its *in vivo* dimerization with zfARNT1. Preliminary data and the supporting literature point to an association between AHR pathway activation and impaired extracellular tissue remodeling. The interactions between cells and ECM are

tightly controlled by membrane proteins, proteolytic enzymes, cytokines and growth factors during numerous physiological processes as well as during regeneration. Inappropriate expression or activity of any of the factors can mediate a variety of pathologies such as tumor metastasis, cardiovascular disease or toxicity. The larval fin regeneration model presented herein can be exploited to unravel the cross talk between AHR activated and other critical signaling pathways.

References

Ahmed Z, Dent RG, Leadbeater WE, Smith C, Berry M and Logan A (2005) Matrix metalloproteases: degradation of the inhibitory environment of the transected optic nerve and the scar by regenerating axons. *Mol Cell Neurosci* **28**:64-78.

Akimenko MA, Johnson SL, Westerfield M and Ekker M (1995) Differential induction of four msx homeobox genes during fin development and regeneration in zebrafish. *Development* **121**:347-57.

Amsterdam A, Burgess S, Golling G, Chen W, Sun Z, Townsend K, Farrington S, Haldi M and Hopkins N (1999) A large-scale insertional mutagenesis screen in zebrafish. *Genes Dev* **13**:2713-2724.

Andreasen EA, Hahn ME, Heideman W, Peterson RE and Tanguay RL (2002a) The zebrafish (*Danio rerio*) aryl hydrocarbon receptor type 1 (zfAHR1) is a novel vertebrate receptor. *Mol Pharmacol* **62**:234-249.

Andreasen EA, Spitsbergen JM, Tanguay RL, Stegeman JJ, Heideman W and Peterson RE (2002b) Tissue-specific expression of AHR2, ARNT2, and CYP1A in zebrafish embryos and larvae: effects of developmental stage and 2,3,7,8-tetrachlorodibenzo-*p*-dioxin exposure. *Tox Sci* **68**:403-419.

Bai S, Thummel R, Godwin AR, Nagase H, Itoh Y, Li L, Evans R, McDermott J, Seiki M and Sarras MP, Jr. (2005) Matrix metalloproteinase expression and function during fin regeneration in zebrafish: analysis of MT1-MMP, MMP2 and TIMP2. *Matrix Biol* **24**:247-60.

Becker CG, Schweitzer J, Feldner J, Schachner M and Becker T (2004) Tenascin-R as a repellent guidance molecule for newly growing and regenerating optic axons in adult zebrafish. *Mol Cell Neurosci* **26**:376-89.

Geraudie J, Monnot MJ, Brulfert A and Ferretti P (1995) Caudal fin regeneration in wild type and long-fin mutant zebrafish is affected by retinoic acid. *Int J Dev Biol* **39**:373-81.

Gonzalez FJ and Fernandez-Salguero P (1998) The aryl hydrocarbon receptor: studies using the AHR-null mice. *Drug Metab Dispos* **26**:1194-8.

Hahn ME, Karchner SI, Shapiro MA and Perera SA (1997) Molecular evolution of two vertebrate aryl hydrocarbon (dioxin) receptors (AHR1 and AHR2) and the PAS family. *Proc Natl Acad Sci U S A* **94**:13743-8.

Haque M, Francis J and Sehgal I (2005) Aryl hydrocarbon exposure induces expression of MMP-9 in human prostate cancer cell lines. *Cancer Lett* **225**:159-66.

Henry EC, Kent TA and Gasiewicz TA (1997) DNA binding and transcriptional enhancement by purified TCDD.Ah receptor complex. *Arch Biochem Biophys* **339**:305-14.

Hosoya T, Oda Y, Takahashi S, Morita M, Kawauchi S, Ema M, Yamamoto M and Fujii-Kuriyama Y (2001) Defective development of secretory neurones in the hypothalamus of Arnt2-knockout mice. *Genes Cells* **6**:361-74.

Karchner SI, Franks DG and Hahn ME (2005) AHR1B, a new functional aryl hydrocarbon receptor in zebrafish: tandem arrangement of ahr1b and ahr2 genes. *Biochem. J.*

Kawakami A, Fukazawa T and Takeda H (2004) Early fin primordia of zebrafish larvae regenerate by a similar growth control mechanism with adult regeneration. *Dev Dyn* **231**:693-9.

Lahvis GP, Lindell SL, Thomas RS, McCuskey RS, Murphy C, Glover E, Bentz M, Southard J and Bradfield CA (2000) Portosystemic shunting and persistent fetal vascular structures in aryl hydrocarbon receptor-deficient mice. *Proc Natl Acad Sci U S A* **97**:10442-7.

Martinez JM, Afshari CA, Bushel PR, Masuda A, Takahashi T and Walker NJ (2002) Differential toxicogenomic responses to 2,3,7,8-tetrachlorodibenzo-p-dioxin in malignant and nonmalignant human airway epithelial cells. *Toxicol Sci* **69**:409-23.

Mimura J, Ema M, Sogawa K and Fujii-Kuriyama Y (1999) Identification of a novel mechanism of regulation of Ah (dioxin) receptor function. *Genes Dev* **13**:20-5.

Murphy KA, Villano CM, Dorn R and White LA (2004) Interaction between the aryl hydrocarbon receptor and retinoic acid pathways increases matrix metalloproteinase-1 expression in keratinocytes. *J Biol Chem* **279**:25284-93.

Nagase H and Woessner JF, Jr. (1999) Matrix metalloproteinases. *J Biol Chem* **274**:21491-4.

Nasevicius A and Ekker SC (2000) Effective targeted gene 'knockdown' in zebrafish. *Nat Genet* **26**:216-20.

Nechiporuk A and Keating MT (2002) A proliferation gradient between proximal and msxb-expressing distal blastema directs zebrafish fin regeneration. *Development* **129**:2607-17.

Poss KD, Shen J and Keating MT (2000a) Induction of lef1 during zebrafish fin regeneration. *Dev Dyn* **219**:282-6.

Poss KD, Shen J, Nechiporuk A, McMahon G, Thisse B, Thisse C and Keating MT (2000b) Roles for Fgf signaling during zebrafish fin regeneration. *Dev Biol* **222**:347-58.

Prasch AL, Heideman W and Peterson RE (2004) ARNT2 is not required for TCDD developmental toxicity in zebrafish. *Toxicol Sci* **82**:250-8.

Prasch AL, Tanguay RL, Mehta V, Heideman W and Peterson RE (In Press) Identification of zebrafish ARNT1 homologs: TCDD toxicity in the developing zebrafish requires ARNT1. *Mol Pharmacol*.

Prasch AL, Teraoka H, Carney SA, Dong W, Hiraga T, Stegeman JJ, Heideman W and Peterson RE (2003) Aryl Hydrocarbon Receptor 2 Mediates 2,3,7,8-Tetrachlorodibenzo-p-dioxin Developmental Toxicity in Zebrafish. *Toxicol Sci* **76**:138-50.

Santamaria JA, Mari-Beffa M, Santos-Ruiz L and Becerra J (1996) Incorporation of bromodeoxyuridine in regenerating fin tissue of the goldfish Carassius auratus. *J Exp Zool* **275**:300-7.

Schmidt JV and Bradfield CA (1996) Ah receptor signaling pathways. *Ann Rev Cell Dev Biol* **12**:55-89.

Tanguay RL, Abnet CC, Heideman W and Peterson RE (1999) Cloning and characterization of the zebrafish (*Danio rerio*) aryl hydrocarbon receptor. *Biochimica Biophys Acta* **1444**:35-48.

Tanguay RL, Andreasen EA, Heideman W and Peterson RE (2000) Identification and expression of alternatively spliced aryl hydrocarbon nuclear translocator2 (ARNT2) cDNAs from zebrafish with distinct functions. *Biochimica et Biophysica Acta* **1494**:117-128.

Thackaberry EA, Jiang Z, Johnson CD, Ramos KS and Walker MK (2005) Toxicogenomic Profile of 2,3,7,8-Tetrachlorodibenzo-p-dioxin in the Murine Fetal Heart: Modulation of Cell Cycle and Extracellular Matrix Genes. *Toxicol Sci*.

Villano CM, Murphy KA, Akintobi A and White LA (2005) 2,3,7,8-tetrachlorodibenzo-p-dioxin (TCDD) induces matrix metalloproteinase (MMP) expression and invasion in A2058 melanoma cells. *Toxicol Appl Pharmacol*.

Vinarsky V, Atkinson DL, Stevenson TJ, Keating MT and Odelberg SJ (2005) Normal newt limb regeneration requires matrix metalloproteinase function. *Dev Biol* **279**:86-98.

Visse R and Nagase H (2003) Matrix metalloproteinases and tissue inhibitors of metalloproteinases: structure, function, and biochemistry. *Circ Res* **92**:827-39.

Walisser JA, Bunger MK, Glover E and Bradfield CA (2004) Gestational exposure of Ahr and Arnt hypomorphs to dioxin rescues vascular development. *Proc Natl Acad Sci U S A* **101**:16677-82.

Wang WW, J. Hsu, H. Kong, Z. Hu,C. (2000) Overexpression of a zebrafish ARNT2-like factor represses CYP1A transcription in ZLE cells. *Marine Biotechnology* **2**:376-386.

Wentworth JN, Buzzeo R and Pollenz RS (2004) Functional characterization of aryl hydrocarbon receptor (zfAHR2) localization and degradation in zebrafish (Danio rerio). *Biochem Pharmacol* **67**:1363-72.

White JA, Boffa MB, Jones B and Petkovich M (1994) A zebrafish retinoic acid receptor expressed in the regenerating caudal fin. *Development* **120**:1861-72.

Zodrow JM and Tanguay RL (2003) 2,3,7,8-Tetrachlorodibenzo-*p*-dioxin inhibits fin regeneration in zebrafish. *Toxicological Sciences* **76**:151-161.

Acknowledgments

We thank Dr. Nancy Hopkins for the *arnt2* mutants and Fred Tilton, Dr. Stacey Harper and Dr. Mark Reimers for helpful discussions on the manuscript. This work was supported in part by NIEHS grants ES10820, ES00210, and ES0385

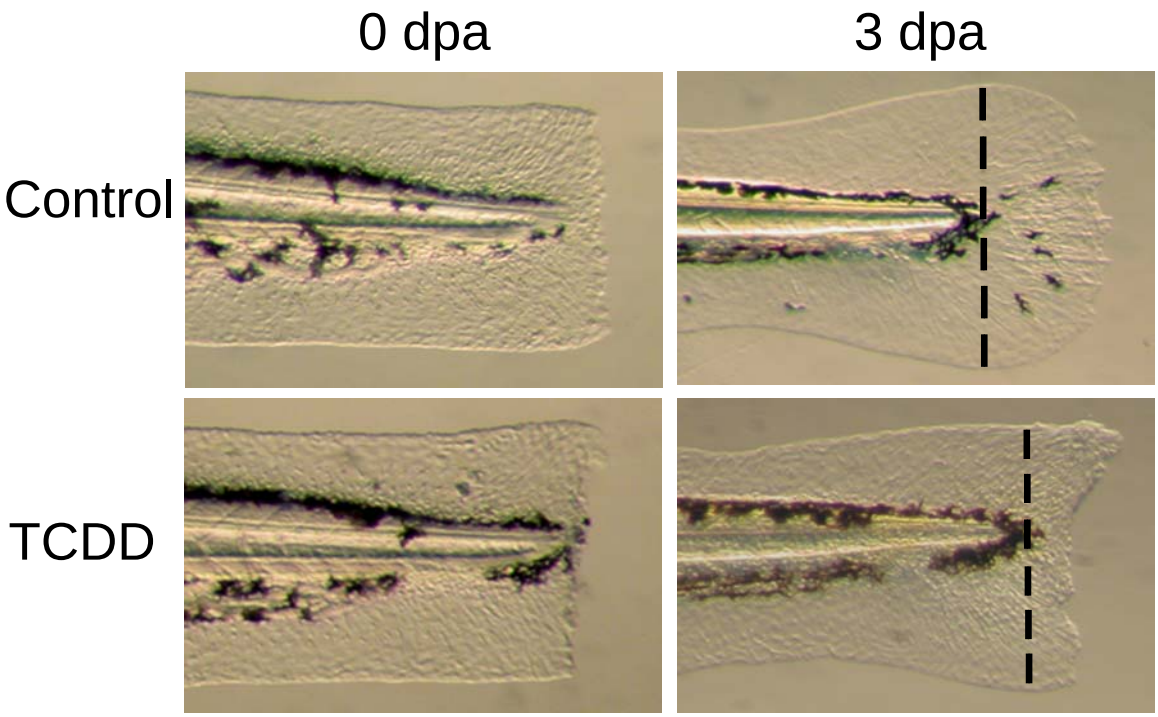

Figure 2-1. TCDD inhibits the regeneration of zebrafish fin primordia. The caudal fin primordia of zebrafish larvae (48 hpf) were surgically ablated just posterior to the notochord. Following amputation, larvae were exposed to TCDD (0.5 ng/mL) or vehicle control (DMSO). The fin regeneration images were captured immediately after amputation (0 dpa) on 3 dpa. The dotted line indicates the plane of amputation at 0 dpa.

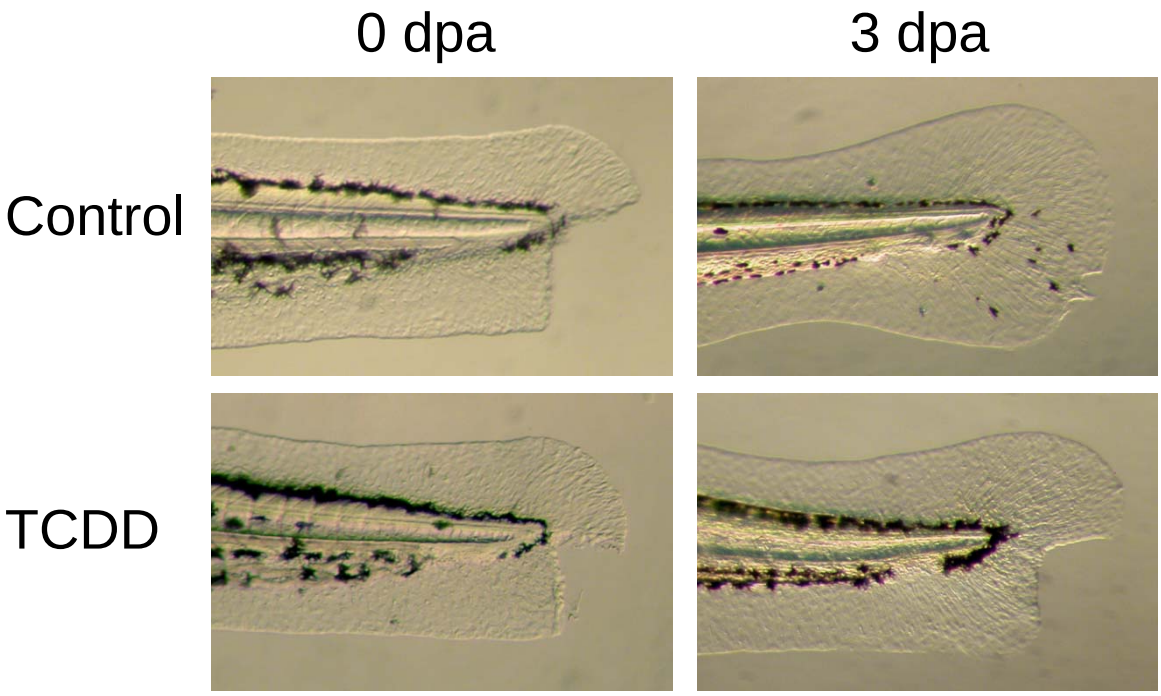

Figure 2-2. The suppression of fin regeneration by TCDD is specific to the regenerating tissue. The ventral half of the caudal fin was amputated followed by the waterborne exposure to TCDD (0.5 ng/mL) or control (DMSO). The embryos were allowed to develop further to analyze whether the TCDD preferentially inhibits the regenerating tissue. Fin regeneration images were acquired on 0 dpa and 3 dpa.

Figure 2-3. TCDD preferentially affects the regenerating fin. (A) The length of maximum outgrowth, the area of regenerated fin tissue and the area of non-amputated fin tissue at 0 and 3 dpa were measured in vehicle and TCDD exposed embryos as described in the schematic diagram. **(B)** The length of maximum ventral caudal fin outgrowth (1 micron = 1.54 pixels) and **(C)** the area of regenerated fin tissue (%) in control larvae were significantly greater than the TCDD exposed embryos ($P<0.001$). **(D)** The measurement of increase in the area of non-amputated tissue from 0-3 dpa will delineate whether TCDD affects the normal growth of fin tissue. The area of the dorsal half of the caudal fin in TCDD exposed larvae was greater than control larvae ($P<0.004$). The dotted line indicates the plane of amputation. The respective values represent the mean $\pm$ SEM (t-test, n =11). All three parameters were measured using the Image Pro-Plus software (Media Cybernetics, Silver Spring, MD).

2-3

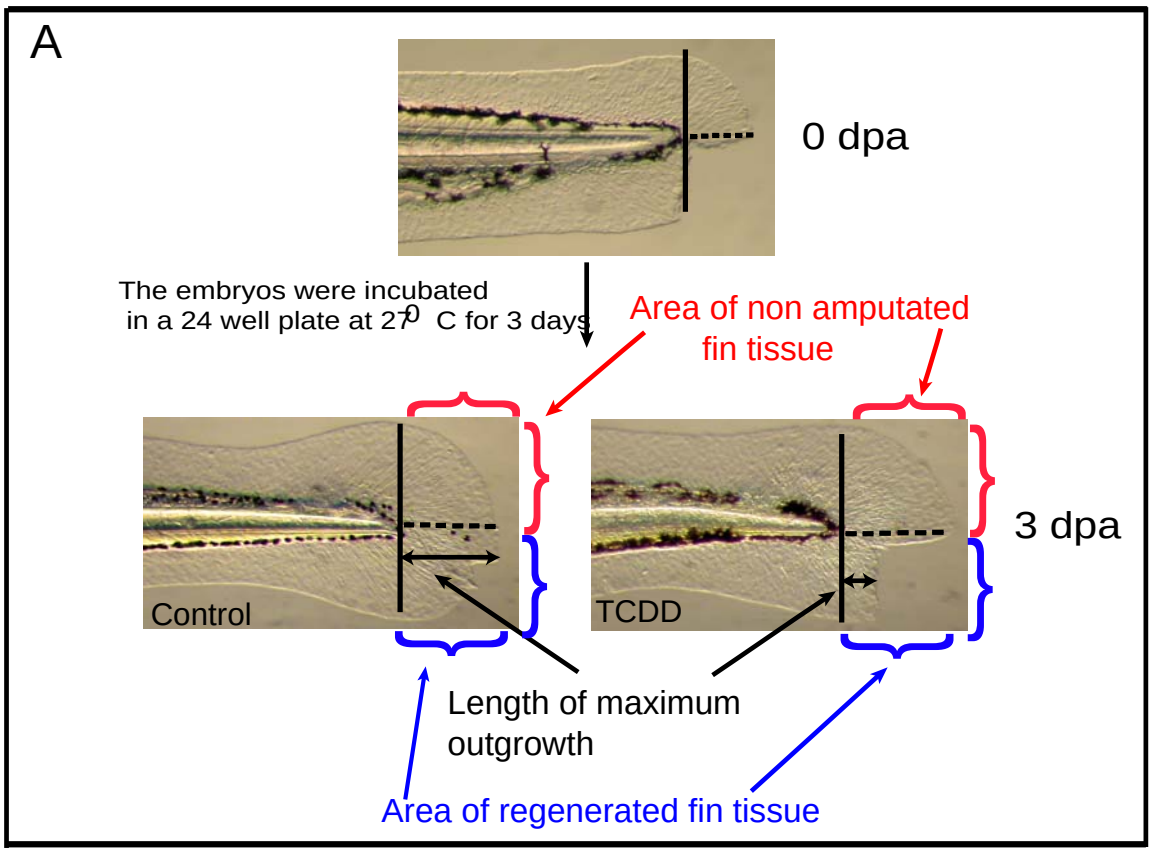
A
0 dpa
The embryos were incubated
in a 24 well plate at 27° C for 3 days
Area of non amputated
fin tissue
Control
TCDD
3 dpa
Length of maximum
outgrowth
Area of regenerated fin tissue

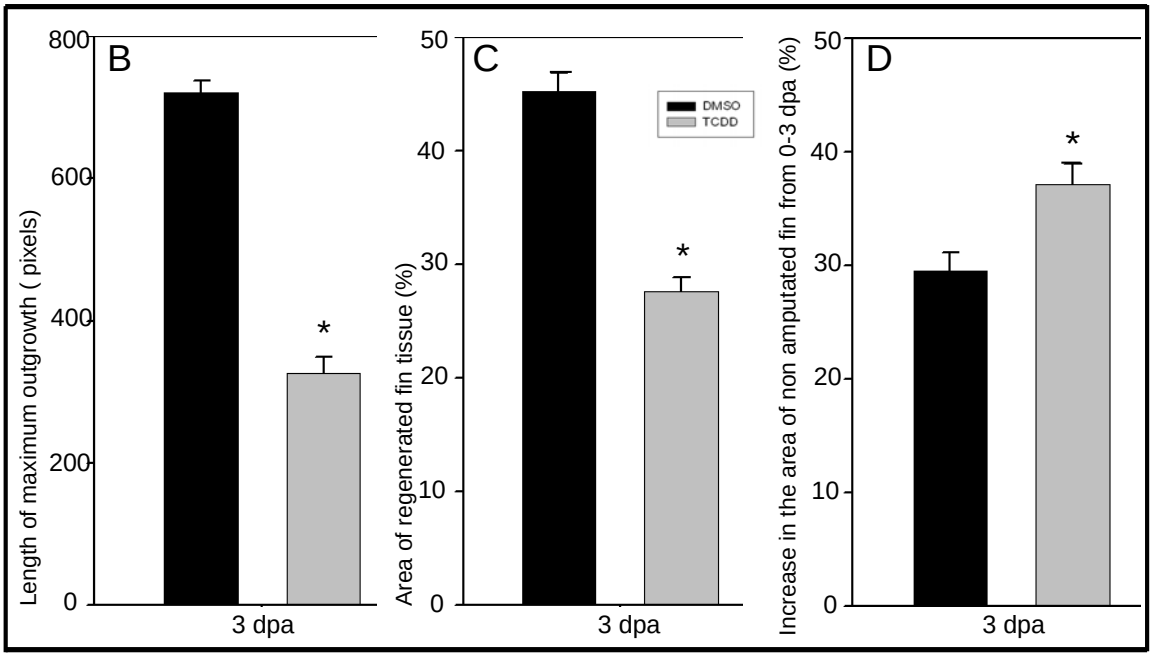
B
Length of maximum outgrowth (pixels)
800
600
400
200
0
*
3 dpa
C
Area of regenerated fin tissue (%)
50
40
30
20
10
0
DMSO
TCDD
*
3 dpa
D
Increase in the area of non amputated fin from 0-3 dpa (%)
50
40
30
20
10
0
*
3 dpa

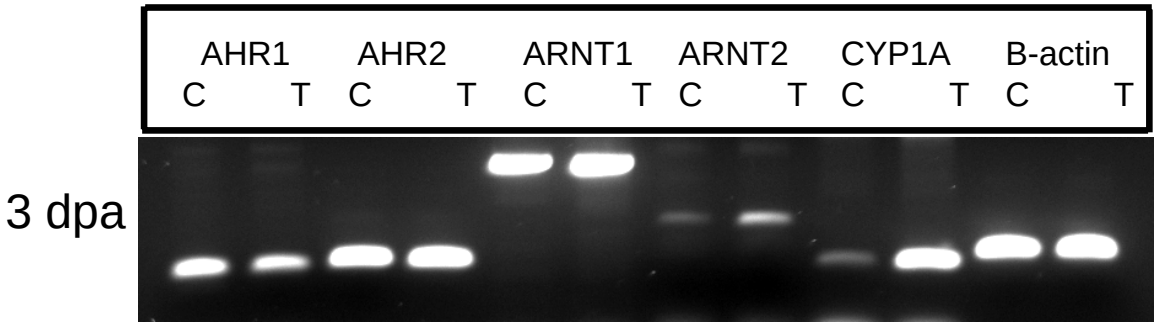

Figure 2-4. Identification of AHR pathway members in the regenerating zebrafish fin tissue by RT-PCR. The 48 hpf larvae were exposed to DMSO (C) or TCDD (T) after amputation and the regenerating fin tissues were harvested for RNA isolation (n = 100). Reverse transcription was conducted followed by PCR using zfAHR1, zfAHR2, zfARNT1, zfARNT2b/c, zfCYP1A and β-actin specific primer pairs. The PCR products were resolved by agarose gel electrophoresis and visualized with ethidium bromide staining.

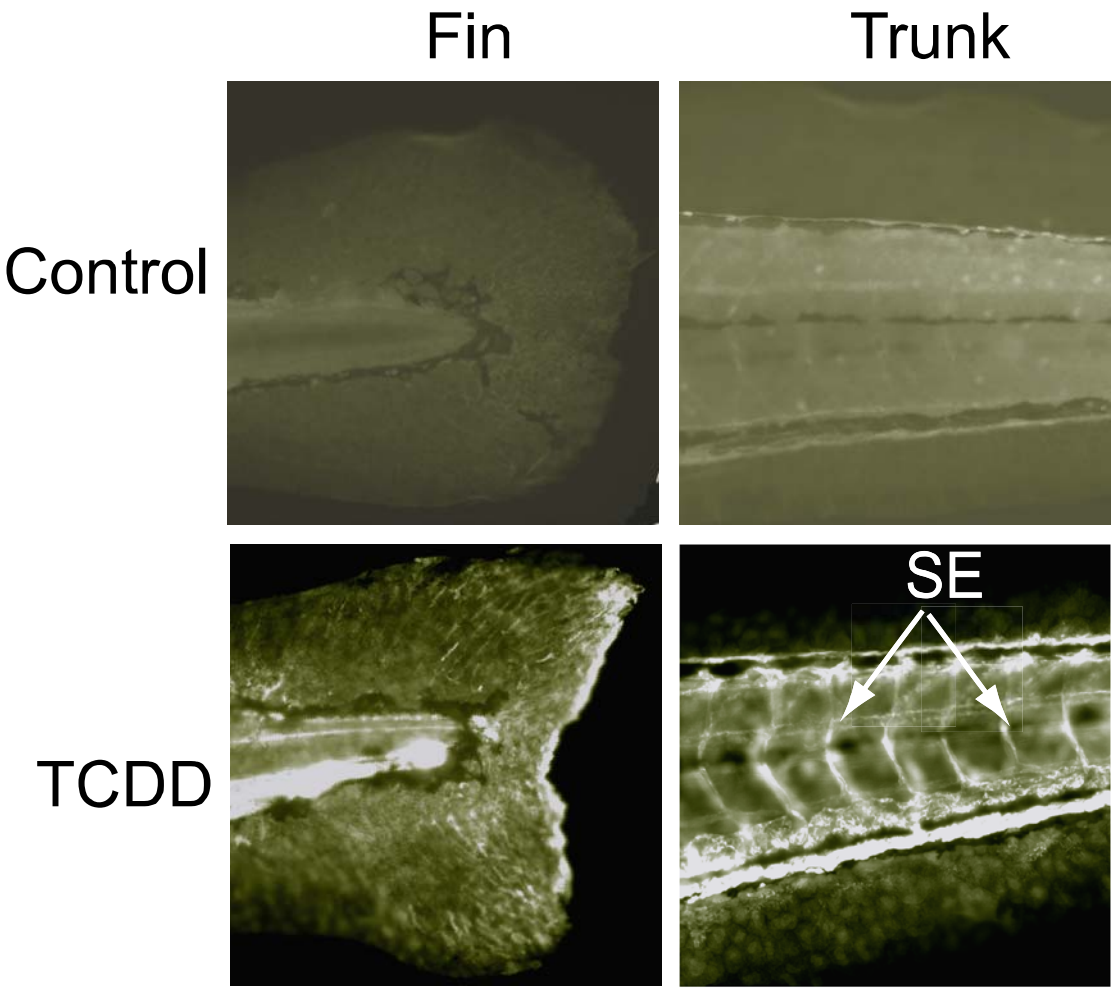

Figure 2-5. Whole mount immunolocalization of zfCYP1A. The immunohistochemical localization of zfCYP1A in control and TCDD exposed larvae at 3 dpa using monoclonal antibody, C107. Depicted are the images of fin tissue and the trunk of the larvae with positive CYP1A localization in the intersegmental vessel (SE).

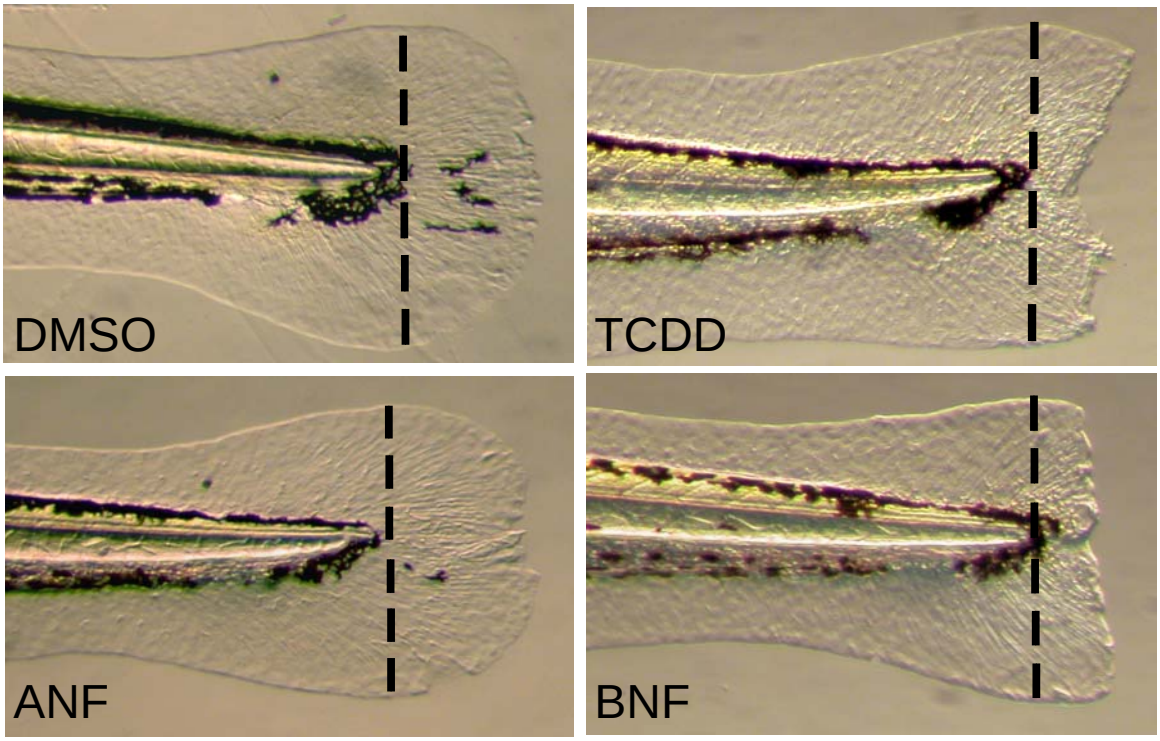

Figure 2-6. Activation of AHR2 by BNF inhibits fin regeneration similarly to TCDD. The caudal fin of 48 hpf larvae were surgically amputated and exposed to control (DMSO), an AHR antagonist ANF, or AHR agonists BNF and TCDD. The images were taken at 3 dpa and the dotted line indicates the plane of ablation of fin tissue.

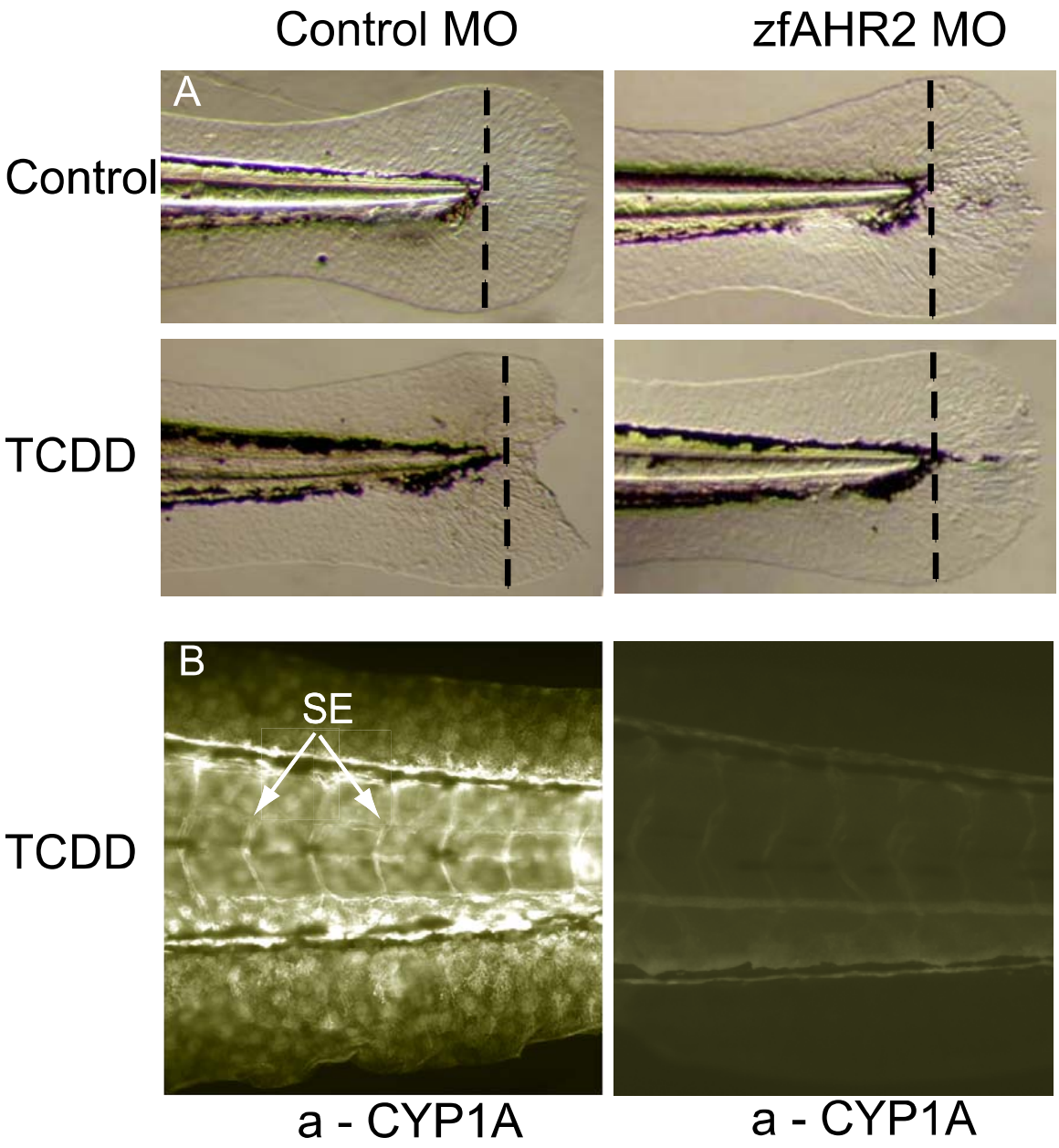

Figure 2-7. Fin regeneration occurs in *zfahr2* morpholino injected embryos in the presence of TCDD. (A) The control morpholino (Control MO) and *zfahr2* morpholino (AHR2 MO) injected embryos were amputated at 48 hpf and exposed to vehicle or TCDD. The fin regeneration images were taken at 3 dpa. Dotted line marks the plane of amputation. **(B)** Immunolocalization of zfCYP1A on Control and *zfahr2* morphants exposed to TCDD. (SE – intersegmental vessel).

Figure 2-8. Role of zfARNT members in the inhibition of fin regeneration by TCDD. **(A)** Heterozygous (HET, *zfarnt2*$^{+/-}$) and homozygous *zfarnt2*$^{-/-}$ mutants were exposed to vehicle or TCDD. The images are of *zfarnt2*$^{+/-}$ and *zfarnt2*$^{-/-}$ larvae characterized genotypically by PCR. The images of the mutants exposed to DMSO are not shown. **(B)** Genotyping the *zfarnt2* mutants by PCR. **(C)** The control (Control MO) and *zfarnt1* morphants (ARNT1 MO) were exposed to vehicle or TCDD at 0 dpa. The images were captured at 3 dpa. Images of the control and *zfarnt1* morphants exposed to DMSO are not shown. **(D)** Whole mount immunolocalization of zfCYP1A in control and *zfarnt1* morphants exposed to TCDD.

2-8

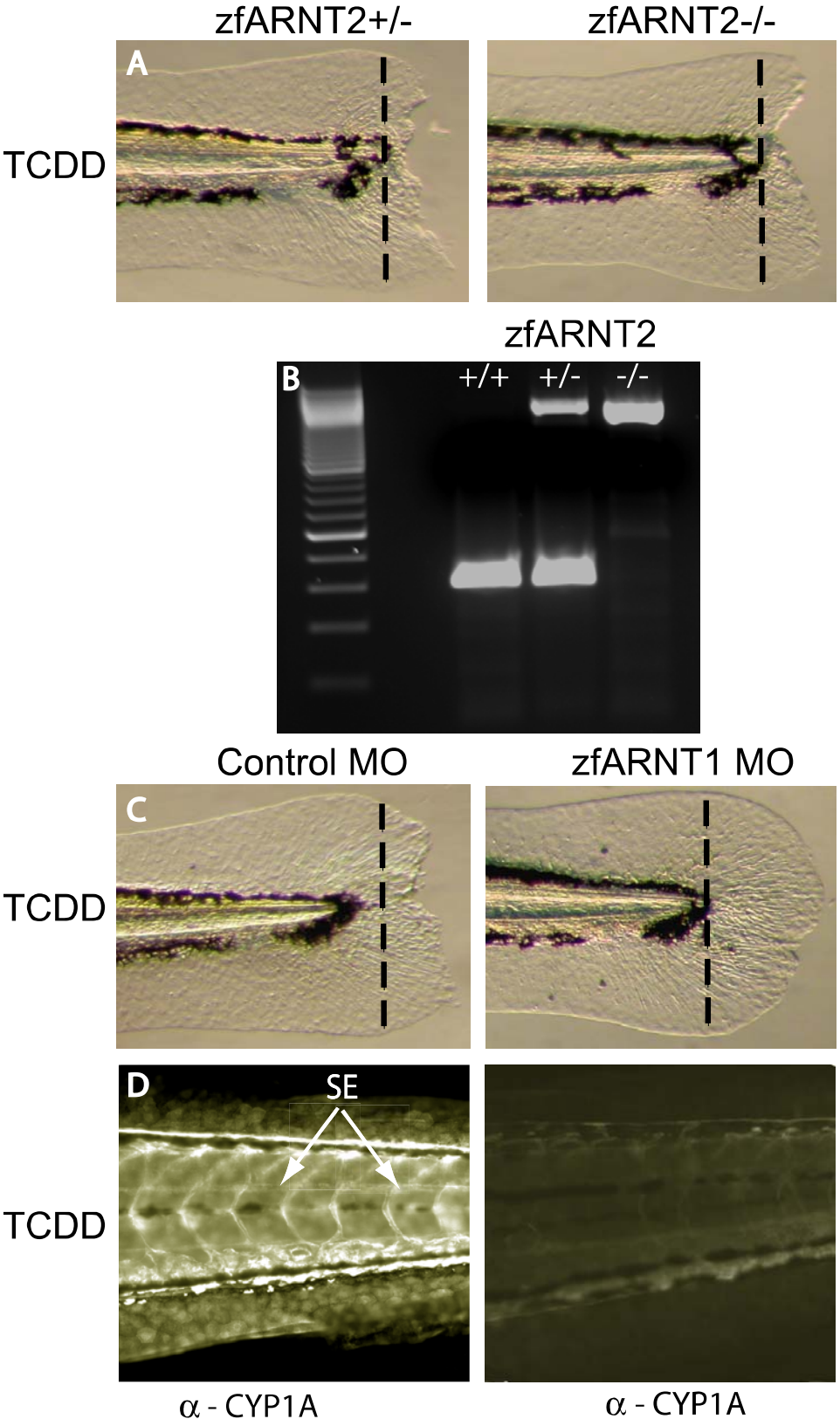
zfARNT2+/-
zfARNT2-/-
A
TCDD
zfARNT2
B
+/+
+/-
-/-
Control MO
zfARNT1 MO
C
TCDD
D
SE
TCDD
α - CYP1A
α - CYP1A

Figure 2-9. Inhibitory effect on the process of fin regeneration by TCDD and FGFR1 inhibitor is different. (A, B) The 48 hpf larvae were amputated and exposed to vehicle, TCDD or FGFR1 inhibitor (SU5402). Images of the TCDD and SU5402 exposed larvae were taken at 3 dpa. **(C, D, F)** Whole mount immunolocalization of acetylated tubulin that stains axons and the peripheral processes of larvae exposed to vehicle, TCDD or FGFR1 inhibitor (SU5402). The arrows indicate the path of diverging peripheral processes **(D, E)** Immunohistochemical staining was done on TCDD exposed larvae with ventral half cuts to delineate the peripheral processes that are diverging at the site of inhibition of fin regeneration. The arrow on the ventral half cut reveals the deviating path of peripheral processes **(D)**. The images are representative of 12 larvae and the images were inverted.

2-9

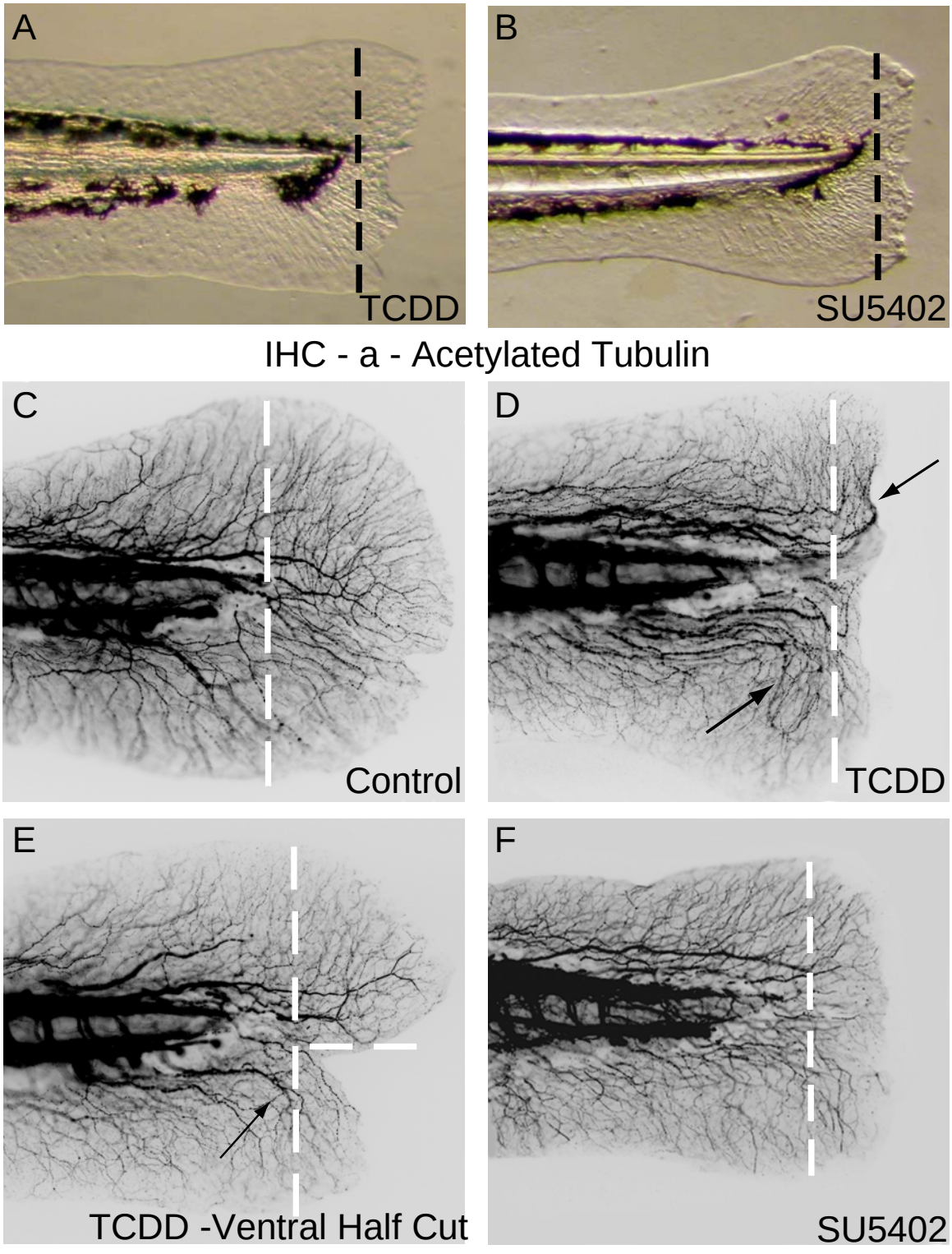
A
TCDD
B
SU5402
IHC - a - Acetylated Tubulin
C
Control
D
TCDD
E
TCDD -Ventral Half Cut
F
SU5402

Table 2-1. Oligonucleotides used for PCR.

Name of Primer	Sequence of the primer (5'-3')
zfAHR1F	TAGACAGCGATATACAGCAG
zfAHR1R	TCTCTCCAACACCATTCATG
zfAHR2F2	ACGGTGAAGCTCTCCCATA
zfAHR2R2	AGTAGGTTTCTCTGGCCAC
zfARNT1F	ATCCTGCGCATGGCCGTATC
zfARNT1R	GATGTAGCCTGTGCAGTGGAC
zfARNT2b/cF	GACTGAATTCCTTTCGCGCCAC
zfARNT2b/cR	CTGGAGCTGCTTGACGTTG
zfCYP1AF	ACAACATCAGAGACATCACC
zfCYP1AR	TCTCTTTGCAGTCGCTCCTGG
zfβ-actinF	AAGCAGGAGTACGATGAGTC
zfβ-actinR	TGGAGTCCTCAGATGCATTG
zfARNT2F1	CGGAAATGTCGCTGTTGTTAGTTGTG
zfARNT2R1	GAACTGAGTTTGCGCGTTTGAGAC
TranspoR	TGCGATGCCGTCTACTTTGA

Crosstalk between AHR and Wnt Signaling Impairs Tissue Regeneration

Lijoy K Mathew, Sumitra S Sengupta, Jane LaDu, Eric A Andreasen, and Robert L Tanguay.

Department of Environmental and Molecular Toxicology, Environmental Health Sciences Center, Oregon State University, Corvallis, OR, 97331.

Formatted for Publication in Molecular and Cellular Biology

Abstract

Exposures to dioxin, including 2,3,7,8-tetrachlorodibenzo-*p*-dioxin (TCDD) cause a variety of toxicities in vertebrates and is mostly mediated through the inappropriate activation of Ahr pathway. Although transcriptional regulation by Ahr is widely studied, the molecular mechanisms responsible for the adverse outcomes after Ahr activation are largely unknown. To identify the important events downstream of Ahr activation that play an actual role in the toxic responses, we employed the zebrafish caudal fin regeneration models since TCDD blocks the regenerative process. Comparative toxicogenomic analysis revealed that both adult and larval fins respond to TCDD during regeneration with mis-expression of Wnt signaling members and Wnt target genes. R-Spondin1, a novel ligand for the Wnt co-receptor was highly induced and we hypothesized that mis-expression of R-Spondin1 is necessary for Ahr activation to block regeneration. Partial antisense repression of R-Spondin1 reversed the inhibitory effect of TCDD and tissue regeneration was restored. Since R-Spondin1 signals through the Wnt co-receptor LRP6, we further demonstrated that the TCDD-mediated block in regeneration is also LRP6 dependent. This is the first report of a cross talk between Ahr and Wnt/β-catenin signaling pathway in any biological system and provide a mechanistic explanation on how ligand-activated Ahr initiates complex adverse *in vivo* responses.

Introduction

The aryl hydrocarbon receptor (AHR) is a basic-helix–loop–helix (bHLH) transcription factor, well known for its ability to bind to environmental contaminants such as 2,3,7,8-tetrachlorodibenzo-*p*-dioxin (TCDD)(Burbach et al., 1992; Hankinson, 1994; Henry and Gasiewicz, 1993). The well accepted mechanism of action of TCDD is that the ligand bound AHR translocates to the nucleus where it binds with its dimerization partner, Ah receptor nuclear translocator (ARNT). The AHR-ARNT complex binds to specific enhancer elements resulting in the transactivation of a variety of genes that induce diverse toxicities including reproductive and developmental toxicity, immunotoxicity, cardiotoxicity, teratogenicity and neurotoxicity at low exposure levels [reviewed in (Schmidt and Bradfield, 1996). Even though the transcriptional regulation of AHR has been widely studied, the molecular mechanisms leading to the manifestation of toxicities are poorly understood. To understand the complex molecular mechanisms after AHR activation, an *in vivo* research model easily amenable to molecular and genetic manipulation would be very useful.

Zebrafish caudal fin regeneration is a well established research model that has been utilized to identify the basic principles of tissue regeneration (Akimenko et al., 2003; Mari-Beffa et al., 1996; Poss et al., 2000b; Santamaria and Becerra, 1991; Santamaria et al., 1996; Whitehead et al., 2005). Zebrafish regenerate their caudal fins by a process referred to as epimorphic regeneration (Mescher, 1996; Nakatani et al., 2007; Poss et al., 2000a; Santamaria and Becerra, 1991; Stoick-Cooper et al., 2007; Whitehead et al., 2005). Immediately after surgical amputation, epithelial cells begin to migrate over the injured site forming a wound cap, which is followed by the de-differentiation of cells proximal to the amputation plane into a cluster of pluripotent cells referred to as blastema (Nakatani et al., 2007; Santamaria and Becerra, 1991; Santos-Ruiz et al., 2002; Whitehead et al., 2005). The blastema cells further proliferate and differentiate into the required cell types to complete the regenerative outgrowth. This complex process is tightly regulated by multiple signaling pathways, and interference by external stimuli could modulate the regeneration process leading to defective regeneration. We have

previously demonstrated that TCDD (2,3,7,8-Tetrachlorodibenzo-*p*-dioxin), an Ahr ligand, inhibits zebrafish fin regeneration at both adult and larval stages (Mathew et al., 2006; Zodrow and Tanguay, 2003). We also have shown that the inhibition of fin regeneration mediated by TCDD is Ahr2 and Arnt1 dependent (Mathew et al., 2006). Therefore, we developed this inhibition of regeneration phenomenon as an *in vivo* platform to identify the molecular signaling pathways downstream of Ahr activation.

Through microarray and morphological analysis, we have previously demonstrated that TCDD affects several components involved in cellular differentiation and extracellular matrix composition in adult tissue regenerates (Andreasen et al., 2007; Andreasen et al., 2006). To determine whether the gene expression changes by TCDD are conserved between the adult and larval fin regeneration models, we performed microarray analysis using the larval regeneration model. Comparative genomic analysis revealed that Ahr activation results in the mis-expression of a number of Wnt signaling genes in both regeneration systems, and we conclusively demonstrate that cross talk between Ahr and Wnt signaling is responsible for the impairment of fin regeneration. Additionally, the identification of the molecular pathways affected by Ahr activation could also reveal essential molecular signaling pathways important for tissue regeneration.

Materials and Methods

Zebrafish Embryos

Fertilized embryos from AB strain zebrafish (University of Oregon, Eugene, OR) were used for all the experiments. All embryos were reared in our laboratory according to standard procedures and each experimental group consisted of 12 larvae (Westerfield, 1995). Sox9b mutant line was a gift from Dr. John H. Postlethwait (University of Oregon, Eugene, OR).

Chemicals

TCDD (>99% pure) was obtained from Chemsyn (Lenexa, KS) and the larval exposures were done at a concentration of 1ng/mL. BIO (6-bromoindirubin-3'-oxime) was bought from EMD Biosciences (San Diego, CA) and the larvae were exposed at a final concentration of 10μM.

Fin RNA Isolation

Caudal fins from two day old embryos (AB strain, Eugene, OR) were amputated and the animals were exposed to either DMSO (vehicle control) or 0.5ng/mL TCDD (>99% pure, Chemsyn, Lenexa, KS) in the water for 1 hr (Figure 1). After several rinses in TCDD free water, the larvae were reared until 2 and 3 days post amputation (dpa) when their regenerating fin tissue was amputated and collected for RNA analysis. RNA was extracted from the fin tissue using the RNAqueous Micro kit (Ambion, Austin, TX). Three groups at each time point and treatment, each comprised of 150 larval fins, were pooled to make an individual replicate. The quality and quantity of RNA was analyzed by UV absorbance. The abundance of ribosomal RNA and degree of degradation was determined in electropherogram patterns using the 2100 Bioanalyzer and RNA 6000 Nano chips (Agilent Technologies, Palo Alto, CA).

Affymetrix Microarray Processing

The microarray processing using the Affymetrix platform was performed by the Center for Genome Research and Biocomputing at Oregon State University, Corvallis OR. A total of 100ng of RNA from the larval fin tissue (+/-TCDD) at 2 and 3 dpa were used to generate biotinylated complementary RNA (cRNA) using the Two-Cycle Target Labeling kit (Affymetrix, Santa Clara, CA). In short, the different RNA samples were reverse transcribed using a T7-$(dT)_{24}$ primer and Superscript II reverse transcriptase (Invitrogen, Carlsbad, CA) and double stranded cDNA was synthesized. Another round of double stranded cDNA synthethis was conducted using the previously synthesized cDNA as the template. Biotinylated cRNA was synthesized from the double stranded cDNA using T7 RNA polymerase and a biotin-conjugated pseudouridine containing nucleotide mixture provided in the IVT Labeling Kit (Affymetrix, Santa Clara, CA). The

biotinylated cRNA was quantified and 10µg of purified and fragmented cRNA from each experimental sample was hybridized to zebrafish genome arrays (Zebrafish430_2) according to the Affymetrix GeneChip Expression Analysis Technical Manual (701021 Rev. 5). Arrays were scanned with an Affymetrix scanner 3000. Each array image was visualized to discount artifactual signals, scratches or debris. Experiments were MIAME certified.

Data analysis was performed by importing the Affymetrix cel files into GeneSpring 7.1 software (Agilent Technologies, Palo Alto, CA). The files were GC-RMA processed to discount for background signal and each transcript was normalized to the median signal to allow comparison between arrays on a relative scale for each gene. The differential gene expression changes by TCDD during regeneration was performed by comparing the experimental samples from the vehicle vs TCDD exposed larvae at 2 and 3dpa by one-way ANOVA assuming equal variance ($p < 0.05$). Only genes that were at least 1.7 fold differentially expressed from the vehicle gene levels were considered for analysis. The annotation of genes were conducted by taking into account the sequence similarity to known mammalian proteins that was determined by conducting a BLAST search of each Affymetrix probe set against the Sanger database (http://www.sanger.ac.uk/Projects/D_rerio/). Moreover, other databases such as Genbank (http://www.ncbi.nlm.nih.gov/BLAST/) and the Zebrafish Affy Chip Annotation Project at Children's Hospital Boston http://134.174.23.160/zfaca/hash/master020106public.aspx) were used simultaneously.

Quantitative RT-PCR

From the larval fin tissue (+/-TCDD), total RNA was isolated in triplicate at 2 and 3 dpa (n = 150/group). cDNA was prepared from 100 ng of total RNA per group using Superscript II (Life Technologies, Gaithersburg, MD) and oligo(dT) primers in a 20 µl volume. Quantitative RT-PCR (qRT-PCR) was performed using gene specific primers (Supplemental Table. 5) with the Opticon 2 real-time PCR detection system (MJ Research, Waltham, MA). According to the manufacturer's instructions (Finnzymes, Espoo Finland), 1 µl of cDNA was used for each PCR reaction using DyNAmo SYBR green qPCR kit. All experimental samples were normalized to their β-actin abundance

and quantitative differences between biological samples were determined by normalizing all samples to a common reference sample. Agarose gel electrophoresis and thermal denaturation (melt curve analysis) were performed to analyze the formation of specific PCR products. Statistical significant differences of mRNA abundance were assessed by one-way ANOVA on $\log_{10}$ transformed data using Tukey method ($p < 0.05$) (SigmaStat software, Chicago, IL).

Oligonucleotides

Oligonucleotide primers were synthesized by MWG-Biotech (High Point, NC). Forward primers are prefixed with an F corresponding to sense strands and antisense reverse primers are designated with an R. Primers were designed to amplify sequence within the Affymetrix probe set sequence. Sequence for each primer can be found in Supplemental Table. 5.

Cloning of zebrafish LRP6 gene

The human LRP6 peptide sequence was blasted against the Sanger database (http://www.sanger.ac.uk/Projects/D_rerio/), and a putative gene (Ensemble gene ID ENSDARG00000063702) with 66% peptide similarity was identified. Three predicted transcripts were enlisted for this gene and based on the number of exons and splicing similarity, we pursued with the transcript ID ENSDART00000093327. Forward and reverse primers were designed from either ends of the predicted coding sequence and PCR was performed using KOD hot start DNA polymerase (Novagen, San Diego, CA) to clone the full length gene (predicted sequence is 4767bp). The gel purified PCR product was incubated with Taq polymerase at 72°C for 1 minute to add "T" at the blunt end and then inserted to the TOPO-XL vector (Invitrogen, Carlsbad, CA). The full length sequence of zfLRP6 gene was sequenced by designing primers within the fragment after each DNA sequencing step. The full length coding sequence of zfLPR6 gene starting form the start to the stop codon is 4953bps.

Morpholinos

The R-Spondin1 gene was specifically targeted by designing a splice junction morpholino (MO) at the intron 1 - exon 2 boundary (Gene Tools, Philomath, OR). The sequence of the fluorescein tagged R-Spondin1 MO is 5'-GTGCTTACTGATGGAGAAAAGACAG-3'. A splice junction MO at the exon 3-intron 4 boundary of the LRP6 gene was designed to transiently knockdown the transcript. The sequence of LRP6 MO is 5'- AGGTGTTCTGACCTGCTGGAGCCGT-3'. Morpholinos were diluted to 3 mM in 1X Danieau's solution (58 mM NaCl, 0.7 mM KCl, 0.4 mM $MgSO_4$, 0.6 mM $Ca(NO_3)_2$, 5 mM HEPES, pH 7.6) as described (Nasevicius and Ekker, 2000). A standard control morpholino (Gene Tools, Philomath, OR) (5'CTCTTACCTCAGTTACAATTTATA 3') was used as the control morpholino (Control-MO). Approximately, 2 nl of 0.3mM of R-Spondin1 MO and 0.5mM of LRP6 MO solution was microinjected into the embryos at the 1–2 cell stage. The control, R-Spondin1 and LRP6 morphants were amputated at 2dpf and exposed to vehicle or TCDD for one hour followed by raising the larvae for 3 days at 28°C.

In situ Hybridization

In situ localization of mRNA was performed on the regenerating fin at respective time points as described previously (Poss et al., 2000a; Schier et al., 1997). The *msxe* and *dlx5a* probes were obtained from Atsushi Kawakami(Kawakami et al., 2004). *Raldh2* probe was prepared by cloning the cDNA by RT-PCR from the RNA isolated from the whole adult zebrafish. *R-Spondin1* probe was generated by cloning the cDNA by RT-PCR from the adult zebrafish RNA.

Results

Gene Expression Changes in Larval Regenerating Tissue after AHR Activation

Previously, we reported that TCDD inhibits both adult and larval fin regeneration (Mathew et al., 2006; Zodrow and Tanguay, 2003). To elucidate the molecular signaling

events downstream of Ahr activation, microarray analysis was conducted using regenerating fin tissue isolated from larval fish in the presence and absence of TCDD (Figure 1). Alterations in gene expression by TCDD were evaluated by first filtering for genes that were at least 1.7 fold differentially abundant at 2 and 3dpa from their time matched control. One Way ANOVA analysis was performed between the time-matched vehicle and TCDD-exposed gene list for statistical significance. A total of 1097 genes were differentially expressed by TCDD exposure (Figure 2A). The genes were categorized into distinct functional groups based on sequence homology and the identified function (Figure 2B). Components related to signal transduction, extracellular matrix remodeling, cytoskeleton dynamics and Wnt signaling pathway were the predominant functional groups significantly affected by TCDD (Table S1 & 2). Transcripts from different functional groups that were differentially expressed by Ahr activation were validated by qRT-PCR (Figure 3A, B), illustrating the validity of the microarray results. Genes known to be transcriptionally upregulated by AHR activation were induced, including xenobiotic metabolizing enzymes such as CYP1A1, confirming the activation of AHR pathway by TCDD in the regenerating larval fin tissue (Figure 3A). The TCDD modulated extracellular matrix genes such as Spondin 2b, Claudin c and CYR61 were induced while, Cartilage link protein (Crtl), Thrompospondin 3 (Thps3), Perisotin and Keratocan were repressed representatively by qRT-PCR (Figure 3A, B). R-Spondin1, a recently identified Wnt ligand was one of the most highly induced transcripts at 2 and 3dpa. In contrast, Sox9b, a transcription factor that plays a major role in chondrogenesis regulation was the gene mostly repressed by TCDD. These larval regeneration responses to TCDD are highly consistent with our previous microarray study on adult fin regeneration after TCDD treatment (Andreasen et al., 2007), and prompted to us to perform a comparative toxicogenomic approach in these two different platforms.

Comparative Toxicogenomic Approach Reveals Mis-regulation of Wnt Signaling by Ahr Activation

Since fin regeneration is inhibited by Ahr activation in both life stages, the key molecular events controlling this phenomenon may be conserved. The transcriptional

response to TCDD in larval fin regeneration system was compared with our previously published gene expression analysis data on adult fin regeneration after TCDD exposure (Andreasen et al., 2006) (Figure S1). We generated a list of genes that were differentially regulated at least 1.7 fold in response to TCDD in both adult and larvae regenerating fins at any time point. One Way ANOVA analysis was conducted to determine the significance of TCDD exposure on time matched samples assuming equal variance ($p<0.05$). Approximately, 50 genes were similarly enhanced and 150 transcripts were repressed due to Ahr activation in the two regenerative models (Table S3 & 4). Distinctively, R-Spondin1 and Sox9b were the genes that were mostly induced and repressed respectively during larval and adult fin regeneration after exposure to TCDD. This is significant because, the structural architecture of the caudal fin tissue at these two life stages is very different. The similar expression pattern of 200 genes in response to Ahr activation in the regenerating fin tissue suggests common mechanisms of action for the inhibitory phenotype. It is noteworthy that transcripts related to extracellular matrix metabolism, cell adhesion and migration dominated the list of differentially expressed genes after TCDD exposure in both the models.

Mis-regulation of Wnt Signaling by Ahr Activation is Mediated through R-Spondin1

In addition to the over-expression of R-Spondin1, numerous Wnt signaling targets were also altered by Ahr activation, in both regeneration models (Table 1). The identification of Wnt target genes was performed with reference to the Wnt home page (http://www.stanford.edu/~rnusse/wntwindow.html) and recognized more than 20 Wnt target genes that were modulated by Ahr activation in these two regenerative models (Table 1). The pattern of the expression of these Wnt target genes suggested that TCDD improperly activates Wnt signaling pathway in tissue regenerates. *In situ* localization of *r-spondin1* revealed high induction of the transcript in the fin tissue of TCDD-exposed larvae, consistent with the microarray and qRT-PCR results (Figure 4). The localization pattern of *r-spondin1* in the regenerating fin tissue was unique as it was expressed in a few rows of cells surrounding the notochord in close proximity to the regenerating fin tissue. Since R-Spondin1 is an upstream modulator of Wnt signaling, we hypothesized

that Ahr-dependent mis-expression of R-Spondin1 may dictate the downstream gene expression changes that collectively result in impaired cellular differentiation, extracellular matrix remodeling and cell adhesion and migration. If the induction of R-Spondin1 is required for TCDD to block the regenerative growth, antisense repression of R-Spondin1 should permit regeneration in the presence of TCDD. A splice junction morpholino (MO) was designed to target R-Spondin1 gene in the I1E2 boundary (Figure 5A). It is noteworthy to mention that complete knockdown of R-Spondin1 gene resulted in the lethality of all the microinjected embryos (morphants) at 24hpf, suggesting an important functional role for this gene during development (data not shown). To avoid a lethal response, we titrated the level of the fluorescent tagged R-Spondin1 MO to obtain partial suppression of the gene to a level that did not completely impair embryonic development. The morphants were screened for fluorescence and the animals with similar intensity were selected for the study. Caudal fins of both control and R-Spondin1 morphants at 48hpf were amputated and were then exposed to vehicle or TCDD and raised for the following 3 days. The control and R-Spondin1 morphants exposed to vehicle regenerated, whereas TCDD blocked the regeneration of control morphants (Figure 5B). However, partial suppression of R-Spondin1 using splice blocking morpholinos abrogated the TCDD-dependent block of regeneration, suggesting that inappropriate induction of R-Spondin1 is required for TCDD to impair regeneration (Figure 5B). The partial repression of R-Spondin1 transcript was analyzed by RT-PCR using specific primers on control and R-Spondin1 morphants at 3dpf (Figure 5A). A mis-spliced transcript was detected as a lower band (Figure 5C) and the size of this product is consistent with the loss of the targeted exon 2. These results are significant because this is for the first time we demonstrate that the adverse *in vivo* responses to AHR activation can be circumvented by modulating a single downstream gene. Moreover, these studies for the first time identify functional cross talk between the Ahr and Wnt signal transduction pathways and indicate the power of zebrafish model to discover and define the molecular pathways that regulate complex *in vivo* biological responses.

LRP6 is Required for TCDD Dependent Inhibition of Regeneration

Recent studies suggest that R-Spondin1 signaling is mediated directly or indirectly through the Wnt co-receptor LRP6 (Binnerts et al., 2007; Wei et al., 2007). We hypothesized that if LRP6 is required for the functioning of R-Spondin1 signaling, antisense repression of LRP6 should permit regeneration even in the presence of TCDD. We designed a splice junction MO against the LRP6 gene in the E3I4 boundary (Figure 6A). Similar to the R-Spondin1 MO experiments, the complete knockdown of LRP6 elicited lethality implicating its functional importance during development. Further titration experiments along with the screening for fluorescence of the control and LRP6 morphants helped us to screen the animals for the studies. The caudal fins of the selected control and LRP6 morphants were amputated at 48hpf and exposed to vehicle or TCDD for an hour, and allowed to develop for the following 3 days. The control and LRP6 morphants exposed to vehicle completely regenerated the fin tissue, suggesting that partial reduction of LRP6 gene did not impact the normal regeneration process. The control morphants exposed to TCDD elicited inhibition of regeneration, while LRP6 morphants regenerated their lost fin tissue in the presence of TCDD (Figure 6B). This clearly suggests that mis-expression of R-Spondin1 requires LRP6 to mediate the signaling to impair regeneration. We further confirmed the efficiency of the splice junction LRP6MO by illustrating the mis-splicing of the gene by PCR (Figure 6C). This result underscores our findings that Ahr activation impacts tissue regeneration by interfering with the normal functional role of Wnt signaling.

Improper Activation of Wnt Signaling Impairs Regeneration

Our microarray data and functional studies with R-Spondin1 support the hypothesis that Ahr activation is inappropriately activating the Wnt signaling pathway through R-Spondin1, which causes the inhibition of regeneration. On the other hand, active Wnt signaling is critical for zebrafish fin regeneration and distinct Wnt pathway members have opposing roles during regeneration, implicating a complex functional role for this pathway (Stoick-Cooper et al., 2007; Zhong et al., 2006). In order to directly test the role of improper activation of Wnt signaling pathway during regeneration, we made use of BIO (6-bromoindirubin-3'-oxime), a specific pharmacological inhibitor of

glycogen synthase kinase-3 (GSK-3) which is a negative regulator of canonical Wnt signaling pathway (Sato et al., 2004). Two day old larvae were amputated and exposed to vehicle or BIO (10μM) for 3 days continuously. In comparison with the vehicle, BIO impaired regeneration in a pattern very similar to TCDD exposed larvae (Figure7A). This study suggest that over-activation of Wnt signaling pathway by BIO inhibits regeneration and explains the requirement for a spatio-temporal fine balance of Wnt signaling during regeneration.

Since our results suggest that TCDD over-activates Wnt signaling pathway, we performed a comparative analysis of molecular markers that specifically define wound epithelium (*dlx5a*) and blastema (*msxe* and *raldh2*) between TCDD and BIO exposed larvae. We performed *in situ* hybridization with *dlx5a msxe* and *raldh2* antisense probes to determine if wound epithelium and blastema were formed properly. When compared with the vehicle control, the expression of *dlx5a*, *msxe* and *raldh2* were lost in TCDD exposed animals in the regenerating fin tissue at 1dpa (Figure 7B), indicating improper wound epithelium and blastema formation. We further analyzed the expression of the above described markers on BIO exposed larvae. Similar to TCDD exposed larvae, the expression of *dlx5a*, *msxe* and *raldh2* were lost in the regenerating fin tissue at 1dpa in the BIO exposed larvae (Figure7B), suggesting that inappropriate activation of Wnt signaling inhibits fin regeneration by impairing the formation of a the wound epithelium and blastema. These results illustrate the importance of appropriate regulation of Wnt signaling pathway for tissue regeneration and supports our hypothesis that TCDD exposure elevates the expression of the Wnt ligand, R-Spondin1, leading to over-activation of Wnt signaling pathway.

Impairment of Regeneration by Ahr Activation is not Completely Sox9b Dependent

Since R-Spondin1 is a Wnt ligand, we further analyzed the relationship between R-Spondin1 and the other Wnt target genes that were mis-expressed following Ahr activation. *Sox9b* was identified as a Wnt target gene in mesenchymal cells during the process of chondrogenic differentiation and this gene was strongly repressed following the activation of Wnt signaling pathway (Day et al., 2005; Hill et al., 2005; Yano et al., 2005). Importantly, in both adult and larval fin regeneration models, *sox9b* was the most

repressed gene by TCDD and we proposed that the activation of Wnt signaling by AHR activation through R-Spondin1 is responsible for the repression of *sox9b*. We performed functional regeneration studies using *sox9b* homozygous mutants to determine if the repression of sox9b itself is enough to impair regeneration. The amputated *sox9b* mutants regenerated their fin tissue by 3dpa, but with defective cartilaginous-like support structures and actinotrichia resulting in a delicate unsupported new tissue (Figure 8). Since SOX9 is also considered as a master regulator of chondrogenesis (Akiyama et al., 2002; Bi et al., 1999; Goldring et al., 2006), these results indicate that the reduced abundance of sox9b by Ahr activation could explain the impairment of cartilage like structures. Moreover, these results also implicate the involvement of other molecular factors downstream to R-Spondin1 and parallel to sox9b.

Discussion

Zebrafish caudal fin regeneration is a well established research model to understand the basic biological mechanisms of the remarkable phenomenon of regeneration. Similar to the adults, early life stage larvae (2dpf) also completely regenerate caudal fins following amputation (Kawakami et al., 2004; Mathew et al., 2006). We have reported that TCDD inhibits both life stages of caudal fin regeneration. The toxicity studies associated with exposure to halogenated aromatic hydrocarbons such as TCDD have resulted in the identification of Ahr as an essential ligand activated transcription factor that mediates most if not all of the toxic effects of TCDD. What remain mostly unknown are the molecular events downstream of Ahr activation that elicits adverse tissue specific responses. To address this information gap, we have exploited TCDD-dependent block in fin regeneration in order to identify the molecular signaling pathways impacted after Ahr activation (Mathew et al., 2006; Zodrow and Tanguay, 2003). In addition to the effect of TCDD on zebrafish fin regeneration, a previous report has demonstrated that treatment of mice with TCDD after partial hepatectomy resulted in the suppression of liver regeneration (Mitchell et al., 2006).

Therefore, since TCDD has a global effect on tissue regeneration, identification of the signaling pathways that cross talk with Ahr will also provide a better understanding of the basic regeneration pathways. Global gene expression analysis in the adult fin regeneration after TCDD exposure suggests that Ahr activation modulates a cluster of genes involved in cellular differentiation and extracellular matrix metabolism (Andreasen et al., 2006). To understand whether the larval fin regeneration is also affected by TCDD at a similar molecular level, we performed microarray analysis in the early life stage regeneration model after TCDD exposure. Similarly to the adult model, TCDD most profoundly altered the abundance of transcripts involved in signal transduction, metabolism and composition of the extracellular matrix during larval fin regeneration.

Comparative analysis performed between the two caudal fin regeneration models revealed a strong similarity in the pattern of gene expression between these two platforms in response to TCDD, even with distinct tissue architecture. Antisense repression of R-Spondin1 resulted in the inability of TCDD to impair regeneration indicating that mis-induction of this gene was absolutely required for Ahr activation to inhibit regeneration. R-Spondin family belongs to a new class of secreted proteins including four members (R-Spondin1-4) and each contains a leading N-terminal signal peptide, two furin-type cysteine rich domains, one thrombospondin type domain and a C-terminal basic amino acid rich domain (Kamata et al., 2004; Kazanskaya et al., 2004). R-Spondins have been identified as novel ligands for the Fdz/LRP receptor complex and induces the β-catenin/TCF dependent gene activation (Kim et al., 2006). Recent studies suggest that human R-Spondin1 is a high affinity ligand for LRP6 and binding of this ligand to the receptor results in the phosphorylation of LRP6 and activation of β-catenin signaling (Wei et al., 2007). However, another recent study conflicts with the previous report and suggests that R-Spondin1 does not directly interact with LRP6, but instead prevents the DKK1/Kremen-mediated internalization of LRP6 thereby facilitating increased LRP6 levels on the cell surface(Binnerts et al., 2007). But both studies acknowledge that LRP6 is required for R-Spondin1 signaling. Even though R-Spondins act through β-catenin stabilization and may synergize with Wnt proteins, multiple *in vitro* and *in vivo* studies in different species suggest that the effect may not be completely dependent on the canonical Wnt signaling pathway (Kazanskaya et al., 2004; Nam et al., 2006). In addition

to human and mouse, R-Spondins have also been identified in other vertebrates such as rat, zebrafish, xenopus and chicken.

Since LRP6 is required for R-Spondin1 signaling, we further tested the functional requirement of LRP6 in the AHR activation mediated inhibition of fin regeneration phenomenon. We observed that partial suppression of LRP6 is sufficient to prevent the inhibitory effect of TCDD on fin regeneration. This demonstrates that R-Spondin1 requires LRP6 to mediate its effect and also underscore our hypothesis that Ahr activation improperly activates the canonical Wnt signaling pathway. These results are very important as a previous study has reported that increased Wnt/β-catenin signaling augments adult zebrafish fin regeneration (Stoick-Cooper et al., 2007). However, our results suggest that over activation of Wnt/β-catenin signaling impairs regeneration. This leads to a question about the threshold level of the Wnt signaling pathway that is required for the completion of the regenerative process. To confirm our results that over activation of Wnt/ β-catenin signaling impairs regeneration, we tested a chemical BIO that is referred to as a small molecule that activates the Wnt/β-catenin signaling pathway by the inhibition of GSK-3 (Meijer et al., 2003; Sato et al., 2004; Tseng et al., 2006). BIO inhibited larval fin regeneration when compared to the vehicle-exposed larvae (Figure 7A), emphasizing our finding that over activation of Wnt/β-catenin signaling impairs regeneration. Analysis of molecular markers suggests that in both TCDD and BIO exposed animals, the expression of *dlx5a*, *msxe* and *raldh2* that defines the wound epithelium and blastema respectively, were lost (Figure 7B). These results suggest that over activation Wnt signaling pathway affects the blastema formation by inhibiting the cellular differentiation process. In support to our speculation, previous studies have reported that even though Wnt signaling is required for hematopoietic stem cell self-renewal, constitutive activation of β-catenin signaling caused multilineage differentiation block impacting the stem cell maintenance (Kirstetter et al., 2006; Scheller et al., 2006). Another recent study demonstrated that muscle stem cells from aged mice convert from a myogenic to fibrogenic lineage resulting in tissue fibrosis and the lineage conversion is associated with activation of canonical Wnt signaling pathway (Brack et al., 2007). Altogether, these studies support that inappropriate activation of Wnt /β-catenin signaling impacts the differentiation process during fin regeneration.

The functional importance of R-Spondin genes were revealed by two recent genetic studies that described different mutations of R-Spondins have been associated with human disease conditions. A rare autosomal recessive condition known as anonychia is linked to the mutation of R-Spo4 and another recessive syndrome characterized by XX sex reversal, palmoplantar hyperkeratosis and predisposition to squamous cell carcinoma is due to the mutation of R-Spondin1(Blaydon et al., 2006; Parma et al., 2006). Mutation of R-Spondin1 causes the XX sex reversal to male and this impact is speculated to be due to the induction of SOX9 promoting the testis development. More clearly, it's been proposed that R-Spondin1 regulates the expression of SOX9 and the mutation of R-Spondin1 resulted in the inappropriate induction of SOX9 levels which indeed resulted in the XX sex reversal (Parma et al., 2006). Therefore, normal expression of R-Spondin1 will result in the repression of SOX9 which will lead to the proper development of the female gonads. These human studies are consistent with our earlier supposition that Ahr-dependent increased expression of R-Spondin1 directly leads to decreased expression of Sox9b. Moreover, SOX9 is also reported to be a Wnt target gene (Blache et al., 2004; Hill et al., 2005; Yano et al., 2005) and hence we propose that the reduced level of Sox9b is caused by the inappropriate induction of R-Spondin1. In addition to the fact that SOX9 is a Wnt target gene and regulated by R-Spondin1, SOX9 is a transcription factor as well as a master regulator that controls chondrogenesis and extracellular matrix composition (ECM) (Akiyama Ddagger et al., 2005; Bi et al., 1999; Goldring et al., 2006; Lefebvre et al., 1997; Mori-Akiyama et al., 2003; Murakami et al., 2000; Tsuchiya et al., 2003). Also, *sox9b* expression in the basal epidermal cell layer of the distal part of the adult regenerating fin tissue has been previously reported (Smith et al., 2006). However, *sox9b* mutants regenerated their fin tissue with defective chondrogenesis, suggesting that mis-expression of *sox9b* which is a regulator of ECM production or cell differentiation could explain the TCDD-dependent changes in ECM transcript abundance and the observed pathology.

In addition to our report of improper activation of Wnt signaling by Ahr activation, other studies have demonstrated the interference of AHR with other developmental signaling pathways. AHR influences TGF-β signaling members in a ligand dependent or independent manner (Chang et al., 2007; Puga et al., 2005; Thomae

et al., 2005). A recent report has illustrated the ligand independent role of AHR in reversing the proliferative and gene expression phenotype of Ahr-/- fibroblasts by inhibiting TGF-β signaling (Chang et al., 2007). Also, another i*n vitro* study has demonstrated that addition of TGFbeta3 into the palate culture model completely prevented the TCDD-mediated block of palatal fusion (Thomae et al., 2005). However, our report is the first to demonstrate the complete reversal of an adverse *in vivo* outcome of Ahr activation by modulating the expression of a single gene and categorically establish the functional crosstalk between Ahr and Wnt signaling pathways (Figure 9). It is noteworthy to mention that mis-regulation of Wnt signaling causes a wide variety of adverse effects such as developmental defects and cancer and these new findings put forward the potential role of environmental AHR ligands in the etiology of different disease conditions. Also, these results demonstrate the absolute requirement of a fine balance of Wnt signaling for the process of epimorphic regeneration (Figure 9). Altogether, our studies demonstrate the power of the zebrafish model to dissect the mechanisms that underlie the *in vivo* responses to environmental exposures.

References

Akimenko MA, Mari-Beffa M, Becerra J and Geraudie J (2003) Old questions, new tools, and some answers to the mystery of fin regeneration. *Dev Dyn* **226**(2):190-201.

Akiyama Ddagger H, Kim Ddagger JE, Nakashima K, Balmes G, Iwai N, Deng JM, Zhang Z, Martin JF, Behringer RR, Nakamura T and de Crombrugghe B (2005) Osteo-chondroprogenitor cells are derived from Sox9 expressing precursors. *Proc Natl Acad Sci U S A* **102**(41):14665-14670.

Akiyama H, Chaboissier MC, Martin JF, Schedl A and de Crombrugghe B (2002) The transcription factor Sox9 has essential roles in successive steps of the chondrocyte differentiation pathway and is required for expression of Sox5 and Sox6. *Genes Dev* **16**(21):2813-2828.

Andreasen EA, Mathew LK, Lohr CV, Hasson R and Tanguay RL (2007) Aryl hydrocarbon receptor activation impairs extracellular matrix remodeling during zebra fish fin regeneration. *Toxicol Sci* **95**(1):215-226.

Andreasen EA, Mathew LK and Tanguay RL (2006) Regenerative Growth is Impacted by TCDD: Gene Expression Analysis Reveals Extracellular Matrix Modulation. *Toxicol Sci* **92**(1):254-269.

Bi W, Deng JM, Zhang Z, Behringer RR and de Crombrugghe B (1999) Sox9 is required for cartilage formation. *Nat Genet* **22**(1):85-89.

Binnerts ME, Kim KA, Bright JM, Patel SM, Tran K, Zhou M, Leung JM, Liu Y, Lomas WE, 3rd, Dixon M, Hazell SA, Wagle M, Nie WS, Tomasevic N, Williams J, Zhan X, Levy MD, Funk WD and Abo A (2007) R-Spondin1 regulates Wnt signaling by inhibiting internalization of LRP6. *Proc Natl Acad Sci U S A*.

Blache P, van de Wetering M, Duluc I, Domon C, Berta P, Freund JN, Clevers H and Jay P (2004) SOX9 is an intestine crypt transcription factor, is regulated by the Wnt pathway, and represses the CDX2 and MUC2 genes. *J Cell Biol* **166**(1):37-47.

Blaydon DC, Ishii Y, O'Toole E A, Unsworth HC, Teh MT, Ruschendorf F, Sinclair C, Hopsu-Havu VK, Tidman N, Moss C, Watson R, de Berker D, Wajid M, Christiano AM and Kelsell DP (2006) The gene encoding R-spondin 4 (RSPO4), a secreted protein implicated in Wnt signaling, is mutated in inherited anonychia. *Nat Genet*.

Brack AS, Conboy MJ, Roy S, Lee M, Kuo CJ, Keller C and Rando TA (2007) Increased Wnt signaling during aging alters muscle stem cell fate and increases fibrosis. *Science* **317**(5839):807-810.

Burbach KM, Poland A and Bradfield CA (1992) Cloning of the Ah-receptor cDNA reveals a distinctive ligand-activated transcription factor. *Proc Natl Acad Sci U S A* **89**(17):8185-8189.

Chang X, Fan Y, Karyala S, Schwemberger S, Tomlinson CR, Sartor MA and Puga A (2007) Ligand-independent regulation of transforming growth factor beta1 expression and cell cycle progression by the aryl hydrocarbon receptor. *Mol Cell Biol* **27**(17):6127-6139.

Day TF, Guo X, Garrett-Beal L and Yang Y (2005) Wnt/beta-catenin signaling in mesenchymal progenitors controls osteoblast and chondrocyte differentiation during vertebrate skeletogenesis. *Dev Cell* **8**(5):739-750.

Goldring MB, Tsuchimochi K and Ijiri K (2006) The control of chondrogenesis. *J Cell Biochem* **97**(1):33-44.

Hankinson O (1994) The role of the aryl hydrocarbon nuclear receptor protein in aryl hydrocarbon receptor action. *TEM* **5**(6):240-244.

Henry EC and Gasiewicz TA (1993) Transformation of the aryl hydrocarbon receptor to a DNA-binding form is accompanied by release of the 90 kDa heat-shock protein and increased affinity for 2,3,7,8-tetrachlorodibenzo-p-dioxin. *Biochem J* **294**(Pt 1):95-101.

Hill TP, Spater D, Taketo MM, Birchmeier W and Hartmann C (2005) Canonical Wnt/beta-catenin signaling prevents osteoblasts from differentiating into chondrocytes. *Dev Cell* **8**(5):727-738.

Kamata T, Katsube K, Michikawa M, Yamada M, Takada S and Mizusawa H (2004) R-spondin, a novel gene with thrombospondin type 1 domain, was expressed in the dorsal neural tube and affected in Wnts mutants. *Biochim Biophys Acta* **1676**(1):51-62.

Kawakami A, Fukazawa T and Takeda H (2004) Early fin primordia of zebrafish larvae regenerate by a similar growth control mechanism with adult regeneration. *Dev Dyn* **231**(4):693-699.

Kazanskaya O, Glinka A, del Barco Barrantes I, Stannek P, Niehrs C and Wu W (2004) R-Spondin2 is a secreted activator of Wnt/beta-catenin signaling and is required for Xenopus myogenesis. *Dev Cell* **7**(4):525-534.

Kim KA, Zhao J, Andarmani S, Kakitani M, Oshima T, Binnerts ME, Abo A, Tomizuka K and Funk WD (2006) R-Spondin proteins: a novel link to beta-catenin activation. *Cell Cycle* **5**(1):23-26.

Kirstetter P, Anderson K, Porse BT, Jacobsen SE and Nerlov C (2006) Activation of the canonical Wnt pathway leads to loss of hematopoietic stem cell repopulation and multilineage differentiation block. *Nat Immunol* **7**(10):1048-1056.

Lefebvre V, Huang W, Harley VR, Goodfellow PN and de Crombrugghe B (1997) SOX9 is a potent activator of the chondrocyte-specific enhancer of the pro alpha1(II) collagen gene. *Mol Cell Biol* **17**(4):2336-2346.

Mari-Beffa M, Mateos I, Palmqvist P and Becerra J (1996) Cell to cell interactions during teleosts fin regeneration. *Int J Dev Biol* **Suppl 1**:179S-180S.

Mathew LK, Andreasen EA and Tanguay RL (2006) Aryl hydrocarbon receptor activation inhibits regenerative growth. *Mol Pharmacol* **69**(1):257-265.

Meijer L, Skaltsounis AL, Magiatis P, Polychronopoulos P, Knockaert M, Leost M, Ryan XP, Vonica CA, Brivanlou A, Dajani R, Crovace C, Tarricone C, Musacchio A, Roe SM, Pearl L and Greengard P (2003) GSK-3-selective inhibitors derived from Tyrian purple indirubins. *Chem Biol* **10**(12):1255-1266.

Mescher AL (1996) The cellular basis of limb regeneration in urodeles. *Int J Dev Biol* **40**(4):785-795.

Mitchell KA, Lockhart CA, Huang G and Elferink CJ (2006) Sustained aryl hydrocarbon receptor activity attenuates liver regeneration. *Mol Pharmacol* **70**(1):163-170.

Mori-Akiyama Y, Akiyama H, Rowitch DH and de Crombrugghe B (2003) Sox9 is required for determination of the chondrogenic cell lineage in the cranial neural crest. *Proc Natl Acad Sci U S A* **100**(16):9360-9365.

Murakami S, Lefebvre V and de Crombrugghe B (2000) Potent inhibition of the master chondrogenic factor Sox9 gene by interleukin-1 and tumor necrosis factor-alpha. *J Biol Chem* **275**(5):3687-3692.

Nakatani Y, Kawakami A and Kudo A (2007) Cellular and molecular processes of regeneration, with special emphasis on fish fins. *Dev Growth Differ* **49**(2):145-154.

Nam JS, Turcotte TJ, Smith PF, Choi S and Yoon JK (2006) Mouse cristin/R-spondin family proteins are novel ligands for the Frizzled 8 and LRP6 receptors and activate beta-catenin-dependent gene expression. *J Biol Chem* **281**(19):13247-13257.

Nasevicius A and Ekker SC (2000) Effective targeted gene 'knockdown' in zebrafish. *Nat Genet* **26**(2):216-220.

Parma P, Radi O, Vidal V, Chaboissier MC, Dellambra E, Valentini S, Guerra L, Schedl A and Camerino G (2006) R-spondin1 is essential in sex determination, skin differentiation and malignancy. *Nat Genet*.

Poss KD, Shen J and Keating MT (2000a) Induction of lef1 during zebrafish fin regeneration. *Dev Dyn* **219**(2):282-286.

Poss KD, Shen J, Nechiporuk A, McMahon G, Thisse B, Thisse C and Keating MT (2000b) Roles for Fgf signaling during zebrafish fin regeneration. *Dev Biol* **222**(2):347-358.

Puga A, Tomlinson CR and Xia Y (2005) Ah receptor signals cross-talk with multiple developmental pathways. *Biochem Pharmacol* **69**(2):199-207.

Santamaria JA and Becerra J (1991) Tail fin regeneration in teleosts: cell-extracellular matrix interaction in blastemal differentiation. *J Anat* **176**:9-21.

Santamaria JA, Mari-Beffa M, Santos-Ruiz L and Becerra J (1996) Incorporation of bromodeoxyuridine in regenerating fin tissue of the goldfish Carassius auratus. *J Exp Zool* **275**(4):300-307.

Santos-Ruiz L, Santamaria JA, Ruiz-Sanchez J and Becerra J (2002) Cell proliferation during blastema formation in the regenerating teleost fin. *Dev Dyn* **223**(2):262-272.

Sato N, Meijer L, Skaltsounis L, Greengard P and Brivanlou AH (2004) Maintenance of pluripotency in human and mouse embryonic stem cells through activation of Wnt signaling by a pharmacological GSK-3-specific inhibitor. *Nat Med* **10**(1):55-63.

Scheller M, Huelsken J, Rosenbauer F, Taketo MM, Birchmeier W, Tenen DG and Leutz A (2006) Hematopoietic stem cell and multilineage defects generated by constitutive beta-catenin activation. *Nat Immunol* **7**(10):1037-1047.

Schier AF, Neuhauss SC, Helde KA, Talbot WS and Driever W (1997) The one-eyed pinhead gene functions in mesoderm and endoderm formation in zebrafish and interacts with no tail. *Development* **124**(2):327-342.

Schmidt JV and Bradfield CA (1996) Ah receptor signaling pathways. *Ann Rev Cell Dev Biol* **12**:55-89.

Smith A, Avaron F, Guay D, Padhi BK and Akimenko MA (2006) Inhibition of BMP signaling during zebrafish fin regeneration disrupts fin growth and scleroblasts differentiation and function. *Dev Biol* **299**(2):438-454.

Stoick-Cooper CL, Weidinger G, Riehle KJ, Hubbert C, Major MB, Fausto N and Moon RT (2007) Distinct Wnt signaling pathways have opposing roles in appendage regeneration. *Development* **134**(3):479-489.

Thomae TL, Stevens EA and Bradfield CA (2005) Transforming growth factor-beta3 restores fusion in palatal shelves exposed to 2,3,7,8-tetrachlorodibenzo-p-dioxin. *J Biol Chem* **280**(13):12742-12746.

Tseng AS, Engel FB and Keating MT (2006) The GSK-3 inhibitor BIO promotes proliferation in mammalian cardiomyocytes. *Chem Biol* **13**(9):957-963.

Tsuchiya H, Kitoh H, Sugiura F and Ishiguro N (2003) Chondrogenesis enhanced by overexpression of sox9 gene in mouse bone marrow-derived mesenchymal stem cells. *Biochem Biophys Res Commun* **301**(2):338-343.

Wei Q, Yokota C, Semenov MV, Doble B, Woodgett J and He X (2007) R-spondin1 is a high affinity ligand for LRP6 and induces LRP6 phosphorylation and beta-catenin signaling. *J Biol Chem* **282**(21):15903-15911.

Westerfield, M. (1995) *The Zebrafish Book*. University of Oregon Press, Eugene, OR.

Whitehead GG, Makino S, Lien CL and Keating MT (2005) fgf20 is essential for initiating zebrafish fin regeneration. *Science* **310**(5756):1957-1960.

Yano F, Kugimiya F, Ohba S, Ikeda T, Chikuda H, Ogasawara T, Ogata N, Takato T, Nakamura K, Kawaguchi H and Chung UI (2005) The canonical Wnt signaling pathway promotes chondrocyte differentiation in a Sox9-dependent manner. *Biochem Biophys Res Commun* **333**(4):1300-1308.

Zhong N, Gersch RP and Hadjiargyrou M (2006) Wnt signaling activation during bone regeneration and the role of Dishevelled in chondrocyte proliferation and differentiation. *Bone*.

Zodrow JM and Tanguay RL (2003) 2,3,7,8-tetrachlorodibenzo-p-dioxin inhibits zebrafish caudal fin regeneration. *Toxicol Sci* **76**(1):151-161.

Acknowledgements

We would like to thank Anne-Marie Girard from the Center for Gene Research and Biotechnology at Oregon State University for her valuable assistance. We also would like to thank Dr. John H. Postlethwait (University of Oregon, Eugene, OR) for the *sox9b* mutant zebrafish line. This work was supported in part by NIEHS grants ES10820, ES00210, and ES03850, Oregon Medical Research Foundation grant and predoctoral fellowship from American Heart Association (LKM).

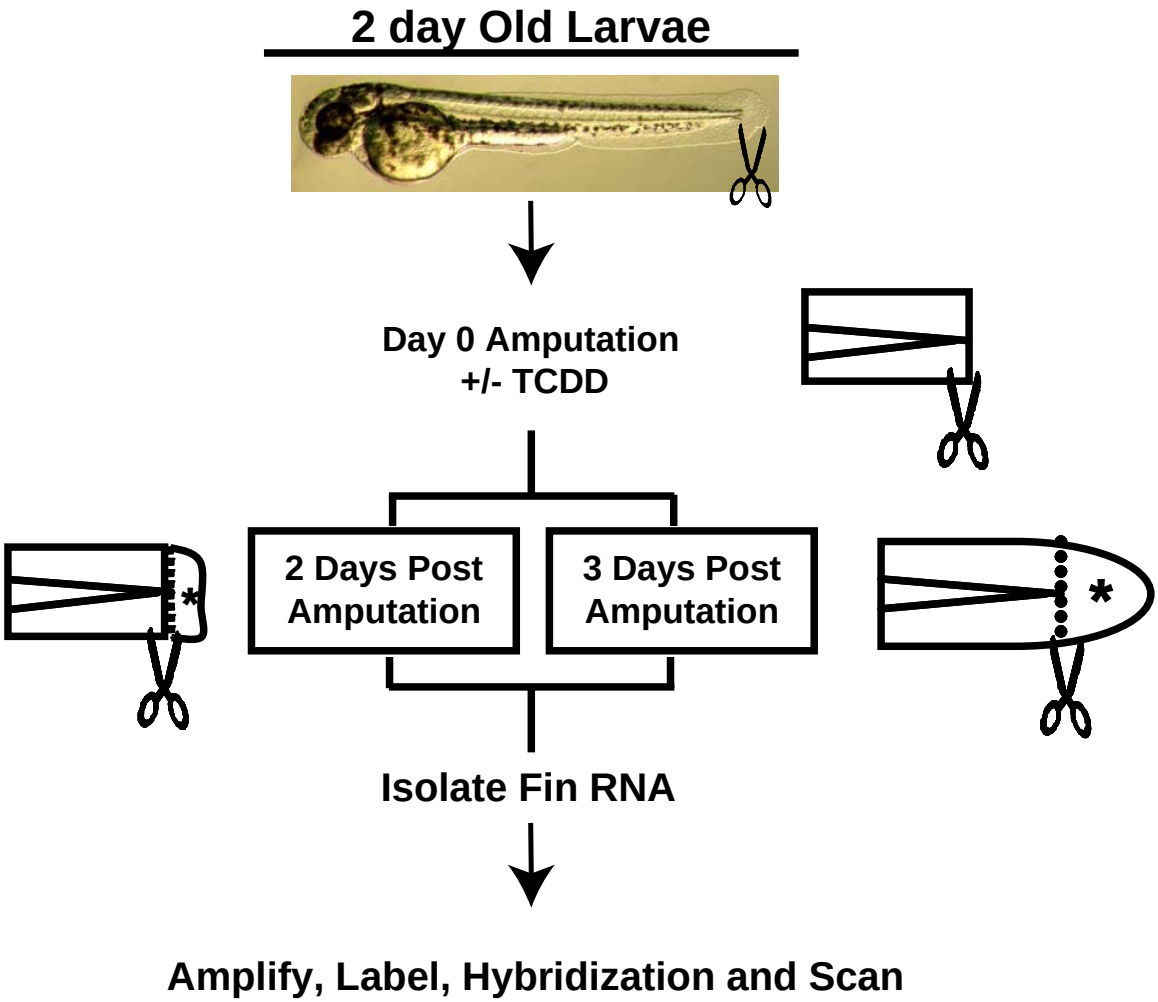

Figure 3-1. Experimental Design of Larval Microarray Analysis. This figure depicts a schematic representation of the microarray analysis from start to the end. Two day old larvae were amputated and exposed to vehicle or TCDD for an hour. Regenerating fin tissues from 150 larvae were pooled for each time point and treatment at 2dpa and 3dpa respectively and the samples were collected in triplicates. This was followed by two step amplification, labeling, hybridization and scanning of the results.

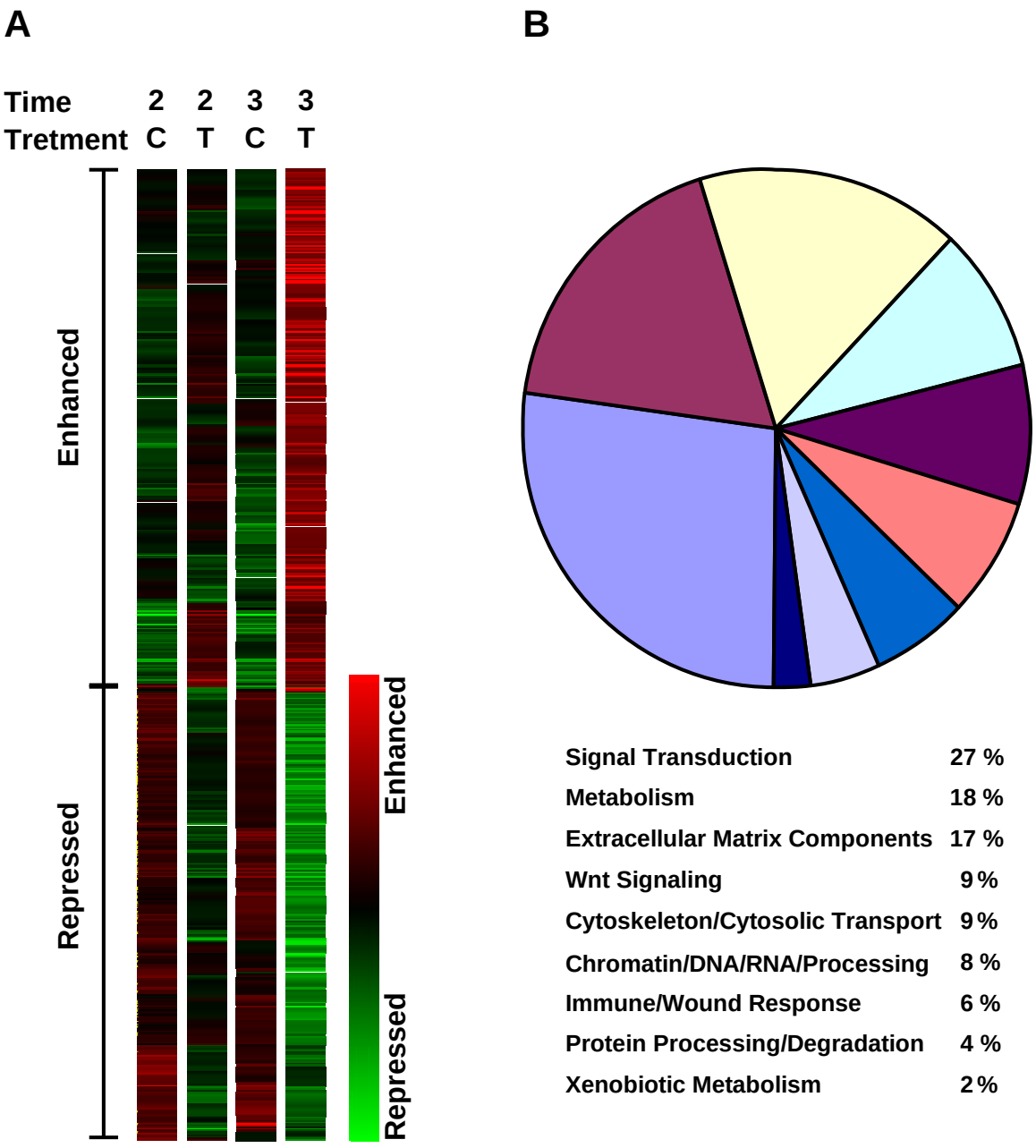

Figure 3-2. Heat map and pie graph depicting altered genes by TCDD exposure in the regenerating fin. A) Heat map illustrating the genes that were enhanced or repressed at least 1.7 fold due to TCDD exposure in comparison to their time matched vehicle controls in larval regenerating fins. One - Way ANOVA analysis assuming equal variance was conducted (n=3, $p<0.05$). Of the potential 14,234 transcripts, 1097 genes were differentially regulated between control or TCDD exposure. **B)** The differentially expressed genes by TCDD exposure were classified into different groups based on its function. C, Control; T, TCDD.

Figure 3-3. Validation of TCDD modulated genes by qRT-PCR in the larval regenerating fin tissue. Gene specific primers were used to quantify the differentially expressed genes using quantitative real-time PCR. The expression pattern of selected **A)** induced genes and **B)** repressed genes were analyzed by qRT-PCR. Not-amputated refers to time matched larval fins that were not amputated until tissue was collected for mRNA isolation. The abundance of each transcript levels were normalized to β-actin expression. One-was ANOVA analyses were performed separately to determine differences in the expression between amputation state and also if there was an effect of TCDD exposure during regeneration. Each bar represents the mean +/- SEM (n =3). If differences were detected, they were followed by Tukeys test. Asterisk (*) indicates significant difference at the same time in regeneration between vehicle (control) and TCDD exposed larvae ($p<0.05$). Letters (a, b) signify a difference between time matched uncut fins (not-amputated) and vehicle exposed fins ($p<0.05$).

3-3

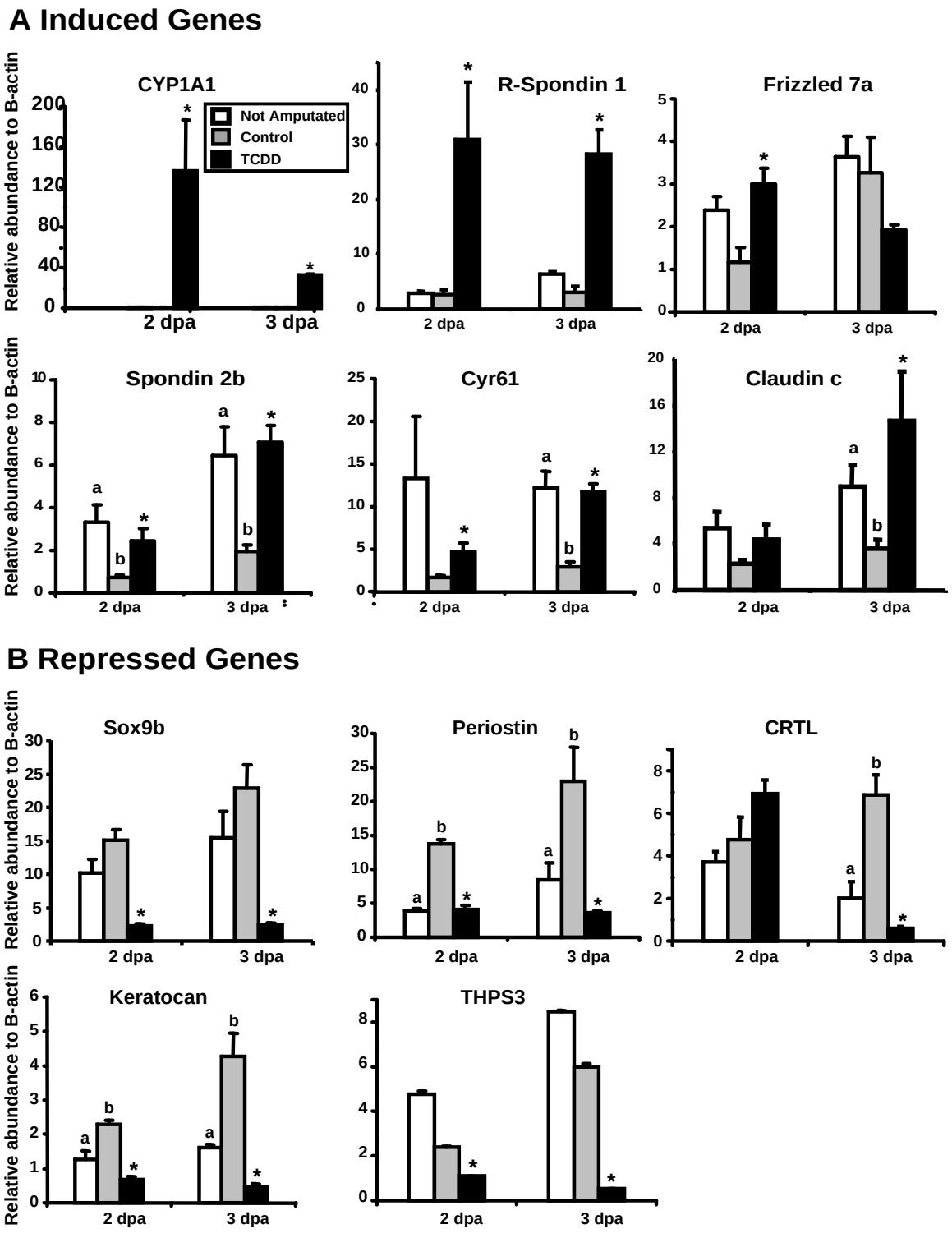
A Induced Genes
CYP1A1
R-Spondin 1
Frizzled 7a
Spondin 2b
Cyr61
Claudin c
Not Amputated
Control
TCDD
Relative abundance to B-actin
2 dpa
3 dpa
B Repressed Genes
Sox9b
Periostin
CRTL
Keratocan
THPS3

Figure 3-4. Partial antisense repression of *R-Spondin1* restores the regenerative ability in the presence of TCDD. A) The bold line at the intron-exon (I1-E2) boundary indicates the gene sequence targeted with the *R-Spondin1* splice variant MO. To analyze the splice blocking efficiency, forward and reverse primers (arrows at E1 and E3) were designed for RT-PCR. The splice variant MO should result in the loss of E2 to get a smaller misspliced PCR product. **B)** Control and zf *R-Spondin1* morphants were amputated at 2dpf and exposed to vehicle or TCDD. The fin regeneration images were taken at 3 dpa. Dotted line marks the plane of amputation. **C)** Analysis of *R-Spondin1* transcript in control and *R-Spondin1* morphants (3 days post fertilization) after qRT-PCR, followed by agarose gel electrophoresis (2%). The lower arrow points to the mispliced *R-Spondin1* variant after the loss of the targeted exon. β-actin expression was used as the loading control.

3-4

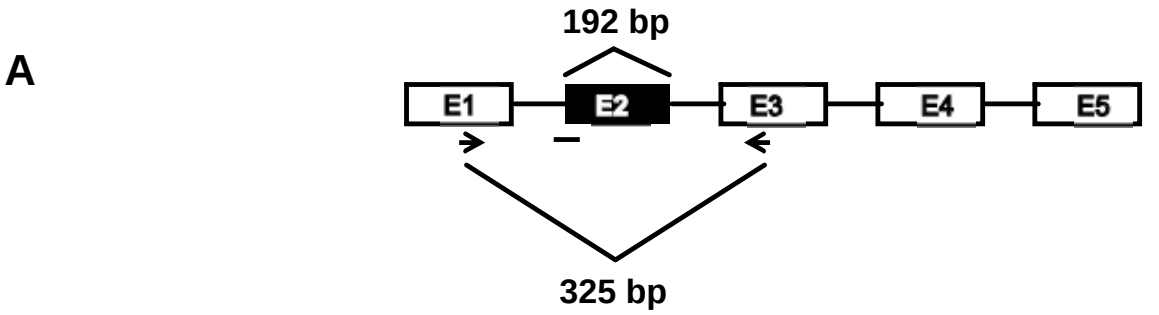
A
192 bp
E1
E2
E3
E4
E5
325 bp

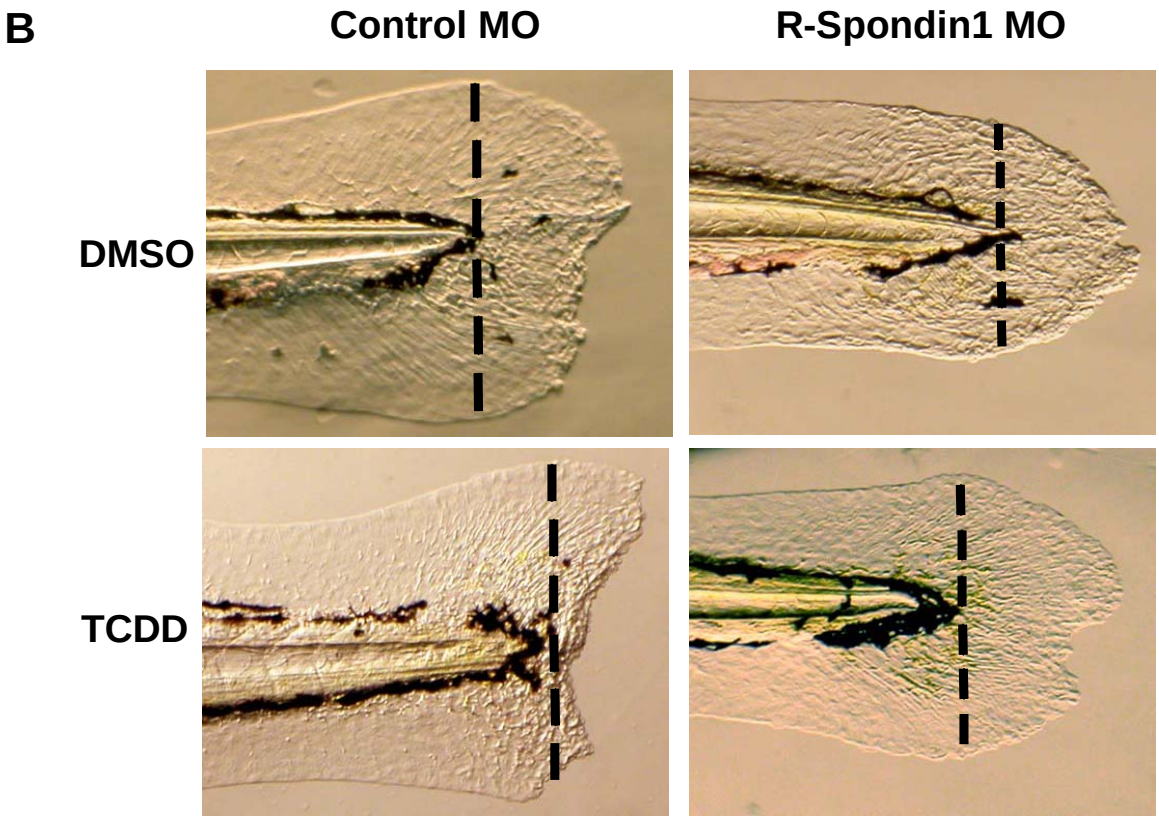
B
Control MO
R-Spondin1 MO
DMSO
TCDD

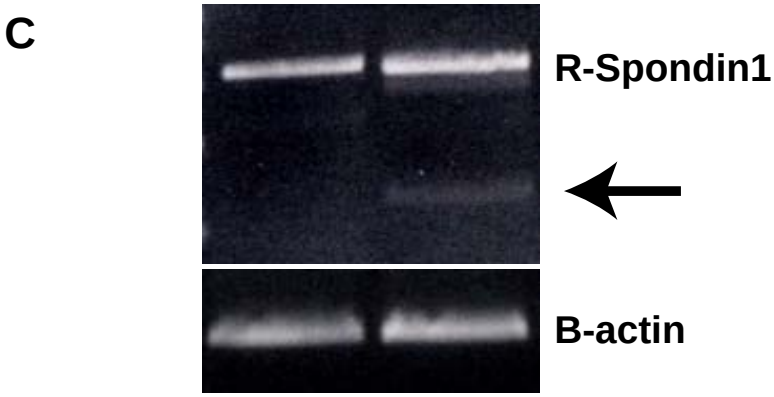
C
R-Spondin1
B-actin

Figure 3-5. LRP6 is required for TCDD to mediate inhibition of regeneration. A) A splice junction MO was designed to target LRP6 at the intron-exon (E3-I3) and the bold line depicts the targeted sequence. The splice variant MO should result in the loss of E3 to get a smaller misspliced PCR product. **B)** The control and zf LRP6 morphants were amputated at 2dpf and exposed to vehicle or TCDD. The fin regeneration images were acquired at 3 dpa and the dotted line marks the plane of amputation. **C)** The splice blocking efficiency was analyzed by RT-PCR with specific forward and reverse primers. The analysis of LRP6 transcript in control and LRP6 morphants (3 days post fertilization) was performed with RT-PCR, followed by agarose gel electrophoresis (2%).Eventhough non-quantitative, a clear reduction of the LRP6 primary transcript was found in the LRP6 morphants. The lower arrow points to the mispliced LRP6 variant after the loss of the targeted exon. β-actin expression was used as the loading control.

3-5

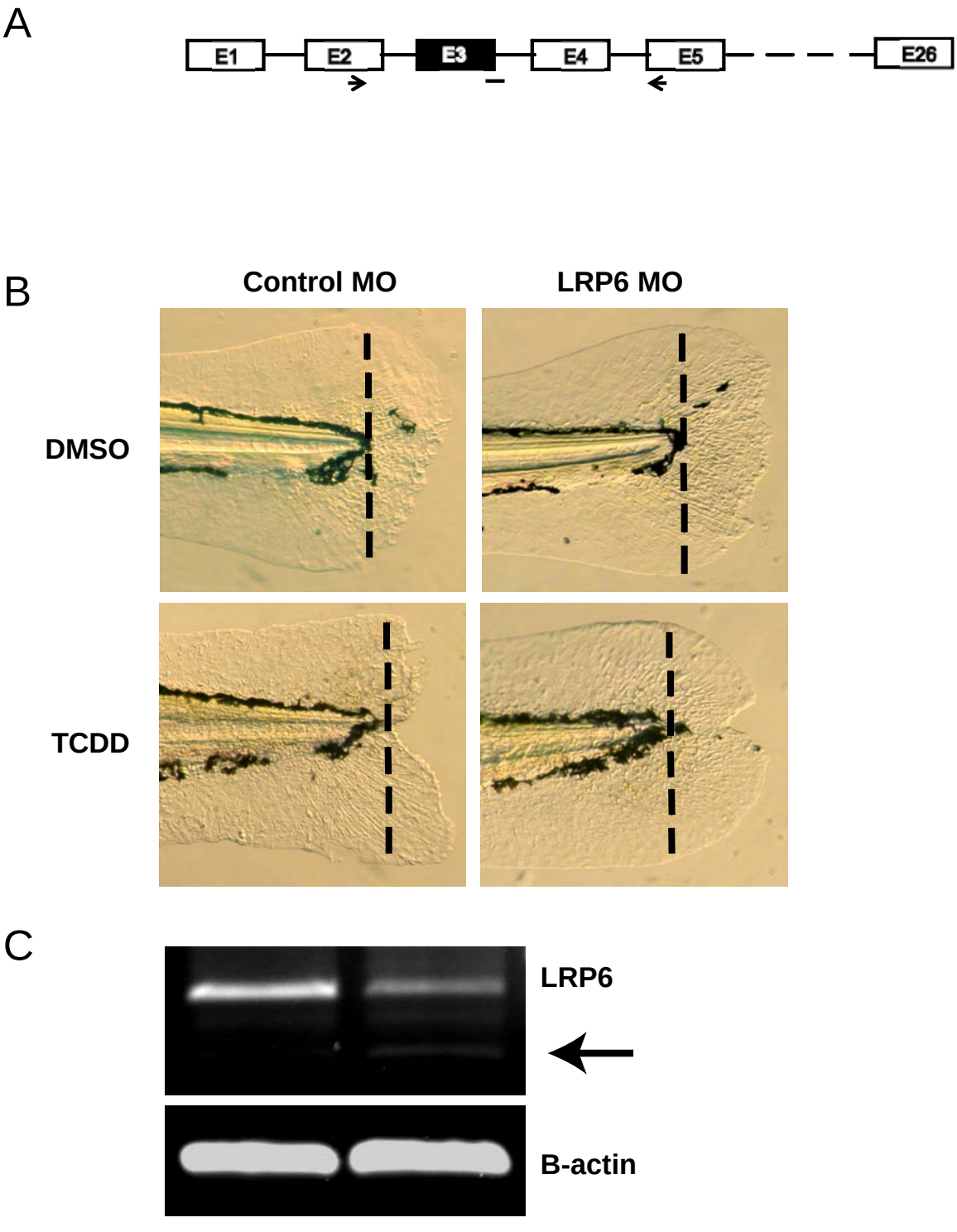

Figure 3-6. GSK3 inhibitor BIO impairs regeneration. A) Two day old larvae were amputated and exposed to vehicle or BIO (6-bromoindirubin-3'-oxime)(GSK3 inhibitor) continuously. The images depicted here are representative images acquired at 3 dpa. **B)** In situ hybridization with *dlx5a*, *msxe* and *raldh2* was performed to analyze the integrity of wound healing and blastema formation after exposure to TCDD and BIO at 1dpa. The images are representative of multiple experiments and more than 25 images per treatment.

3-6

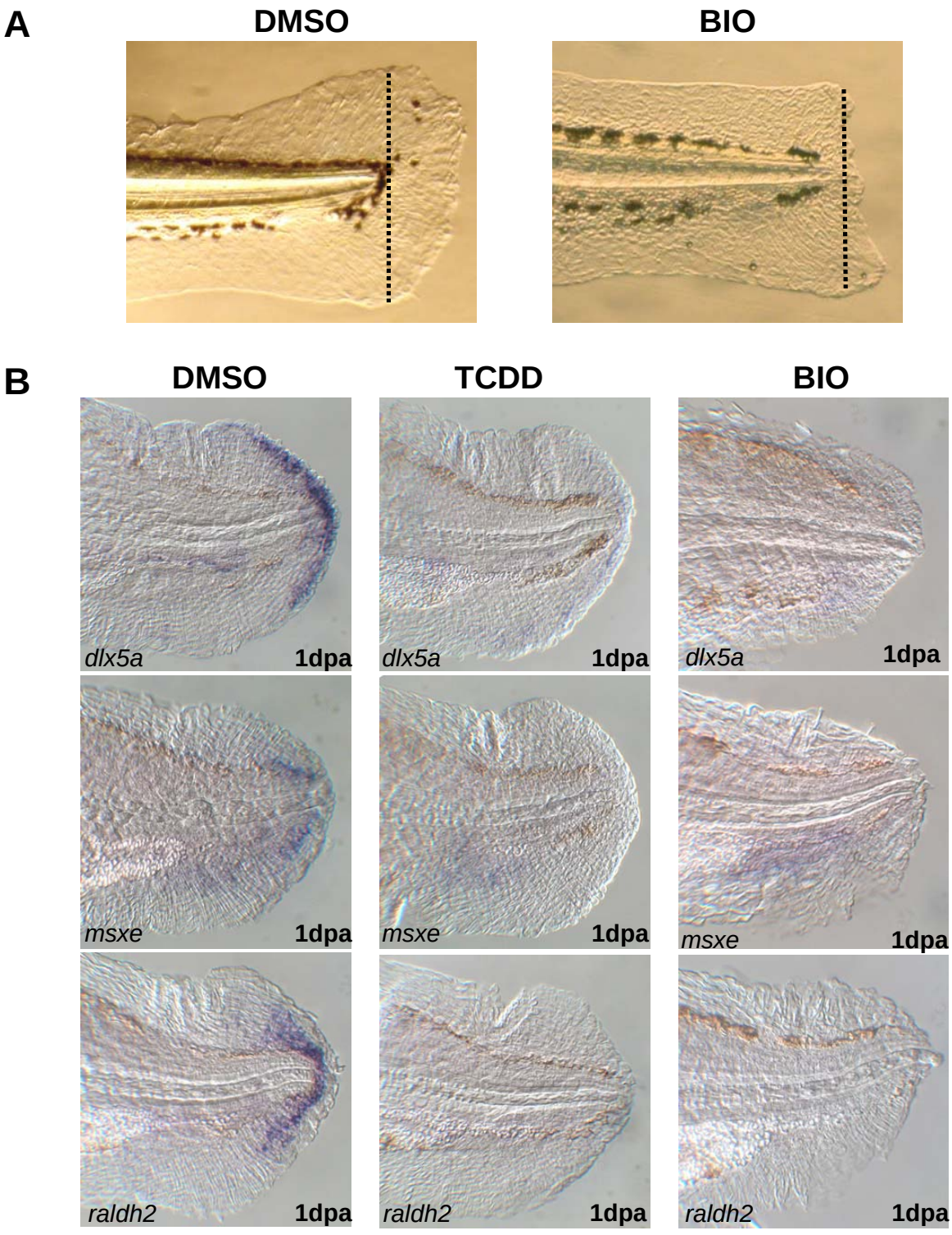

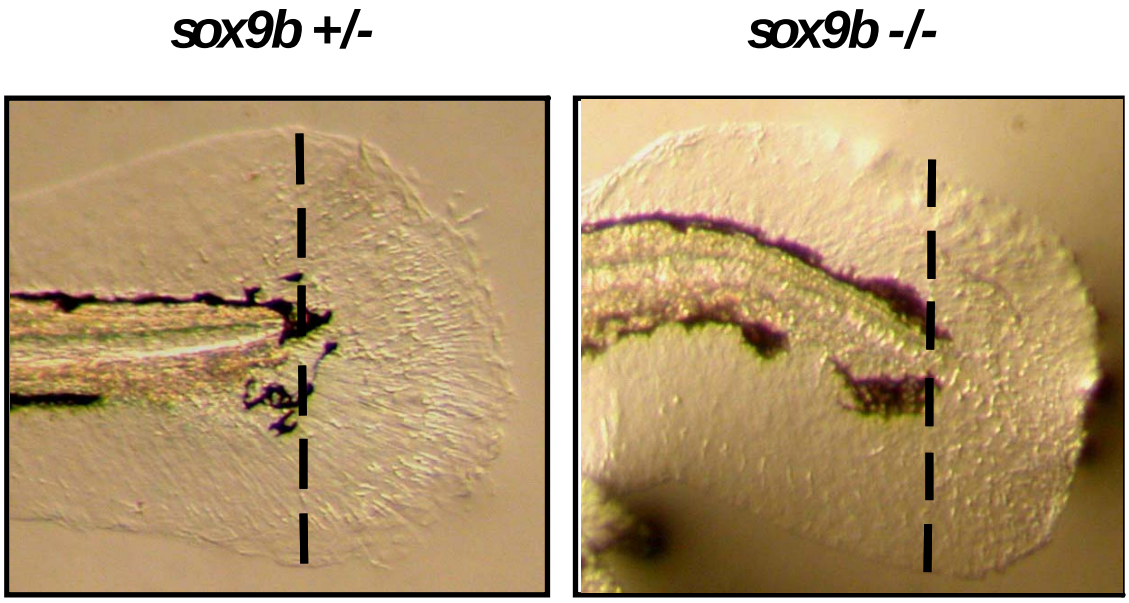

Figure 3-7. *Sox9b* homozygous mutants are not defective of regenerative outgrowth. Homozygous and heterozygous *sox9b* mutants were amputated at 48hpf and allowed to regenerate for 3 days. The images depicted here are representative of pictures taken at 3 dpa.

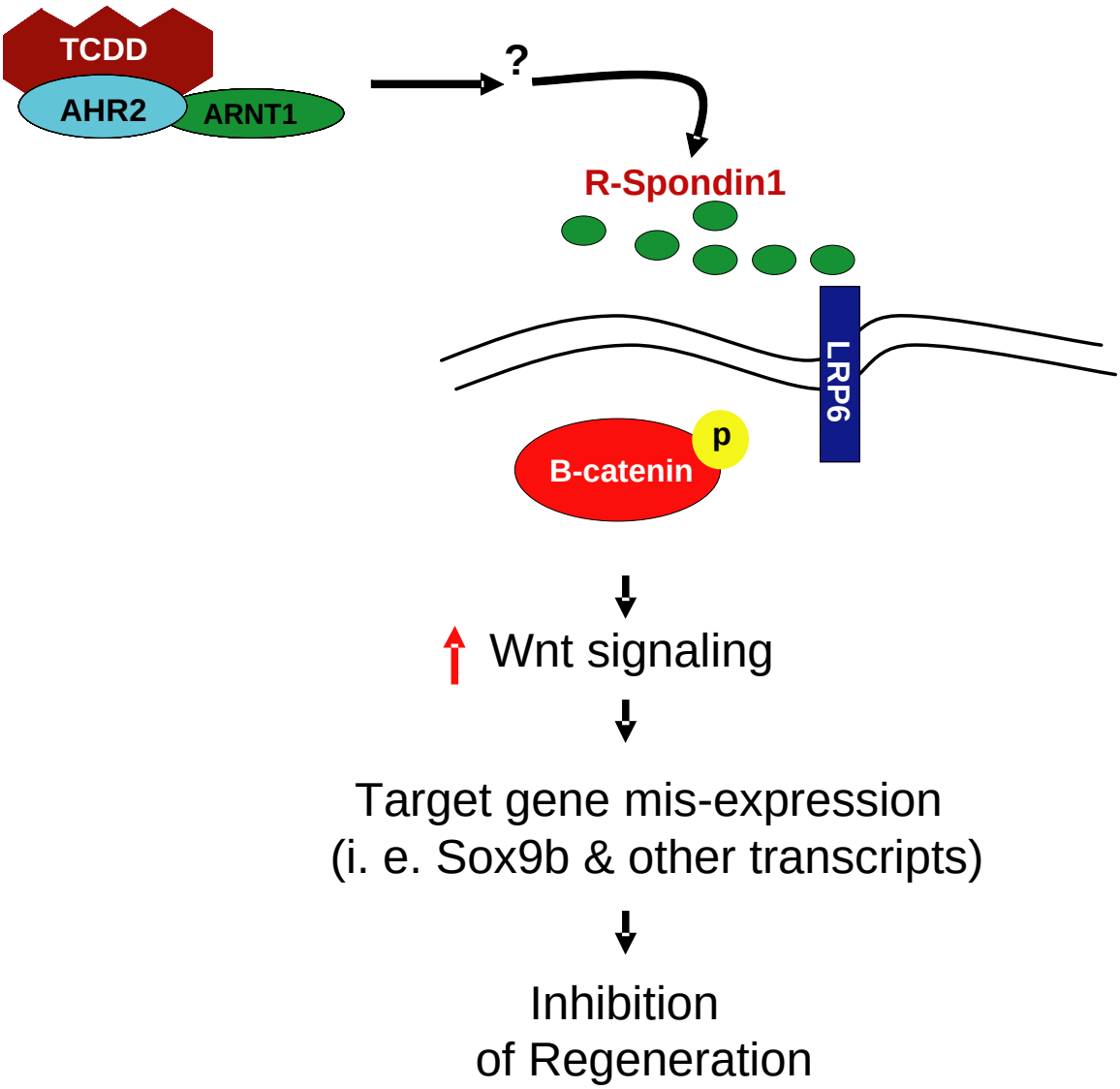

Figure 3-8. Proposed model of mechanism. AHR activation during fin regeneration improperly expresses R-Spondin1, which mediates through LRP6 to activate the Wnt/ β-catenin signaling. Activation of Wnt/ β-catenin signaling results in the phosphorylation of β-catenin which in turn causes the mis-expression of various Wnt target genes including sox9b. The functional consequences of these events collectively results in inhibition of fin regeneration.

Table 3-1. Wnt signaling pathway members and target genes altered by TCDD exposure in the two fin regeneration models.

Table 1. Wnt Signaling Pathway Members and Target Genes

	Fold Difference (p Value)									
	Larvae				Adult					
Wnt Pathway Members	2 dpa		3 dpa		1 dpa		3 dpa		5 dpa	
R-spondin-1	9.02	0.04	15.41	0.01	9.40	0.01	20.46	0.00	15.29	0.00
TCI (C8orf4)			7.82	0.05						
Dickkopf-1			3.35	0.02						
Frizzled 7a	3.45	0.02	3.16	0.00	5.44	0.01	3.84	0.00	3.10	0.01
WNT inhibitory factor 1			2.93	0.01						
Casein kinase 1, epsilon			2.51	0.01						
SOX3	2.79	0.04	2.56	0.02					1.95	0.03
Frizzled 10	0.58	0.05	0.33	0.01						
Frizzled 8a			0.47	0.05						
wnt11r									0.32	0.00
Wnt Target Genes										
Fgf20a			11.20	0.02					2.98	0.02
jagged1a			6.23	0.04					2.20	0.03
Claudin-1			3.94	0.01						
VEGF			3.82	0.01						
Cycloxygenase 2	2.03	0.03	3.29	0.02						
Glucagon			3.12	0.02						
Cholecystokinin			2.86	0.00	5.62	0.01	6.35	0.01	4.18	0.02
Follistatin			2.83	0.01						
CYR 61			2.64	0.01					0.22	0.03
CTGF			2.26	0.01						
Thrombospondin-1	2.26	0.04	2.17	0.01						
TIMP2	1.96	0.04	2.01	0.01					2.77	0.05
Sox9b	0.04	0.02	0.17	0.02	0.11	0.02	0.07	(<0.01)	0.09	(<0.01)
cyp26a1									0.26	0.00
Runx2a									0.40	0.00
twist1									0.35	0.01
c-jun									0.49	0.03
Lysyl oxidase			0.10	0.01	0.42	0.01			0.46	0.05
Connexin 43			0.55	0.02	0.54	0.01	0.22	(<0.01)	0.31	(<0.01)
Col11a1			0.19	0.02	0.37	0.02	0.40	0.02		
Periostin	0.45	0.04	0.36	0.04						
dapper 2							0.35	0.00		
IGF-2							0.47	0.02		
cmyc							0.50	0.00		
Snail1a			0.48	0.01			0.52	(<0.01)		

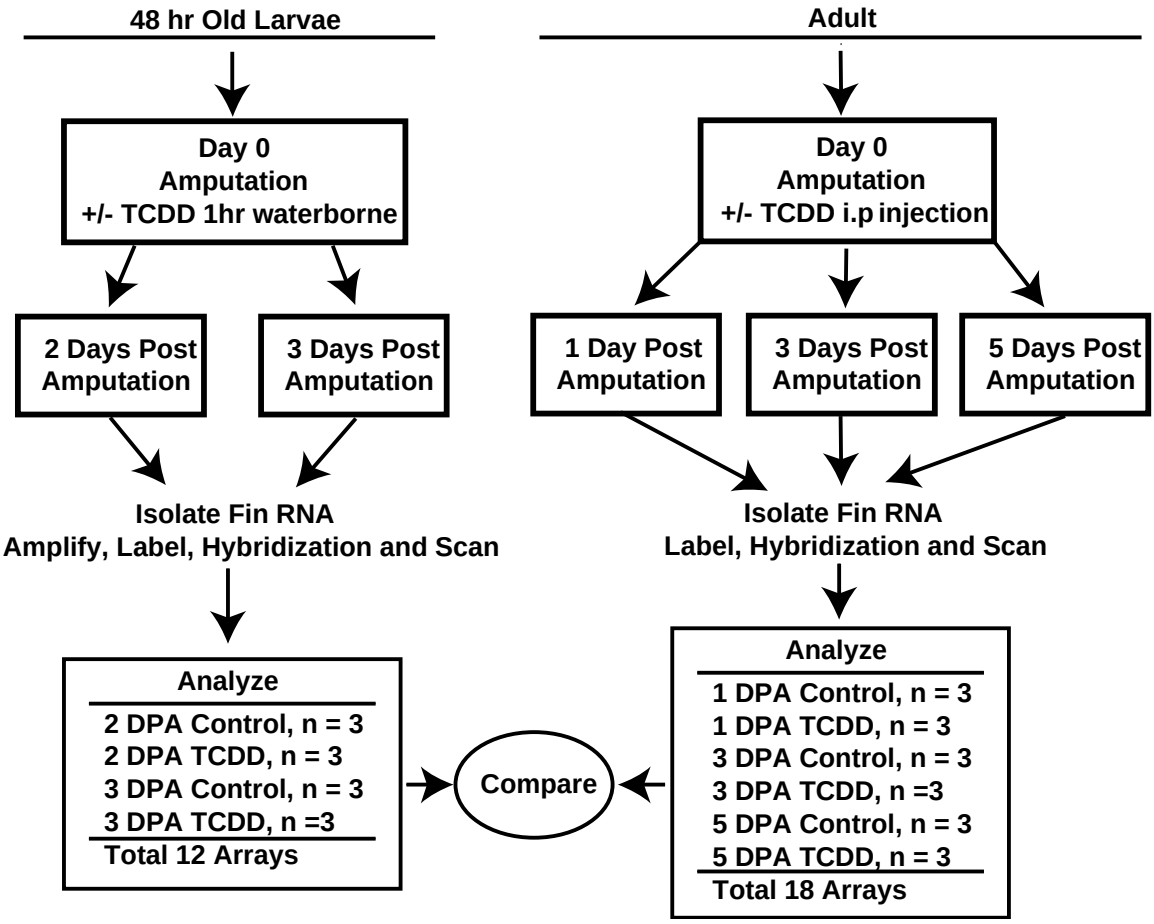

Figure 3S-1. Comparative toxicogenomic analysis. Schematic diagram for Affymetrix microarray analysis of larval and adult regenerating fin tissue. The larvae were amputated at 2dpf, followed by the exposure with DMSO (Control) or TCDD (0.5ng/mL). Three groups, each comprising of regenerating fin tissue from 150 larvae were isolated for each time and treatment. 100 ng of total RNA was used to generate biotinylated complementary RNA (cRNA) for each group using the Two-Cycle Target Labeling kit (Affymetrix, Santa Clara, CA). Adult fins were amputated and the fish i.p. dosed with vehicle or TCDD (50 ng/g) and the regenerating fins were collected 1, 3 and 5 days after amputation and dosing. 10 fins were pooled per time and treatment in triplicate. 2.5 µg of total RNA was used to generate biotylated cRNA using the 1-Cycle Target Labeling kit (Affymetrix, Santa Clara, CA). Common responses to TCDD were then revealed by first comparing microarray results within a life stage and then between larval and adult life stages.

Table 3S-1. Genes Enhanced at Least 1.7 Fold by TCDD Exposure in Larval Regenerating Fins.

Gene	Affymetrix	Fold Induced (p Value) 2 DPA		3DPA	
Xenobiotic Metabolism					
CYP1A	Dr.9478.1.S1_at	163.6	(0.01)	194.5	< (0.01)
CYP1C1	Dr.12329.1.A1_at	56.36	(0.02)	40.90	(0.03)
Cytochrome b5	Dr.5040.1.S1_at			6.73	(0.01)
UDPGT	Dr.5410.1.A1_at	17.06	(0.01)	10.44	(0.02)
CYP1B	DrAffx.2.29.S1_at	8.84	(0.02)	6.07	(0.01)
Sulfotransferase	Dr.3583.1.S1_at	2.34	(0.02)	2.47	(0.02)
Extracellular Matrix Components					
Matrix Metabolism / Components					
TIMP2	Dr.22985.1.A1_at			11.20	(0.01)
MMP13	Dr.10314.1.S1_a_at			5.61	(0.02)
Connective tissue growth factor(CTGF)	Dr.10431.1.S1_at			3.82	(0.01)
Mucin 2	Dr.14396.1.A1_at			3.47	(0.02)
Thrombospondin-1	Dr.2712.1.A1_at	1.96	(0.04)	2.86	(0.01)
MMP9	Dr.967.1.S1_at			2.84	(0.03)
Cell Adhesion / Cell Guidance					
Claudin c	Dr.12596.1.S1_at			22.74	(0.01)
Spondin 2b	Dr.563.1.S1_at			7.81	(0.01)
Tetraspanin-7	Dr.3559.1.A1_at			7.74	(0.02)
CYR 61	Dr.15501.1.S1_at			6.23	< (0.01)
Endocan (Endothelial cell-specific molecule 1)	Dr.19483.1.A1_at			4.29	(0.02)
Claudin 11	Dr.12486.1.S1_at			3.60	(0.02)
Cytoskeleton / Cytosolic Transport					
Synaptobrevin 2	Dr.23433.1.A1_at			6.48	(0.01)
Syntaxin 11	Dr.12309.1.A1_at			4.68	(0.01)
Synaptotagmin 4	Dr.13868.1.S1_at			3.29	(0.01)
Breast cancer associated protein BRAP1	Dr.7929.1.S1_at			3.21	(0.03)
Exportin 1	Dr.12499.1.A1_at			3.11	(0.02)
Transgelin-3	Dr.3966.1.A1_at			2.96	(0.02)
Cell Cycle / Chromatin / DNA / RNA Processing					
NSE2 protein	Dr.10424.1.A1_at			3.28	(0.03)
H1 histone family member X	Dr.24246.1.S1_at			2.92	(0.05)
Methyl-CpG binding domain protein 2	Dr.23525.1.A1_at			2.88	(0.02)
Chromatin modifying protein 5	Dr.25531.1.A1_at			2.75	(0.01)
RFX2	Dr.2654.1.A1_at			2.21	(0.02)
UBTF	Dr.10946.1.A1_at			2.21	(0.01)
Protein Processing / Degradation					
Ubiquitin thiolesterase	Dr.8724.1.S1_at			8.96	(0.01)
Peptidylprolyl isomerase (cyclophilin)-like 1	Dr.24858.2.S1_s_at			3.97	(0.01)
Ring finger protein 28	Dr.436.1.A1_at			3.17	(0.01)
Smad-specific E3 ubiquitin ligase 1	Dr.4117.1.A1_at			2.55	(0.03)
F-box only protein 32	Dr.11532.1.S1_at			2.43	(0.02)
Cullin 1b	Dr.7761.1.A1_at			2.19	(0.04)
Immune / Wound Response					
Immune-responsive protein 1	Dr.10914.1.A1_at			27.20	(0.02)
CC chemokine CCL1	Dr.8113.1.S1_at			11.45	(0.02)
Neutrophil cytosol factor 1	Dr.2973.1.A1_at			8.37	(0.03)
Macrophage stimulating 1	Dr.12399.1.S1_at			6.76	(0.02)
Nonspecific cytotoxic cell receptor protein 1	Dr.1180.1.S1_at			3.53	(0.03)
Annexin A5	Dr.20555.1.S1 s at			2.70	(0.02)

Signal Transduction					
HSP70	Dr.20198.2.S1_x_at			59.63	< (0.01)
HSP 90 alpha	Dr.25536.1.A1_at			21.54	(0.01)
Dual specificity protein phosphatase 2	Dr.22685.1.A1_at			20.23	(0.02)
CCAAT/enhancer binding protein beta	Dr.6575.1.S1_at			10.34	(0.03)
Insulin-like growth factor binding protein 1	Dr.8587.1.A1_at			10.30	(0.02)
GADD45B	Dr.13161.1.S1_at			6.97	(0.01)
Wnt Signaling					
R-spondin-1	Dr.11481.1.A1_at	9.02	0.04	15.41	0.01
TCl (C8orf4)	Dr.1131.2.S1_at			7.82	(0.05)
Dickkopf-1	Dr.8056.1.S1_at			3.35	(0.02)
Frizzled 7a	Dr.4823.1.S1_at	3.45	(0.02)	3.16	< (0.01)
WNT inhibitory factor 1	Dr.3690.1.S1_at			2.93	(0.01)
Casein kinase 1, epsilon	Dr.7400.1.A1_at			2.51	(0.01)
Metabolism					
Arginase type II	Dr.2022.1.A1_at			33.66	(0.02)
Pp1r3a	Dr.6604.2.A1_a_at			17.32	(0.01)
Monocarboxylate transporter 3	Dr.7337.1.S1_at			12.32	(0.01)
Phosphofructokinase-P	Dr.12547.1.A1_at			10.01	< (0.01)
Transcobalamin II	Dr.6550.1.A1_at			7.43	(0.01)
Fructose-bisphosphate aldolase C	Dr.19223.1.S2_at			7.17	< (0.01)
Other					
ES1 protein mitochondrial precursor	Dr.6709.1.S1_at			29.00	(0.02)
Cryptochrome 2	Dr.10332.1.S2_at			5.92	(0.04)
Protein C20orf149	Dr.7102.1.S1_at			4.46	(0.03)
Tropomyosin 4	Dr.913.1.S1_at			3.49	(0.02)
Cholecystokinin	Dr.14080.1.A1_at	2.03	(0.03)	3.29	(0.02)
Leftover	Dr.17145.1.S1_at			3.07	(0.01)

Table 3S-2. Genes Repressed at Least 1.7 Fold by TCDD in Regenerating Fins of Larvae.

Gene	Affymetrix	Fold Reduced (p) 2 DPA		3DPA	
Extracellular Matrix Components					
Chondrogenesis Regulation					
Sox9b	Dr.11850.1.S2_at	27.78	(0.02)	5.95	(.02)
Collagen Modification and Catabolism					
FK506 binding protein 5	Dr.2675.1.A1_at			10.12	(.03)
Lysyl oxidase precursor	Dr.11427.1.S1_at			9.89	(.01)
Lysyl oxidase 2 precursor	Dr.23096.1.A1_at			9.49	(.01)
Proline 4-hydroxylase alpha 1	Dr.3932.1.S1_at			3.49	(.02)
FK506 binding protein 10	Dr.3212.1.S1_at			4.99	(.01)
FK506 binding protein 9	Dr.23890.1.S1_at			3.95	(.01)
Extracellular Matrix Components					
Cartilage Link Protein	Dr.24236.1.S1_at			22.09	(.05)
Keratocan precursor	Dr.9880.1.A1_at	6.85	(0.04)	8.17	(.01)
Bone/cartilage proteoglycan I	Dr.14064.1.S1_at			5.57	(.01)
Col11a1	Dr.3536.1.A1_at			5.34	(.02)
Thrombospondin 3	Dr.1089.1.S1_at	2	(0.03)	5.06	(.01)
Chondromodulin I	Dr.4827.1.A1_x_at			4.6	(.02)
Cell Adhesion / Cell Guidance					
Paired related homeobox 1	Dr.1221.1.A1_at	1.79	(0.04)	3.46	(.01)
Repulsive guidance molecule A precursor	Dr.18272.1.S1_at			3.04	(.03)
Periostin	Dr.23788.3.S1_at	2.24	(0.04)	2.79	(.02)
Laminin beta 1	Dr.4129.1.S1_at			2.43	(.02)
Astrotactin	Dr.14729.2.A1_at			2.19	(.03)
Kangai 1	Dr.18088.1.S1_at			2.18	(.01)
Cytoskeletion / Cytosolic Transport					
ERGIC-53 protein	Dr.6822.1.A1_at			5.26	(.02)
Alpha- tubulin 2	Dr.20214.1.A1_at			4.95	(.02)
Myosin I alpha	Dr.4817.1.A1_at			4.45	(.01)
KDEL receptor 3	Dr.6027.1.A1_at			4.27	(.02)
Karyopherin alpha 2	Dr.1691.4.A1_at	1.79	(0.04)	3.17	(.05)
Coatomer protein complex subunit zeta 1	Dr.8160.1.S1_at			3.11	(.03)
Cell Cycle / Chromatin / DNA / RNA / Processing					
MCM3	Dr.784.1.S1_at			5.32	(.01)
Deoxycytidine kinase	Dr.25378.1.A1_at			4.95	(.02)
dUTP pyrophosphatase	Dr.1438.1.S1_at			4.68	(.01)
Origin recognition complex subunit 5-like	Dr.17944.1.S1_at	1.89	(0.02)	3.27	(.01)
Origin recognition complex subunit 3-like	Dr.2362.1.S1_at			3.12	(.01)
Ribonuclease UK114	Dr.18514.1.S1_at			3.01	(.01)
Protein Processing / Degradation					
F-box only protein 16	Dr.18466.1.A1_at	2.19	(0.04)		
UDP-glucose ceramide glucosyltransferase-like 1	Dr.6344.1.S1_at			3.24	(.02)
Protein disulfide isomerase-related protein	Dr.3085.1.A1_at			2.86	(.01)
Peptidyl arginine deiminase type II	Dr.8670.1.A1_at			2.75	(.02)
Appbp1	Dr.7212.1.S1_at			2.2	(.01)
Ubiquitin-activating enzyme E1-domain containing 1	Dr.13754.1.S1_at			2.12	(.04)
Immune / Wound Response					
Complement factor D precursor	Dr.1999.1.S1_at			13.23	(.02)
Granulin 1	Dr.4748.1.S1_at	5.76	(0.02)		
Complement C1q tumor necrosis factor-related protein 5	Dr.965.1.S1 at			4.88	(.01)

Chemokine-like factor super family member 3	Dr.14592.1.A1_at			4.24	(.01)
Tissue factor pathway inhibitor 1	Dr.20029.1.A1_at			3.4	(.01)
Chemokine (C-X-C motif) receptor 4.	Dr.6798.1.S1_at			3.39	(.01)
Signal Transduction					
Kruppel-like factor 2a (KLF2a)	Dr.3448.1.S1_at			13.75	(.01)
Insulin-like growth factor binding protein 2	Dr.8149.1.A1_at	2.32	(0.02)	8.92	(.01)
NR2F1	Dr.16.1.S1_at	1.97	(0.02)	5.97	(.03)
Ataxin 2-binding protein variant 1	Dr.11261.1.A1_at			3.9	(.03)
Heat shock protein 1	Dr.12378.1.S1_at	2.9	(0.02)		
Id2	Dr.12836.2.A1_at			3.51	(.03)
Wnt Signaling					
Frizzled 10	Dr.8067.1.S1_at			3.07	(.01)
Frizzled 8a	Dr.8830.1.S1_at			2.11	(.05)
Metabolism					
Sulfatase FP2b	Dr.12108.1.A1_at			6.77	(.01)
Glutamate receptor 5	Dr.14817.1.A1_at	5.01	(0.02)		
Zinc transporter SLC39A7	Dr.3818.2.A1_at			3.87	(.01)
GTP cyclohydrolase 1	Dr.14668.1.S1_at			3.75	(.02)
Glutamate receptor ionotropic kainate 2	Dr.3211.1.A1_at	3.64	(0.04)		
Pyridoxal kinase	Dr.835.1.A1_at			3.61	(.01)
Calcium Signaling					
Reticulocalbin 1	Dr.1232.1.A1_at			19.2	(.01)
Enkurin	Dr.14980.1.S1_at	3.08	(0.04)		
Calreticulin	Dr.1809.1.A1_at			2.35	(.01)
Nucleobindin 1	Dr.6259.1.S1_at			2.06	(.02)
Oxygen Transport / Storage					
Myoglobin	Dr.636.1.S1_at	8.62	(0.01)	16.01	(.02)
Cytoglobin	Dr.4925.1.S1_x_at	4.12	(0.02)	8.49	(.01)
Other					
Keratin 13	Dr.12425.1.S1_x_at			7.62	(.03)
Type I cytokeratin, enveloping layer (cyt1)	Dr.5531.1.S1_a_at			7.41	(.02)
Keratin 8	Dr.24487.1.A1_at			6.93	(.05)
Selenophosphate synthetase 1	Dr.20919.1.S1_at			5.19	(.01)
Sperm associated antigen 6	Dr.17566.1.A1_at	2.96	(0.04)		
Transcription factor RAM2 splice variant b	Dr.3481.1.A1_at			3.93	(.01)

Table 3S-3. Transcripts enhanced at least 1.7 fold by TCDD exposure in regenerating fins of larvae and adults.

		Fold Induction (p Value)				
		Adult			Larvae	
Gene	Affymetrix	1 dpa	3 dpa	5 dpa	2 dpa	3 dpa
Xenobiotic Metabolism						
CYP1A	Dr.9478.1.S1_at	91.5 (0.009)	122.5 (0.009)	40.9 (0.046)	163.6 (0.0)	368.3 (0.0)
CYP1C1	Dr.12329.1.A1_at	52.4 (0.002)	73.0 (0.002)	50.9 (0.031)	56.4 (0.0)	40.9 (0.017)
UDPGT	Dr.5410.1.A1_at	8.1 (0.002)	9.4 (0.002)	8.2 (0.025)	17.1 (0.0)	10.4 (0.009)
Cytochrome b5	Dr.5040.1.S1_at	6.7 (0.002)	7.7 (0.002)	6.6 (0.024)	6.7 (0.0)	8.3 (0.0)
Sulfotransferase	Dr.3583.1.S1_at	3.2 (0.003)	2.5 (0.003)	2.1 (0.016)	2.3 (0.0)	2.5 (0.008)
Glutathione peroxidase	Dr.8000.1.S1_at		2.5 (0.007)	3.7 (0.0)	3.7 (0.016)	
Extracellular Matrix and Metabolsim						
MMP13	Dr.10314.1.S1_a_at	5.6 (0.025)	9.3 (0.043)	5.6 (0.001)		5.6 (0.008)
Cadherin-19	Dr.14830.1.S1_at	3.2 (0.004)	3.4 (0.004)	3.2 (0.002)	2.6 (0.006)	
Thioredoxin	Dr.8723.1.S1_at			2.0 (0.02)		2.3 (0.026)
Vascular						
Edg-3	Dr.13774.1.S1_at	8.2 (0.007)	4.5 (0.007)		2.5 (0.008)	3.6 (0.002)
ESM-1	Dr.19483.1.A1_at	2.2 (0.004)	2.8 (0.004)	2.7 (0.009)		4.3 (0.006)
Vamp2	Dr.17950.1.S1_at			1.9 (0.028)		4.0 (0.005)
Signaling and Development						
R-Spondin 1	Dr.11481.1.A1_at	9.4 (0.008)	20.5 (0.008)	15.3 (0.015)	9.2 (0.002)	15.4 (0.0)
Frizzled 7a	Dr.4823.1.S1_at	5.4 (0.008)	3.8 (0.008)	3.1 (0.017)	3.5 (0.0)	3.2 (0.0)
Dlx4b	Dr.153.1.S1_at	2.5 (0.012)	2.1 (0.012)	2.1 (0.03)	3.8 (0.003)	2.5 (0.008)
Fgf20a	Dr.17781.1.A1_at			3.0 (0.023)		2.0 (0.023)
ANKH	Dr.22947.1.A1_at			3.0 (0.02)		3.7 (0.004)
Jagged1a	Dr.12590.1.S1_at			2.2 (0.027)		2.2 (0.024)
S-100A1	Dr.7197.1.S1_at			1.9 (0.021)		3.8 (0.038)
VSG lipase	Dr.2577.1.A1_at			1.8 (0.04)	4.6 (0.002)	
Nervous System						
Sox3	Dr.20010.8.A1_at			2.0 (0.029)	2.8 (0.002)	2.6 (0.005)
NSP2	Dr.25676.1.A1_at			1.7 (0.001)	1.9 (0.003)	3.2 (0.002)
Immune						
CC chemokine CCL1	Dr.8113.1.S1_at	2.3 (0.015)	3.4 (0.015)	4.5 (0.017)	6.4 (0.0)	
MAPK14a	Dr.7930.1.S1_at		1.7 (0.017)			1.9 (0.002)
Chromatin/DNA/RNA Synthethis and Processing						
BTB (POZ) domain	Dr.11749.1.A1_at			3.1 (0.014)	1.8 (0.02)	
MID1 interacting protein 1	Dr.428.1.S1_at	2.4 (0.014)	2.4 (0.014)			1.8 (0.006)
Metabolism						
cholecystokinin	Dr.14080.1.A1_at	5.6 (0.008)	6.3 (0.008)	4.2 (0.017)	2.0 (0.001)	3.3 (0.004)
Pp1r3a	Dr.6604.2.A1_a_at	3.0 (0.002)	2.7 (0.002)	2.1 (0.039)	1.8 (0.012)	17.3 (0.0)
Transcobalamin II	Dr.6550.1.A1_at			1.9 (0.035)		7.4 (0.003)
Glutathione reductase	Dr.17468.1.A1_at			1.9 (0.025)		2.0 (0.002)

Table 3S-4. Transcripts repressed at least 1.7 fold by TCDD exposure in regenerating fins of larvae and adults.

		Fold Reduced (p Value)									
		Adult						Larvae			
Gene	Affymetrix	1 dpa		3 dpa		5 dpa		2 dpa		3 dpa	
Matrix Components/Metabolism											
Chondrogenesis Regulation											
Sox9b	Dr.11850.1.S2_at	9.4	(0.02)	14.4	(<0.01)	10.8	(<0.01)	27.6	(<0.01)	6.0	(0.01)
Collagen Modification and Catabolism											
Lysyl oxidase precursor	Dr.11427.1.S1_at			6.1	(0.01)	9.6	(<0.01)	1.9	(0.01)	9.9	(<0.01)
Lysyl oxidase 2 precursor	Dr.23096.1.A1_at	2.4	(0.01)	1.9	(0.01)	2.2	(0.05)	2.0	(0.04)	9.5	(<0.01)
FK506 binding protein 9	Dr.23890.1.S1_at					1.7	(0.02)			4.0	(<0.01)
FK506 binding protein 10	Dr.3212.1.S1_at			2.0	(<0.01)	1.8	(0.03)			5.0	(<0.01)
FK506 binding protein 14	Dr.6003.1.S1_at			2.8	(<0.01)	2.5	(0.03)			3.8	(<0.01)
Proline 4-hydroxylase alpha 1	Dr.3932.1.S1_at	2.0	(0.02)	4.7	(<0.01)	2.3	(0.04)			3.5	(0.01)
Lysyl hydroxylase	Dr.7688.1.A1_at			2.7	(0.01)	2.5	(0.03)			2.4	(<0.01)
Extracellular Matrix Components											
Cartilage Link Protein	Dr.24236.1.S1_at	6.6	(0.01)	12.9	(0.02)	7.6	(0.01)			22.1	(0.03)
Dermacan	Dr.4338.1.A1_at	3.2	(0.03)	3.6	(<0.01)	3.8	(0.02)			4.0	(<0.01)
Protogalectin Gal1-L2	Dr.13015.1.S1_at	2.4	(0.01)	2.2	(0.04)	2.0	(0.01)	2.3	(0.02)		
Col11a1 like	Dr.3536.1.A1_at	2.7	(0.02)	2.5	(0.02)					5.3	(0.01)
Col5a2	Dr.741.1.S1_at					1.8	(0.02)			2.1	(0.01)
Cell-Cell Cell-Matrix Interaction											
Thrombospondin 3	Dr.1089.1.S1_at			2.7	(0.02)	2.0	(0.04)	2.0	(<0.01)	5.1	(<0.01)
Cadherin-11	Dr.251.1.S1_at			1.9	(0.04)	2.2	(0.01)	1.8	(0.01)		
Bone Formation											
Connexin 43	Dr.582.1.S1_a_at	1.8	(0.01)	4.7	(<0.01)	3.2	(<0.01)			1.8	(0.04)
Non-Collagen Extracellular Matrix Metabolism											
Sulfatase FP2b	Dr.12108.1.A1_at			2.2	(0.01)			2.6	(0.02)	6.8	(<0.01)
Immune/Wound Response											
Granulin	Dr.4748.1.S1_at	2.3	(0.01)					5.8	(<0.01)		
Granulin-A precursor	Dr.5809.1.A1_at	1.8	(0.01)							3.2	(<0.01)
Coagulation factor XIII A chain	Dr.16206.1.A1_s_at	1.9	(<0.01)			3.9	(<0.01)	2.3	(<0.01)		
Chemokine-like factor member 3	Dr.14592.1.A1_at			2.0	(<0.01)	1.7	(0.03)	1.9	(0.01)	4.2	(<0.01)
Chemokine (C-X-C motif) ligand 12a	Dr.822.1.S3_at			2.5	(0.03)	2.7	(<0.01)	3.5	(0.01)		
Complement factor D precursor	Dr.1999.1.S1_at					5.2	(0.04)	2.8	(0.02)	13.2	(0.01)
Cytoglobin	Dr.4925.1.S1_x_at			2.4	(<0.01)			4.1	(<0.01)	8.5	(<0.01)
Complement C1q TNF 5	Dr.965.1.S1_at			2.0	(<0.01)					4.9	(<0.01)
Signaling											
GTP cyclohydrolase 1	Dr.14668.1.S1_at			3.0	(0.01)	5.4	(<0.01)	3.1	(0.02)	3.7	(0.01)
FK506 binding protein 5	Dr.2675.1.A1_at					3.9	(0.01)			10.1	(0.01)
Fgfr3	Dr.10434.1.S1_at					1.7	(0.01)	1.7	(<0.01)		
Nervous System											
Grik2	Dr.3211.1.A1_at			1.8	(0.03)	1.9	(0.01)	3.6	(<0.01)		
Snai1a	Dr.15.1.S1_a_at			1.9	(<0.01)					2.1	(0.01)
Ataxin 2-binding protein variant 1	Dr.11261.1.A1_at					1.7	(0.03)			3.9	(0.03)
Synaptogyrin-2	Dr.24743.1.A1_at					1.7	(<0.01)			2.4	(0.02)
Metabolism											
Glucose transporter type 9	Dr.14747.1.A1_at					3.8	(<0.01)			2.6	(<0.01)
Glucose transporter type 10	Dr.17311.1.A1_at			2.1	(0.01)					3.3	(<0.01)
Igf2b	Dr.8145.1.S1_at					3.3	(<0.01)	1.8	(<0.01)		
Igf2	Dr.9288.1.S1_at			2.1	(0.02)					2.6	(0.03)
Development											
Lunatic fringe homolog	Dr.1831.1.S1_at	1.9	(0.04)							2.1	(<0.01)
Zic family member 3 heterotaxy 1	Dr.25653.1.A1_at			2.1	(0.01)					2.0	(0.03)

Table 3S-5. Oligonucleotides used for qRT-PCR.

Target Gene	Sequence 5′ to 3′	Affymetrix Probe Set Number
F Cartilage Link Protein	GAAAGGGCGGCATTAACACC	Dr.24236.1.s1
R Cartilage Link Protein	AAGCTGCATCATTCATGTGG	Dr.24236.1.s1
F CYP1A	TGTGCTTTCAAACATACCGC	DR.9478.1.S1_at
R CYP1A	TGTGCATATTGAAACAGCCG	DR.9478.1.S1_at
F CYR61	ATCCTCATTAGCTGCGTCCC	DR.15501.1.S1_at
R CYR61	TGATGTTGGTTTCCTCTAGC	DR.15501.1.S1_at
F R-Spondin 1	GCGACATACAATATCAGAGG	Dr.11481.1.A1_at
R R-Spondin 1	GTTCGGTGTCATAATTCTCC	Dr.11481.1.A1_at
F Claudin c	CTCTCCTATCTGTGTACGTG	Dr.12596.1.s1_at
R Claudin c	GTAGTGCTGAAAACAACGAC	Dr.12596.1.s1_at
F Frizzled7a	TCGAGTACGCATTAGGATCCG	Dr.4823.1.S1_at
R Frizzled7a	ACTGTACAGATACAAAGGTC	Dr.4823.1.S1_at
F Keratocan	TCTGCAACACCTAAACCACC	DR.9880.1.A1_AT
R Keratocan	GAAATCCAGTAAACCACCAC	DR.9880.1.A1_AT
F Periostin	TGTATTTTTCTGGGATGCGG	Dr.23788.3.s1
R Periostin	AGGATTGAGCACATCTGTCC	Dr.23788.3.s1
F Spondin 2b	CTTTGTAAGGGTCAGTGTGG	Dr.563.1.S1_at
R Spondin 2b	GTGGCCTAGACTGTTTCAGC	Dr.563.1.S1_at
F Sox9b	TGACGAGTTGTTCTCCAGAG	Dr.11850.1.s2; Dr.11850.1.S1
R Sox9b	AGGCCACACGTCTATAACCC	Dr.11850.1.s2; Dr.11850.1.S1
F Thrombospondin-3	TCAGTTCACACCGTAAGCAG	DR.1089.1.S1_at
R Thrombospondin-3	ACACATTATACAGCTCCACG	DR.1089.1.S1_at
F β-actin	AAGCAGGAGTACGATGAGTC	Dr.1109.1.S1_at
R β-actin	TGGAGTCCTCAGATGCATTG	Dr.1109.1.S1_at

Chapter 4. Unraveling Tissue Regeneration Pathways Using Chemical Genetics

Lijoy K. Mathew[1,2,3,] Sumitra Sengupta[1,2,3], Atsushi Kawakami[4], Eric, A. Andreasen[1,2,3], Christiane V. Löhr[1,2,5], Catherine A. Loynes[6], Stephen A. Renshaw[6], Randall T. Peterson[7], and Robert L. Tanguay[1,2,3*]

[1]Department of Environmental and Molecular Toxicology, [2]Environmental Health Sciences Center, [3]Marine and Freshwater Biomedical Sciences Center, [5]Department of Veterinary Medicine, Oregon State University, Corvallis, OR, 97331, [4]Department of Biological Information, Tokyo Institute of Technology, Japan. [5]Department of Veterinary Medicine, Oregon State University, Corvallis, OR, 97331. [6]MRC Centre Development for Developmental and Biomedical Genetics, University of Sheffield, Western Bank, Sheffield, S10 2TN, UK. [7]Developmental Biology Laboratory, Cardiovascular Research Center, Massachusetts General Hospital, Charlestown, MA 02129.

Abstract

Identifying the molecular pathways that are required for regeneration remains one of the great challenges of regenerative medicine. Although genetic mutations have been useful for identifying some molecular pathways, small molecule probes of regenerative pathways might offer some advantages, including the ability to disrupt pathway function with precise temporal control. However, a vertebrate regeneration model amenable to rapid throughput small molecule screening is not currently available. We report here the development of a zebrafish early life stage fin regeneration model and its use in screening for small molecules that modulate tissue regeneration. By screening 2000 biologically active small molecules, we identified 17 that specifically inhibited regeneration. These compounds include a cluster of glucocorticoids, and we demonstrate that transient activation of the glucocorticoid receptor is sufficient to block regeneration, but only if activation occurs during a narrow window of time during wound healing/blastema formation. We further demonstrate that glucocorticoid exposure inhibit blastema formation. In addition, knockdown of the glucocorticoid receptor restores regenerative capability to non-regenerative, glucocorticoid-exposed zebrafish. To test whether the classical anti-inflammatory action of glucocorticoids is responsible for blocking regeneration, we prevented acute inflammation following amputation by antisense repression of the Pu.1 gene. Although loss of Pu.1 prevents the inflammatory response by neutrophils and macrophages, regeneration is not affected. Collectively, these results indicate that signaling from exogenous glucocorticoids impairs blastema formation and limits regenerative capability in vertebrates through an acute inflammation-independent mechanism. These studies demonstrate the feasibility of exploiting chemical genetics to define the pathways that govern vertebrate regeneration.

Introduction

The promise of regenerative medicine is that therapies will be devised to promote the repair or replacement of damaged or diseased tissues and organs. This emerging field is approached from two distinct lines of attack. In recent years, stem cell based models have been developed to generate a suite of differentiated cells for therapeutic applications. The use of high throughput chemical genetic screening to identify modulators of stem cell fate offers great promise (Ding and Schultz, 2004). The alternative approach exploits the inherent regenerative capacity of non-mammalian models to define the molecular events that permit tissue regeneration (Brockes and Kumar, 2005). There are several regenerative animal models including salamanders, newts, zebrafish, hydra and flatworms that are established to evaluate tissue regeneration (Akimenko et al., 2003; Bader and Oberpriller, 1978; Fujisawa, 2003; Mescher, 1996); what is currently lacking is the availability of a vertebrate regeneration model that is amenable to rapid throughput assessments.

Zebrafish have the remarkable capability to regenerate their fins, optic nerve, scales, heart and spinal cord (Poss et al., 2003). Adult caudal fin regeneration is the most well-studied model for dissecting the molecular signaling that controls regenerative growth and angiogenesis (Bayliss et al., 2006; Poss et al., 2003). Comparative genomics indicate significant genetic conservation between mammals and lower vertebrates, which begs the question: what are the molecular differences that permit tissue regeneration in zebrafish, and make mammalian tissues recalcitrant to regeneration? Answers to this question will provide a path for comparative studies in mammals. Zebrafish recover the lost caudal fin tissue after amputation through a process of epimorphic regeneration and this occurs in a stepwise manner with the formation of an epithelial wound cap, followed by blastema formation and finally the regenerative outgrowth (Akimenko et al., 2003; Poss et al., 2003) (Fig.1). This complex regenerative process is orchestrated by sequential interactions between biomolecules and cells in a spatio-temporal manner. Global gene expression analysis on heart and fin regeneration in adult zebrafish illustrates the involvement of multiple signaling pathways mediated through the differential expression

of hundreds of genes during this remarkable process (Andreasen et al., 2006; Lien et al., 2006; Schebesta et al., 2006). The identification of the signaling molecules that control these interactions will offer avenues to rapidly advance the field of regenerative medicine. The characterization of key regulators such as FGF and Wnt as critical factors during regeneration emphasizes the likely involvement of multiple signaling pathways in fin regeneration (Poss et al., 2000b; Stoick-Cooper et al., 2007). This again underscores the importance of a comprehensive approach to identify the full repertoire of molecular players required for tissue regeneration. Although adult zebrafish regeneration models have proven useful, many of the molecular and genetic tools that are useful for embryonic and larval studies are not easily applied to adult stage animals (Poss et al., 2003). Recent results indicate that these technical barriers may be overcome by using an early life stage regeneration model. Specifically, two-day-old zebrafish larvae completely regenerate their fin primordia within three days following amputation (Kawakami et al., 2004; Mathew et al., 2006; Nakatani et al., 2007). Since this life stage is inherently amenable to molecular and genetic manipulations such as transient and stable transgenics, genetic mutant screens and chemical genetics, this model offers a powerful new way to identify novel regulators of tissue regeneration.

In vivo high throughput small molecule screening has the potential to target any biological process (Love et al., 2004; MacRae and Peterson, 2003; Peterson and Fishman, 2004; Peterson et al., 2000; Peterson et al., 2004; Shafizadeh et al., 2004; Zon and Peterson, 2005); however, this approach has not been applied in a vertebrate regenerative system. To probe tissue regeneration, an inhibitory screen was developed. The underlying premise is that if a chemical inhibits or modulates an essential molecular target, then regeneration will be impacted. The identification of the chemical target will thus help to reveal underlying molecular pathways that permit tissue regeneration. Previous larval fin regeneration studies demonstrated the feasibility of this general inhibitory approach; inhibition of FGFR-1 with SU5402, or activation of the aryl hydrocarbon receptor (AHR) disrupted tissue regeneration (Kawakami et al., 2004; Mathew et al., 2006; Nakatani et al., 2007). We report here for the first time an *in vivo* vertebrate regeneration assay that employs a rapid small molecule library screening to identify pathways essential for tissue regeneration. We also demonstrate that this regenerative platform is well suited to

identify the molecular targets of small molecules and to define the molecular and cellular mechanism underlying the chemical response.

Materials and Methods

Screening for Inhibitors of Larval Fin Regeneration

Fertilized eggs were obtained from AB strain zebrafish (University of Oregon, Eugene, OR) for all the experiments. All embryos were raised in our laboratory according to standard procedures. Two-day-old embryos were dechorionated and anesthetized with 3-amino benzoic acid ethylester (tricaine). The larvae were laid on an agar plate and the caudal fin primordia were amputated with a surgical blade just posterior to the notochord. Two amputated larvae were arrayed per well in 96-well plates containing 50 µL E3 embryo buffer (5 mM NaCl, 0.17 mM KCl, 0.33 mM $CaCl_2$, 0.33 mM $MgSO_4$). The small molecules (2,000 bioactives from MicroSource Discovery Systems (Gaylordsville, CT), were added individually to the test wells at a final concentration of 25 µM. The amputated larvae were incubated for 3 days at 28°C, and at 3 dpa, the larvae were anesthetized and assessed visually to score regenerative progression. After the primary screen, Beclomethasone dipropionate (Beclomethasone, Sigma-Aldrich, St.Louis, MO) was used as a prototype GR agonist. For all functional studies, Beclomethasone was used at 1 µM final concentration.

Adult Zebrafish Study

Adult male zebrafish (AB strain) were pre-exposed for one day to vehicle or Beclomethasone with waterborne concentrations ranging from 0.05 - 0.0005mg/L. The concentration that was used for the study reported here is 0.005mg/L (n=6). After pre-exposure, the fish were anesthetized, and their caudal fins were surgically amputated. The fish were transferred back to the tanks and were continuously exposed to vehicle or Beclomethasone until the end of the study. The exposure solutions were changed daily.

Quantitative Real Time PCR

The larvae were amputated at 2dpf and exposed to vehicle or Beclomethasone and the regenerating fin tissue was specifically isolated at 1dpa. Total RNA was extracted from the regenerating fin tissue using the RNAqueous Micro kit (Ambion, Austin, TX). Three groups per treatment, each comprised of 150 larval fins, were pooled to make an individual replicate. For RNA from whole embryo, the amputated larvae exposed to vehicle or Beclomethasone at 2dpf were sampled at 3dpf. Total RNA was isolated from triplicate groups of whole embryos using RNeasy Mini kit (Qiagen, CA) according to manufacturer's instructions. Data was quantitatively expressed as the fold change in the mRNA levels between Beclomethasone-exposed embryos and vehicle-exposed embryos after normalizing to β-actin abundance. The *p* values represent the significant difference of transcript level between groups as calculated using One Way ANOVA and Tukey method (SigmaStat, Chicago, IL) (Fig. 4A). To quantify GR transcript morpholino knockdown, RNA was isolated from the control or GR morphants at 2dpf (Fig. 4D). The transcript levels were normalized to β-actin abundance. The *p* value represents significance as determined by One Way ANOVA. For all the experiments, cDNA was synthesized from 3μg of total RNA per group using Superscript II (Life Technologies, Gaithersburg, MD) and oligo(dT) primers in a 20 μl volume. Quantitative PCR was conducted using gene-specific primers with the Opticon-2 real-time PCR detection system (MJ Research, Waltham, MA). Briefly, 1 μl of cDNA was used for each PCR reaction in the presence of SYBR Green, using DyNAmo SYBR green qPCR kit according to the manufacturer's instructions (Finnzymes, Espoo, Finland). Agarose gel electrophoresis (Fig. 4C) and thermal denaturation (melt curve analysis) were conducted to ensure formation of specific products. Primer sequences used were as follows: FKBP5, 5'-CACGTTCACAAACACACTGC-3', 5'-ATCAAACGAACAAGCGGGTC-3'; GILZ, 5'- CGACTTGTTTATATGGGCTG-3', 5'-TCTTCAGACACCAACATGCC-3'; SOX9b, 5'-TGACGAGTTGTTCTCCAGAG-3', 5'- AGGCCACACGTCTATAACCC-3'; GR, 5'-CAAATGGGCTAAAGCTCTGC-3', 5'-TCTTCAACCCATCCTTCGGC-3'.

Morpholinos

Antisense repression of GR was performed using splice variant morpholino (MO) oligonucleotides (Gene Tools, Philomath, OR). A putative zebrafish GR ortholog was identified (Genbank accession number AB218424). Since there were three predicted transcripts based on alternative splicing, a MO was designed at an intron-exon boundary that was conserved between predicted transcripts. The sequence of GR splice variant MO was 5'-CTGCTTCATGTATTTTAGGGTTCCG-3'. The sequence of PU.1 MO is 5′-GATATACTGATACTCCATTGGTGGT-3′ (Gene Tools, Philomath, OR). Morpholinos were diluted to 3 mM in 1X Danieau's solution (58 mM NaCl, 0.7 mM KCl, 0.4 mM $MgSO_4$, 0.6 mM $Ca(NO_3)_2$, 5 mM HEPES, pH 7.6) as described (Nasevicius and Ekker, 2000). A standard control morpholino (Gene Tools, Philomath, OR) (5'CTCTTACCTCAGTTACAATTTATA 3') was used as the control morpholino (Control-MO). Approximately 2 nl of the appropriate MO solution was microinjected into the embryos at the 1–2 cell stage. The 3' end of the MOs was fluorescein-tagged to screen microinjection success at 24hpf. The control and GR morphants at 2dpf were amputated and exposed to vehicle or Beclomethasone and raised for 3 days at 28°C. The control and PU.1 morphants were amputated and allowed to grow for 3 days at 28°C.

In situ Hybridization

Whole mount in situ hybridization was conducted on the regenerating fin at different time points as described previously (Poss et al., 2000a; Schier et al., 1997). The *msxe* and *dlx5a* probes were obtained from Atsushi Kawakami(Kawakami et al., 2004). The *junbl* probe is a gift from Atsushi Kawakami (Ishida and Kawakami., manuscript in preparation).

Brdu Incorporation Analysis by Immunohistochemistry

The amputated larvae that were exposed to vehicle or Beclomethasone were incubated with Brdu (Roche, Indianapolis, IN) for 6hrs starting from 6hpa or 24hpa. The larvae were labeled with Brdu (10mM) in a 96-well plate with one larva in each well at 28°C. After 6hrs of incubation with Brdu, the animals were euthanized with tricaine and fixed in 4% paraformaldehyde (PFA) overnight. The fixed larvae were dehydrated with

methanol and then stored in methanol at -20°C. For performing immunohistochemistry, the larvae were rehydrated using a graded methanol/PBST (phosphate-buffered saline (PBS) and 0.1% Tween-20) series. The larvae were then treated with Proteinase K (10µg/Ml) in PBST for 20 minutes at room temperature (RT) and then rinsed several times with PBST. The larvae were refixed in 4% PFA for 30 minutes and then rinsed several times in water. This was followed by quick rinses in 2N HCL, then incubated in 2N HCL at RT for an hour and washed with PBST several times. The larvae were then blocked with 1% normal goat serum in PBST for an hour at RT and then incubated with anti-Brdu antibody (1:100; G3G4; Developmental Studies Hybridoma Bank, Iowa City, IA) overnight at 4°C. After 4x for 30 min washes with PBST, the larvae were incubated with a secondary antibody (1:1000; Alexa-546 conjugated goat anti mouse; Molecular Probes, Eugene, OR) for 4 hrs at RT. The larvae were then washed 4x for 30 min in PBST and visualized by epifluorescence microscopy. The Brdu-labeled fluorescent cells were quantified with the images using ImagePro Plus software program (Media Cybernetics, Inc., Silver Spring, MD).

Morphologic Characterization by Histological Analysis

The amputated larvae exposed to vehicle or Beclomethasone were euthanized and fixed in 4% paraformaldehyde at 1dpa. The fixed larvae were post fixed in 1% osmium tetroxide and embedded in Embed 812-Araldite 502 resin. Semi-thin serial sections were cut at 1 micrometer, stained with toluidine blue, and analyzed by light microscopy.

Neutrophil and Macrophage Migration Assay

The Tg(BACmpo:gfp)^{i114} transgenic line larvae were anaesthetized and amputated at 3dpf as described above. At the time points indicated, amputated larvae were taken from predetermined wells and the numbers of GFP-positive neutrophils counted (Renshaw et al., 2006) at the same time, and in the same fish the number of neutral red positive macrophages were assessed. For macrophage count, the amputated larvae at 3dpf were exposed to neutral red at a final concentration of 2.5µg/mL for 4 hours prior to

assessment. The macrophages are stained red and were counted at the amputation site periodically as given in Fig. 8C, D.

Results and Discussion

Development of Rapid Throughput Zebrafish Regeneration Assay

Since regeneration is accomplished by an orchestrated coordination of multiple pathways and signaling events, a vertebrate regeneration assay was developed to identify small molecules that specifically modulated tissue regeneration. To demonstrate the power of this approach, a 2000-member structurally diverse bioactive small molecule library was screened to identify inhibitors of regeneration. Two day post fertilization (dpf) larvae were amputated and transferred to 96-well plates and continuously exposed to individual chemicals. At 3 days post amputation (dpa), the larvae were microscopically imaged to assess regenerative progression. A total of 17 small molecules (approximately, 0.8% of the library) inhibited tissue regeneration. These inhibitory chemicals comprised several different functional classes such as anti-inflammatory, keratolytic, cytochrome P-450 inhibitor, etc. Representative images of complete and impaired regeneration are depicted (Fig. 2A, B). Although a number of small molecules produced overt toxicity at the test concentration (25 μM) leading to systemic edema by the end of the assay, these animals completely regenerated their fin tissue (Fig. 2C). This specificity indicates that a toxic response can be uncoupled from the regenerative response.

Identification of Glucocorticoids as Modulators of Regeneration

The positive “hits” were of different chemical classes and using structure function analysis, a major cluster of compounds was identified as glucocorticoids (5 of the “hit” compounds). Although the main focus of this study was to demonstrate the feasibility of using small molecules to probe tissue regeneration, we also wanted to demonstrate the ability to rapidly identify small molecule targets during early life stages. We selected glucocorticoids for further studies since this was the largest cluster of “hits”.

Glucocorticoids consistently and specifically inhibited regeneration without inhibiting normal growth, creating a "V" shaped fin (Fig. 3A). This characteristic morphology occurs because the tissue lateral to the amputation plane continues to grow and partially collapses around the amputation plane. Glucocorticoids are steroid hormones that exert most of their actions by binding the glucocorticoid receptor (GR) (Carlstedt-Duke and Gustafsson, 1987; Gustafsson et al., 1987; Schaaf and Cidlowski, 2002). From mammalian studies it is clear that there are several isoforms of GR due to differential splicing and alternative translation initiation sites, of which GRα and GRβ are the most well-studied (Lu and Cidlowski, 2004; Lu and Cidlowski, 2006; Schaaf and Cidlowski, 2002). Binding of glucocorticoid activates GRα transcriptional activity, leading to the initiation or repression of transcription, whereas GRβ is not able to bind ligands and has a dominant negative activity through inhibition of GRα transcriptional activity (Oakley et al., 1999). In addition to the classical genomic model of GR activation, non-genomic activities have also been reported at high concentrations of glucocorticoids (Croxtall et al., 2002; Goulding, 2004). In order to broadly analyze the mechanism of action from the positive "hits", dose response studies were completed with selected glucocorticoids by measuring the length of maximum outgrowth. The length of maximum outgrowth is the distance from the center of the amputation plane to the tip of the regenerating fin (Mathew et al., 2006), and the IC_{50} for regeneration ranged from 200-400 nM (Fig. 3B). Beclomethasone dipropionate (Beclomethasone) has a potent inhibitory effect on regeneration at the lower nanomolar range, and hence this small molecule was selected for further experiments.

Since the adult fin regeneration model is more widely studied, it was important to determine if chemical "hits" identified in the larval screen would be predictive for the adult fin regeneration responses. Therefore, the regeneration response to glucocorticoid exposure on fin regeneration was also assessed in adult zebrafish. Similar to the larvae, Beclomethasone exposure inhibited adult caudal fin regeneration and small projection-like structures were observed at the plane of amputation (Fig. 3C). The similar inhibitory response suggested that a common underlying molecular target was targeted by this chemical.

Beclomethasone Induces Expression of GR Target Genes

Since the IC_{50} of glucocorticoids for regeneration was in the nanomolar range, it is highly likely that the glucocorticoids are acting *via* activation of the GR. To test whether Beclomethasone activates the GR pathway, three primary GR target genes were identified including the glucocorticoid induced leucine zipper (GILZ), the FK506 binding protein 5 (FKBP5) and the SRY-box containing gene 9b (SOX9b) (Chen et al., 2006; Rogatsky et al., 2003; Sekiya et al., 2001; Wang et al., 2004). To analyze the expression of these genes, qRT-PCR was conducted using RNA from the larval regenerating fin tissue at 1dpa in the presence and absence of Beclomethasone. All three genes were significantly induced in response to Beclomethasone exposure, indicating that the GR is activated by glucocorticoids in this regeneration model (Fig. 4). Similarly, qRT-PCR analysis was performed in the whole embryo at 3dpf after exposure to Beclomethasone at 2dpf, and the global expression of those genes was similar in pattern to the regenerating fin tissue (Supplemental Fig.1). These results suggest that Beclomethasone is activating the GR and the inhibitory effect on regeneration could be mediated through inappropriate GR activation.

GR Activation is Required for Beclomethasone to Inhibit Regeneration

To directly determine if the GR was the molecular target of Beclomethasone and to determine if the GR was necessary for the glucocorticoid-mediated inhibition of regeneration, a morpholino was designed to block splicing of the exons encoding the well conserved GR ligand binding domain (Fig. 5B). Transient knockdown of GR did not elicit obvious early developmental defects, suggesting that the GR is not essential for early embryonic development (data not shown). The standard control morpholinos-microinjected larvae (morphants) and GR morphants were amputated at 2dpf and continuously exposed for 3 days to vehicle or Beclomethasone. It is noteworthy that the control and GR morphants exposed to vehicle completely regenerated their fin tissue, emphasizing that endogenous GR is not required for larval fin regeneration (Fig. 5A). Control morphants exposed to Beclomethasone failed to regenerate, whereas knockdown of GR completely restored regenerative capacity in the presence of Beclomethasone (Fig. 5A). These results indicate that impaired regeneration by Beclomethasone is mediated

through ligand activated GR. To confirm GR morpholino efficacy, qRT-PCR was performed with GR-specific primers in control and GR morphants. The GR primary transcript was detected in the control morphants, but was not detected in the GR morphants indicating efficient knockdown of GR transcripts (Fig. 5C). The predicted misspliced transcript was also detected as a lower band (Fig. 5C) and the size of this product is consistent with the loss of the targeted exon. Additionally, qRT-PCR analysis revealed significant reduction in the GR transcript between control and GR morphants (Fig. 5D). These results indicate that the molecular target for glucocorticoids identified in the small molecule screen is the GR. Collectively, inappropriate ligand-activated GR blocks tissue regeneration, and the next goal was to begin to identify the events downstream of GR that mediate this response.

Glucocorticoids Target Early Stages of Regeneration

A significant advantage of chemical genetics is that the initiation and termination of the chemical exposure can be tightly controlled; therefore, the screen can be designed to probe any stages of this complex process. Previously we have reported that AHR ligands block regeneration at both early and late stages in adult and larval zebrafish (Mathew et al., 2006; Zodrow and Tanguay, 2003). To define the regenerative stage that is most responsive to GR activation, Beclomethasone (1μM) was added beginning at a number of distinct time windows post amputation. Larvae that were exposed to Beclomethasone immediately following amputation for just four hours failed to regenerate (Fig. 6A, B). However, larvae exposed to Beclomethasone beginning at 4hpa and then continuously until 3 dpa were non-responsive, as they completely regenerated their fins. These data indicate that glucocorticoids exclusively target early stages of regeneration, which encompass wound healing/blastema stages in larvae (Fig. 6C, D). In adult zebrafish, Beclomethasone exposure for just 1dpa was not sufficient enough to block regeneration when assessed at 5dpa (data not shown), indicating slight differences in the regenerative window of sensitivity. The differential response in adult zebrafish could be due to variations in the pharmacokinetics, metabolism, and drug efficiency in the complex adult regeneration system.

Beclomethasone Impairs Wound Epithelium and Blastema Formation

Since the sensitive window of exposure in larval zebrafish is within the first four hours of regeneration, we performed *in situ* localization with a molecular marker that defines the wound epithelium, which is the first step of regeneration that occurs after amputation of the fin tissue. The expression of a basal wound epidermis marker, *dlx5a* (Kawakami et al., 2004; Schebesta et al., 2006) was used to assess whether Beclomethasone exposure affected the formation of an intact wound epithelium. The larvae exposed to vehicle revealed a strong expression of *dlx5a* at 1dpa in the wound epithelium of the regenerating fin, whereas the larvae exposed to Beclomethasone failed to express *dlx5a* (Fig. 7 A,B). This indicates that the wound epithelium is not properly formed in the Beclomethasone-exposed larvae and the wound epithelium could be the primary target of GR activation, which indeed supports the sensitivity of the critical window of early exposure.

To further characterize whether blastema formation is impacted by Beclomethasone, we assessed the expression of two blastema markers *msxe* (Kawakami et al., 2004) and *junbl* (Ishida and Kawakami, manuscript in preparation and our unpublished data) by in situ hybridization. The normal expression of *msxe* in the blastema region just beneath the plane of amputation was present in the vehicle-exposed larvae at 1dpa, but *msxe* expression was absent in the Beclomethasone exposed larvae (Fig. 7. C,D). Similarly, the *junbl* blastema marker which was highly expressed in the blastema of the vehicle-exposed larvae at 1 dpa was completely absent in Beclomethasone-exposed larvae (Fig. 7.E,F), suggesting that, GR activation by Beclomethasone inhibits blastema formation which is essential for fin regeneration. Additionally, we also assessed the formation of blastema at 1dpa by light microscopic analysis of semi-thin sections of vehicle- or Beclomethasone-exposed larvae. In the vehicle-exposed larva, a solid dense blastema (B) was formed immediately proximally to the amputation site (Fig. 7. G). In the Beclomethasone-exposed larvae, cells were very loosely arranged and separated by wide empty spaces (intercellular spongiosis/edema) immediately proximal to the amputation site, resulting in the formation of abnormal blastema (aB) (Fig. 7 H1, H2). In addition, many of the epithelial cells (E) in Beclomethasone-treated larvae displayed cytoplasmic vacuolation and the epithelium was separated from deeper cell layers.

Altogether, these results indicate that, inappropriate GR activation impacts signaling molecules critical for wound healing and blastema formation.

Cell Proliferation is Affected by Beclomethasone

To determine the impact of GR activation on early regeneration stage cellular proliferation, bromodeoxyuridine (Brdu) incorporation proliferation studies were competed at 6-12hpa and 24-30hpa, reflective of pre- and post-blastema formation in larval fin regenerates. At 6-12hpa, many Brdu-labeled cells were observed just beneath the plane of amputation in the vehicle-exposed larvae, whereas there was significant reduction in the number of proliferating cells in the Beclomethasone-exposed larvae (Fig. 8A). There was also a significant reduction in cellular proliferation in the Beclomethasone-exposed larvae when compared to vehicle at 24-30hpa (Fig. 8A), and at 12-24hpa (data not shown). Similar to previous reports, we also observed a cluster of Brdu-labeled cells at the posterior and ventral side of the notochord, which are likely to contribute to the normal development of the caudal fin region (Kawakami et al., 2004). Irrespective of the chemical treatment, there was no difference in the number of cells at the ventral side of the notochord, suggesting that the normal growth of the caudal fin region is not affected by Beclomethasone, and rather, the inhibitory effect is very specific to the regenerating fin tissue. Altogether these results indicate that GR activation results in the inhibition of cell proliferation at multiple regenerative stages.

Neutrophils and Macrophages are Not Essential for Regeneration

Of the multiple actions of glucocorticoids, perhaps the best understood is the immunosuppressive effects on the acute-phase inflammatory response (Schaaf and Cidlowski, 2002; Schoneveld et al., 2004). It is known that amputation of caudal fin in zebrafish induces neutrophilic inflammation (Oyewumi et al., 2003; Renshaw et al., 2006), and work from other model systems suggests that newly recruited neutrophils and macrophages secrete cell-signaling molecules, such as growth factors and cytokines that are considered important for wound healing and tissue repair. We therefore hypothesized that the action of glucocorticoids on inhibiting regeneration might occur via inhibition of macrophage or neutrophil migration to the site of injury. In order to assess whether

Beclomethasone affects the infiltration of neutrophils or macrophages to the amputation site, we utilized the Tg(BACmpo:gfp)^{i114} line that expresses green fluorescent protein (GFP) under control of the neutrophil-specific myeloperoxidase (mpo/mpx) regulatory region (Renshaw et al., 2006). Tg(BACmpo:gfp)^{i114} larvae were amputated at 72hpf and exposed to vehicle or Beclomethasone as described above. There was a modest reduction in the number of neutrophils (GFP positive cells) at the amputation site of the Beclomethasone exposed larvae at 4 and 8hpa when compared to vehicle-exposed larvae, raising the possibility that the glucocorticoid response could be mediated by a small reduction in neutrophils (Fig. 9A,B). Similarly, the number of macrophages that migrate to the amputation site was quantified by neutral red staining and there was no significant difference in the number of macrophages between vehicle- or Beclomethasone-exposed larvae (Fig. 9C,D). It remained a possibility that the block in regeneration by glucocorticoids was mediated by either a reduction in neutrophils at the amputation site, or by the suppression of important regenerative cytokine produced by invading inflammatory cells. To directly determine the importance of myeloid cells in larval fin regeneration, we used antisense morpholinos to target the Pu.1, a transcription factor required to permit myeloid cell development (Hsu et al., 2004; Lieschke et al., 2002; Rhodes et al., 2005). After amputation, Pu.1 morphants completely regenerated their caudal fin indistinguishable from control morphants indicating that neutrophils and macrophages are not required for normal larval fin regeneration (Fig. 9E, F). This significantly extends the findings of wound healing studies in the Pu.1 null mice where tissue repair proceeds in the complete absence of neutrophils and macrophages (Redd et al., 2004). The efficiency of Pu.1 MO was confirmed by assessing the GPF positive cells for neutrophils and performing neutral red staining for macrophages. Both neutrophils and macrophages were detected in the control morphants, but were completely absent at the amputation site in the Pu.1 morphants at 8hpa (Fig. 9G,H,I,J). These results for the first time illustrate that acute inflammation through neutrophils and macrophages are not absolutely required for the initiation of regeneration in zebrafish. Moreover, the similarity in the functional role of Pu.1 gene during wound healing between mice and zebrafish underscores the conserved function of genes across different vertebrate animals.

Conclusions

Numerous human conditions could be significantly improved if therapies that encourage tissue regeneration were available. Our findings illustrate the power of *in vivo* chemical genetics to identify novel bioactive compounds, and their molecular targets, that together function to modulate tissue regeneration. The genetic and molecular utilities of this early life stage regeneration model such as transient and stable transgenics, genetic mutant screens, rapid antisense repression, and the controlled use of chemical genetics makes this vertebrate regeneration model an outstanding discovery platform. The results generated can be rapidly evaluated in other regenerative models. By utilizing the power of comparative approaches, the most exciting outcome will be a molecular explanation for the observed differences in regenerative capacity across taxa, and will reveal pathways for therapeutic interventions.

References

Akimenko MA, Mari-Beffa M, Becerra J and Geraudie J (2003) Old questions, new tools, and some answers to the mystery of fin regeneration. *Dev Dyn* **226**:190-201.

Andreasen EA, Mathew LK and Tanguay RL (2006) Regenerative Growth is Impacted by TCDD: Gene Expression Analysis Reveals Extracellular Matrix Modulation. *Toxicol Sci* **92**:254-269.

Bader D and Oberpriller JO (1978) Repair and reorganization of minced cardiac muscle in the adult newt (Notophthalmus viridescens). *J Morphol* **155**:349-57.

Bayliss PE, Bellavance KL, Whitehead GG, Abrams JM, Aegerter S, Robbins HS, Cowan DB, Keating MT, O'Reilly T, Wood JM, Roberts TM and Chan J (2006) Chemical modulation of receptor signaling inhibits regenerative angiogenesis in adult zebrafish. *Nat Chem Biol* **2**:265-73.

Brockes JP and Kumar A (2005) Appendage regeneration in adult vertebrates and implications for regenerative medicine. *Science* **310**:1919-23.

Carlstedt-Duke J and Gustafsson JA (1987) Structure and function of the glucocorticoid receptor. *J Steroid Biochem* **27**:99-104.

Chen W, Rogatsky I and Garabedian MJ (2006) MED14 and MED1 differentially regulate target-specific gene activation by the glucocorticoid receptor. *Mol Endocrinol* **20**:560-72.

Croxtall JD, van Hal PT, Choudhury Q, Gilroy DW and Flower RJ (2002) Different glucocorticoids vary in their genomic and non-genomic mechanism of action in A549 cells. *Br J Pharmacol* **135**:511-9.

Ding S and Schultz PG (2004) A role for chemistry in stem cell biology. *Nat Biotechnol* **22**:833-40.

Fujisawa T (2003) Hydra regeneration and epitheliopeptides. *Dev Dyn* **226**:182-9.

Goulding NJ (2004) The molecular complexity of glucocorticoid actions in inflammation - a four-ring circus. *Curr Opin Pharmacol* **4**:629-36.

Gustafsson JA, Carlstedt-Duke J, Poellinger L, Okret S, Wikstrom AC, Bronnegard M, Gillner M, Dong Y, Fuxe K and Cintra A (1987) Biochemistry, molecular biology, and physiology of the glucocorticoid receptor. *Endocr Rev* **8**:185-234.

Hsu K, Traver D, Kutok JL, Hagen A, Liu TX, Paw BH, Rhodes J, Berman JN, Zon LI, Kanki JP and Look AT (2004) The pu.1 promoter drives myeloid gene expression in zebrafish. *Blood* **104**:1291-7.

Kawakami A, Fukazawa T and Takeda H (2004) Early fin primordia of zebrafish larvae regenerate by a similar growth control mechanism with adult regeneration. *Dev Dyn* **231**:693-9.

Lien CL, Schebesta M, Makino S, Weber GJ and Keating MT (2006) Gene Expression Analysis of Zebrafish Heart Regeneration. *PLoS Biol* **4**.

Lieschke GJ, Oates AC, Paw BH, Thompson MA, Hall NE, Ward AC, Ho RK, Zon LI and Layton JE (2002) Zebrafish SPI-1 (PU.1) marks a site of myeloid development independent of primitive erythropoiesis: implications for axial patterning. *Dev Biol* **246**:274-95.

Love DR, Pichler FB, Dodd A, Copp BR and Greenwood DR (2004) Technology for high-throughput screens: the present and future using zebrafish. *Curr Opin Biotechnol* **15**:564-71.

Lu NZ and Cidlowski JA (2004) The origin and functions of multiple human glucocorticoid receptor isoforms. *Ann N Y Acad Sci* **1024**:102-23.

Lu NZ and Cidlowski JA (2006) Glucocorticoid receptor isoforms generate transcription specificity. *Trends Cell Biol*.

MacRae CA and Peterson RT (2003) Zebrafish-based small molecule discovery. *Chem Biol* **10**:901-8.

Mathew LK, Andreasen EA and Tanguay RL (2006) Aryl hydrocarbon receptor activation inhibits regenerative growth. *Mol Pharmacol* **69**:257-65.

Mescher AL (1996) The cellular basis of limb regeneration in urodeles. *Int J Dev Biol* **40**:785-95.

Nakatani Y, Kawakami A and Kudo A (2007) Cellular and molecular processes of regeneration, with special emphasis on fish fins. *Dev Growth Differ* **49**:145-54.

Nasevicius A and Ekker SC (2000) Effective targeted gene 'knockdown' in zebrafish. *Nat Genet* **26**:216-20.

Oakley RH, Jewell CM, Yudt MR, Bofetiado DM and Cidlowski JA (1999) The dominant negative activity of the human glucocorticoid receptor beta isoform. Specificity and mechanisms of action. *J Biol Chem* **274**:27857-66.

Oyewumi MO, Liu S, Moscow JA and Mumper RJ (2003) Specific association of thiamine-coated gadolinium nanoparticles with human breast cancer cells expressing thiamine transporters. *Bioconjug Chem* **14**:404-11.

Peterson RT and Fishman MC (2004) Discovery and use of small molecules for probing biological processes in zebrafish. *Methods Cell Biol* **76**:569-91.

Peterson RT, Link BA, Dowling JE and Schreiber SL (2000) Small molecule developmental screens reveal the logic and timing of vertebrate development. *Proc Natl Acad Sci U S A* **97**:12965-9.

Peterson RT, Shaw SY, Peterson TA, Milan DJ, Zhong TP, Schreiber SL, MacRae CA and Fishman MC (2004) Chemical suppression of a genetic mutation in a zebrafish model of aortic coarctation. *Nat Biotechnol* **22**:595-9.

Poss KD, Keating MT and Nechiporuk A (2003) Tales of regeneration in zebrafish. *Dev Dyn* **226**:202-210.

Poss KD, Shen J and Keating MT (2000a) Induction of lef1 during zebrafish fin regeneration. *Dev Dyn* **219**:282-6.

Poss KD, Shen J, Nechiporuk A, McMahon G, Thisse B, Thisse C and Keating MT (2000b) Roles for Fgf signaling during zebrafish fin regeneration. *Dev Biol* **222**:347-58.

Redd MJ, Cooper L, Wood W, Stramer B and Martin P (2004) Wound healing and inflammation: embryos reveal the way to perfect repair. *Philos Trans R Soc Lond B Biol Sci* **359**:777-84.

Renshaw SA, Loynes CA, Trushell DM, Elworthy S, Ingham PW and Whyte MK (2006) A transgenic zebrafish model of neutrophilic inflammation. *Blood* **108**:3976-8.

Rhodes J, Hagen A, Hsu K, Deng M, Liu TX, Look AT and Kanki JP (2005) Interplay of pu.1 and gata1 determines myelo-erythroid progenitor cell fate in zebrafish. *Dev Cell* **8**:97-108.

Rogatsky I, Wang JC, Derynck MK, Nonaka DF, Khodabakhsh DB, Haqq CM, Darimont BD, Garabedian MJ and Yamamoto KR (2003) Target-specific utilization of transcriptional regulatory surfaces by the glucocorticoid receptor. *Proc Natl Acad Sci U S A* **100**:13845-50.

Schaaf MJ and Cidlowski JA (2002) Molecular mechanisms of glucocorticoid action and resistance. *J Steroid Biochem Mol Biol* **83**:37-48.

Schebesta M, Lien CL, Engel FB and Keating MT (2006) Transcriptional profiling of caudal fin regeneration in zebrafish. *ScientificWorldJournal* **6**:38-54.

Schier AF, Neuhauss SC, Helde KA, Talbot WS and Driever W (1997) The one-eyed pinhead gene functions in mesoderm and endoderm formation in zebrafish and interacts with no tail. *Development* **124**:327-42.

Schoneveld OJ, Gaemers IC and Lamers WH (2004) Mechanisms of glucocorticoid signalling. *Biochim Biophys Acta* **1680**:114-28.

Sekiya I, Koopman P, Tsuji K, Mertin S, Harley V, Yamada Y, Shinomiya K, Nifuji A and Noda M (2001) Dexamethasone enhances SOX9 expression in chondrocytes. *J Endocrinol* **169**:573-9.

Shafizadeh E, Peterson RT and Lin S (2004) Induction of reversible hemolytic anemia in living zebrafish using a novel small molecule. *Comp Biochem Physiol C Toxicol Pharmacol* **138**:245-9.

Stoick-Cooper CL, Weidinger G, Riehle KJ, Hubbert C, Major MB, Fausto N and Moon RT (2007) Distinct Wnt signaling pathways have opposing roles in appendage regeneration. *Development* **134**:479-89.

Wang JC, Derynck MK, Nonaka DF, Khodabakhsh DB, Haqq C and Yamamoto KR (2004) Chromatin immunoprecipitation (ChIP) scanning identifies primary glucocorticoid receptor target genes. *Proc Natl Acad Sci U S A* **101**:15603-8.

Zodrow JM and Tanguay RL (2003) 2,3,7,8-tetrachlorodibenzo-p-dioxin inhibits zebrafish caudal fin regeneration. *Toxicol Sci* **76**:151-161.

Zon LI and Peterson RT (2005) In vivo drug discovery in the zebrafish. *Nat Rev Drug Discov* **4**:35-44.

Acknowledgements

We would like to thank Ms. Jane LaDu, Kay Fischer, Jessica Perry and Laura Young for their technical assistance. These studies were supported in part by NIEHS grants ES10820, ES00210, and ES03850, Oregon Medical Research Foundation grant and pre-doctoral fellowship from American Heart Association (LKM).

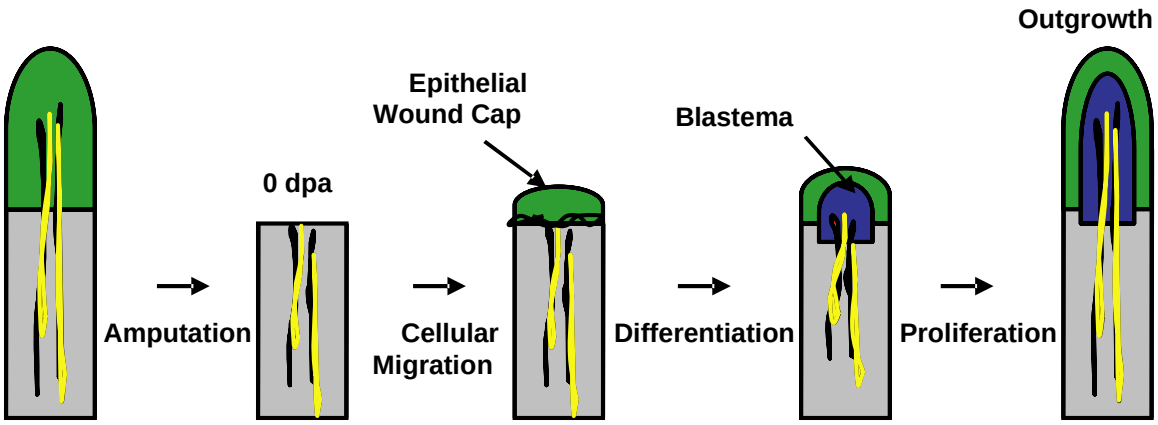

Figure 4-1. Network of molecular signaling during regeneration. Schematic diagram depicting the three steps of epimorphic regeneration: 1) Wound healing, 2) Blastema formation and 3) Regenerative outgrowth.

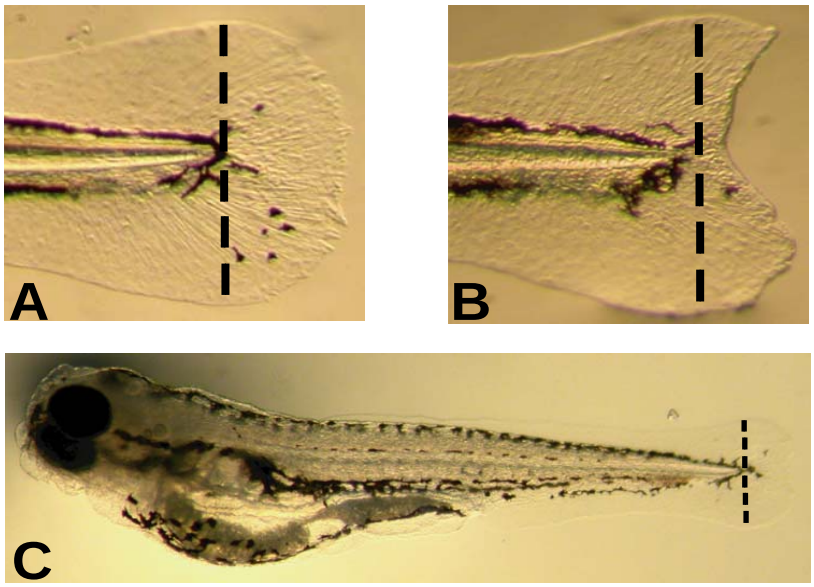

Figure 4-2. Rapid screening for inhibitors of larval fin regeneration. The 2dpf larvae were surgically amputated and exposed to the chemicals in a 96 well plate continuously for 3 days at 28°C. The larvae were screened for inhibitors of larval fin regeneration at 3 dpa. **A)** A typical example of complete regeneration, **B)** impaired regeneration and **C)** a larvae that is able to regenerate its fin, but displaying overt embryo toxicity.

Figure 4-3. Glucocorticoids inhibit regeneration. A) The caudal fin primordia of larvae at 2 dpf were amputated and exposed to vehicle or glucocorticoid continuously for 3 days at 28°C. The regeneration images were captured at 3 dpa and the broken line indicates the plane of amputation. These images are representative of 12 larvae. **B)** Tissue regenerate length from the original plane of amputation measured at 3 dpa in the presence of the indicated concentrations of selected glucocorticoids. The regenerate length was calculated from the center of the plane of amputation to the tip of the regenerating fin. **C)** The inhibitory effect of glucocorticoids on regeneration was also assessed in adults to determine if chemical "hits" from the larval screen would be predictive for the more well-established adult regeneration model. Adult zebrafish were amputated and continuously exposed to Beclomethasone (0.005mg/L) (n=6). The images were captured at 5 dpa and the arrow indicates the plane of amputation.

4-3

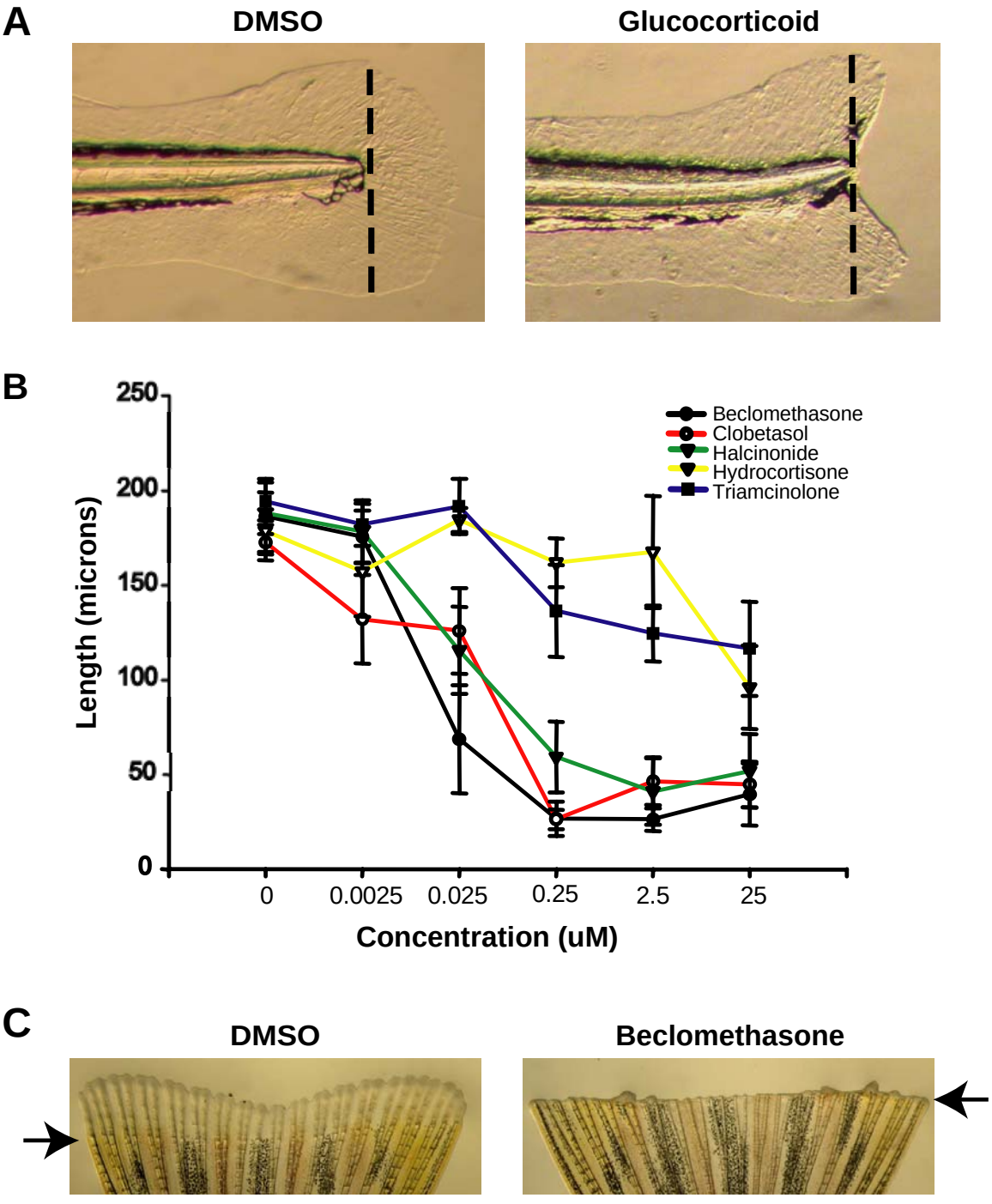
A
DMSO
Glucocorticoid
B
Length (microns)
250
200
150
100
50
0
0
0.0025
0.025
0.25
2.5
25
Concentration (uM)
Beclomethasone
Clobetasol
Halcinonide
Hydrocortisone
Triamcinolone
C
DMSO
Beclomethasone

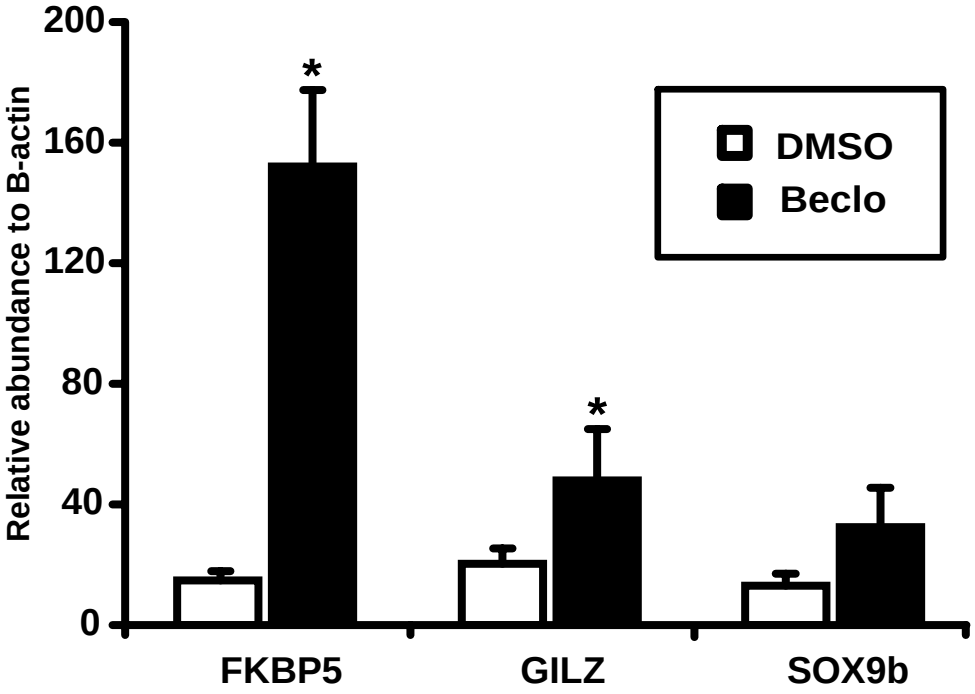

Figure 4-4. Expression of GR primary target genes are induced by Beclomethasone. Two day old larvae were amputated and exposed to vehicle or Beclomethasone. qRT-PCR was conducted on the regenerating fin tissue using gene specific primers for the primary GR target genes FKBP5, GILZ and SOX9b. The abundance of the message levels were normalized to β-actin expression. The expression of FKBP5 ($p<0.004$) and GILZ ($p<0.024$) were significantly induced in Beclomethasone exposed larval fin tissue. The respective values represent the mean $\pm$ S.E.M and the * sign refers to the significant difference statistically (One Way ANOVA, n=3).

Figure 4-5. Activation of GR is required for inhibition of regeneration by Beclomethasone. A) Control and GR morphants were amputated and exposed to vehicle or Beclomethasone at 2dpf for 3 days. The images were acquired on 3 dpa. **B)** The bold line at the intron-exon (I5-E6) boundary designates the gene sequence targeted with the GR splice variant MO. The arrows at E5 and E8 indicate the forward and reverse primers designed for qRT-PCR to analyze the splice blocking efficiency. The splice variant MO should result in the loss of E6 to get a smaller mis-spliced PCR product. **C)** Analysis of GR transcript in control and GR morphants after qRT-PCR, followed by agarose gel electrophoresis. The upper arrow denotes the PCR product for the primary GR transcript and the lower arrow points to the mis-spliced GR variant after the loss of targeted E6. β-actin expression was used as the loading control. **D)** qRT-PCR analysis for GR gene between control and GR morphants. The relative abundance of GR mRNA levels is illustrated ($p<0.045$) and the * sign refers to the significant difference statistically (One-way ANOVA, n=3).

4-5

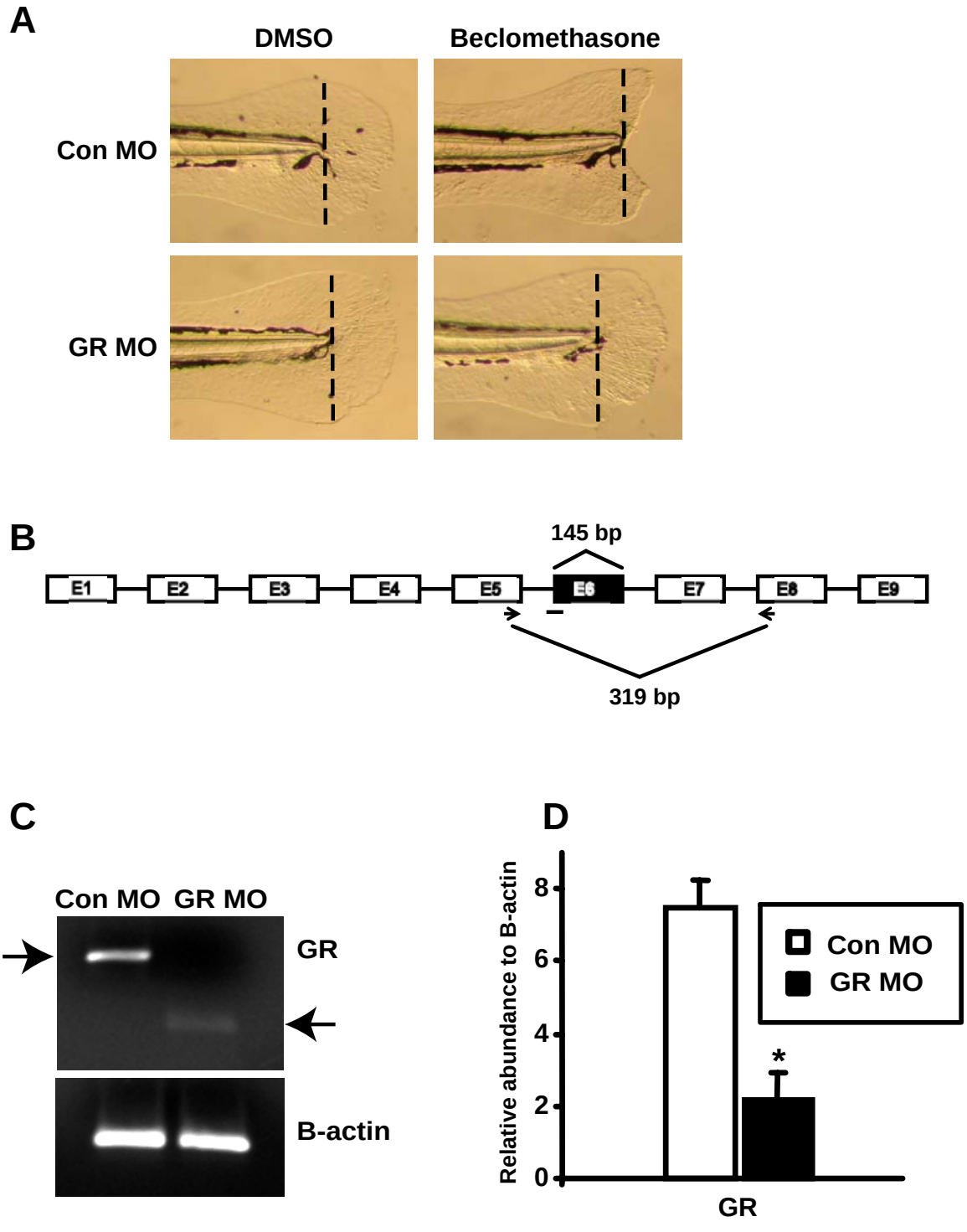
A
DMSO
Beclomethasone
Con MO
GR MO
B
145 bp
E1
E2
E3
E4
E5
E6
E7
E8
E9
319 bp
C
Con MO
GR MO
GR
B-actin
D
Relative abundance to B-actin
8
6
4
2
0
Con MO
GR MO
*
GR

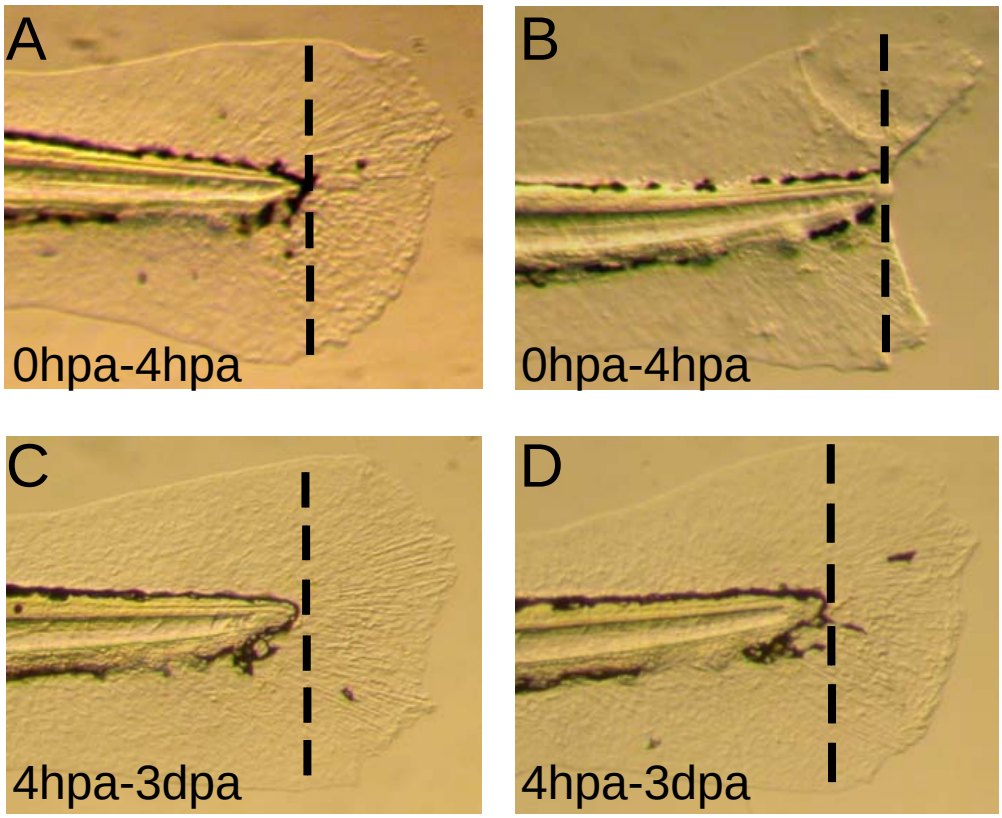

Figure 4-6. Beclomethasone specifically impact early stages of regeneration. The larvae were amputated at 2dpf and exposed to **A)** vehicle or **B)** Beclomethasone (1μM) until 4hpa and then raised in fish water for 3 days. Images were acquired three days later (3 dpa). Larvae were amputated at 2dpf and were allowed to regenerate for just four hours before continuous exposure to **C)** vehicle or **D)** Beclomethasone (1μM) until image acquisition at 3dpa. Beclomethasone was used at varying concentrations from 0.25 μM to 25 μM to confirm these results (data not shown).12 larvae were used per group.

Figure 4-7. Wound healing and blastema formation is affected by Beclomethasone. In situ hybridization was performed with amputated larvae exposed and vehicle or Beclomethasone using different molecular markers at 1dpa. The expression of wound epithelium and blastema markers in the regenerating fin at 1dpa exposed to vehicle or Beclomethasone, **A,B)** *dlx5a* **C,D)** msxe and **E,F)** *junbl.* **G)** Images are of methylene blue-stained semi-thin sections of larvae taken at 400x by light microscopy. Two images of the same Beclomethasone exposed larvae sectioned at different levels are depicted as **H1** and **H2**. Orientation of Beclomethasone treated larvae within the blocks was slightly oblique. The level of the amputation site was identified by the presence of multifocal necrosis with the notochord. The arrowhead indicates the plane of amputation. Blastema – B; Abnormal Blastema – aB; Epithelium – E; Melanocyte – M; Notochord – N.

4-7

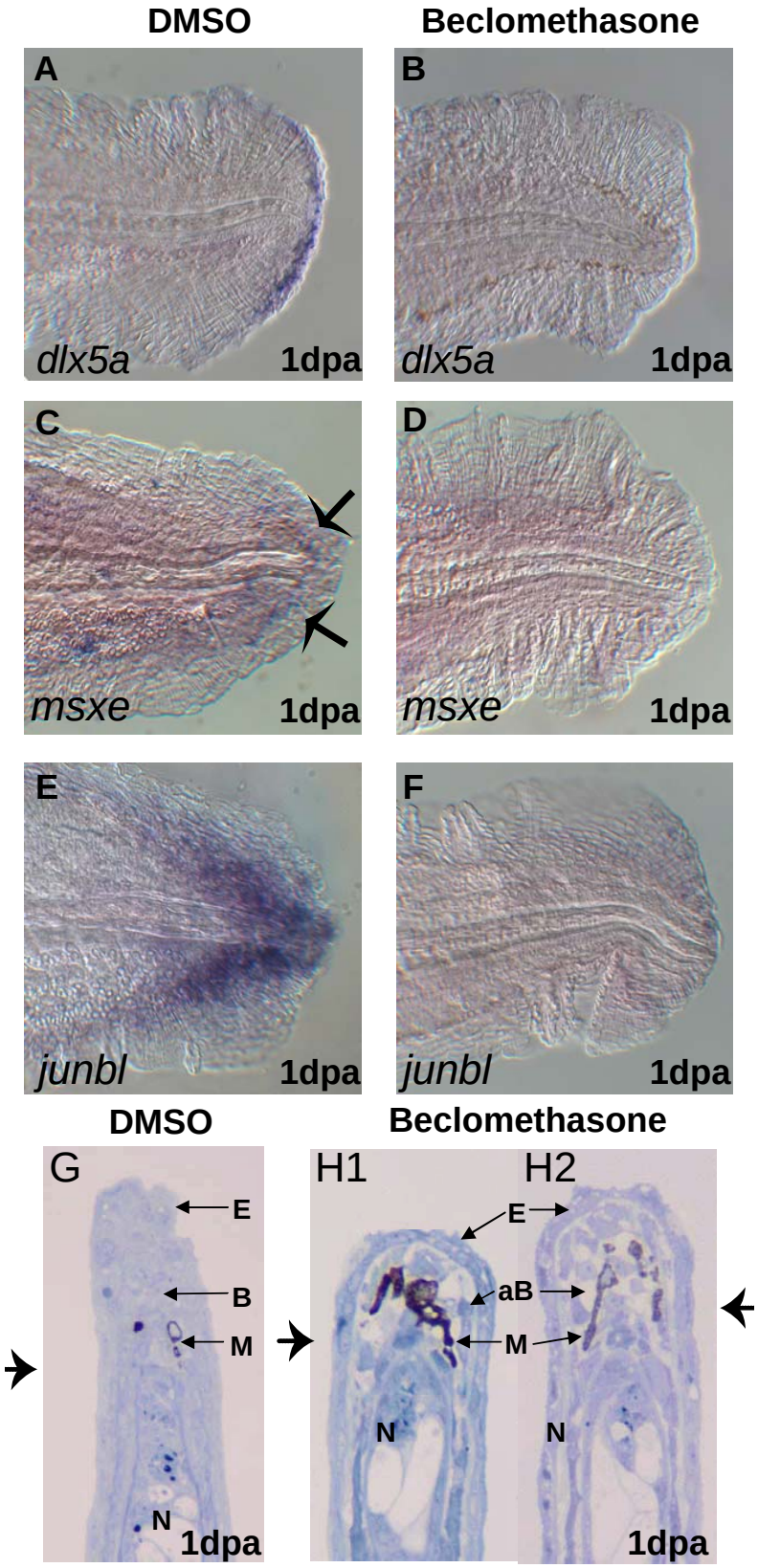
DMSO
Beclomethasone
A
dlx5a
1dpa
B
dlx5a
1dpa
C
msxe
1dpa
D
msxe
1dpa
E
junbl
1dpa
F
junbl
1dpa
DMSO
Beclomethasone
G
E
B
M
N
1dpa
H1
H2
E
E
aB
M
M
N
N
1dpa

Figure 4-8. Proliferation of cells is impacted by Beclomethasone at different regenerative stages. A) Amputated larvae exposed to vehicle or Beclomethasone were incubated with Brdu at 6-12 and 24-30hpa. Brdu labeled cells between vehicle or Beclomethasone exposed larvae at 6-12hpa and 24-30hpa. The images are representative of a total number of seven larvae and the experiment was repeated twice. The bracket represents the area analyzed for the count of proliferating cells. The dotted line represents the boundary of the regenerating fin. **B)** Quantification of the cell proliferation between vehicle or Beclomethasone exposed larvae. The respective values represent the mean $\pm$ S.E.M (One way ANOVA and Tukey method, n =7). There was statistical significant reduction (*) in the number of proliferating cells in the Beclomethasone exposed larvae compared to vehicle at both time points ($p< 0.005$). All the parameters were measured using the Image Pro-Plus software (Media Cybernetics, Silver Spring, MD).

4-8

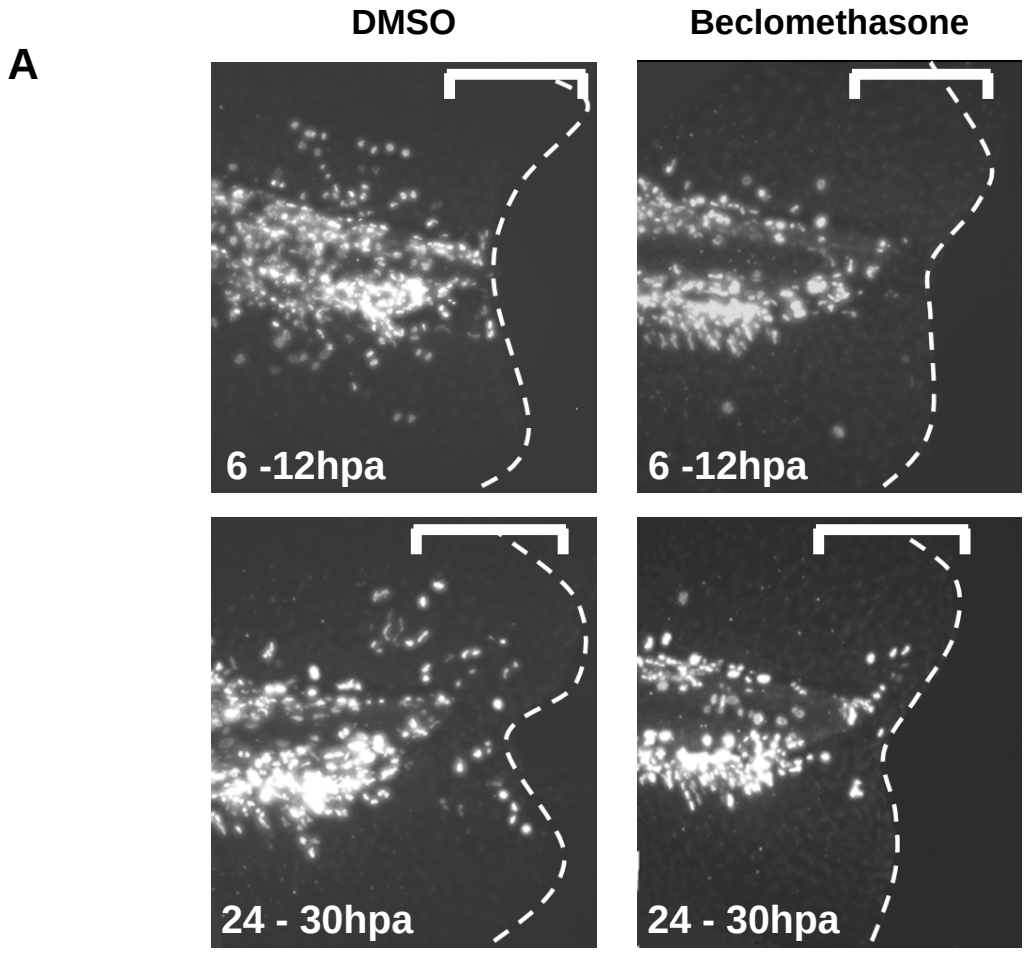
A
DMSO
Beclomethasone
6 -12hpa
6 -12hpa
24 - 30hpa
24 - 30hpa
B
25
20
15
10
5
0
DMSO
Beclo
*
*
6-12 hpa
24-30hpa

Figure 4-9. Neutrophils and Macrophages are not critical for regeneration. A) Neutrophil migration assay performed on vehicle or Beclomethasone exposed larvae at various time points. **B)** An image depicting the neutrophil migration to the wound site and the GFP positive cells were counted as part of the development of this assay. **C)** Macrophage migration assay was performed as described above using neutral red staining. **D)** A representative image showing the macrophages that are stained red at the amputation site. **E)** Control morphants and **F)** Pu.1 morphants completely regenerate the fin tissue. Images of **G)** control and **H)** Pu.1 morphant stained with neutral red at 8hpa.12 larvae were used for each group. The statistical analysis was conducted by One way ANOVA, with Bonferroni post test correction for multiple comparisons (Prism, GraphPad) and the (*) sign refers that the difference between number of neutrophils at 4 and 8hpa are statistically significant.

4-9

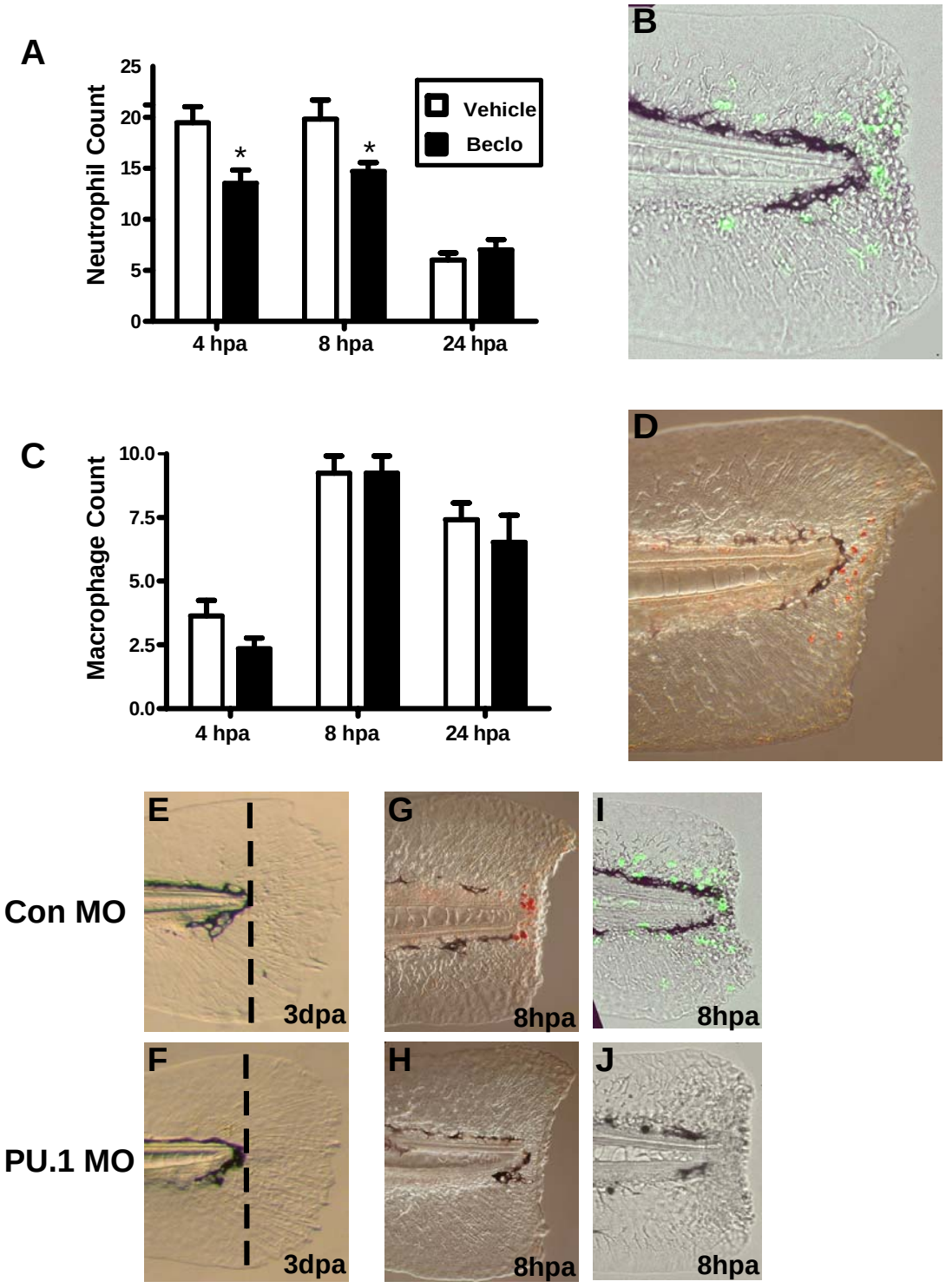
A
Neutrophil Count
25
20
15
10
5
0
Vehicle
Beclo
*
*
4 hpa
8 hpa
24 hpa
B
C
Macrophage Count
10.0
7.5
5.0
2.5
0.0
4 hpa
8 hpa
24 hpa
D
Con MO
PU.1 MO
E
F
G
H
I
J
3dpa
3dpa
8hpa
8hpa
8hpa
8hpa

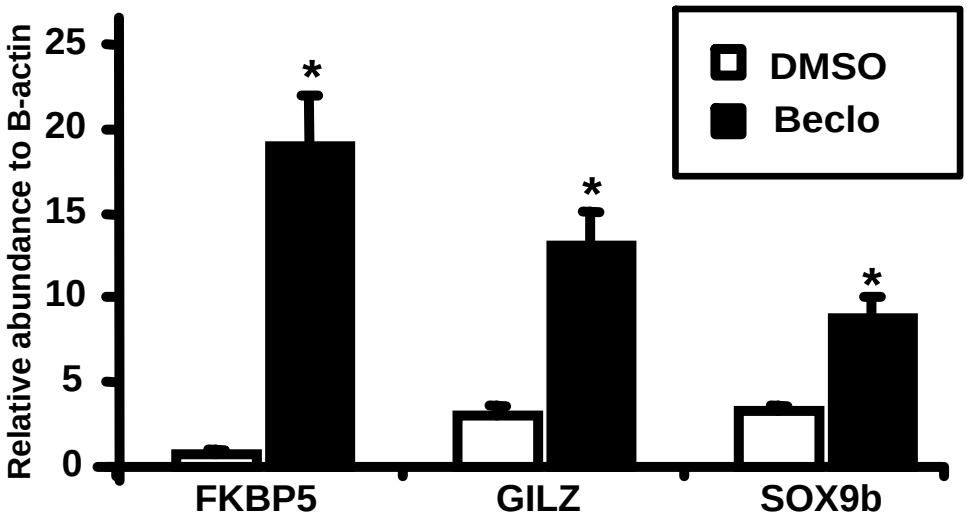

Figure 4S-1. Beclomethasone induced the global gene expression of GR primary target genes. Two day old larvae were exposed to vehicle or Beclomethasone at 2dpf and qRT-PCR was performed on the RNA isolated from whole embryonic tissue at 3dpf. The gene expression of primary GR target genes such as FKBP5, GILZ and SOX9b were analyzed. The abundance of the message levels were normalized to β-actin expression. The expression of all three genes was induced significantly in Beclomethasone exposed embryos ($p<0.004$). The respective values represent the mean $\pm$ S.E.M. (One Way ANOVA, n=3).

Chapter 5. Comparative Genomic Profiling Reveals Common Regenerative Pathways

Lijoy K Mathew, Sumitra Sengupta, Jessica Perry, Jane LaDu, Eric A Andreasen, Robert L Tanguay.

Department of Environmental and Molecular Toxicology, Environmental Health Sciences Center, Oregon State University, Corvallis, OR, 97331.

Formatted for Publication in PLoS Genetics.

Abstract

Zebrafish have the remarkable ability to regenerate body parts including the heart, spinal cord and fins by a process referred to as epimorphic regeneration. Recent studies have illustrated that similar to adult zebrafish, early life stage-larvae also possess the ability to regenerate the caudal fin. A comparative genomic analysis was used to determine the degree of conservation in gene expression among the regenerating adult caudal fin, adult heart and larval fin. Results indicate that these tissues respond to amputation/injury with strikingly similar genomic responses. Comparative analysis revealed *raldh2*, a rate-limiting enzyme for the synthesis of Retinoic acid (RA), as one of the highly induced genes across the three regeneration platforms. *In situ* localization and functional studies suggest that *raldh2* expression is critical for the complete formation of wound epithelium and blastema, processes which are indispensable for epimorphic regeneration. Patterning during regenerative outgrowth was previously considered to be the primary function of RA signaling during regeneration; however our results suggest that RA signaling is also essential for the initiation of regenerative events. We further demonstrate that the expression of *raldh2* is regulated by Wnt, Fgf and *actβA* signaling during regeneration. Since the early life stage larvae are highly amenable to molecular and genetic manipulations, the larval fin regeneration model offers an outstanding platform to rapidly identify the molecular signaling events that are required to accomplish tissue regeneration.

Introduction

Injury, disease and aging all result in a loss of tissue and reduced quality of life. Numerous human conditions could be significantly improved if therapies that encourage tissue regeneration were available. Most adult tissues and organs, especially in human beings and other mammals, have lost their regenerative potential. As a result, injury to a tissue or organ usually results in permanent damage from scarring to disability. The field of regenerative medicine is aimed at developing strategies to restore individual cell types, complex tissues, or structures that are lost or damaged. Currently, one of the main approaches in the field of regenerative medicine is to understand more about the differentiation of stem cells into specific cell types and then into complex structures (Bianco and Robey 2001). Alternatively, another strategy is to comprehend how some organisms have retained the ability to regenerate their tissues, organs and appendages (Morgan 1900; O'Steen and Walker 1962; Kemp and Park 1970) (reviewed in (Brockes et al. 2001). By understanding the molecular and genetic pathways that differentially function in these "lower" animals to accomplish regeneration, we will be in a stronger position to figure out why mammals fail to respond to tissue injury with a regenerative mechanism.

Lower vertebrate model systems such as urodele amphibians and teleost fish have the remarkable ability to regenerate organs such as the heart, spinal cord, retina and limbs/fins (Santamaria and Becerra 1991; Brockes 1994; Yamada et al. 1995; Akimenko et al. 2003; Poss et al. 2003). Adult fin regeneration has been studied in a number of teleost fishes, including goldfish (Morgan 1902; Santamaria et al. 1992; Santamaria et al. 1996), trout (Alonso et al. 2000), tilapia (Kemp and Park 1970; Santamaria et al. 1992) and minnows (Morgan 1900; Geraudie and Singer 1977), indicating that regenerative growth is functionally similar in teleosts. In recent years, emergence of the zebrafish model has reinvigorated the field of adult fin regeneration and has been established as a research model for the identification of critical molecular signaling pathways that govern the process of regeneration (Poss et al. 2000b; Nechiporuk and Keating 2002; Poss et al. 2002a; Quint et al. 2002; Akimenko et al. 2003; Poss et al. 2003). Adult zebrafish caudal

fin regeneration is completed by a process termed epimorphic regeneration, which involves reprogramming and differentiation of blastema cells to different cell types to restore the tissue to its original form (Geraudie et al. 1993; Akimenko et al. 1995; Mari-Beffa et al. 1996; Nechiporuk and Keating 2002; Poss et al. 2003). A genetic zebrafish mutant study revealed that fgf20a is absolutely required for the initiation and formation of blastema, whereas recent reports suggest that Wnt/β-catenin signaling seems to act upstream of FGF signaling (Whitehead et al. 2005; Stoick-Cooper et al. 2007). Even though major progress has been made in the identification of some of the essential pathways for regeneration such as FGF, Wnt and *Activin-βA* (*actβA*) signaling, most would agree that we are still at the early stages of gene discovery (Poss et al. 2000a; Poss et al. 2000b; Poss et al. 2003; Whitehead et al. 2005; Kawakami et al. 2006b; Jazwinska et al. 2007; Stoick-Cooper et al. 2007).

The adult fin regeneration model has unique advantages, but technical barriers have slowed progress. Recently it was reported that the fin primordia is capable of complete regeneration (2-5 days post fertilization) (Kawakami et al. 2004). Morphologically, the larval fin regenerates similarly to the adult by the development of a wound epithelium followed by blastema formation, which later proliferates and differentiates into the required cell types (Kawakami et al. 2004). Also not surprisingly, similar to the adult zebrafish, chemical inhibition of FGFR1 by SU5402, aryl hydrocarbon receptor (AHR) activation by TCDD and Glucocorticoid receptor (GR) activation by Beclomethasone abrogates larval fin regeneration (Poss et al. 2000b; Zodrow and Tanguay 2003; Kawakami et al. 2004; Mathew et al. 2006; Mathew et al. 2007) suggesting that there are similarities at the cellular and molecular level between adult and larval regeneration. Since many of the experimental advantages of zebrafish lie at the earliest life stages, the possibility of evaluating fin regeneration during this experimentally tractable life stage is enticing.

A comprehensive microarray analysis of adult zebrafish fin and adult heart regeneration identified some conserved genomic responses to amputation in these distinct regeneration models (Lien et al. 2006; Schebesta et al. 2006). This suggests that the molecular signaling pathways essential for the initiation of regeneration may be conserved. To identify whether there are corresponding similarities in the regenerative

gene expression response in the early life stage models, we conducted global genomic analysis of larval and adult fin regeneration and compared the gene expression changes. Larval microarray analysis revealed that the major functional groups altered were wound healing, signal transduction, transcriptional regulation and extracellular matrix components. Comparative analysis between larval and the adult fin regeneration systems indicated high degree of similarity between the two gene expression profiles. When the larval gene list was compared with the published zebrafish heart regeneration gene list, similar pattern of gene expression changes were also observed. Since the tissue architecture of larval fin, adult fin and heart are very different; the significant commonality in the gene expression changes must be due to the conserved molecular signaling events that are required for this remarkable process. To demonstrate the power of the larval model to investigate candidate gene function, we analyzed the role of RA signaling and performed functional studies with the larval regeneration model. Collectively, our results demonstrate that the larval model is well-suited to rapidly unravel critical molecular signaling pathways essential for tissue regeneration.

Materials and Methods

Zebrafish lines and care:

For the larval fin regeneration studies, fertilized eggs were obtained from AB strain zebrafish (University of Oregon, Eugene, OR). For the adult *in situ* hybridization study, 2 month old AB strain zebrafish were used. The fin amputations were performed as previously described (Poss et al. 2000b; Mathew et al. 2006; Andreasen et al. 2007; Mathew et al. 2007). The *Tg(hsp70l:tcf3-GFP)* line was obtained from ZIRC.

Chemicals:

The RA synthesis inhibitors DEAB and Citral were from Sigma Aldrich (St. Louis, MO). The amputated larvae were exposed to DEAB and Citral at a final concentration of 200 and 20μM, respectively, and the solutions were changed daily until

3 dpa. The ERK1/2 inhibitor U0126 was purchased from EMD Biosciences (San Diego, CA) and SB431542 from Sigma Aldrich (St. Louis, MO).UU0126 and SB431542 were continuously exposed at a final concentration of 10 and 100μM respectively.

Fin Development:

The development of the fin vasculature was analyzed using a transgenic fish (Tg-fli-GFP) that expresses green fluorescent protein in the vasculature under the control of the fli promoter. Periodically, bright field pictures were taken to analyze the development of the fin rays and overall structural changes. Simultaneously, fluorescent pictures at 488nM were taken to observe the development of the vasculature.

Isolation of Fin RNA:

The caudal fin tissue of 2dpf embryos were amputated and the fin tissues were pooled together for RNA isolation and these samples were used as non-regenerating fin tissue (0 dpa). The amputated larvae were allowed to grow for 1, 2, or 3 days and the fin tissues were re-amputated and pooled as described above for the respective 1, 2, and 3 dpa time points. Three technical replicates, each comprisied of regenerating fin tissue from 150 larvae were isolated for each time point. RNA was isolated from the fin tissue using the RNAqueous Micro kit (Ambion, Austin, TX). Adult zebrafish were amputated and the intact fin tissues were used as non regenerating fin tissue. The fin tissues were re-amputated at 1, 3, and 5 dpa for RNA isolation. Each replicate consisted of 10 fins. RNAlater was removed from the samples and total RNA was purified with TRI reagent (Molecular Research Laboratories, Cincinnati, OH) according to the manufacturer's instructions. The quality and quantity of RNA was determined by UV absorbance. Ribosomal RNA abundance and degree of degradation was determined in electropherogram patterns using the 2100 Bioanalyzer and RNA 6000 Nano chips (Agilent Technologies, Palo Alto, CA).

Affymetrix Microarray Processing:

The microarray processing including probe synthesis, hybridization and scanning were conducted by the Center for Genome Research and Biocomputing at Oregon State

University, Corvallis OR. For analysis of larval transcript abundance, 100 ng of total RNA from 0,1, 2 and 3 dpa larval fin tissue were used to generate biotinylated complementary RNA (cRNA) using the Two-Cycle Target Labeling kit (Affymetrix, Santa Clara, CA). Briefly, RNA samples were reverse transcribed using a T7-$(dT)_{24}$ primer and Superscript II reverse transcriptase (Invitrogen, Carlsbad, CA) and double stranded cDNA was synthesized. This was then used as a template for *in vitro* transcription for another round of double-stranded cDNA synthethis. For the adult fin regeneration study, 2.5 µg of total RNA was used to generate biotinylated cRNA for each treatment group using the One-Cycle Target Labeling kit (Affymetrix, Santa Clara, CA). From the double-stranded cDNA, biotinylated cRNA was synthesized using T7 RNA polymerase and a biotin-conjugated pseudouridine containing nucleotide mixture provided in the IVT Labeling Kit (Affymetrix, Santa Clara, CA). For both larval and adult fin regeneration experiments, 10µg of purified and fragmented cRNA from each experimental sample was hybridized to zebrafish genome arrays (Zebrafish430_2) according to the Affymetrix GeneChip Expression Analysis Technical Manual (701021 Rev. 5). Arrays were scanned with an Affymetrix scanner 3000. Each array image was visualized to discount artifactual signals, scratches or debris. Experiments were MIAME certified.

For data analysis, the Affymetrix cel files were imported into GeneSpring 7.1 software (Agilent Technologies, Palo Alto, CA). The files were GC-RMA processed to discount for background signal and each transcript was normalized to the median signal to allow comparison between arrays on a relative scale for each gene. The differential effect of time on regeneration was performed by comparing the non-regenerating fin tissue (0 dpa) to other time points by one-way ANOVA assuming equal variance employing Benjamini and Hochberg multiple testing corrections ($p < 0.05$). Only genes that were at least 1.7 fold differentially expressed from the 0 dpa gene levels were considered for analysis. The annotation of genes was performed by considering the sequence similarity to known mammalian proteins that was determined by conducting a BLAST search of each Affymetrix probe set against the Sanger database (http://www.sanger.ac.uk/Projects/D_rerio/). Additionally, other databases such as Genbank (http://www.ncbi.nlm.nih.gov/BLAST/) and the Zebrafish Affy Chip

Annotation Project at Children's Hospital Boston (http://134.174.23.160/zfaca/hash/master020106public.aspx) were utilized.

Quantitative RT-PCR:

Total RNA was isolated in triplicate from the regenerating fins at 0, 1, 2 and 3 dpa (n = 150/group). From the larval fin RNA, cDNA was prepared from 100 ng of total RNA per group using Superscript II (Life Technologies, Gaithersburg, MD) and oligo(dT) primers in a 20 µl volume. Quantitative RT-PCR (qRT-PCR) was conducted using gene specific primers (Supplemental Table 7) with the Opticon 2 real-time PCR detection system (MJ Research, Waltham, MA). Briefly, 1 µl of cDNA was used for each PCR reaction in the presence of SYBR Green, using DyNAmo SYBR green qPCR kit according to the manufacturer's instructions (Finnzymes, Espoo Finland). All samples were normalized to their β-actin abundance. Quantitative differences between biological samples were determined by normalizing all samples to a common reference sample. Agarose gel electrophoresis and thermal denaturation (melt curve analysis) were conducted to ensure formation of specific products. Significant differences of mRNA abundance were assessed by one-way ANOVA on $\log_{10}$ transformed data using Tukey method ($p < 0.05$) (SigmaStat software, Chicago, IL).

Morpholinos:

The fluorescein tagged *raldh2* morpholino (Gene Tools, Philomath, OR) was used to transiently knockdown *raldh2* gene. The sequence of *raldh2* morpholino is 5'-GTTCAACTTCACTGGAGGTCATCGC-3'. Morpholinos were diluted to 3 mM in 1X Danieau's solution (58 mM NaCl, 0.7 mM KCl, 0.4 mM $MgSO_4$, 0.6 mM $Ca(NO_3)_2$, 5 mM HEPES, pH 7.6) as described (Nasevicius and Ekker 2000). A standard control morpholino (Gene Tools, Philomath, OR) (5'CTCTTACCTCAGTTACAATTTATA 3') was used as the control morpholino (Control-MO). Approximately 2 nl of 0.3mM MO solution was microinjected into the embryos at the 1–2 cell stage. The fin tissue of control and *raldh2* morphants were amputated at 2dpf and exposed and allowed to grow for 3 days at 28°C.

Whole Mount *In situ* Hybridization:

In situ hybridization was performed on the regenerating fin at respective time points as described previously (Schier et al. 1997; Poss et al. 2000a). The *msxe* and *dlx5a* probes were obtained from Atsushi Kawakami (Kawakami et al. 2004). *Raldh2* probe was prepared by cloning the cDNA by RT-PCR from the RNA isolated from the whole adult zebrafish. The *wnt10a* probe was a gift from Gilbert Weidinger (Biotechnological Center, Technical University of Dresden, Germany). The embryos were reared in phenylthiourea (Sigma) at a final concentration of 100μM from 24hpf to inhibit formation of pigmentation.

Cell Proliferation Assay:

The cell proliferation assay was conducted as previously described (Mathew et al. 2007) on the regenerating fin tissue after pulse labeling with Brdu (Roche, Indianapolis, IN) for 6hrs starting from 24 hpa or 48 hpa. Brdu assay was performed on vehicle- or DEAB exposed amputated larvae and similarly on the amputated control or *raldh2* morphants at the respective time points. After 6hrs of incubation with Brdu at 28°C, the larvae were fixed in 4% paraformaldehyde (PFA) overnight. The fixed larvae were dehydrated with methanol and then stored in methanol at -20°C. Briefly, immunochemistry was conducted on the stored larvae by rehydrating with a graded methanol/PBST (phosphate-buffered saline (PBS) and 0.1% Tween-20) series. The larvae were then treated with Proteinase K in PBST for 20 minutes at room temperature (RT) and then rinsed several times with PBST. The larvae were refixed in 4% PFA for 30 minutes and then washed several times in water, followed by quick rinses in 2N HCL and incubation in 2N HCL at RT for an hour. After several washes, the larvae were then blocked with 1% normal goat serum in PBST for an hour at RT and then incubated with anti-Brdu antibody (1:100; G3G4; Developmental Studies Hybridoma Bank, Iowa City, IA) overnight at 4°C. After four or more 30 min washes with PBST, the larvae were incubated with a secondary antibody (1:1000; Alexa-546 conjugated goat anti mouse; Molecular Probes, Eugene, OR) for 4 hrs at RT. The larvae were then washed 4x for 30 min in PBST and visualized by epifluorescence microscopy. The Brdu-labeled

fluorescent cells were quantified with the acquired images using ImagePro Plus software program (Media Cybernetics, Inc., Silver Spring, MD).

Results

Structural Morphogenesis of Larval to Adult Fin:

Although both larvae and adult zebrafish regenerate their caudal fins following amputation, it is clear that there are structural differences in the regenerating tissues between the two life stages. Bright field imaging revealed that the lepidotrichia (fin rays) are not yet present in larvae at 5 days post fertilization (dpf). Instead, the larval fin primordia contained an abundance of actinotrichia (composed of collagenous fibrils) which populate the tissue. It is also noteworthy that the larval fin at this stage is not vascularized as revealed by *in vivo* imaging of the *Fli1-GFP* transgenic line. This led us to ask the question: when does the larval fin take on an adult fin morphology? To answer this question, fin developmental progression was systematically assessed to identify the structural morphogenesis until the fin developed an adult-like phenotype (Supplemental Fig. 1). Although vasculature in the trunk was functional with strong blood flow in 3- and 7- day-old zebrafish, vascularization of the caudal fin was not apparent until after 10dpf. At approximately 10dpf, the posterior end of the notochord begins to bend dorsally, and soon after, clusters of actinotrichia gather, like corn stalks tied with twine, to form ray-like structures ventral to the notochord (Supplemental Fig. 1). Concomitant with the formation of rays, the vasculature forms along these rigid tracks. By 19 dpf, 18 rays had developed, become vascularized and innervated (neuronal immunohistochemistry data not shown). By approximately 3 weeks, the caudal fin appears similar to the adult morphologically, with fully formed vasculature including intersegmental vascular loops. These studies illustrate there are significant structural differences between the adult and 2 day old larval fin structures, yet at both life stages, the animals are equally able to regenerate their fin tissues following amputation.

Comparative Genomic Analysis Revealed Common Signaling Pathways during Zebrafish Regeneration.

Since regeneration is an orchestrated process of molecular events, we designed a global microarray approach to identify the gene expression changes that occur specifically in the isolated regenerates over time in the larval fin tissue. The differential gene expression profile for 1, 2 and 3 days post amputation (dpa) were created by filtering for genes that were at least 1.7 fold differentially abundant relevant to the non-regenerating fin (0 dpa). One-way ANOVA analysis was conducted for statistical significance and a total of 1851 genes were altered in at least in one regeneration time point from 0 dpa (Fig. 1A). From the total 1851 genes, a shorter gene list was created and annotated by filtering for genes that were at least 2.5 fold differentially abundant at any regenerating time point when compared to 0 dpa (Supplemental Table 1). These transcripts were grouped into functional categories such as wound healing and immune response, signal transduction, extracellular matrix and cell adhesion (Fig. 1B). Our results were consistent with the previous studies conducted in two different regeneration models such as adult zebrafish caudal fin and heart (Lien et al. 2006; Schebesta et al. 2006), and prompted us to perform a comparative genomic analysis across three different regeneration platforms. We performed a comparative genomic analysis between the larval and the adult fin regeneration expression profiles. Similar to the larvae, an adult fin regeneration gene list was created by filtering genes that were at least 1.7 fold differentially expressed at 1, 3 or 5 dpa when compared to the non-regenerating 0 dpa fin. Statistical significance was analyzed by one-way ANOVA and a total of 3762 genes were changed at 1, 3, or 5 dpa from 0 dpa. The larval and the adult regenerating fin gene list that were at least 1.7 fold differentially expressed from the 0 dpa time point were compared to each other. 658 genes were identified as common genes, which is approximately 36% of the larval gene list (Figure 1C). We further narrowed the common gene list by filtering for the genes that were at least 1.7 fold differentially abundant at 1 dpa in the larval gene list and this reduced the number of genes to 341. To acquire more meaningful data, we then analyzed the pattern of gene expression changes by assessing the similarity in the gene regulation between the larval and adult gene lists. Out of the 341 genes that were common in both gene lists, 109 and 107 genes were similarly

induced and repressed respectively, which comprised about 64% resemblance in the pattern of gene regulation between the two regenerating tissue platforms (Supplemental Table 2). Similar to the previous adult regeneration studies, many genes involved in wound healing, signal transduction, transcriptional regulation and extracellular matrix components were regulated in both the fin regeneration models (Supplemental Table 3.) In addition to the common gene expression changes, *fgf20a*, which is considered to be an initiator of adult fin regeneration was highly induced in the larval regenerating fin underscoring the commonality at the molecular level between the two systems (Supplemental Table 1) (Whitehead et al. 2005).

The common gene expression profile identified during these two distinct fin regeneration models directed us to compare larval fin regeneration genomic response to the response in the regenerating adult heart. To perform this comparative analysis, we utilized the published data from the study performed on zebrafish regenerating heart (Lien et al. 2006). A total of 662 genes were differentially expressed in the regenerating zebrafish heart in at least one of the three time points, 3, 7 or 14 dpa (Lien et al. 2006). The larval fin regeneration gene list was compared to the adult heart regeneration gene list to identify common gene expression profiles. We identified 189 common gene expression changes (Figure 1D). Of these genes, 116 were similarly induced and 18 were similarly repressed, which constitutes about 89% and 31% similarity in the gene regulation, respectively, between larval fin and adult heart regeneration (Supplemental Table 4). This suggests the existence of conserved biomolecules that are generally required for tissue regeneration (Supplemental Table 5).

To further mine regeneration expression data, we performed a comparative analysis across three regeneration platforms, the two fin regeneration models and the zebrafish heart regeneration system. The goal was to identify the gene expression changes that are similarly modulated after amputation (Figure 1D). A total of 91 genes were common and 54% of these genes were similarly regulated across all three platforms (Supplemental Table 6). A number of genes that were induced or repressed in either adult fin or heart regeneration were validated by qRT-PCR with the larval fin RNA (Supplemental Fig. 2). Wound healing transcripts such as *galectin 9, cathepsin S, C,* and *B* were similarly regulated indicating that the immediate response to amputation is

conserved across the three regeneration platforms. Two members of the Maf protein family such as *krml2* and *krml2.2* which are involved in the control of cellular differentiation were also similarly regulated across three different platforms (Schvarzstein et al. 1999; Kajihara et al. 2001). The extracellular matrix components *timp2* and *mmp14* were highly induced indicating the importance for a proper foundation for the proliferating cells to migrate and adhere in a regulated fashion. Most importantly, *raldh2* (retaldehyde dehydrogenase 2) was one of the genes that was highly induced across three regeneration models. The profound induction of this gene in the epicardium after amputation of zebrafish heart has been recently reported (Lepilina et al. 2006; Lien et al. 2006). This is significant as the caudal fin and heart are morphologically completely different, yet at the level of gene expression; common genomic responses to amputation were observed, again suggesting that there are likely conserved "regenerative mechanisms".

***Raldh2* is Highly Expressed During Caudal Fin Regeneration:**

From the comparative genomic analysis, r*aldh2*, a rate limiting enzyme for Retinoic acid (RA) synthesis was one of the highly induced genes during regeneration across the three regeneration platforms. The induction of *raldh2* gene was validated by qRT-PCR with the larval fin RNA (Supplemental Fig. 2). *In situ* localization in the larval regenerating fin tissue revealed that *raldh2* gene was highly expressed as early as 4 hours post amputation (hpa) through 96 hpa (3 dpa) (Figure 2A). The *raldh2* transcript was expressed beneath the wound epithelium and presumably plays a role in the development of blastema as the expression of *raldh2* was observed as early as 4 hpa. The expression of *raldh2* at 12 hpa and 24 hpa was specifically localized in the blastema region indicating a functional role of RA signaling during the early phases of regeneration. Even though not quantitative, the signal intensity of the *raldh2* gene at 48 (2 dpa) and 72 hpa (3 dpa) was notably high. This high induction of *raldh2* transcript is very consistent with the results obtained from microarray and qRT-PCR (Supplemental Table1 and Supplemental Fig. 2), indicating the importance of this rate limiting enzyme at the post-blastema phase of regeneration. We further analyzed the localization pattern of *raldh2* in the adult regenerating fin tissue at 3 dpa. The expression of *raldh2* was localized in the distal

blastemal region just beneath the wound epithelium (Fig. 2B). This is consistent with the expression of *rar-γ* transcript in the adult regenerating fin tissue at the ray ends beneath the wound epithelium at 2 dpa (White et al. 1994), depicting the overlapping expression of RA signaling members in the regenerating fin tissue. In support of our data, previous mRNA localization studies have revealed that *raldh2* is very highly expressed in epicardium surrounding the ventricle, atrium and outflow tract as early as 1 dpa after partial ventricular amputation in zebrafish heart (Lepilina et al. 2006). Altogether, the qRT-PCR data and the mRNA localization studies confirm the enhanced expression of *raldh2* during caudal fin regeneration in zebrafish.

RA Signaling is Required for Larval Fin Regeneration:

The high induction of *raldh2* in three different regeneration systems suggests that *raldh2* is an active component required for regeneration. We hypothesized that, if RA signaling is critical for regeneration, inhibition of RA synthesis by specific inhibitors should block regeneration. To test this hypothesis, we used a *raldh2* inhibitor, 4-diethylaminobenzaldehyde (DEAB) and a RA synthesis inhibitor, 3,7-Dimethyl-2,6-Octadienal (Citral). The larvae at 2dpf were amputated and exposed continuously to DEAB (250μM) and Citral (25 μM) and the effects on regeneration were assessed at 3 dpa. The larvae exposed to DEAB were not able to regenerate their amputated fins, whereas, the larvae exposed to vehicle completely regenerated their lost fin tissue (Fig. 3A, B). Similar to DEAB, Citral also blocked tissue regeneration indicating the importance of RA signaling for tissue regeneration (Fig. 3A, C). To further demonstrate the specific requirement of *raldh2* during regeneration, we attempted to utilize the available *raldh2/neckless* mutant, but the larvae were severely deformed making regeneration assessments impossible. As an alternative, we performed morpholino (MO) antisense repression of *raldh2* and analyzed the regeneration potential of the *raldh2* morphants. Transient knockdown of gene expression during regeneration is feasible using MO in adult fins by electroporation (Thummel et al. 2006; Jazwinska et al. 2007) and in larval fins by embryonic microinjection (Mathew et al. 2006; Mathew et al. 2007). Our previous larval fin regeneration studies demonstrated that morpholinos can be effectively delivered at the one-cell stage and efficacy lasts for several days (Mathew et al. 2006;

Mathew et al. 2007). Since complete knockdown of *raldh2* is detrimental to normal embryonic development and leads to early mortality, (Begemann et al. 2001; Dobbs-McAuliffe et al. 2004), we carefully titrated the amount of *raldh2* morpholino to only partially repress protein synthesis, and optimized the concentration of the *raldh2* morpholino to a level which did not affect normal fin development (data not shown). The control morphants completely regenerated their fin tissue after amputation at 3 dpa, whereas the *raldh2* morphants failed to regenerate (Fig. 3D, E). These results underscore the utility of the larval fin regeneration model to rapidly perform functional studies.

To further understand the phase(s) of regeneration affected by the inhibition of RA signaling, we performed *in situ* hybridization with molecular markers *dlx5a* and *msxe,* which define the wound epithelium and the blastema, respectively. *In situ* hybridization was performed on larvae exposed to the RA inhibitors, DEAB and Citral at 1 dpa and the expression of *dlx5a* and *msxe* was evaluated. The basal wound epithelium marker *dlx5a* was strongly expressed in the vehicle exposed larvae at 1 dpa in the regenerating fin, while the expression was completely lost in the DEAB and Citral exposed larvae (Fig. 3F, G, H). Similarly, the blastema marker *msxe* was highly reduced by exposure to both the RA synthesis inhibitors at 1 dpa (Fig. 3K, L, M). To confirm the results that *raldh2* expression is essential for proper formation of wound epithelium and blastema, we further performed mRNA localization studies with the same markers in *raldh2* morphants. Very similar to the RA synthesis inhibitors, the expression of both *dlx5a* and *msxe* were significantly reduced in the regenerating fin tissue of the *raldh2* morphants when compared with the control morphants at 1 dpa (Fig. 3I, J, N, O). Altogether, these results indicated that inhibition of RA signaling is important for the the proper formation of the wound epithelium and the blastema, and the expression of *raldh2* is required for fin regeneration in zebrafish.

RA Signaling is Important for Cellular Proliferation at Distinct Regenerative Stages:

Since inhibition of RA signaling affects proper blastema formation, we next examined the role of *raldh2* specifically on cell proliferation by performing *in vivo* Bromodeoxyuridine (Brdu) incorporation assays. Cell proliferation assays were

conducted on larvae exposed to vehicle or DEAB, a *raldh2* specific inhibitor, at 24-30 hpa and 48-54 hpa. There was significant reduction in the number of Brdu-labeled cells in the regenerates of DEAB-exposed larvae at both 24-30 hpa and 48-54 hpa when compared to the vehicle-exposed larvae (Supplemental Fig. 3A, B). We also performed Brdu incorporation assay on *raldh2* morphants to identify whether cellular proliferation is similarly affected using the antisense approach. Similar to the DEAB-exposed larvae, *raldh2* morphants had a significant reduction in the number of Brdu labeled cells at 24-30 hpa and 48-54 hpa when compared to the standard control morphants (Supplemental Fig. 3C, D). It is noteworthy to mention that the inhibitory effects on cell proliferation is similar between DEAB-exposed larvae and *raldh2* morphants with a reduction of Brdu labeled cells at the posterior and ventral side of the notochord (Kawakami et al. 2004; Mathew et al. 2007), suggesting that active RA signaling is required for the normal development of caudal fin. Altogether, these results suggest that the expression of *raldh2* is required for cell proliferation at different regenerative stages.

Wnt Signaling Regulates the Expression of *Raldh2* during Fin Regeneration:

Since *raldh2* is highly expressed and is functionally important for fin regeneration, it is important to identify the signaling molecules/factors that control *raldh2* expression. The functional importance of Wnt signaling during zebrafish adult fin regeneration was recently reported, and the activation of Wnt signaling is upstream of the Fgf signaling pathway (Kawakami et al. 2006a; Stoick-Cooper et al. 2007). As a primary step before assessing whether Wnt signaling controls the expression of *raldh2*, we first analyzed the role of Wnt signaling during larval fin regeneration. To characterize the functional importance of Wnt/ β-catenin signaling during larval fin regeneration, we used an inducible transgenic zebrafish line (Tg(hsp70:ΔTCF-GFP) that simultaneously expresses GFP and inhibits Wnt/ β-catenin signaling. In this transgenic fish line, the truncated and GFP-fused TCF3 acts as a dominant repressor of Wnt-mediated transcription. The expression of this transgene is controlled by the hsp70 promoter, thus it can be conditionally expressed by a brief heat shock to shut down the β-catenin-dependent transcriptional pathways (Lewis et al. 2004). Two day old larvae were heat shocked for 2 hrs at 37^0C followed by amputation, and regeneration progress was

assessed at 3 dpa. Wild type larvae completely regenerated their fin tissue at 3 dpa, whereas the hsp70:ΔTCF-GFP transgenic larvae were unable to regenerate their lost fin tissues (Fig. 4A). We analyzed whether inhibition of Wnt signaling impacted wound epithelium and blastema formation in larvae by evaluating *dlx5a* and *msxe gene expression*. *In situ* localization studies revealed loss of expression of *dlx5a* and *msxe* in the hsp70:ΔTCF-GFP transgenic larvae when compared to the wild type larvae at 1 dpa suggesting that inhibition of Wnt signaling impairs wound epithelium and blastema formation in the larval stage of regeneration (Fig. 4B, C). These results demonstrate that, similar to adult zebrafish regeneration, the early life stage regeneration model also requires active Wnt signaling and further indicates the commonality between the different regeneration models. To directly test whether Wnt signaling regulates the expression of *raldh2*, we performed *raldh2 in situ* hybridization in the hsp70:ΔTCF-GFP transgenic larvae at 1 dpa. The expression of *raldh2* in regenerates was completely absent in the hsp70:ΔTCF-GFP transgenic larvae when compared to the wild type larvae at 1 dpa, indicating that Wnt signaling controls *raldh2* expression (Fig.4D) and suggests that RA signaling is downstream of Wnt signaling.

Activation of ERK1/2 Signaling is Required for the Expression of *Raldh2* during Fin Regeneration:

One of the most well studied signaling pathways in zebrafish regeneration is Ffg signaling where *fgf20a* has been identified as an initiator of regeneration (Poss et al. 2000b; Kawakami et al. 2004; Lee et al. 2005; Whitehead et al. 2005; Mathew et al. 2006). Since Fgf signaling is mediated through the phosphorylation of ERK1/2, we used an ERK1/2 inhibitor (U0126) to determine whether activation of ERK1/2 is required for the expression of *raldh2*. As the effect of U0126 on fin regeneration is not reported, two day old larvae were amputated and exposed to vehicle or U0126 (10Mm) continuously for 3 days to assess whether inhibition of the phosphorylation of ERK1/2 impacts larval fin regeneration. The vehicle-exposed larvae completely regenerated the fin tissue, whereas exposure to U0126 inhibited fin regeneration (Fig. 5A). We further analyzed the expression of the wound epithelium and blastema markers in the U0126 exposed larvae at 1 dpa. U0126 exposure leads to a complete loss of *dlx5a* and *msxe* expression in the

regenerates at 1 dpa when compared to the vehicle control indicating that activation of ERK1/2 is required for wound epithelium and blastema formation (Fig. 5B, C). The next goal was to determine if ERK activation was required for *raldh2* expression. Inhibition of ERK1/2 activation completely abolishes the expression of *raldh2* when compared to the vehicle control, suggesting that activation is ERK1/2 is absolutely required for the expression of *raldh2* (Fig. 5D). Since the classical Fgf pathway functions through the phosphorylation of ERK1/2, we propose that the expression of *raldh2* is controlled by Fgf signaling pathway during fin regeneration is zebrafish.

Activin-βA Signaling *Regulates Raldh2* Expression During Fin Regeneration:

The importance of *actβA* signaling for adult zebrafish caudal fin regeneration was recently reported (Jazwinska et al. 2007). It was relevant to determine whether *actβA* signaling is required for larval fin regeneration and to determine the regulatory role of *actβA* signaling for the expression of *raldh2*. Since *actβA* signaling is mediated through a serine threonine kinase complex including type 1 receptor ActBIB (Alk4) (Shi and Massague 2003), we used the small molecule SB431542 to specifically inhibit the Alk4/5/7 receptor. Recent studies using the adult regeneration model have demonstrated that SB431542 effectively inhibited *actβA* signaling and caudal fin regeneration (Jazwinska et al. 2007). To assess the requirement of *actβA* signaling for larval fin regeneration, amputated two day old larvae were exposed to vehicle or SB431542 (100μM) continuously for 3 days. Regeneration was completely inhibited by SB431542 exposure (Fig. 6A). The formation of the wound epithelium and blastema formation were analyzed by mRNA localization studies using the *dlx5a* and *msxe* probes, respectively. In comparison with the vehicle-exposed larvae, the SB431542-exposed larvae failed to express *dlx5a* in the regenerating fin at 1 dpa (Fig. 6B), indicating that wound epithelium is not formed with the inhibition of *actβA* signaling. The expression of *msxe* was distinctly present in the regenerating fin tissue of the vehicle-exposed larvae, whereas SB431542-exposed larvae exhibited only weak *msxe* expression in a few cells behind the amputation plane (Fig. 6C). These results are consistent with the adult fin regeneration studies, where expression of *msxb* was detectable in a single row of mesenchymal cells distal to the amputation plane at 2 dpa (Jazwinska et al. 2007), and underscores the

conserved functional role of *actβA* signaling for fin regeneration. It was also revealed that in the presence of SB431542, the expression of *raldh2* was completely absent in the regenerating fin tissue compared to vehicle-exposed larvae. (Fig. 6D). These results indicate that *actβA* signaling controls *raldh2* expression.

Finally, since *wnt10a* is proposed to be one of the key players of Wnt signaling during regeneration, we also analyzed whether *wnt10a* is expressed in the regenerating fin tissue when *actβA* signaling is blocked with SB431542. The expression of *wnt10a* was present in both vehicle and SB431542-exposed larvae in the regenerating fin tissue distal to the amputation plane at 1 dpa (Fig. 6E), suggesting that Wnt10a signaling is upstream to *actβA*. Altogether, these results suggest that that, Wnt signaling is at the top of the hierarchy of the known signaling pathways and RA signaling is downstream to Wnt, Fgf and *actβA* signaling during zebrafish fin regeneration (Fig. 7).

Discussion

Since the early life stages of zebrafish are amenable to molecular and genetic techniques, the development of the larval fin regeneration model provides a unique platform to rapidly identify the gene products required for regeneration (Kawakami et al. 2004; Mathew et al. 2006). The major goal of this study was to discern whether regeneration mechanisms are conserved in morphologically distinct zebrafish tissues. By exploiting the power of comparative gene expression analysis, it was revealed that there are significant common gene expression profiles in larval fin, adult caudal fin and in heart regenerating tissues, suggesting the possible existence of common molecular pathways that choreograph the regeneration process.

The physiological progression of fin regeneration in larvae and adults is similar, as both initiating with the formation of a wound epithelium, blastema formation and the distal to proximal propagation of cell proliferation pattern (Poss et al. 2003; Kawakami et al. 2004). Furthermore, there is also growing evidence to suggest that heart regeneration in zebrafish has a high degree of commonality with fin regeneration with respect to the

order of events which occur after a surgical wound. Both tissues regenerate through the blastema formation followed by proliferation of cells to complete outgrowth (Poss et al. 2002b; Poss et al. 2003; Raya et al. 2003; Raya et al. 2004; Lepilina et al. 2006). Gene expression of *msxB* and *msxC* encoding homeo-domain containing transcription factors are re-induced in regenerating zebrafish hearts as early as 3 dpa (Raya et al. 2003; Raya et al. 2004) and also in regenerating fin blastema (Akimenko et al. 1995). Additionally, the expression pattern of *notch1b* and *deltaC*, members of the Notch signaling pathway, are induced very early after heart amputation and in the regenerating fin blastema (Raya et al. 2003). None of the four genes described above were detected in the non-amputated fin or heart tissue, indicating that the re-induction of these genes was specific to the regenerating tissue. Altogether, the current literature supports the comparative gene expression analysis, indicating that there are conserved molecular mechanisms during regeneration across the three different platforms.

Recent studies illustrate that a proper balance of Wnt/β-catenin signaling is also critical for the formation and proliferation of blastemal cells (Kawakami et al. 2006b; Stoick-Cooper et al. 2007). This is consistent with our result observed in the larval model: when canonical Wnt signaling is blocked, the formation of wound epithelium and blastema are blocked (Fig. 4A, B, and C). Moreover, Wif1, a feedback regulator of Wnt signaling pathway was one of the repressed transcripts in both adult and larval fin regeneration models suggesting that the Wnt signaling pathway is well-regulated during regeneration. Moreover, a significant number of Wnt target genes were identified in both the larval and adult fin regeneration gene expression list (Supplemental Fig. 2).

Fgf signaling is one of the well-studied signaling pathways during zebrafish regeneration. The necessity of Fgf signaling during adult zebrafish fin and heart regeneration was demonstrated with the use of the Fgfr 1 inhibitor (SU5402) and the transgenic line (*hsp70:dn-fgfr1*) that expresses the dominant negative Fgfr1 protein upon heat shock (Poss et al. 2000b; Lee et al. 2005; Lepilina et al. 2006). Predictably, the larval fin regeneration system also requires Fgf signaling since SU5402 also blocked the early life stage regeneration (Kawakami et al. 2004; Mathew et al. 2006). Moreover, *fgf20a* which was identified as an initiator of blastema formation in adult regenerating fin (Whitehead et al. 2005) is also highly induced in the larval fin tissue (Supplemental Table

1). Even though *fgf20a* was detected by microarray analysis, the expression was too low to detect by *in situ* hybridization in the larval fin tissue. During zebrafish heart regeneration, among the several Fgf ligands tested, only *fgf17b* was strongly expressed in the cardiomyocytes at the apical edge of the regenerating heart tissue (Lepilina et al. 2006). The expression of different Fgf ligands in these tissues is not unexpected considering the diversity of the regenerating tissues. But the data strongly indicates that, epimorphic tissue regeneration requires functional Fgf signaling in the early stages of the regenerative process.

Similar to Wnt and Fgf signaling, *actβA* is also required for tissue regeneration in adult and larval fin regeneration. The inhibition of *actβA* signaling by SB431542 in the adult caudal fin impaired cellular migration during wound healing and inhibited blastemal cell proliferation (Jazwinska et al. 2007). When *actβA* signaling was inhibited during larval fin regeneration, the wound epithelium was not properly formed. Furthermore, similar to the reduced expression of *msxb* to a row of mesenchymal cells beneath the wound epidermis of the SB431542-exposed adult zebrafish (Jazwinska et al. 2007), *msxe* expression becomes restricted to a few cells beneath the amputation plane of the SB431542 exposed larvae. The functional requirement of *actβA* signaling between the two models underscores the conserved requirement for this pathway for zebrafish tissue regeneration.

Raldh2, a rate limiting enzyme for RA synthesis was one of the most highly induced genes in all three regeneration models. Previous *in situ* localization studies have revealed that *raldh2* was highly expressed in epicardium surrounding the ventricle, atrium and outflow tract as early as 1 dpa after partial ventricular amputation in zebrafish heart (Lepilina et al. 2006). RALDH2 enzyme activity is also highly induced in NG-2 cells after spinal cord injury in rats (Mey et al. 2005), and raldh2 expressing cells have been characterized in a subpopulation of activated oligodendrocyte precursors or polydendrocytes (Kern et al. 2007). During deer antler regeneration, in addition to the other RA signaling members, raldh2 is also expressed in the skin and perichondrium and in perivascular cells in cartilage, indicating the requirement for this RA rate limiting enzyme during the process of regeneration (Allen et al. 2002). Whole body regeneration from a miniscule blood vessel fragment has been illustrated in the colonial urochordate

Botrylloides leachi and the homologue of the RA receptor and raldh-related gene were exclusively expressed in blood cells in the regeneration niches, suggesting the ancestral involvement of RA signaling during regeneration and body restoration events (Rinkevich et al. 2007).

The induction of *raldh2* in the regenerating larval fin as early as 4 hpa suggests the involvement of active RA signaling during the early phases of regeneration. The functional role of RA signaling during amphibian and zebrafish regeneration has been studied for decades and RA is even referred to as a regeneration-inducing molecule (Brockes 1990; White et al. 1994; Ferretti and Geraudie 1995; Viviano and Brockes 1996; Maden and Hind 2003). RA is mainly characterized as a signaling molecule that is required for the vertebrate pattern formation both in developing and regenerating tissues. Amphibian regeneration studies revealed that exposure of regenerating axolotl and urodele limbs to RA results in the modification of positional memory in the proximodistal axis and caused patterning defects such as duplication of the stump (Stocum and Thoms 1984; Thoms and Stocum 1984; Kim and Stocum 1986; Brockes 1991; Geraudie et al. 1993). Similarly, exposure of zebrafish with RA during fin regeneration resulted in remarkable morphological effects suggesting that exogenous RA can respecify patterns in the regenerating fin tissue (White et al. 1994). Most of the regeneration studies with RA signaling are related with the patterning of the structures during regeneration and very little information is currently available about whether RA signaling is critically required for the initiation of regeneration, mainly for the formation of wound epithelium and blastema formation.

Our chemical inhibition and antisense repression of *raldh2* suggests that RA signaling is indeed required for the complete formation of the wound epithelium and the blastema. The reduced expression of *msxe* in the presence of RA synthesis inhibitors and *raldh2* morphants could be due to the absence of blastema formation or its inhibitory effect on blastemal cell proliferation at 24 and 48 hpa (Supplemental Fig.3). The complete understanding of the RA signaling requirement for wound epithelium and blastema formation requires further studies. Since the expression of *raldh2* was continuously present from 4 hpa to 3 dpa, we presume that the requirement of RA signaling is continuous from the initiation of regeneration through pattern formation and

regenerative outgrowth (Fig. 2, 7). However, the increased expression of *raldh2* at 2 dpa raises the possibility for a distinct flux of RA signaling (Fig. 2, 7 and Supplemental Fig.2), and suggests a dual phase of RA signaling during regeneration. In support of our two-phase RA signaling during regeneration, vertebrate limb developmental studies in mice have illustrated the existence of an early phase of RA signaling to initiate forelimb development, followed by a late phase of RA signaling required to develop the apical ectodermal ridge fully along the distal ectoderm to complete the limb outgrowth (Mic et al. 2004). Moreover, studies with the *raldh2/neckless* zebrafish mutant has demonstrated that RA signaling is required for the induction of pectoral fin field and also to establish a prepattern of anteroposterior fates in the condensing fin mesenchyme (Gibert et al. 2006). Therefore, in addition to the established functional role of RA signaling during the regenerative outgrowth, this signaling pathway is also essential in the early stages of regeneration, suggesting the existence of two phases of RA signaling during regeneration.

Finally, we illustrated that, the expression of *raldh2* is controlled by Wnt, Fgf and *actβA* signaling during zebrafish regeneration (Fig. 7). Even though multiple signaling pathways are active during regeneration, the functional requirement of each pathway for completing the process of regeneration from a wound/injury is still not completely understood. Collectively, these studies reveal that there is a conservation of fundamental regenerative networks and pathways that control epimorphic tissue regeneration. Since the larval fin regeneration model is amenable to rapid molecular and genetic manipulations, this early life stage fin regeneration model is a powerful platform to discover and unravel regenerative mechanisms.

References

Akimenko MA, Johnson SL, Westerfield M and Ekker M (1995) Differential induction of four msx homeobox genes during fin development and regeneration in zebrafish. *Development* **121**:347-57.

Akimenko MA, Mari-Beffa M, Becerra J and Geraudie J (2003) Old questions, new tools, and some answers to the mystery of fin regeneration. *Dev Dyn* **226**:190-201.

Allen SP, Maden M and Price JS (2002) A role for retinoic acid in regulating the regeneration of deer antlers. *Dev Biol* **251**:409-23.

Alonso M, Tabata YA, Rigolino MG and Tsukamoto RY (2000) Effect of induced triploidy on fin regeneration of juvenile rainbow trout, Oncorhynchus mykiss. *J Exp Zool* **287**:493-502.

Andreasen EA, Mathew LK, Lohr CV, Hasson R and Tanguay RL (2007) Aryl hydrocarbon receptor activation impairs extracellular matrix remodeling during zebra fish fin regeneration. *Toxicol Sci* **95**:215-26.

Begemann G, Schilling TF, Rauch GJ, Geisler R and Ingham PW (2001) The zebrafish neckless mutation reveals a requirement for raldh2 in mesodermal signals that pattern the hindbrain. *Development* **128**:3081-94.

Bianco P and Robey PG (2001) Stem cells in tissue engineering. *Nature* **414**:118-21.

Brockes JP (1990) Retinoic acid and limb regeneration. *J Cell Sci Suppl* **13**:191-8.

Brockes JP (1991) Some current problems in amphibian limb regeneration. *Philos Trans R Soc Lond B Biol Sci* **331**:287-90.

Brockes JP (1994) New approaches to amphibian limb regeneration. *Trends Genet* **10**:169-73.

Brockes JP, Kumar A and Velloso CP (2001) Regeneration as an evolutionary variable. *J Anat* **199**:3-11.

Dobbs-McAuliffe B, Zhao Q and Linney E (2004) Feedback mechanisms regulate retinoic acid production and degradation in the zebrafish embryo. *Mech Dev* **121**:339-50.

Ferretti P and Geraudie J (1995) Retinoic acid-induced cell death in the wound epidermis of regenerating zebrafish fins. *Dev Dyn* **202**:271-83.

Geraudie J, Monnot MJ, Ridet A, Thorogood P and Ferretti P (1993) Is exogenous retinoic acid necessary to alter positional information during regeneration of the fin in zebrafish? *Prog Clin Biol Res* **383B**:803-14.

Geraudie J and Singer M (1977) Relation between nerve fiber number and pectoral fin regeneration in the teleost. *J Exp Zool* **199**:1-8.

Gibert Y, Gajewski A, Meyer A and Begemann G (2006) Induction and prepatterning of the zebrafish pectoral fin bud requires axial retinoic acid signaling. *Development* **133**:2649-59.

Jazwinska A, Badakov R and Keating MT (2007) Activin-betaA Signaling Is Required for Zebrafish Fin Regeneration. *Curr Biol*.

Kajihara M, Kawauchi S, Kobayashi M, Ogino H, Takahashi S and Yasuda K (2001) Isolation, characterization, and expression analysis of zebrafish large Mafs. *J Biochem (Tokyo)* **129**:139-46.

Kawakami A, Fukazawa T and Takeda H (2004) Early fin primordia of zebrafish larvae regenerate by a similar growth control mechanism with adult regeneration. *Dev Dyn* **231**:693-9.

Kawakami Y, Rodriguez Esteban C, Raya M, Kawakami H, Marti M, Dubova I and Izpisua Belmonte JC (2006a) Wnt/beta-catenin signaling regulates vertebrate limb regeneration. *Genes Dev* **20**:3232-7.

Kawakami Y, Rodriguez Esteban C, Raya M, Kawakami H, Martí M, Dubova I and Izpisua Belmonte JC (2006b) Wnt/-catenin signaling regulates vertebrate limb regeneration. *Genes and Dev* **Dec 2006; 20: 3232 - 3237 ; doi:10.1101/gad.1475106**.

Kemp NE and Park JH (1970) Regeneration of lepidotrichia and actinotrichia in the tailfin of the teleost Tilapia mossambica. *Dev Biol* **22**:321-42.

Kern J, Schrage K, Koopmans GC, Joosten EA, McCaffery P and Mey J (2007) Characterization of retinaldehyde dehydrogenase-2 induction in NG2-positive glia after spinal cord contusion injury. *Int J Dev Neurosci* **25**:7-16.

Kim WS and Stocum DL (1986) Retinoic acid modifies positional memory in the anteroposterior axis of regenerating axolotl limbs. *Dev Biol* **114**:170-9.

Lee Y, Grill S, Sanchez A, Murphy-Ryan M and Poss KD (2005) Fgf signaling instructs position-dependent growth rate during zebrafish fin regeneration. *Development*.

Lepilina A, Coon AN, Kikuchi K, Holdway JE, Roberts RW, Burns CG and Poss KD (2006) A dynamic epicardial injury response supports progenitor cell activity during zebrafish heart regeneration. *Cell* **127**:607-19.

Lewis JL, Bonner J, Modrell M, Ragland JW, Moon RT, Dorsky RI and Raible DW (2004) Reiterated Wnt signaling during zebrafish neural crest development. *Development* **131**:1299-308.

Lien CL, Schebesta M, Makino S, Weber GJ and Keating MT (2006) Gene Expression Analysis of Zebrafish Heart Regeneration. *PLoS Biol* **4**.

Maden M and Hind M (2003) Retinoic acid, a regeneration-inducing molecule. *Dev Dyn* **226**:237-44.

Mari-Beffa M, Mateos I, Palmqvist P and Becerra J (1996) Cell to cell interactions during teleosts fin regeneration. *Int J Dev Biol* **Suppl 1**:179S-180S.

Mathew LK, Andreasen EA and Tanguay RL (2006) Aryl hydrocarbon receptor activation inhibits regenerative growth. *Mol Pharmacol* **69**:257-65.

Mathew LK, Sengupta S, Kawakami A, Andreasen EA, Lohr CV, Loynes CA, Renshaw SA, Peterson RT and Tanguay RL (2007) Unraveling tissue regeneration pathways using chemical genetics. *J Biol Chem*.

Mey J, D JM, Brook G, Liu RH, Zhang YP, Koopmans G and McCaffery P (2005) Retinoic acid synthesis by a population of NG2-positive cells in the injured spinal cord. *Eur J Neurosci* **21**:1555-68.

Mic FA, Sirbu IO and Duester G (2004) Retinoic acid synthesis controlled by Raldh2 is required early for limb bud initiation and then later as a proximodistal signal during apical ectodermal ridge formation. *J Biol Chem* **279**:26698-706.

Morgan TH (1900) Regeneration in teleosts. *Arch Entw Org* **10**:120-131.

Morgan TH (1902) Further experiments on the regeneration of the tail fins of fishes. *Arch Entw MEch* **14**:539-561.

Nasevicius A and Ekker SC (2000) Effective targeted gene 'knockdown' in zebrafish. *Nat Genet* **26**:216-20.

Nechiporuk A and Keating MT (2002) A proliferation gradient between proximal and msxb-expressing distal blastema directs zebrafish fin regeneration. *Development* **129**:2607-17.

O'Steen WK and Walker BE (1962) Radioautographic studies or regeneration in the common newt. III. Regeneration and repair of the intestine. *Anat Rec* **142**:179-87.

Poss KD, Keating MT and Nechiporuk A (2003) Tales of regeneration in zebrafish. *Dev Dyn* **226**:202-210.

Poss KD, Nechiporuk A, Hillam AM, Johnson SL and Keating MT (2002a) Mps1 defines a proximal blastemal proliferative compartment essential for zebrafish fin regeneration. *Development* **129**:5141-9.

Poss KD, Shen J and Keating MT (2000a) Induction of lef1 during zebrafish fin regeneration. *Dev Dyn* **219**:282-6.

Poss KD, Shen J, Nechiporuk A, McMahon G, Thisse B, Thisse C and Keating MT (2000b) Roles for Fgf signaling during zebrafish fin regeneration. *Dev Biol* **222**:347-58.

Poss KD, Wilson LG and Keating MT (2002b) Heart regeneration in zebrafish. *Science* **298**:2188-90.

Quint E, Smith A, Avaron F, Laforest L, Miles J, Gaffield W and Akimenko MA (2002) Bone patterning is altered in the regenerating zebrafish caudal fin after ectopic expression of sonic hedgehog and bmp2b or exposure to cyclopamine. *Proc Natl Acad Sci U S A* **99**:8713-8.

Raya A, Consiglio A, Kawakami Y, Rodriguez-Esteban C and Izpisua-Belmonte JC (2004) The zebrafish as a model of heart regeneration. *Cloning Stem Cells* **6**:345-51.

Raya A, Koth CM, Buscher D, Kawakami Y, Itoh T, Raya RM, Sternik G, Tsai HJ, Rodriguez-Esteban C and Izpisua-Belmonte JC (2003) Activation of Notch signaling pathway precedes heart regeneration in zebrafish. *Proc Natl Acad Sci U S A* **100 Suppl 1**:11889-95.

Rinkevich Y, Paz G, Rinkevich B and Reshef R (2007) Systemic Bud Induction and Retinoic Acid Signaling Underlie Whole Body Regeneration in the Urochordate Botrylloides leachi. *PLoS Biol* **5**:e71.

Santamaria JA and Becerra J (1991) Tail fin regeneration in teleosts: cell-extracellular matrix interaction in blastemal differentiation. *J Anat* **176**:9-21.

Santamaria JA, Mari-Beffa M and Becerra J (1992) Interactions of the lepidotrichial matrix components during tail fin regeneration in teleosts. *Differentiation* **49**:143-50.

Santamaria JA, Mari-Beffa M, Santos-Ruiz L and Becerra J (1996) Incorporation of bromodeoxyuridine in regenerating fin tissue of the goldfish Carassius auratus. *J Exp Zool* **275**:300-7.

Schebesta M, Lien CL, Engel FB and Keating MT (2006) Transcriptional profiling of caudal fin regeneration in zebrafish. *ScientificWorldJournal* **6**:38-54.

Schier AF, Neuhauss SC, Helde KA, Talbot WS and Driever W (1997) The one-eyed pinhead gene functions in mesoderm and endoderm formation in zebrafish and interacts with no tail. *Development* **124**:327-42.

Schvarzstein M, Kirn A, Haffter P and Cordes SP (1999) Expression of Zkrml2, a homologue of the Krml1/val segmentation gene, during embryonic patterning of the zebrafish (Danio rerio). *Mech Dev* **80**:223-6.

Shi Y and Massague J (2003) Mechanisms of TGF-beta signaling from cell membrane to the nucleus. *Cell* **113**:685-700.

Stocum DL and Thoms SD (1984) Retinoic-acid-induced pattern completion in regenerating double anterior limbs of urodeles. *J Exp Zool* **232**:207-15.

Stoick-Cooper CL, Weidinger G, Riehle KJ, Hubbert C, Major MB, Fausto N and Moon RT (2007) Distinct Wnt signaling pathways have opposing roles in appendage regeneration. *Development* **134**:479-89.

Thoms SD and Stocum DL (1984) Retinoic acid-induced pattern duplication in regenerating urodele limbs. *Dev Biol* **103**:319-28.

Thummel R, Bai S, Sarras MP, Jr., Song P, McDermott J, Brewer J, Perry M, Zhang X, Hyde DR and Godwin AR (2006) Inhibition of zebrafish fin regeneration using in vivo electroporation of morpholinos against fgfr1 and msxb. *Dev Dyn* **235**:336-46.

Viviano CM and Brockes JP (1996) Is retinoic acid an endogenous ligand during urodele limb regeneration? *Int J Dev Biol* **40**:817-22.

White JA, Boffa MB, Jones B and Petkovich M (1994) A zebrafish retinoic acid receptor expressed in the regenerating caudal fin. *Development* **120**:1861-72.

Whitehead GG, Makino S, Lien CL and Keating MT (2005) fgf20 is essential for initiating zebrafish fin regeneration. *Science* **310**:1957-60.

Yamada H, Miyake T and Kitamura T (1995) Regeneration of axons in transection of the carp spinal cord. *Zoolog Sci* **12**:325-32.

Zodrow JM and Tanguay RL (2003) 2,3,7,8-tetrachlorodibenzo-p-dioxin inhibits zebrafish caudal fin regeneration. *Toxicol Sci* **76**:151-161.

Acknowledgements

We would like to thank Anne-Marie Girard from the Center for Gene Research and Biotechnology at Oregon State University for her valuable assistance. The vascular specific fli directed gfp transgenic fish was kindly provided by Dr. Brant Weinstein of the Unit on Vertebrate Organogenesis at the National Institutes of Health, Bathesda, MD. The *Tg(hsp70l:tcf3-GFP)* line was obtained from ZIRC.

Figure 5-1. Comparative genomic analysis during zebrafish regeneration. A) Heat map illustrating the changes in gene expression during the progression of larval fin regeneration. The unamputated fin tissue at 2dpf (0dpa) was used as the control to compare with the regenerating fin at 1, 2 and 3dpa. **B)** The genes that were at least 2 fold differentially expressed were grouped based on the known function of the proteins. Comparative gene expression profiling was performed between larval fin, adult fin and adult heart regeneration systems in zebrafish. The venn diagram comparing the genes that were modulated during regeneration between the **C)** larval and the adult fin regeneration, **D)** larval fin and the adult heart regeneration and **E)** larval fin, adult fin and adult heart regeneration models.

5-1

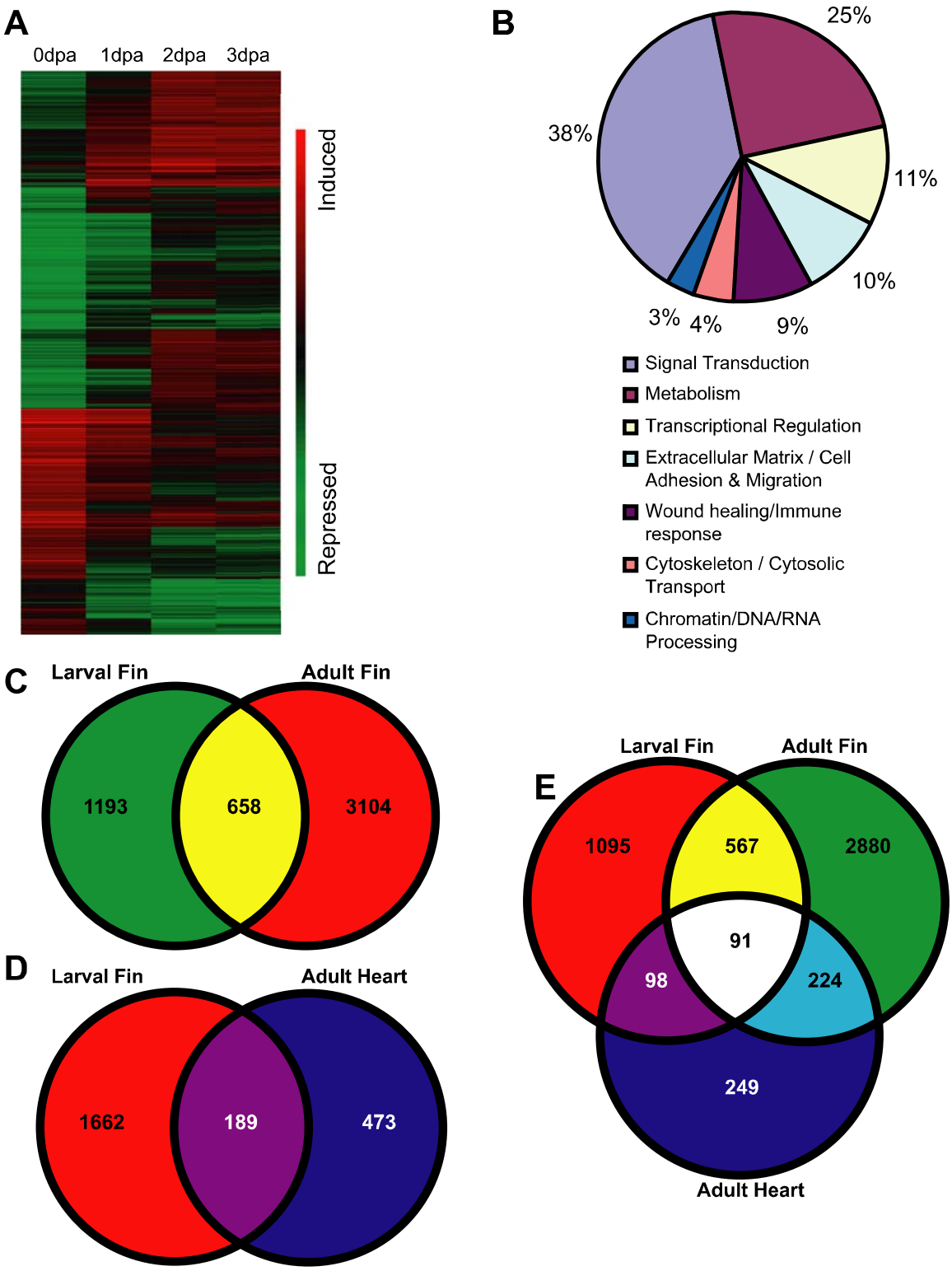
A
0dpa
1dpa
2dpa
3dpa
Induced
Repressed
B
25%
38%
11%
10%
3%
4%
9%
Signal Transduction
Metabolism
Transcriptional Regulation
Extracellular Matrix / Cell Adhesion & Migration
Wound healing/Immune response
Cytoskeleton / Cytosolic Transport
Chromatin/DNA/RNA Processing
C
Larval Fin
Adult Fin
1193
658
3104
D
Larval Fin
Adult Heart
1662
189
473
E
Larval Fin
Adult Fin
1095
567
2880
91
98
224
249
Adult Heart

Figure 5-2. *In situ* localization of *raldh2* in the larval and adult regenerating fin tissue. A) The mRNA localization of *raldh2* was performed in the regenerating fin tissue at various time points in the larval fin tissue. The expression was detected in the larval regenerate as early as 4hpa and continuously till 3dpa. The *raldh2* is clearly expressed beneath the wound epithelium at 4 & 8hpa and in the blastema region at 12hpa and 1dpa. Similar to the microarray and qRT-PCR data, *raldh2* is highly expressed at 2dpa when compared to the other time points. **B)** The expression of *raldh2* is present in the distal blastema region in the adult regenerating fin at 3dpa and the transcript is completely absent in the uncut adult fin.

5-2

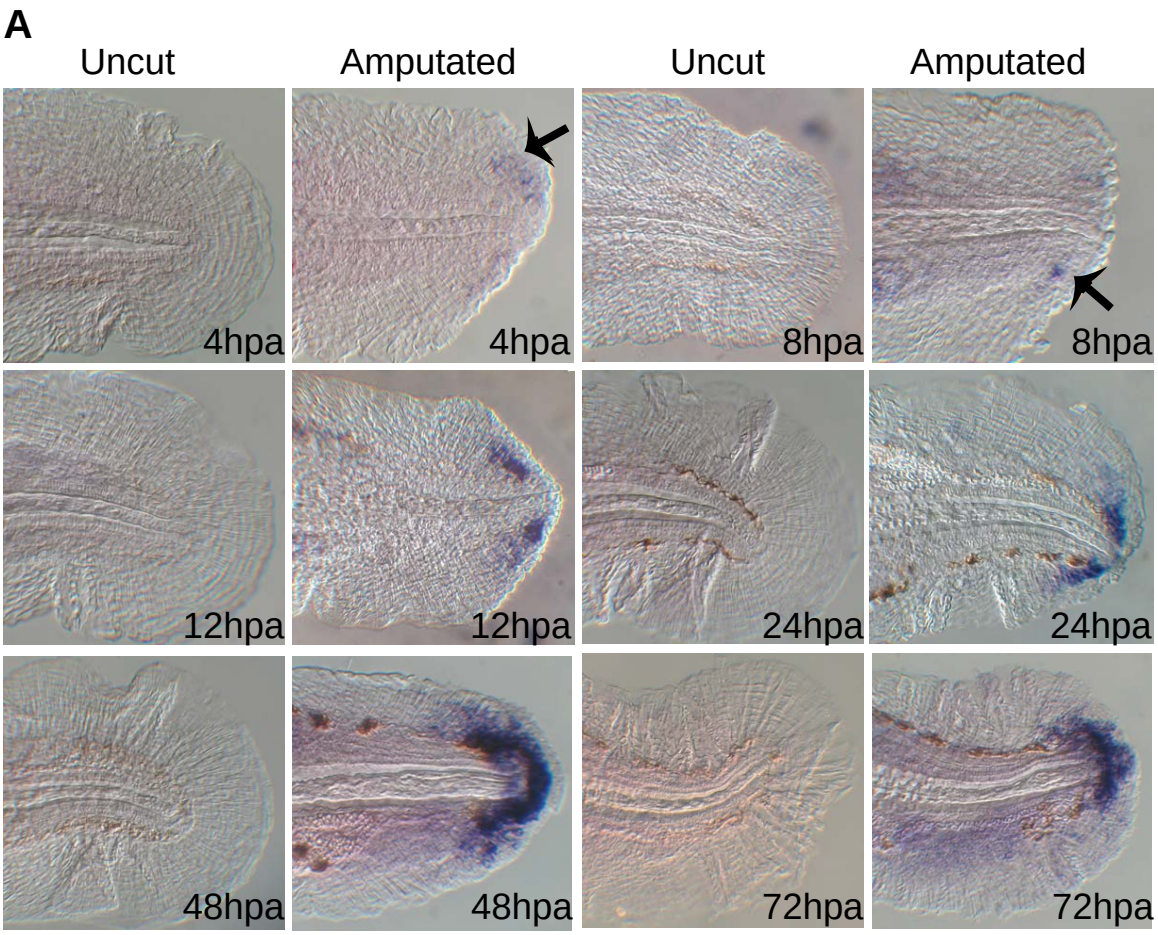
A
Uncut
Amputated
Uncut
Amputated
4hpa
4hpa
8hpa
8hpa
12hpa
12hpa
24hpa
24hpa
48hpa
48hpa
72hpa
72hpa
B
Uncut
Amputated - 3dpa

Figure 5-3. Inhibition of RA signaling impairs fin regeneration with impaired wound epithelium and blastema formation. A, B, C) Two day old larvae were amputated and exposed to vehicle, DEAB or Citral and the regeneration potential was assessed at 3dpa. DEAB and Citral exposed larvae depicted inhibition of regeneration at 3dpa. **D, E)** Control and *raldh2* morphants were amputated and allowed to grow for 3 days at 28°C. Similar to the DEAB and Citral exposed larvae, *raldh2* morphants also had impairment of fin regeneration. The expression of wound epithelium marker *dlx5a* and blastema marker *msxe* were assessed in the regenerating fin at 1dpa by in situ hybridization in the vehicle, DEAB and Citral exposed larvae. **G, H, L, M)** DEAB and Citral exposed larvae didn't express both *dlx5a* and *msxe* when compared with the **F, K,)** vehicle exposed larvae. The expression of *dlx5a* and *msxe* in the regenerating fin at 1dpa were lost in the **N, O)** *raldh2* morphants in comparison with the **I, J)** standard control morphants. All these experiments were conducted multiple times and the pictures are representative of more than 50 animals.

5-3

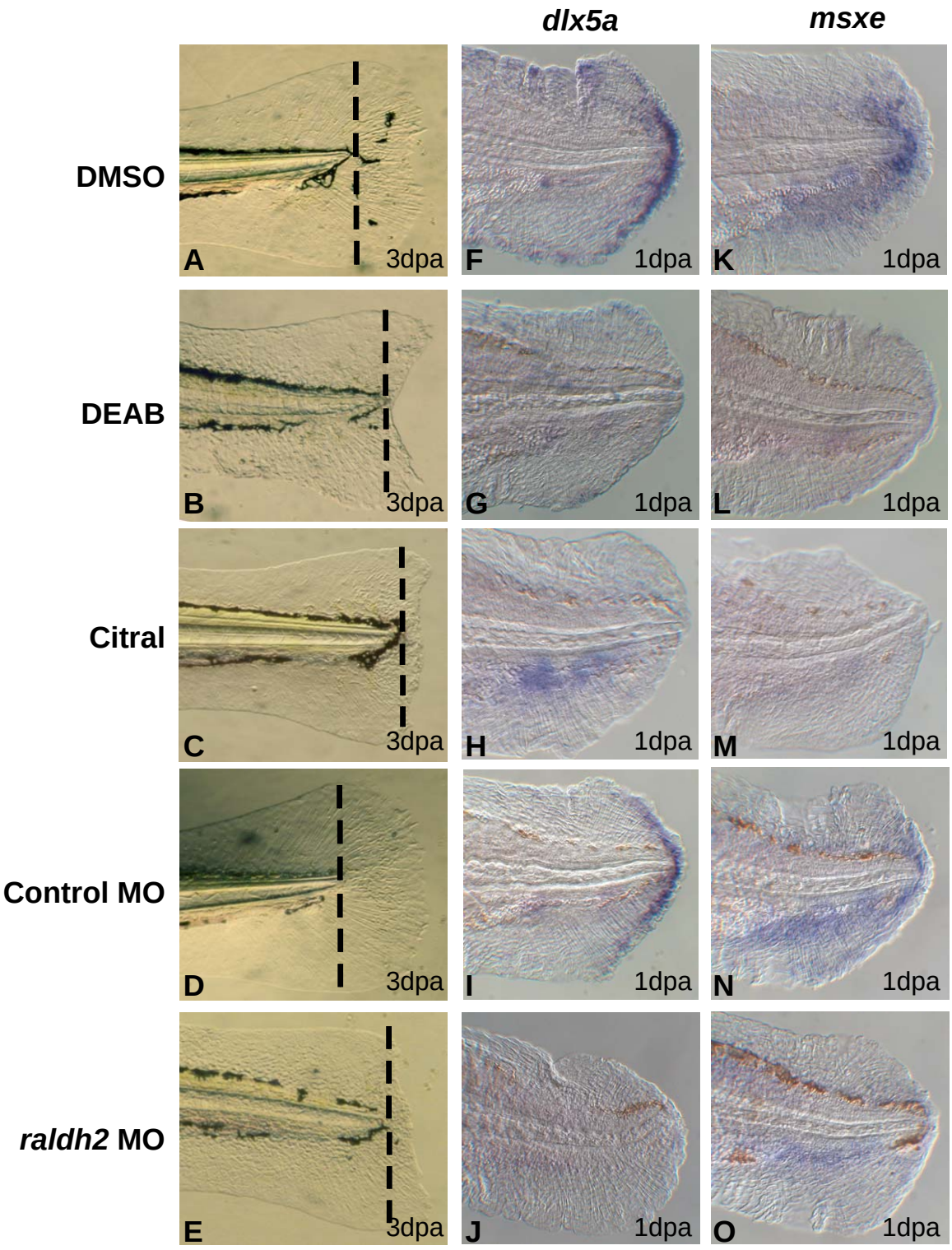
dlx5a
msxe
DMSO
DEAB
Citral
Control MO
raldh2 MO
A
3dpa
B
3dpa
C
3dpa
D
3dpa
E
3dpa
F
1dpa
G
1dpa
H
1dpa
I
1dpa
J
1dpa
K
1dpa
L
1dpa
M
1dpa
N
1dpa
O
1dpa

Figure 5-4. Raldh2 expression during fin regeneration is controlled by Wnt Signaling. Two day old wild type or homozygous *Tg(hsp70l:tcf3-GFP)* larvae were heat shocked at 37°C for 2hours followed by amputation after a few hours of heat shock. **A)** The *Tg(hsp70l:tcf3-GFP)* larvae had impaired regeneration at 3dpa when compared to the wild type. The dotted line indicates the plane of amputation. **B, C)** The expression of *dlx5a* in the wound epithelium and *msxe* in the blastema were not detectable in the *Tg(hsp70l:tcf3-GFP)* larvae in comparison with the wild type larvae. **D)** The expression of raldh2 was completely lost in the *Tg(hsp70l:tcf3-GFP)* larvae, whereas raldh2 is clearly expressed in the wild type larvae at 1dpa.

5-4

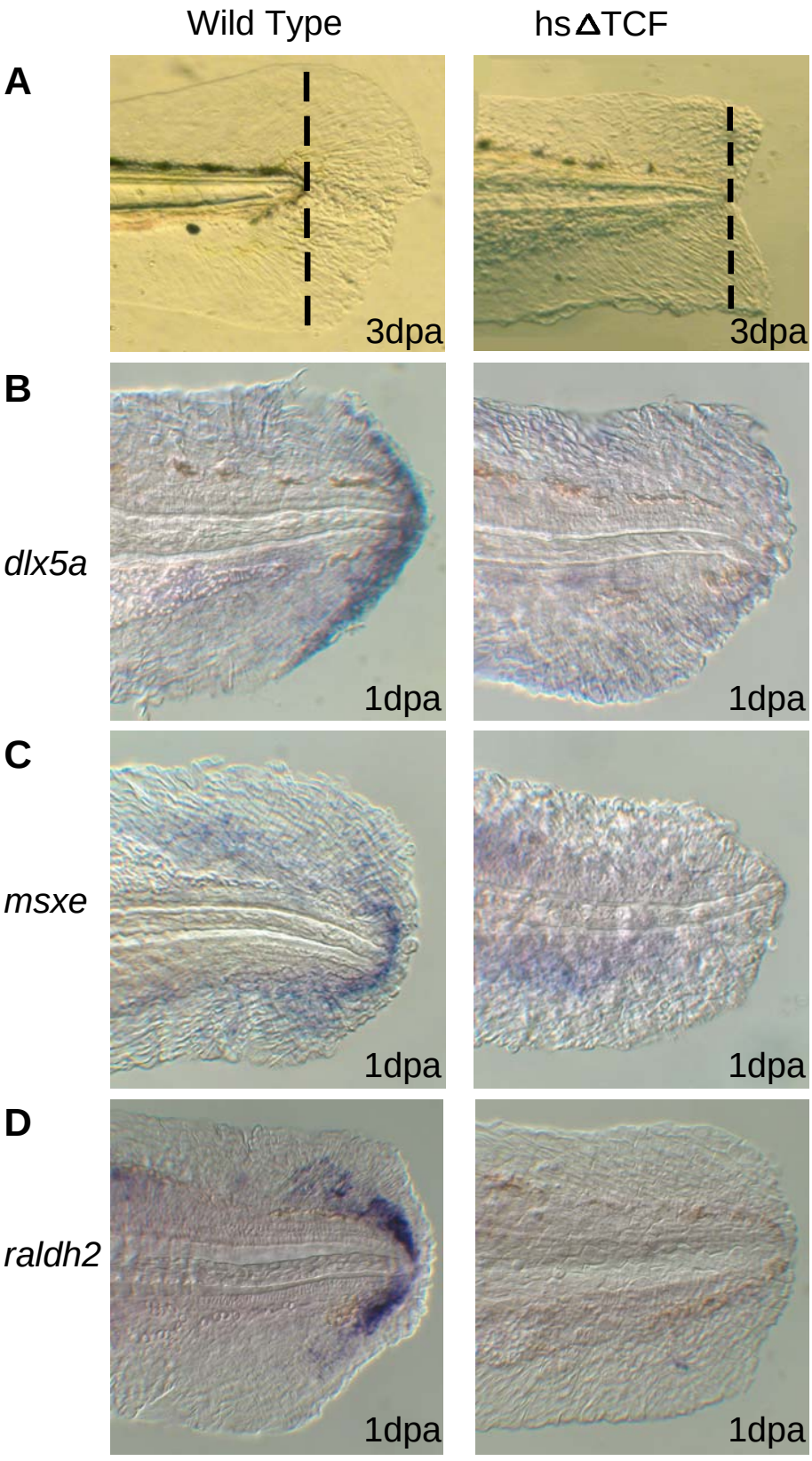
Wild Type
hsΔTCF
A
3dpa
3dpa
B
dlx5a
1dpa
1dpa
C
msxe
1dpa
1dpa
D
raldh2
1dpa
1dpa

Figure 5-5. Expression of *raldh2* is dependent on the phosphorylation of ERK1/2 during fin regeneration. The amputated larvae at 2dpf were exposed to vehicle or U0126 and regeneration was assessed at 3dpa. **A)** The vehicle exposed larvae completely regenerated by 3dpa, whereas, U0126 exposed larvae had inhibition of fin regeneration. The dotted line indicates the plane of amputation. **B, C)** The wound epithelium marker *dlx5a* and blastema marker *msxe* were expressed in the vehicle exposed larvae and is not detectable in the U0126 exposed larvae. **D)** *Raldh2* expression is present in the blastema area in the vehicle exposed larvae at 1dpa and is not detectable in the U0126 exposed larvae.

5-5

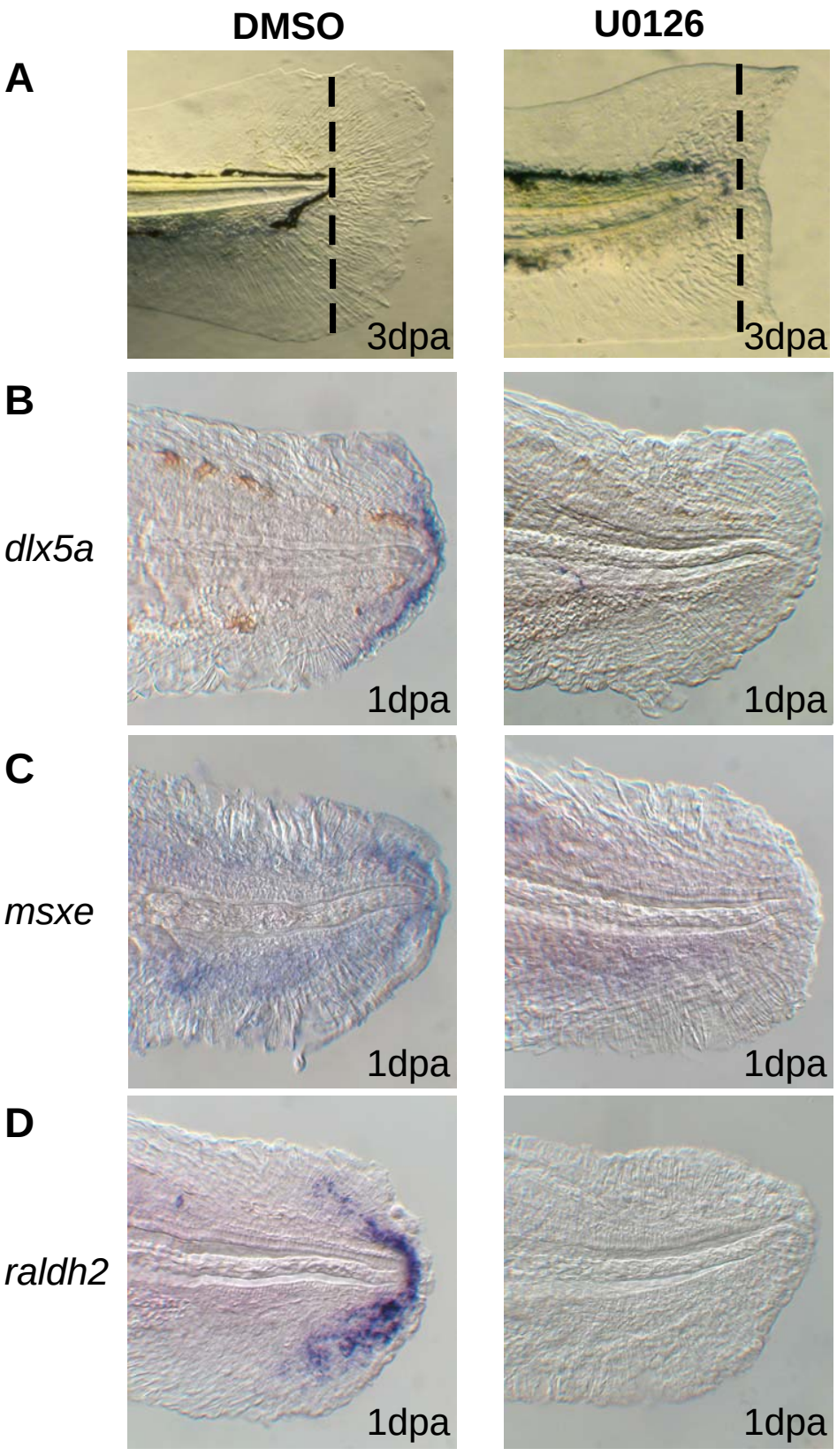
DMSO
U0126
A
3dpa
3dpa
B
dlx5a
1dpa
1dpa
C
msxe
1dpa
1dpa
D
raldh2
1dpa
1dpa

Figure 5-6. *Activin-βA* Signaling regulates *raldh2* expression during regeneration. A) Inhibition of a*ctivin-βA* signaling by SB431542 completely blocks larval fin regeneration. The dotted line indicates the plane of amputation. **B, C)** The wound epithelium and blastema markers such as *dlx5a* and *msxe* respectively are completely repressed in the SB431542 exposed larval regenerating fin at 1dpa. **D)** Exposure to SB431542 results in the loss of expression of *raldh2* in the regenerating fin at 1dpa in comparison with the vehicle exposed larvae. **E)** The Wnt signaling molecule *wnt10a* is expressed in the regenerating fin of both vehicle as well as SB431542 exposed larvae at 1dpa.

5-6

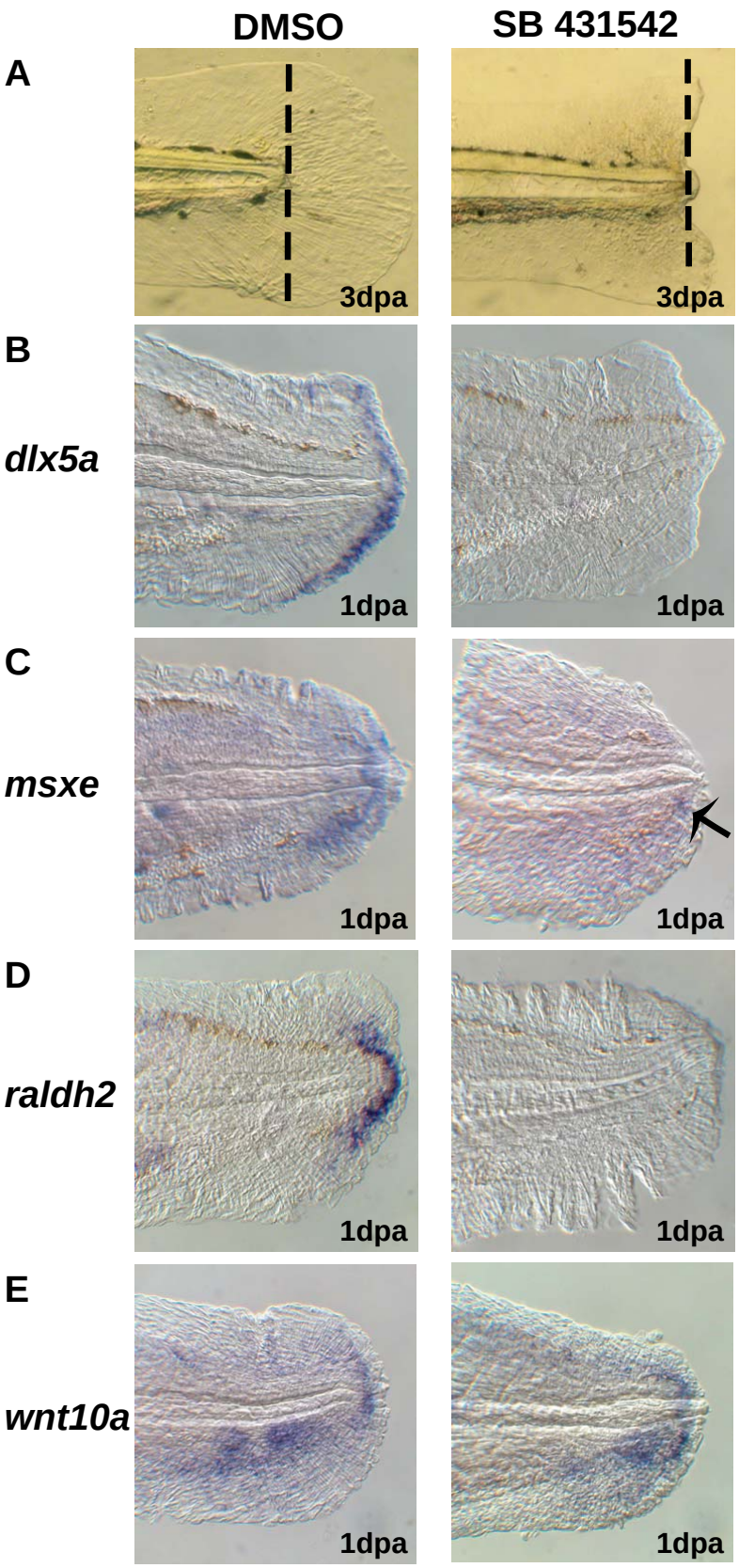
DMSO
SB 431542
A
3dpa
3dpa
B
dlx5a
1dpa
1dpa
C
msxe
1dpa
1dpa
D
raldh2
1dpa
1dpa
E
wnt10a
1dpa
1dpa

Figure 5-7. Proposed model of essential molecular pathways controlling fin regeneration. Zebrafish, unlike mammals and human beings have the remarkable ability to regenerate several organs including heart, spinal cord, and caudal fin after surgical amputation or injury. Based on the comparative genomic and functional analysis, we propose that, the hierarchy of molecular signaling pathways actively involved during the process of regeneration is highly conserved across different regeneration platforms and life stages. Since the expression of *fgf20a* is regulated by Wnt signaling and the expression of *wnt10a* is detectable in the regenerating fin with the inhibition of a*ctivin-βA* signaling, we propose that Wnt signaling pathway is upstream to all the signaling pathways studied during fin regeneration. Raldh2, a rate limiting enzyme for the synthesis of retinoic acid is regulated by Wnt signaling and is also dependent on the phosphorylation of ERK1/2, implicating the involvement of Fgf pathway as Fgf signaling is mediated through the phosphorylation of ERK1/2. A*ctivin-βA* signaling is also involved in the regulation of raldh2, suggesting that, raldh2 is downstream to Wnt, Fgf and a*ctivin-βA* signaling during regeneration. The possibility of Wnt controlling the expression of raldh2 directly is also plausible. Similarly, whether the regulation of raldh2 by a*ctivin-βA* signaling is Fgf dependent or not has to be studied further.

5-7

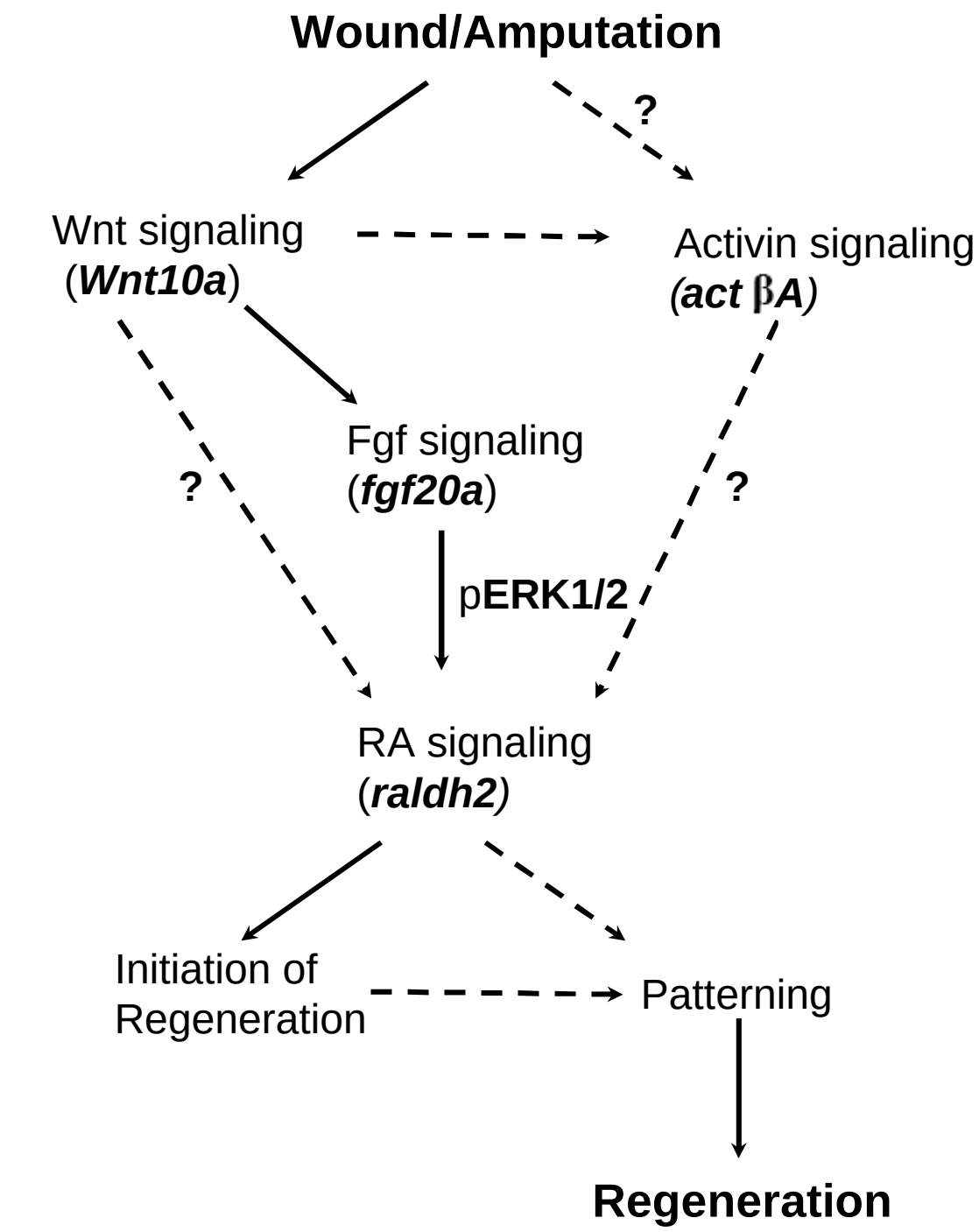
Wound/Amputation
?
Wnt signaling
(Wnt10a)
Activin signaling
(act βA)
Fgf signaling
(fgf20a)
?
?
pERK1/2
RA signaling
(raldh2)
Initiation of
Regeneration
Patterning
Regeneration

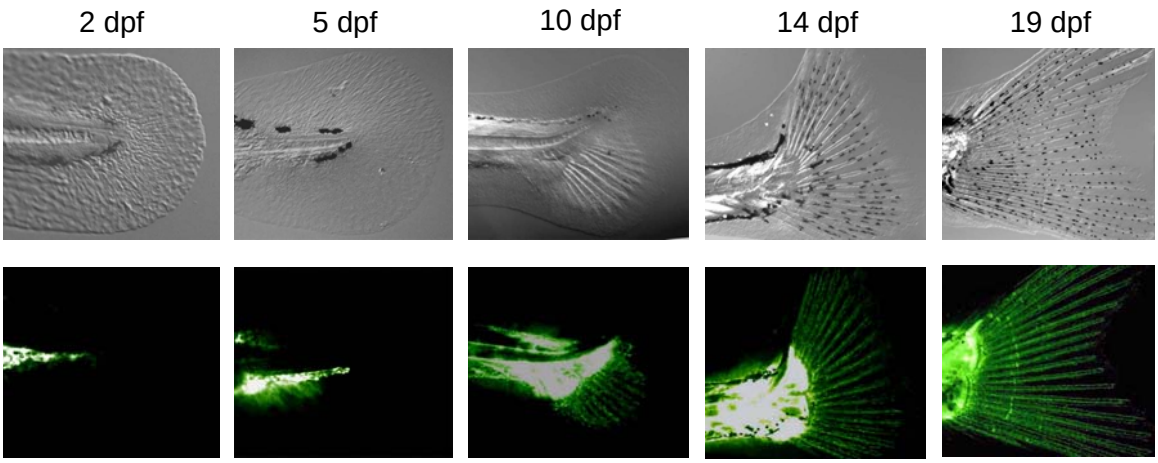

Figure 5S-1. Fin Morphogenesis. The development of the caudal fin was assessed and images were acquired periodically from 2-19dpf. The transgenic line (Fli-GFP) was used to analyze the development of blood vessels in the caudal fin and also illustrates that the 18 bony rays are formed by the end of 3rd week of development.

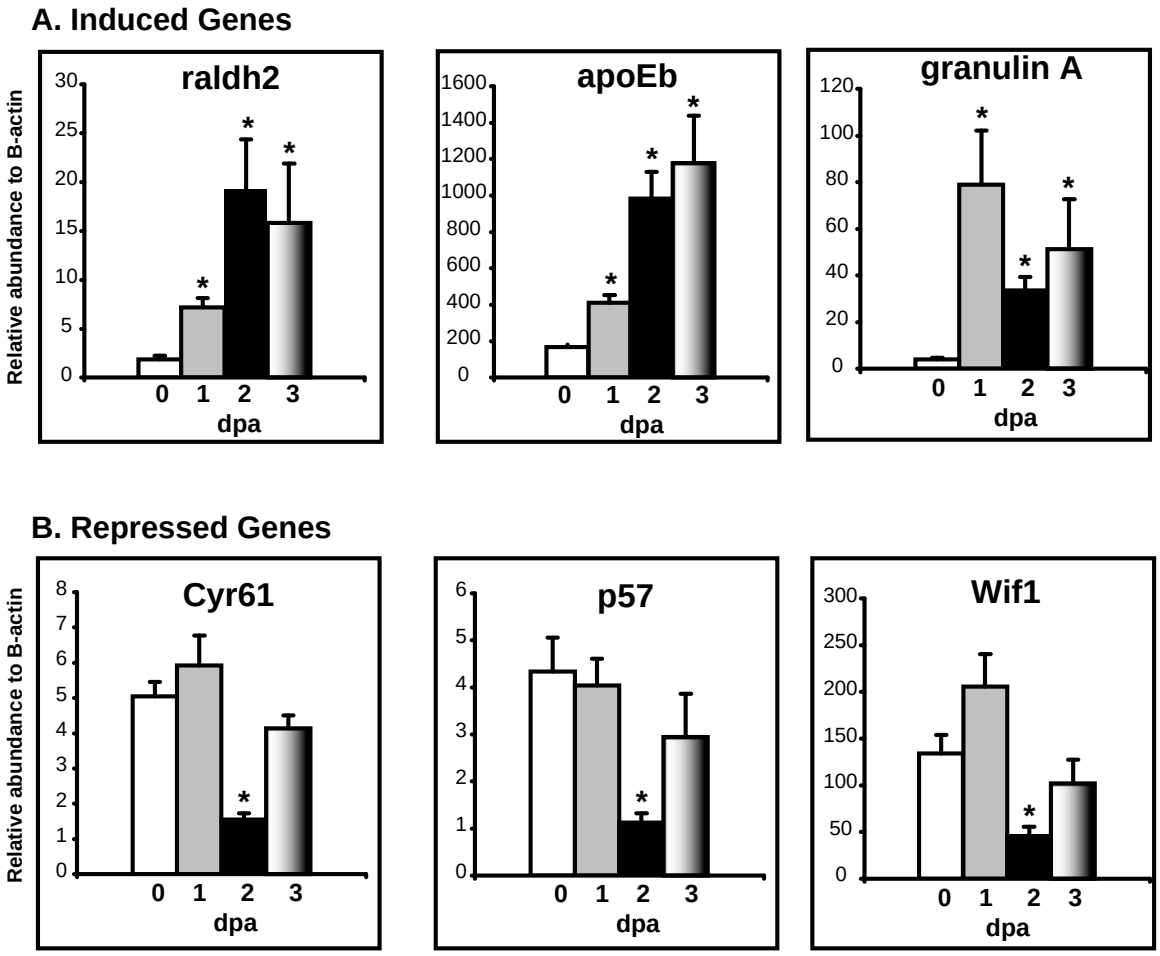

Figure 5S-2. Validation of selected genes by quantitative real time PCR (qRT-PCR). List of genes that were commonly expressed during regeneration between the three different regeneration models were confirmed by qRT-PCR with the larval regenerating fin tissue. qRT-PCR was conducted using gene specific primers for *raldh2, apoEb, granulinA*, *cyr61, p57* and *wif1*. The abundance of the message levels were normalized to β-actin expression. The expression of *raldh2* ($p < 0.002$), *apoEb* ($p < 0.001$), *granulinA* ($p < 0.001$) were significantly induced in all the three regeneration time points and *cyr61* ($p < 0.001$), *p57* ($p<0.010$) and *wif1* ($p<0.005$) were statistically significant at 2dpa only. The respective values represent the mean $\pm$ S.E.M. (One Way ANOVA, n=3).

Figure 5S-3. Inhibition of RA signaling impacts cell proliferation during larval fin regeneration. A) The amputated larvae exposed to vehicle or DEAB and Citral were incubated with Brdu at 24-30 and 48-54hpa. The bracket represents the area analyzed for the count of proliferating cells. **B)** The cell proliferation were quantified between vehicle or DEAB (n=7) and Citral (n=9) exposed larvae. The respective values represent the mean $\pm$ S.E.M (One way ANOVA and Tukey method). The Brdu labeled cells were significantly reduced in DEAB and Citral exposed larvae at 24-30 and 48-54hpa when compared with the vehicle ($p< 0.001$). **C)** The control and raldh2 morphants were amputated and Brdu assay was performed as described above. **D)** Quantification of the cell proliferation between control and *raldh2* morphants. There was significant reduction in the number of proliferating cells in the raldh2 morphants at both 24-30 and 48-54hpa when compared to the control morphants ($p< 0.001$). All the parameters were measured using the Image Pro-Plus software (Media Cybernetics, Silver Spring, MD).

5S-3

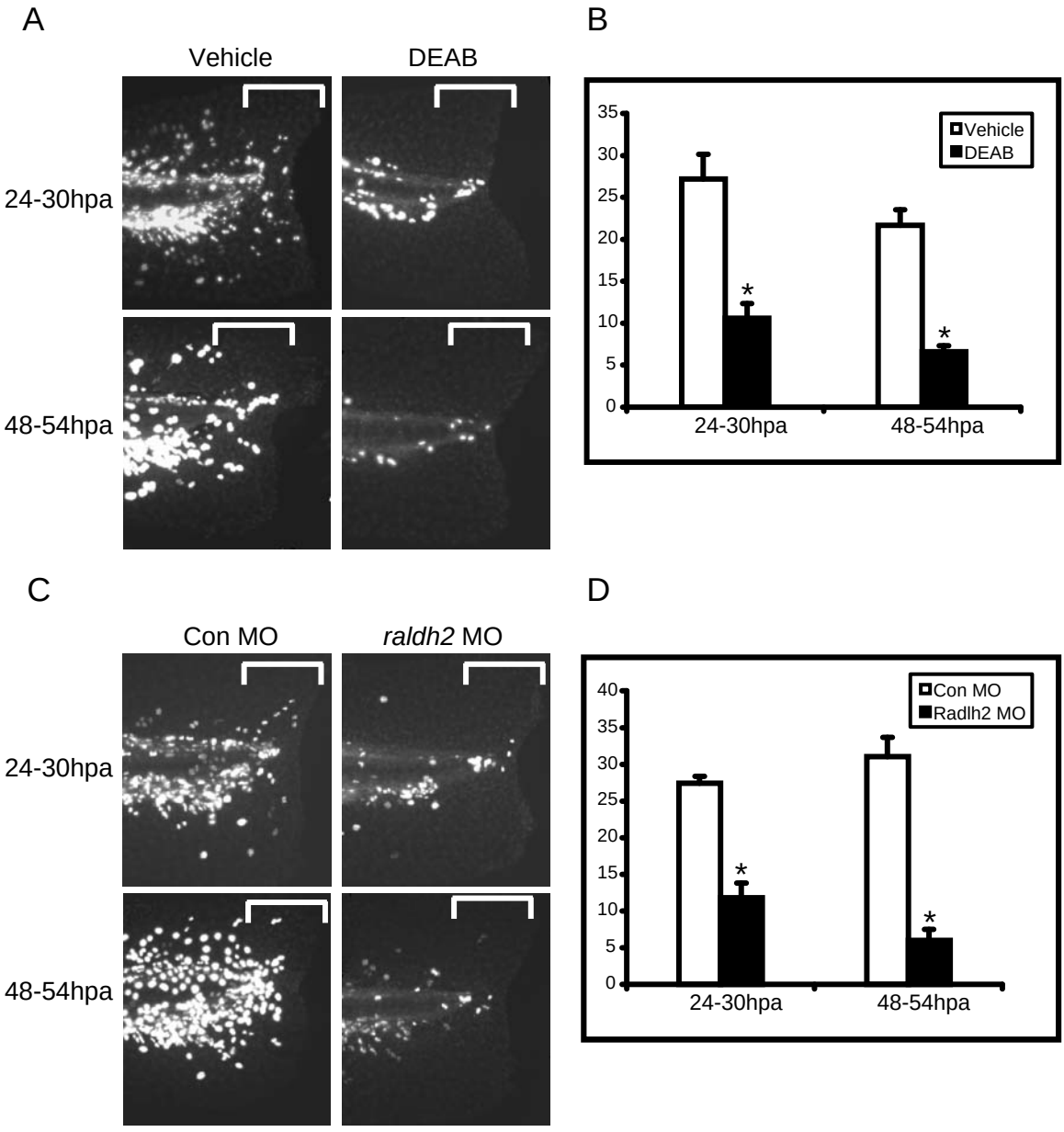
A
Vehicle
DEAB
24-30hpa
48-54hpa
B
Vehicle
DEAB
35
30
25
20
15
10
5
0
*
*
24-30hpa
48-54hpa
C
Con MO
raldh2 MO
24-30hpa
48-54hpa
D
Con MO
Radlh2 MO
40
35
30
25
20
15
10
5
0
*
*
24-30hpa
48-54hpa

Table 5S-1. List of selected genes that were at least 2.5 fold differentially abundant at any regenerating time point when compared to 0dpa during larval fin regeneration.

Gene	Affymetrix ID	Larval Fin Regeneration Fold Change 1 DPA	2 DPA	3DPA
Wound healing/Immune response				
cathepsin L2	Dr.15507.2.A1_at	202.16	87.16	106.55
granulin 2	Dr.4748.1.S1_at	11.71	33.73	19.66
cathepsin S	Dr.24219.5.S1_at	11.35	4.95	4.53
complement component 4B proprotein	Dr.12491.1.A1_at	11.30	17.33	26.12
lactotransferrin	Dr.1889.1.S1_at	9.88	2.39	2.72
granulin A	Dr.5809.1.A1_at	9.19	3.49	4.85
legumain	Dr.24341.1.S1_at	5.22	3.08	2.88
socs-3	Dr.6431.1.S1_at	5.10	14.54	8.92
complement component 6	Dr.16392.1.A1_at	3.60	4.65	5.54
cathepsin C	Dr.4782.1.S1_at	3.30	2.51	2.36
TCIRG1	Dr.3804.2.A1_a_at	2.99	2.47	2.17
galectin 9	Dr.4573.1.A1_at	2.76	4.02	3.24
cathepsin B	Dr.3374.2.S1_at	2.75	2.17	2.27
eosinophil peroxidase	Dr.9478.3.S1_a_at	2.68	2.17	1.62
Napsin 1 precursor	Dr.19238.1.S1_at	2.56	2.90	2.46
Galectin 8, isoform b	Dr.25862.1.A1_at	2.38	1.83	1.50
cathepsin K	Dr.4048.1.S1_at	2.25	4.41	3.63
cathepsin L	Dr.19902.1.S1_at	2.14	3.77	2.85
granulin 1	DrAffx.2.25.A1_at	2.08	4.02	2.52
TFPI	Dr.20029.1.A1_at	1.91	3.77	3.33
thromboxane A synthase 1	Dr.9661.1.A1_at	1.55	2.72	2.40
annexin A1	Dr.26404.1.S1_at	-2.08	-2.34	-2.75
interferon-related developmental regulator 1	Dr.5617.1.A1_at	-2.52	-1.64	-1.70
Thy-1 cell surface antigen	Dr.20019.1.S1_at	-2.54	-1.36	-1.48
Myelin and lymphocyte protein	Dr.1248.1.S1_at	-2.66	-3.11	-2.65
Signal Transduction				
raldh2	Dr.5206.1.S1_at	11.75	49.47	26.03
ms4a4a	Dr.22334.1.S1_at	8.39	21.60	15.68
CBFA2T1	Dr.10668.1.S2_at	7.21	2.40	2.87
protease, serine, 12	Dr.26268.1.A1_at	6.90	3.19	3.65
glia maturation factor, gamma	Dr.18605.1.A1_at	6.37	3.88	3.18
F-box only protein 25	Dr.25520.1.A1_at	4.44	13.67	11.31
fgf20a	Dr.17781.1.A1_at	4.29	10.41	4.57
IGFBP1	Dr.8587.1.A2_at	4.29	5.31	2.98
SAMSN1	Dr.919.1.A1_at	4.22	2.62	2.22
interferon regulatory factor 1	Dr.914.1.A1_a_at	4.04	3.27	25.85
PSME1	Dr.8135.1.S1_at	4.03	6.85	6.39
protein kinase C-like 2	Dr.16985.1.A1_at	3.15	1.89	1.95
PSME2	Dr.8134.1.S1_at	2.91	3.67	4.29
Apoptosis-inducing protein	Dr.13076.1.S1_at	2.88	7.48	5.60
ring finger protein 11	Dr.26465.1.S1_at	2.74	6.32	6.38
phospholipase C, gamma 2	Dr.11512.1.A1_at	2.60	3.57	4.44
glutamate receptor, ionotropic, kainate 2	Dr.3211.1.A1_at	2.60	2.11	1.91
rasl11b	Dr.2953.1.S1_at	2.59	3.11	1.64
SPRY domain-containing SOCS box protein 4	Dr.10211.1.A1_at	2.58	2.83	2.74
Serine/threonine protein kinase VRK2	Dr.15781.1.S1_at	2.55	2.76	3.78

arrestin domain containing 2	Dr.2047.1.A1_at	2.55	6.99	5.67
B-cell translocation gene 1	Dr.25187.3.S1_at	2.49	3.24	2.03
MPP1	Dr.1842.1.A1_at	2.48	3.88	3.46
mesoderm specific transcript	Dr.8060.1.S1_at	2.47	3.24	3.14
EIF4EBP3	Dr.4647.1.S1_at	2.38	4.31	3.40
pyruvate kinase, muscle	Dr.7952.1.S1_at	2.38	2.21	1.86
BCL2-like 10	Dr.15057.1.S2_at	2.35	8.03	4.88
G protein-coupled receptor 137ba	Dr.6999.1.A1_at	2.35	2.38	2.55
PSMA6	Dr.10120.1.S1_at	2.35	4.17	3.93
PSMB7	Dr.15777.1.A1_at	2.35	4.20	6.93
NR4A1	Dr.9243.1.A1_at	2.27	7.08	4.60
Ubiquitin-conjugating enzyme E2H	Dr.17520.1.S1_at	2.27	3.56	3.13
GADD45B	Dr.1378.1.S1_at	2.14	4.94	4.00
ankyrin repeat and SOCS box-containing 8	Dr.26472.1.S1_at	2.12	2.99	3.14
ADP-ribosylation factor-like 4	Dr.11322.1.S1_at	2.12	4.03	3.06
GBP1	Dr.14275.1.A1_at	2.08	3.13	5.89
syndecan binding protein	Dr.1778.1.S1_at	2.07	2.83	2.14
apolipoprotein Eb	Dr.1246.1.S1_at	2.05	3.47	3.17
serum/glucocorticoid regulated kinase	Dr.10320.1.S1_at	2.04	3.13	2.07
GTP cyclohydrolase I feedback regulatory	Dr.12454.1.S1_at	2.01	3.97	4.26
GABARAPL2	Dr.16079.1.S1_at	2.00	3.32	3.22
secernin 3	Dr.7392.1.S1_at	1.99	2.19	2.56
myeloid cell leukemia sequence 1a	Dr.4957.1.S1_at	1.89	2.79	2.73
C-type natriuretic peptide 4	Dr.18242.1.A1_at	1.85	5.60	3.14
Inositol hexakisphosphate kinase 2	Dr.15620.1.S1_at	1.74	3.67	3.81
maf	Dr.10168.1.S1_at	1.70	4.45	3.73
ADP-ribosylation factor-like protein 5B	Dr.15961.1.A1_at	1.68	3.52	2.66
Elongation factor 2 kinase	Dr.523.1.A1_at	1.64	2.56	2.27
dual specificity phosphatase 1	Dr.2413.1.S1_at	1.63	8.85	5.57
2-peptidylprolyl isomerase A	Dr.9654.1.A1_at	1.62	5.03	5.80
Caspase-9 precursor	Dr.16035.1.S1_at	1.58	3.07	2.34
early growth response 1	Dr.10183.1.S2_at	1.54	3.08	4.40
B-cell translocation gene 2	Dr.6511.1.S1_at	1.53	4.49	2.53
Ras-related protein Rab-1A	Dr.21919.1.A1_at	1.51	2.55	2.50
dachshund homolog	Dr.3413.1.S1_at	1.51	3.07	2.14
interferon regulatory factor 7	Dr.10428.1.S1_at	1.50	2.46	2.75
Secernin-2	Dr.12696.1.A1_at	1.47	3.72	2.91
Breast cancer associated protein BRAP1	Dr.7929.1.S1_at	1.44	2.70	2.45
inositol polyphosphate phosphatase-like 1	Dr.21368.1.A1_at	1.42	2.42	3.10
lipopolysaccharide-induced TNF factor	Dr.20110.1.S1_at	1.41	2.85	2.21
GADD45G	Dr.11828.1.A1_at	1.40	2.66	1.77
cyclin G2	Dr.20083.1.A1_at	1.38	3.23	2.35
Programmed cell death 4	Dr.14306.1.S1_a_at	1.35	2.67	3.04
bmp5	Dr.10625.1.A1_at	1.33	2.63	2.32
TGF-beta-inducible nuclear protein 1	Dr.10477.1.S1_at	1.30	2.76	2.62
E3 ubiquitin-protein ligase IBRDC2	Dr.17207.1.A1_at	1.29	4.83	3.33
FGF10	Dr.8853.1.S1_at	1.29	2.56	2.41
interleukin-1 receptor-associated kinase 4	Dr.13000.1.S1_at	1.28	3.07	2.44
SERPINE2 protein	Dr.10097.1.S1_at	1.21	1.86	2.60
WNT inhibitory factor 1	Dr.3690.1.S1_at	-1.17	-3.96	-4.29
caveolin 1	Dr.5678.1.S1_s_at	-1.24	-4.87	-3.72
Receptor expression-enhancing protein 2	Dr.16638.1.A1_at	-1.27	-2.61	-2.12
activated leukocyte cell adhesion molecule	Dr.20912.1.S2_at	-1.31	-3.41	-3.13
DLG7	Dr.20429.2.S1_a_at	-1.33	-3.30	-2.66
Transgelin-3	Dr.3966.1.A1_at	-1.34	-1.82	-2.68
fgfr4	Dr.409.1.S1_at	-1.37	-2.47	-3.20
cyclin D1	Dr.24753.1.S2_at	-1.37	-2.68	-1.93

calmodulin 3b	Dr.17933.1.S1_at	-1.38	-2.58	-2.35
cardiomyopathy associated 1	Dr.152.1.A1_at	-1.42	-4.40	-4.65
ODZ1	Dr.8281.1.S1_at	-1.42	-3.11	-3.37
GA17 protein	Dr.25580.1.S1_at	-1.47	-1.99	-2.63
neuropilin 1a	Dr.26440.1.S1_at	-1.58	-3.00	-2.86
p57	Dr.3502.1.S1_at	-1.61	-3.77	-4.65
elavl3	Dr.20167.3.S1_at	-1.64	-6.38	-5.03
protein kinase C, beta 1	Dr.15087.1.A1_at	-1.65	-2.98	-3.96
IMP-1	Dr.9189.1.A1_at	-1.78	-2.21	-3.00
pou23	Dr.21068.1.S1_s_at	-1.95	-3.18	-2.79
Ictacalcin	Dr.25140.5.S1_at	-1.97	-2.05	-3.90
Benzodiazapine receptor	Dr.20778.1.S1_at	-1.99	-2.60	-4.03
Oxidative stress induced growth inhibitor 2	Dr.6154.1.A1_at	-2.07	-7.57	-13.06
heat shock 70kDa protein 12A	Dr.15969.1.A1_at	-2.08	-2.98	-2.91
kdelr2	Dr.6631.1.A1_at	-2.11	-5.27	-5.12
pgrmc2	Dr.2911.1.S1_at	-2.14	-4.06	-4.21
stromal interaction molecule 1	Dr.25937.1.A1_at	-2.14	-2.42	-2.72
hey2	Dr.1899.3.A1_at	-2.20	-2.85	-2.89
lipoprotein lipase	Dr.20185.1.S1_at	-2.41	-3.32	-3.05
hsp90a	Dr.610.1.S1_at	-2.52	-11.72	-8.25
Purkinje cell protein 4 like 1	Dr.17014.1.S1_at	-2.52	-2.32	-2.35
calpain 2, (m/II) large subunit	Dr.10119.1.A1_at	-2.67	-3.52	-3.48
ITPK1	Dr.22569.1.S1_at	-2.75	-1.62	-1.33
cryptochrome 1	Dr.10329.1.S1_at	-2.88	-1.88	-2.15
calpain 9	Dr.4236.1.S1_at	-2.99	-4.51	-2.94
GTP cyclohydrolase 1	Dr.14668.1.S1_at	-3.05	-4.51	-8.58
insulin induced gene 1	Dr.19560.1.S1_at	-3.82	-2.15	-3.22
cryptochrome 2	Dr.10332.1.S1_at	-4.56	-5.24	-5.10
anterior gradient 2 homolog	Dr.25277.1.S1_at	-4.79	-8.07	-10.02
ppp1r3b	Dr.4453.1.S1_at	-8.78	-8.99	-10.89
ECM/Cell Adhesion & Migration				
versican	Dr.9682.1.A1_at	8.31	5.76	7.11
fibronectin 1b	Dr.24233.1.S1_at	4.94	3.12	2.63
col17a1	Dr.10041.1.A1_at	4.44	2.77	2.95
meprin A, beta	Dr.17470.1.S1_at	3.91	2.29	1.87
clusterin	Dr.20131.2.A1_at	3.41	6.06	5.06
Olfactomedin-like protein precursor	Dr.1154.1.S1_at	2.93	4.54	5.82
TIMP2	Dr.15281.1.A1_at	2.37	3.88	2.89
cartilage oligomeric matrix protein	Dr.1089.1.S1_at	2.28	2.60	4.06
FREM2	Dr.3300.2.A1_at	2.15	3.41	1.54
SPON2	Dr.563.1.S1_at	2.13	2.86	4.17
AAMP protein	Dr.11399.1.A1_at	2.07	2.31	2.81
Latexin	Dr.23294.1.S1_at	1.95	4.59	4.70
transmembrane 7 superfamily member 1	Dr.14044.1.A1_at	1.95	2.86	2.35
mmp14	Dr.23324.1.A1_at	1.86	3.46	3.65
lysyl oxidase	Dr.11427.1.S1_at	1.85	8.70	12.99
mmp14a	Dr.4229.1.S1_at	1.29	2.90	2.85
col1a2	Dr.5521.1.S1_at	-1.16	-3.58	-3.67
spondin 1b	Dr.565.1.S1_at	-1.33	-2.88	-3.82
fibronectin 1	Dr.19965.1.S1_at	-1.38	-3.44	-2.30
netrin 1	Dr.545.1.S1_at	-1.61	-4.17	-4.09
desmoplakin	Dr.4929.1.A1_at	-1.76	-2.35	-2.39
semaphorin 3aa	Dr.5060.1.A1_at	-1.89	-2.46	-2.71
EFEMP2	Dr.4543.1.S1_at	-2.73	-1.78	-3.86
Advillin	Dr.26109.1.A1_at	-2.98	-2.23	-3.23
claudin 9	Dr.12596.1.S1_at	-5.20	-8.21	-5.76

contactin 4	Dr.21041.1.S1_at	-9.99	-4.15	-4.15
Transcriptional Regulation				
krml2	Dr.23470.1.S1_s_at	8.82	4.67	4.88
krml2.2	Dr.8198.1.A1_at	7.67	4.98	4.80
spi1	Dr.7612.1.A1_at	5.31	2.45	2.30
junb	Dr.10326.1.S1_at	4.55	10.72	7.93
E74-like factor 3	Dr.1909.1.S1_at	3.62	5.10	4.66
Fos-related antigen 2	Dr.10410.1.A1_at	3.52	7.73	5.94
junbl	Dr.737.1.A1_at	2.98	4.65	3.58
stat1	Dr.257.1.A1_at	2.63	6.66	7.31
Kruppel-like factor 2a	Dr.3448.1.S1_at	2.55	6.29	7.80
sox4a	Dr.20124.1.A1_at	2.54	1.58	1.82
fos	Dr.12986.1.A1_a_at	2.37	6.88	5.71
histone deacetylase 9	Dr.14159.1.A1_at	2.23	3.02	3.59
suppressor of Ty 3 homolog	Dr.14718.1.A1_at	2.18	3.65	3.36
homeo box C12	Dr.10124.1.A1_at	2.00	3.83	2.52
transcription elongation factor A (SII), 3	Dr.15634.1.S1_at	1.49	3.21	1.48
sox9b	Dr.11850.1.S2_at	1.39	3.49	3.23
sox21b	Dr.14800.1.A1_at	-1.31	-3.53	-2.98
deltaD	Dr.20958.1.S1_at	-1.32	-5.99	-4.61
hoxb3a	Dr.5779.1.S1_at	-1.32	-5.90	-6.29
foxa	Dr.588.1.S1_at	-1.36	-3.44	-3.62
sox3	Dr.1691.12.S1_at	-1.38	-1.53	-2.61
hmgb2	Dr.9746.12.S1_at	-1.40	-2.12	-2.78
hoxa2b	Dr.5772.1.S1_at	-1.46	-3.28	-3.48
transcription factor 2, hepatic	Dr.14662.1.S2_at	-1.47	-2.61	-2.13
dmrt2	Dr.8088.1.S1_at	-1.59	-2.98	-3.02
sox19a	Dr.20910.1.S1_at	-1.71	-3.41	-6.28
deltaB	Dr.574.1.S1_at	-1.73	-6.38	-10.78
Kruppel-like factor 2b	Dr.9976.1.S1_at	-1.75	-2.50	-2.93
pou50	Dr.57.1.S1_at	-2.20	-4.27	-4.71
cdx4	Dr.11836.1.S1_at	-2.38	-4.21	-3.96
gastrulation brain homeo box 2	Dr.17548.1.S1_at	-3.38	-7.49	-7.65
endothelial PAS domain protein 1	Dr.25865.1.S1_at	-5.05	-5.27	-6.81
Chromatin/DNA/RNA Processing				
poly(A) binding protein cytoplasmic 1	Dr.12233.1.S1_at	1.59	2.98	2.32
chromodomain helicase DNA binding protein 2	Dr.859.1.S1_at	1.58	1.84	2.63
RNA binding motif protein 25	Dr.2606.1.A1_at	1.55	2.20	3.44
lamin B1	Dr.25051.1.S2_at	-1.26	-3.82	-3.46
Exportin-1	Dr.12499.1.A1_at	-1.31	-2.70	-2.56
SNRP70	Dr.25566.1.S1_at	-2.00	-2.72	-2.42
poly(A) binding protein cytoplasmic 1	Dr.12233.1.S1_at	1.59	2.98	2.32
chromodomain helicase DNA binding protein 2	Dr.859.1.S1_at	1.58	1.84	2.63
Cytoskeleton/Cytosolic Transport				
keratin 14	Dr.25556.1.S1_at	7.09	3.12	1.96
syntaxin 11	Dr.12309.1.A1_at	3.00	3.57	2.44
MYLIP	Dr.20935.1.S1_at	2.88	4.65	4.69
profilin family, member 4	Dr.16239.1.A1_at	2.17	3.78	3.83
nipsnap homolog 3A	Dr.17452.1.S1_at	1.87	2.18	2.67
Tubulin beta-2A chain	Dr.7928.1.A1_at	-1.26	-3.10	-3.01
secretory carrier membrane protein 5	Dr.19471.1.A1_at	-1.35	-4.12	-3.39
actin, alpha 1	Dr.24891.1.S1_at	-2.02	-4.60	-7.89
periplakin	Dr.9761.1.S1_at	-2.29	-2.69	-2.08

tubulin, alpha 1	Dr.7506.1.A1_at	-2.31	-2.68	-3.14
p76	Dr.349.1.A1_at	-2.59	-2.18	-2.43
envoplakin	Dr.5577.1.A1_at	-4.56	-6.73	-6.42
Metabolism				
ferritin, heavy polypeptide 1	Dr.12425.5.S1_at	14.25	35.56	14.56
Y+L amino acid transporter 1	Dr.18441.1.A1_at	6.43	7.15	6.16
acid phosphatase 5, tartrate resistant	Dr.1508.1.S1_at	5.35	2.34	2.72
Rhesus blood group, B glycoprotein	Dr.12749.1.A1_at	5.27	2.38	3.31
Palmitoyltransferase ZDHHC2	Dr.9870.1.A1_at	4.09	7.09	10.49
glucosamine-6-phosphate deaminase 1	Dr.18431.1.S1_at	4.07	6.57	5.75
argininosuccinate synthetase	Dr.4095.1.A1_at	3.67	2.86	2.32
cytoglobin	Dr.4925.1.S1_x_at	3.53	5.35	4.57
Cytochrome c oxidase subunit 4 isoform 2	Dr.12760.1.A1_at	3.47	2.47	5.61
SLC7A8	Dr.3789.1.A1_at	3.33	2.38	3.05
mpdu1a	Dr.1439.1.S1_at	-3.19	-4.08	-2.98
enolase 2	Dr.13441.1.A1_at	3.18	8.96	4.54
aldose reductase	Dr.6142.1.A1_at	3.18	9.79	7.99
carboxypeptidase N, polypeptide 1	Dr.1128.1.S1_at	2.98	1.77	2.28
UGT1A1	Dr.3029.1.A1_at	2.78	2.63	2.07
Multidrug resistance protein 1	Dr.8645.1.A1_at	2.51	1.70	4.08
SLC15A4	Dr.13966.1.S1_at	2.42	2.97	2.91
carboxypeptidase M	Dr.14571.1.A1_at	2.41	6.42	4.97
uncoupling protein 3	Dr.4905.1.S1_at	2.38	5.95	21.21
carboxypeptidase, vitellogenic-like	Dr.506.1.S1_at	2.33	2.63	2.54
argininosuccinate lyase	Dr.11501.1.S1_at	2.18	2.83	2.56
creatine kinase, muscle	Dr.22156.1.A1_at	2.15	2.69	3.69
CYP27A1	Dr.25700.1.A1_at	2.08	3.57	4.93
ATP6V1E1	Dr.4617.1.A1_at	2.06	2.63	2.20
glutathione peroxidase 2	Dr.8000.1.S1_at	2.01	2.35	3.27
cytochrome b-245, alpha polypeptide	Dr.17749.2.A1_a_at	2.00	2.84	2.57
glycogenin 1	Dr.13604.1.S1_at	2.00	2.85	2.77
Sialin	Dr.15485.1.A1_at	1.99	2.50	2.42
Phytanic acid oxidase	Dr.10186.1.A1_at	1.99	2.18	2.75
lysophospholipase 3	Dr.360.1.A1_at	1.96	3.20	3.02
bckdk	Dr.25159.1.S1_at	1.93	2.60	2.45
cyp3c1	Dr.938.1.S1_at	1.89	3.05	2.79
selenoprotein X, 1	Dr.147.1.A1_at	1.88	2.54	2.51
glutamate-ammonia ligase	Dr.4147.1.S1_at	1.86	5.48	4.78
peptidylprolyl isomerase A (cyclophilin A)	Dr.6264.1.A1_at	1.85	2.65	2.24
ywhabl	Dr.4607.1.A1_at	-1.67	-2.43	-2.76
Malonyl CoA-acyl carrier protein transacylase	Dr.13862.1.S1_at	1.61	5.21	4.14
methionine sulfoxide reductase A	Dr.14650.1.A1_at	1.51	4.79	4.26
slc40a1	Dr.8152.1.S1_at	1.43	2.73	2.26
Intestinal alkaline phosphatase 1	Dr.1104.1.A1_at	1.31	4.55	3.18
slc38a3	Dr.5364.1.A1_at	1.30	2.98	2.62
adenosine monophosphate deaminase 3	Dr.11670.1.S1_at	1.30	2.56	1.66
HSD3B7	Dr.10542.1.S1_at	1.17	2.86	2.87
atp1a1a.2	Dr.10343.1.S1_at	-1.25	-3.67	-3.49
cytochrome c oxidase subunit Vib polypeptide 1	Dr.956.1.S1_at	-1.28	-1.77	-2.58
Troponin I, fast skeletal muscle	Dr.17891.1.S1_at	-1.42	-13.19	-11.69
selenoprotein M	Dr.5565.1.S1_at	-1.43	-1.75	-2.62
alcohol dehydrogenase 8b	Dr.16130.1.S1_at	-1.45	-2.17	-2.54
lactate dehydrogenase B	Dr.4212.1.S1_at	-1.54	-3.10	-3.07
acetyl-CoA acetyltransferase 2	Dr.813.1.S1_at	-1.66	-3.33	-3.45
MTHFD2	Dr.5222.1.S1_at	-1.83	-2.43	-2.90

creatine kinase, mitochondrial 1	Dr.771.1.S1_at	-1.87	-2.73	-4.18
ABCF2	Dr.24208.1.S1_at	-1.87	-2.34	-2.91
atp1a1a.1	Dr.25976.1.A1_at	-2.15	-2.48	-3.13
SLC6A1	Dr.7076.1.A1_at	-2.15	-7.39	-5.74
phosphoserine aminotransferase 1	Dr.11425.1.S1_at	-2.28	-2.44	-3.59
7-dehydrocholesterol reductase	Dr.18226.1.A1_at	-2.51	-2.30	-1.90
cyp51	Dr.1603.1.A1_at	-2.55	-5.83	-6.27
ribonucleotide reductase M2 b	Dr.23801.1.A1_at	-2.59	-1.43	-1.86
phosphomannomutase 2	Dr.13747.1.S1_at	-2.60	-2.85	-3.30
adenylate kinase 3	Dr.1707.1.S1_at	-2.60	-2.37	-1.42
Cytidine deaminase	Dr.25811.1.S1_at	-2.65	-1.64	-2.13
phosphoglycerate dehydrogenase	Dr.24995.5.A1_at	-2.66	-2.41	-3.12
HMGCS1	Dr.2051.1.S1_at	-2.67	-3.26	-2.73
phosphoglucomutase 3	Dr.21347.1.S1_at	-2.68	-3.98	-4.45
galactose-4-epimerase, UDP-	Dr.987.1.S1_at	-2.82	-3.99	-3.94
cyp17a1	Dr.25390.1.A1_s_at	-2.86	-2.24	-3.96
N-acylsphingosine amidohydrolase	Dr.25118.1.S1_at	-2.92	-2.23	-2.24
SLC25A22	Dr.25199.1.A1_at	-4.43	-3.27	-3.77
folate hydrolase	Dr.16405.1.S1_at	-6.90	-10.71	-12.76

Table 5S-2. Summary of the pattern of gene regulation between adult and larval fin regeneration.

	Induced	Repressed	Total
Common Genes	179	166	341
Similarly Regulated	109	107	216
Similarly Regulated (%)	60.9	64.5	63.3

Table 5S-3. Selected genes that were commonly expressed between larval and adult fin regeneration.

		Larval Fin			Adult Fin		
		Fold Change			Fold Change		
Gene	Affymetrix ID	1DPA	2DPA	3DPA	1DPA	3DPA	5DPA
Wound healing/Immune response							
cathepsin S	Dr.24219.5.S1_at	11.35	4.95	4.53	2.18	1.53	1.75
legumain	Dr.24341.1.S1_at	5.22	3.08	2.88	3.23	2.07	2.29
socs-3	Dr.9617.1.A1_at	4.54	7.59	4.12	4.09	4.20	2.19
cathepsin C	Dr.4782.1.S1_at	3.30	2.51	2.36	1.80	1.91	1.69
cathepsin L	Dr.19902.1.S1_at	2.14	3.77	2.85	4.22	3.56	3.60
granulin 1	DrAffx.2.25.A1_at	2.08	4.02	2.52	11.61	2.53	3.47
Signal Transduction							
raldh2	Dr.5206.1.S1_at	11.75	49.47	26.03	12.37	14.34	7.47
ms4a4a	Dr.22334.1.S1_at	8.39	21.60	15.68	1.85	2.26	1.87
fgf20a	Dr.17781.1.A1_at	4.29	10.41	4.57	11.50	9.62	3.17
Igfbp1	Dr.8587.1.A2_at	4.29	5.31	2.98	3.41	2.00	2.01
WNT inhibitory factor 1	Dr.3690.1.S1_at	-1.17	-3.96	-4.29	-3.04	-4.12	-3.36
deltaD	Dr.20958.1.S1_at	-1.32	-5.99	-4.61	-2.27	-1.79	-1.28
Notch 2	Dr.16720.1.A1_at	-1.39	-1.93	-1.79	-1.75	-1.43	-1.42
regulator of G-protein signalling 16	Dr.9926.1.S1_at	-1.71	-1.49	-1.53	-3.36	-3.37	-1.26
ECM/ Cell Adhesion & Migration							
fibronectin 1b	Dr.24233.1.S1_at	4.94	3.12	2.63	9.17	5.05	3.80
galectin 9	Dr.4573.1.A1_at	2.76	4.02	3.24	3.36	3.58	1.48
TIMP2	Dr.15281.1.A1_at	2.37	3.88	2.89	58.91	15.31	4.75
MMP14	Dr.23324.1.A1_at	1.86	3.46	3.65	2.81	5.13	5.39
metrn	Dr.3745.1.A1_at	-1.32	-2.15	-2.22	-4.83	-3.83	-3.03
semaphorin 3aa	Dr.5060.1.A1_at	-1.89	-2.46	-2.71	-2.32	-2.67	-1.61
envoplakin	Dr.5577.1.A1_at	-4.56	-6.73	-6.42	-2.02	-1.75	-1.52
Transcriptional Regulation							
krml2	Dr.23470.1.S1_s_at	8.82	4.67	4.88	2.12	1.75	1.64
krml2.2	Dr.8198.1.A1_at	7.67	4.98	4.80	2.36	2.20	1.86
spi1	Dr.7612.1.A1_at	5.31	2.45	2.30	3.78	2.56	2.78
Kruppel-like factor 2	Dr.3448.1.S1_at	2.55	6.29	7.80	3.16	3.89	4.73
sox4a	Dr.20124.1.A1_at	2.54	1.58	1.82	1.96	3.55	2.71
dachshund c	Dr.3413.1.S1_at	1.51	3.07	2.14	5.06	12.59	8.80
hes6	Dr.19467.1.A1_at	-1.19	-1.53	-1.93	-2.18	-1.71	-2.17
sox3	Dr.20010.8.A1_at	-1.78	-2.08	-2.80	-3.20	-2.02	-1.91
pou50	Dr.57.1.S1_at	-2.20	-4.27	-4.71	-1.85	-1.89	-1.85
Cytoskeleton/Cytosolic Transport							
nipsnap homolog 3A	Dr.17452.1.S1_at	1.87	2.18	2.67	2.86	3.65	2.81
vac14	Dr.18964.1.A1_at	1.60	1.59	2.13	2.91	2.01	1.34
keratin 18	Dr.890.1.S1_at	1.54	2.43	1.68	2.06	2.30	2.08
Clathrin-associated protein 19	Dr.1084.1.A1_at	-1.84	-1.89	-2.43	-2.49	-2.64	-1.95
tubulin, alpha 1	Dr.7506.1.A1_at	-2.31	-2.68	-3.14	-1.60	-2.05	-1.80
p76	Dr.349.1.A1_at	-2.59	-2.18	-2.43	-3.09	-2.28	-2.09
Chromatin/DNA/RNA Processing							
histone deacetylase 8	Dr.3849.1.A1_at	2.06	1.63	1.71	1.90	1.84	1.38

Orc6L	Dr.24945.1.S1_at	1.96	2.29	1.85	3.22	2.15	1.70
poly(A) binding protein cytoplasmic 1	Dr.12233.1.S1_at	1.59	2.98	2.32	25.99	12.39	23.62
HLA-B associated transcript 1	Dr.5423.1.A1_at	-1.39	-1.84	-1.71	-1.55	-1.93	-2.23
deoxyribonuclease I-like 3	Dr.20334.1.S1_at	-2.08	-1.31	-1.60	-3.35	-2.64	-1.90
ribonucleotide reductase M2 b	Dr.23801.1.A1_at	-2.59	-1.43	-1.86	-2.52	-2.34	-2.39

Table 5S-4. Summary of the pattern of gene regulation between larval fin and adult heart regeneration.

	Induced	Repressed	Total
Common Genes	131	58	189
Similarly Regulated	116	18	132
Similarly Regulated (%)	88.5	31.0	69.8

Table 5S-5. Selected genes that were commonly expressed between larval and adult heart regeneration.

		Larval Fin			Adult Heart		
		Fold Change			Fold Change		
Gene	Affymetrix ID	1DPA	2DPA	3DPA	3DPA	7DPA	14DPA
Wound healing/Immune response							
granulin 2	Dr.4748.1.S1_at	11.71	33.73	19.66	3.31	2.29	1.91
cathepsin S	Dr.24219.5.S1_at	11.35	4.95	4.53	3.27	2.14	1.13
lactotransferrin	Dr.1889.1.S1_at	9.88	2.39	2.72	0.81	2.44	1.44
granulin a	Dr.5809.1.A1_at	9.19	3.49	4.85	3.04	2.17	1.05
legumain	Dr.24341.1.S1_at	5.22	3.08	2.88	2.48	1.68	0.85
galectin 9	Dr.4573.1.A1_at	2.76	4.02	3.24	1.96	0.97	0.94
Signal Transduction							
raldh2	Dr.5206.1.S1_at	11.75	49.47	26.03	1.66	1.35	0.32
krml2	Dr.23470.1.S1_s_at	8.82	4.67	4.88	1.98	0.78	0.02
krml2.2	Dr.8198.1.A1_at	7.67	4.98	4.80	1.96	0.90	0.12
jun B proto-oncogene	Dr.10326.1.S1_at	4.55	10.72	7.93	1.31	1.44	1.08
apolipoprotein Eb	Dr.1246.1.S1_at	2.05	3.47	3.17	3.94	2.14	0.23
CYR61	Dr.15501.1.S1_at	-1.34	-2.36	-1.83	0.76	1.60	0.82
p57 (kip2)	Dr.3502.1.S1_at	-1.61	-3.77	-4.65	-1.08	-1.06	-0.35
hsp90a	Dr.610.1.S1_at	-2.52	-11.72	-8.25	-1.63	-1.39	-1.32
ECM/ Cell Adhesion & Migration							
glia maturation factor, gamma	Dr.18605.1.A1_at	6.37	3.88	3.18	1.92	1.32	0.62
clusterin	Dr.20131.2.A1_at	3.41	6.06	5.06	0.45	2.89	1.77
TIMP2	Dr.15281.1.A1_at	2.37	3.88	2.89	3.45	2.69	1.44
MMP14	Dr.23324.1.A1_at	1.86	3.46	3.65	1.35	1.90	1.96
MMP2	Dr.2408.1.A1_at	1.40	2.24	2.55	0.17	1.62	1.40
decorin	Dr.16078.1.S1_at	-1.13	-2.16	-1.96	0.54	1.45	1.04
Transcriptional Regulation							
spi1	Dr.7612.1.A1_at	5.31	2.45	2.30	2.05	1.81	1.46
Negative elongation factor C/D	Dr.25468.1.A1_at	2.73	2.29	2.67	3.02	1.89	0.87
activating transcription factor 3	Dr.14282.1.S1_at	2.04	2.36	1.58	-0.47	1.24	0.47
Orc6L	Dr.24945.1.S1_at	1.96	2.29	1.85	1.85	1.45	0.51
Cytoskeleton/Cytosolic Transport							
syntaxin 11	Dr.12309.1.A1_at	3.00	3.57	2.44	1.50	0.89	0.60
keratin 18	Dr.890.1.S1_at	1.54	2.43	1.68	2.67	2.20	1.47
keratin 8	Dr.4387.1.S1_at	-1.22	-1.40	-1.89	1.96	1.49	0.36
unc45b	Dr.345.1.S1_at	-1.49	-2.59	-2.23	-1.12	-0.72	-0.52
p76	Dr.349.1.A1_at	-2.59	-2.18	-2.43	1.25	1.39	1.06
Metabolism							
ferritin, heavy polypeptide 1	Dr.12425.5.S1_at	14.25	35.56	14.56	5.58	4.27	2.50
Y+L amino acid transporter 1	Dr.18441.1.A1_at	6.43	7.15	6.16	4.00	2.78	1.30
glucosamine-6-phosphate deaminase1	Dr.18431.1.S1_at	4.07	6.57	5.75	3.88	3.14	2.06
Thioredoxin	Dr.8723.1.S1_at	1.52	2.08	1.50	2.51	2.14	0.90
mical3	Dr.14768.1.A1_at	-1.88	-1.81	-1.60	-1.30	-0.65	-0.40
atp1a1a.1	Dr.25976.1.A1_at	-2.15	-2.48	-3.13	-1.07	-0.83	-0.27

Table 5S-6. List of selected genes commonly present between larval fin, adult fin and adult heart regeneration systems.

	Larval Fin			Adult Fin			Adult Heart		
	Fold Change			Fold Change			Fold Change		
Gene	1DPA	2DPA	3DPA	1DPA	3DPA	5DPA	3DPA	7DPA	14DPA
Wound healing/Immune response									
cathepsin S	11.35	4.95	4.53	2.18	1.53	1.75	3.27	2.14	1.13
legumain	5.22	3.08	2.88	3.23	2.07	2.29	2.48	1.68	0.85
cathepsin C	3.30	2.51	2.36	1.80	1.91	1.69	2.35	1.49	0.98
galectin 9	2.76	4.02	3.24	3.36	3.58	1.48	1.96	0.97	0.94
cathepsin B	2.75	2.17	2.27	2.16	1.64	1.63	2.10	0.99	-0.82
Napsin 1 precursor	2.56	2.90	2.46	2.18	1.77	1.95	2.06	1.22	0.43
Signal Transduction									
raldh2	11.75	49.47	26.03	12.37	14.34	7.47	1.66	1.35	0.32
krml2.2	8.82	4.67	4.88	2.12	1.75	1.64	1.98	0.78	0.02
krml2	7.67	4.98	4.80	2.36	2.20	1.86	1.96	0.90	0.12
Fos-related antigen 2	3.31	3.44	2.48	4.07	2.99	1.94	0.87	1.32	0.94
C-type natriuretic peptide 4	1.85	5.60	3.14	20.34	11.37	4.12	2.01	3.58	1.43
paired related homeobox 1	1.47	2.04	1.90	1.72	2.94	3.06	1.67	1.43	0.64
ECM/ Cell Adhesion & Migration									
fibronectin 1b	4.94	3.12	2.63	9.17	5.05	3.80	0.75	1.59	0.99
Olfactomedin-like protein precursor	2.93	4.54	5.82	2.80	6.60	5.72	1.92	2.09	1.21
TIMP2	2.37	3.88	2.89	58.91	15.31	4.75	3.45	2.69	1.44
MMP14	1.86	3.46	3.65	2.81	5.13	5.39	1.35	1.90	1.96

Table 5S-7. List of gene specific primers used for qRT-PCR and cloning of raldh2 for probe synthesis.

Target Gene	Sequence 5′ to 3′
F raldh2	GGGGTAAAGTGGTAAAACGC
R raldh2	GCAGTGGTCAAAAGCATGGC
F apoEb	AGCTGCAGGAAGTCATGGAC
R apoEb	GTGCTAGTCCAATTGAGTCC
F granulin A	GAAGGACGTTCAGTGTGGTG
R granulin A	GGGCTCGTTTCTTTTTGGAG
F cyr 61	ATCCTCATTAGCTGCGTCCC
R cyr 61	TGATGTTGGTTTCCTCTAGC
F p57	TACATACATCAGTCCACCTG
R p57	CTGTTTAGAGCACTGTGGTC
F wif1	TAAGAGATTTCGCGGAGGAG
R wif1	TGAAATGGAGGTGCCTTGGC
F β-actin	AAGCAGGAGTACGATGAGTC
R β-actin	TGGAGTCCTCAGATGCATTG
F raldh2 for cloning cDNA	ACCGGCATCTTCAATAGACG
R raldh2 for cloning cDNA	ATCAGCTTGCCTACCTCAGT

Chapter 6. Conclusion

Zebrafish caudal fin regeneration system is an exceptional platform to decipher the complex molecular pathways during epimorphic regeneration. We took advantage of the early life stage fin regeneration model because of its amenability for various molecular and genetic manipulations. First, we utilized a toxicological approach to impair the larval fin regeneration using an AHR ligand, TCDD. By antisense repression techniques, we demonstrated that AHR2 and ARNT1 are the *in vivo* molecular partners for TCDD to inhibit fin regeneration. We developed this *in vivo* platform for two purposes, first to understand the downstream target genes of AHR activation and second to unravel the essential regenerative signaling pathways affected by TCDD. Comparative toxicogenomic analysis between the adult and larval fin regeneration models after treatment with TCDD revealed that, AHR activation misexpressed Wnt signaling family members as well as Wnt target genes. We hypothesized that misexpression of R-Spondin1, a TCDD- induced gene, which is a novel ligand for Wnt co-receptor LRP6 is responsible for the differential expression of the Wnt target genes in the regenerating fin tissue after AHR activation. By partial antisense approaches, we demonstrated that, mis-induction of R-Spondin1 is absolutely required for TCDD-mediated inhibition of regeneration. This is for the first time a toxic phenomenon of AHR activation is completely reversed by modulating a single downstream target gene *in vivo*. Moreover, our studies for the first time identify functional cross talk between Wnt and AHR signal transduction pathways and indicate the power of zebrafish model to discover and define molecular pathways that regulate complex *in vivo* biological responses. Further studies have to be performed to identify the regulation of R-Spondin1 by AHR activation which will provide more insight how TCDD elicits toxic responses. Moreover, it is also important to understand how improper induction of R-Spondin1 impaired regeneration and is critical to identify the target genes responsible for this effect. This will eventually lead to the identification of critical signaling molecules during regeneration, which have numerous clinical implications in the emerging field of regenerative medicine.

Second, we used an unbiased chemical genetic approach and we developed an *in vivo* rapid throughput regeneration assay to identify novel molecular signaling pathways important for regeneration. Glucocorticoids were identified as modulators of regeneration and we demonstrated that transient activation of the glucocorticoid receptor is sufficient to block regeneration, but only if activation occurs during a narrow window of time during wound healing/blastema formation. We further showed that neutrophils and macrophages are not required for fin regeneration and these results indicate that signaling from exogenous glucocorticoids impairs blastema formation and limits regenerative capability in vertebrates through an acute inflammation-independent mechanism. Our findings illustrate the power of *in vivo* chemical genetics to identify novel bioactive compounds, and their molecular targets, that together function to modulate tissue regeneration. The signaling molecules affected by glucocorticoids have to be identified and the results will provide more understanding about tissue regeneration. Moreover, the use of additional small molecules to probe tissue regeneration will definitely lead to identification of novel regenerative pathways which will enhance the field of regenerative medicine.

Lastly, we took a comparative genomic approach to identify commonality in gene expression changes across different zebrafish regeneration models. We identified and functionally evaluated the role of RA signaling during fin regeneration. Most of the previous regeneration studies with RA signaling are related with the patterning of the structures during the regenerative outgrowth phase, but we illustrated that, RA signaling is also essential for the initiation of regeneration. Therefore, in addition to the established functional role of RA signaling during the regenerative outgrowth, RA signaling pathway is also essential in the early stages of regeneration, suggesting the existence of a dual phase of RA signaling during regeneration. Collectively, our studies revealed that there is conservation of fundamental regenerative networks and pathways that control epimorphic tissue regeneration.

Since the larval fin regeneration model is amenable to rapid molecular and genetic manipulations, this early life stage fin regeneration model is a powerful platform to discover and unravel regenerative mechanisms. By utilizing the power of chemical genetic and comparative approaches, the most exciting outcome will be a molecular

explanation for the observed differences in regenerative capacity across taxa, and will reveal pathways for therapeutic interventions.